Ghent University
Faculty of Science
Department of Plant Biotechnology and Genetics

Molecular genetic analysis of PIN polarity and auxin transport

Urszula Kania

Promotor: Prof. Dr. Jiří Friml

VIB / Plant Systems Biology
Technologiepark 927, B-9000 Ghent, Belgium

This thesis is submitted as fulfillment of the requirements for the degree of
Doctor (PhD) in Sciences: Biochemistry and Biotechnology
Academic year 2014-2015

This work was conducted in the Department of Plant Systems Biology of the Flanders Institute for Biotechnology

PROMOTOR

Prof. Dr. Jiří Friml
Institute of Science and Technology Austria (IST Austria)
Am Campus 1
3400 Klosterneuburg, Austria
Jiri.Friml@ist.ac.at

EXAMINATION BOARD

Prof. Dr. Wout Boerjan **(Chair)**
VIB Department of Plant Systems Biology, UGent
Technologiepark 927
9052 Gent
Wout.Boerjan@psb.vib-ugent.be

Prof. Dr. Stéphanie Robert
SLU/Umeå Plant Science Center
Department of Forest Genetics and Plant Physiology
901 83 Umeå, Sweden
Stephanie.Robert@slu.se

Prof. Dr. Danny Geelen
Coupure Links 653 Bl. A
9000 Gent
Danny.Geelen@UGent.be

Prof. Dr. Markus Geisler
University of Fribourg
Department of Biology - Plant Biology
Rue Albert-Gockel 3
CH-1700 Fribourg, Switzerland
Markus.Geisler@unifr.ch

Prof. Dr. Jenny Russinova
VIB Department of Plant Systems Biology, UGent
Technologiepark 927
9052 GENT
Jenny.Russinova@psb.vib-ugent.be

Prof. Dr. Moritz Nowack
VIB Department of Plant Systems Biology, UGent
Technologiepark 927 B
9052 Gent, Belgium
Moritz.Nowack@psb.vib-ugent.be

Dr. Boris Parizot
VIB Department of Plant Systems Biology, UGent
Technologiepark 927
9052 GENT
Boris.Parizot@psb.vib-ugent.be

Dr. Kiril Mishev
VIB Department of Plant Systems Biology, UGent
Technologiepark 927
9052 GENT
Kiril.Mishev@psb.vib-ugent.be

SUMMARY

In order to adapt to ever-changing environmental conditions and to respond to environmental stimuli, plants with their sessile lifestyle developed different strategies than animals. The plan of a plant's body is dynamically changing through its life span. These changes involve postembryonic development of new organs and formation of new meristems. The body plan of animals is already established during embryogenesis and postembryonic changes involve mainly tissue and organ growth. This amazing plant plasticity is regulated most prominently by the phytohormone auxin. Polar transport and local accumulation or depletions of this hormone in plant tissues underline the basis of this regulatory mechanism. Auxin is transported from one cell to another by PIN auxin efflux carriers, which, by feedback loop, regulate auxin concentration in cells. Polar localization of PIN proteins is crucial for establishing auxin gradient within plant tissues.

In **Chapter 1** we introduced the importance of polarity in the development of multicellular organisms and described factors which are known to play a role in the establishment and maintenance of polarity. Although the core mechanism regulating the delivery of proteins to their polar domains is similar in plants and animals, the genes responsible for polar targeting differ between those two kingdoms. Animal epithelial cells provide a good model system to study polarity as they display basolateral and luminal apical polarities separated by tight junctions. In plants, most of the knowledge about polar protein localization comes from PIN family studies. In this chapter we have presented forward and reverse genetics methods for studying polarity in plants and pointed out chemical genetics as a promising tool, which can overcome limitations of classical genetics.

In the **Chapter 2** and **3** we described two small molecules, endosidin 4 (ES4) and endosidin 6 (ES6) identified in chemical genomics screen. Both chemicals were identified as factors affecting polar PIN1 localization in *PIN2:PIN1-GFP; pin2* line (Drakakaki et al., 2011). We confirmed the initial results of the screen by immunolocalization of PIN1 protein in *PIN2:PIN1-GFP; pin2* line. Both chemicals induced apicalization of PIN1 in epidermal cells of this line.

Further characterization of ES4 described in **Chapter 2** revealed its effect on various morphological and intracellular features of plant phenotype, including shortening of the root of wild type plants, inversion of gravitropic defect observed in PIN2:PIN1-HA;pin2 line, induction of various intracellular trafficking markers agglomeration and inhibition of BFA bodies formation. Among all mutants analyzed for their root growth sensitivity to ES4, *arf-gefs* were those most affected, with the strongest inhibition of root growth displayed by *gnl1*. Root growth of wild-type plants was examined also on medium co-supplemented with ES4

and BFA at various concentrations. When combined, these two chemicals displayed additive effect on root growth indicating that they most likely affect different trafficking pathway. In this chapter we presented the results of forward genetic screen performed to identify mutants resistant to ES4. For this purpose we assessed the root length of PIN1:PIN1-GFP EMS mutagenized population grown on medium supplemented with ES4. Map-based cloning and sequencing of *es4r1* mutant selected in the screen revealed a mutation in the δ subunit of the COPI coatomer (δ-COPI). δ-COPI belongs to medium subunit family protein of clathrin adaptor complexes. Haploinsufficiency test was also conducted on heterozygous deletion yeast strains for the sensitivity to ES4 of various intracellular trafficking regulators like genes encoding different ARF, ARF GEFs and subunits of COPI coatomer. Among tested strains the only mutant that displayed a severely increased ES4 sensitivity was a *sec7*/SEC7 ARF GEF. In addition the impact of ES4 on the wild-type (*ARF1*^{WT}), GTP-locked (*ARF1*^{Q71L}), and GDP-locked (*ARF*^{T31N}) forms of ARF1 (Xu and Scheres, 2005) in transgenic *Arabidopsis* plants was tested. The only GTP-locked ARF1^{Q71L} was resistant to the ES4 treatment. Altogether the above results indicate that ES4 affects ARF1/ARF-GEF dependent trafficking pathways.

In **Chapter 3** we characterized morphological, intracellular and biochemical phenotypes of *Arabidopsis* plants treated with ES6. This small molecule inhibited root and hypocotyl growth, induced root hairs outgrowth and auxin accumulation. Among all test marker proteins only the cellulose synthase A proteins (GFP:CESAs) were affected by ES6. Additionally ES6 induced formation of Microtubule Associated Cellulose Synthase Compartments MASCs. Isoxaben is a chemical known to inhibit cell wall cellulose synthesis. We have compared its effect to ES6 on cell wall cellulose and hemicellulose composition. ES6 affected different sugars than isoxaben, indicating distinct mechanism of action for these two compounds. The above results demonstrated that ES6 affected cell wall composition. What is more, among all mutants tested for their sensitivity to ES6, the only resistant one was *rcn1*, defective in a1 subunit of protein phosphatase 2 (PP2Aa1). *rcn1* revealed smaller reduction in root and hypocotyl growth when compared to the control. The connection between the effects of ES6 on cell wall and PP2AA1 protein needs to be further investigated.

In **Chapter 4** we designed and initiated the study of sequence encoded cues for directionality of auxin transport in PIN proteins. PIN5 and PIN8, in contrast to other PM localized PIN proteins, are localized to the ER membranes. Both proteins are capable of transporting auxin, but in opposite directions. Genetic analysis of the knock-out and overexpression lines revealed that PIN5 and PIN8 can potentially compensate each other function, in maintaining auxin homeostasis and thus presumably contribute to antagonistic developmental responses observed in these lines. Alignment of PIN protein sequences in CLUSTAL X revealed two

sequences characteristic only for PIN8 protein. To address the possible involvement of these two domains in opposite auxin fluxes, we generated the set of constructs with mutated versions of the two specific domains.

In the closing **Chapter 5** we summarized the main conclusions of the thesis and proposed future experiments beneficial for broader understanding of mechanisms regulating polar localization of PIN proteins and opposite auxin fluxes.

LIST OF ABBREVIATIONS

A	ALANINE
ABCB	ATP BINDING OF B-TYPE
ABP	AUXIN BINDING PROTEIN
AEE	APICAL EARLY ENDOSOME
AFB	AUXIN SIGNALING F BOX
ALA	ALANINE
AP	ADAPTOR PROTEIN
aPKC	ATYPICAL PROTEIN KINASE C
AMPK	AMP-ACTIVATED PROTEIN KINASE
ARE	APICAL RECYCLING ENDOSOME
ARF	ADP-RIBOSYLATION FACTOR
ASP	ASPARTIC ACID
At	ARABIDOPSIS THALIANA
AUX	AUXIN RESISTANT
AXR	AUXIN RESISTANT
BEE	BASOLATERAL EARLY ENDOSOME
BEN	BFA-VISUALIZED ENDOCYTIC TRAFFICKING DEFECTIVE
BEX	BFA-VISUALIZED EXOCYTIC TRAFFICKING DEFECTIVE
BFA	BREFELDIN A
BRI	BRASSINOSTEROID INSENSITIVE
CaMV	CAULIFLOWER MOSAIC VIRUS
CAPS	CLEAVED AMPLIFIED POLYMORPHIC SEQUENCES
CDC	CELL DIVISION CONTROL
CDS	CODING SEQUENCE
CEV	CONSTITUTIVE EXPRESSION OF VEGETATIVE STORAGE PROTEIN
CES	CELLULOSE SYNTHASE
CFP	CYAN FLUORESCENT PROTEIN
CHC	CLATHRIN HEAVY CHAIN
CLC	CLATHRIN LIGHT CHAIN
CLSM	CONFOCAL SCANNING LASER MICROSCOPY
CME	CLATHRIN MEDIATED ENDOCYTOSIS
CO	CORTEX
Col	COLUMBIA
COP	COATOMER PROTEIN COMPLEX
CRE	COMMON RECYCLING ENDOSOME
CSC	CELLULOSE SYNTHASE COMPLEX
CSLD	*CELLULOSE* SYNTHASE (CESA)-LIKE PROTEIN
D	ASPARTIC ACID
DARTS	DRAG AFFINITY RESPONSIVE TARGET STABILITY
DLG	DISCS LARGE
DMSO	DIMETHYL SULFOXIDE
DNA	DEOXYRIBO NUCLEIC ACID
DRP	DYNAMIN RELATED PROTEIN
EDTA	ETHYLENEDIAMINETETRAACETIC ACID
EE	EARLY ENDOSOME
ELI	ECTOPIC LIGNIN
EMB	EMBRYO DEFECTIVE
EMS	ETHYL METHANESULFONATE
ENP	ENHANCER OF PINOID
EP	EPIDERMIS
ER	ENDOPLASMATIC RETICULUM
ES	ENDOSIDIN

EXO	EXOCYST
FRAP	FLUORESCENCE RECOVERY AFTER PHOTOBLEACHING
FYPP	PHYTOCHROME-ASSOCIATED SERINE/THREONINE PROTEIN PHOSPHATASE
GAP	GTPASE ACTIVATING PROTEIN
GBF	GOLGI-ASSOCIATED BREFELDINA-RESISTANT GUANINE NUCLEOTIDE EXCHANGE FACTOR
GDI	GDP DISSOCIATION INHIBITOR
GDP	GUANOSINE DIPHOSPHATE
GEF	GUANINE NUCLEOTIDE EXCHANGE FACTOR
GFP	GREEN FLUORESCENT PROTEIN
GN	GNOM
GNL	GNOM LIKE
GTP	GUANOSINE-5'-TRIPHOSPHATE
GUS	β-GLUCURONIDASE
H	HISTIDINE
HA	HUMAN INFLUENZA HEMAGGLUTININ
HIS	HISTIDINE
HSP	HEAT SHOCK PROMOTER
IAA	INDOLE-3 ACETIC ACID
ICR	INTERACTOR OF CONSTITUTIVE ACTIVE ROP
IX	ISOXABEN
IXR	ISOXABEN RESISTANT
LAX	LIKE AUX1
L*er*	LANDSBERG *ERECTA*
LGL	LETHAL GIANT LARVAE
LKB	LIVER KINASE B
MAB	MACCHI-BOU
MAP	MICROTUBULE ASSOCIATED PROTEIN
MASC	MICROTUBULE ASSOCIATED CELLULOSE SYNTHASE COMPARTMENTS
MBD	MICROTUBULE BINDING DOMAIN
MDCA	MADIN-DARBY CANINE KIDNEY
MDR	MULTIDRUG RESISTANCE
MHD	μ HOMOLOGY DOMAIN
MS	MURASHIGE AND SKOOG
MUNC	MAMMALIAN UNCOORDINATED
MVB	MULTIVESICULAR BODY
NAA	α-NAPHTHALENEACETIC ACID
NPA	1-N-NAPHTHYLPHTHALAMIC ACID
NPY	NAKED PINS IN YUC MUTANTS
OD	OPTICAL DENSITY
OE	OVEREXPRESSING
PALS	CRUMBS/PROTEINS ASSOCIATED WITH LIN SEVEN
PAR	PARTITIONING DEFECTIVE
PAT	POLAR AUXIN TRANSPORT
PATJ	PALS-ASSOCIATED TIGHT JUNCTION
PCR	POLYMERASE CHAIN REACTION
PGP	PHOSPHOGLYCOPROTEIN
PID	PINOID
PILS	PIN-LIKES
PIN	PIN-PINFORMED
PIP	PLASMA MEMBRANE INTRINSIC PROTEIN
PK	PROTEIN KINASE
PM	PLASMA MEMBRANE

PP	PROTEIN PHOSPHATASE
PRC	PROCUSTE
PVC	PREVACUOLAR COMPARTMENT
RCN	ROOTS CURL IN NPA
RE	RECYCLING ENDOSOME
REPP	REGULATOR OF PIN POLARITY
RIC	ROP-INTERACTIVE CRIB MOTIF-CONTAINING PROTEIN
RNA	RIBONUCLEIC ACID
ROP	RHO OF PLANTS
RPM	ROUNDS PER MINUTE
RPS5A	RIBOSOMAL PROTEIN5A
RSW	RADIAL SWELLING
SAC	SUPPRESSOR OF ACTIN
SAL	SAPS DOMAIN-LIKE
SAR	STRUCTURE ACTIVITY RELATIONSHIP
SCR	SKP1/CULLIN1/F-BOX
SD	STANDARD DEVIATION
SE	STANDARD ERROR
SEC	SECRETORY
SNX	SORTIN NEXIN
SSLP	SINGLE SEQUENCE LENGTH POLYMORPHISM
ST	SIALYLTRANSFERASE
SYP	SYNTAXIN OF PLANTS
TALEN	TRANSCRIPTION ACTIVATOR-LIKEEFFECTOR NUCLEASES
TAP	TANDEM AFFINITY PURIFICATION
TEM	TRANSMISSION ELECTRON MICROSCOPY
TGN	TRANS GOLGI NETWORK
THE1	THESEUS1
TIBA	2,3,5-TRIIODOBENZOIC ACID
TILLING	TARGETING-INDUCED LOCAL LESIONS IN GENOMES
TIR	TRANSPORT INHIBITOR RESPONSE
TMK	TRANSMEMBRANE KINASE
TXR	THAXTOMIN A RESISTANT
VAN	VASCULAR NETWORK DEFECTIVE
VHAa1	VACUOLAR H^+-ATPase SUBUNIT A1
VPS	VACUOLAR PROTEIN SORTING
VTI	VESICLE TRANSPORT V-SNARE
WAG	WAVY ROOT GROWTH
Ws	WASSILEWSKIJA
WT	WILD TYPE
X-GLUC	5-BROMO-4-CHLORO-3-INDOLYL-BETA-D-GLUCURONIC ACID
YFP	YELLOW FLUORESCENT PROTEIN
YPD	YEAST EXTRACT/PEPTONE/DEXTROSE
ZFN	ZINC FINGER NUCLEASES

TABLE OF CONTENT

RESEARCH OBJECTIVES

Phytohormone auxin, through local accumulation and coordinated polar transport, plays a pivotal role in the developmental and environmental responses of plants. The aim of this work was to obtain a better insight into the mechanisms regulating polar localization of PIN proteins in the model plant *Arabidopsis thaliana*, using a chemical genomic approach. So far the topic was mostly studied using classical genetics approaches, including knock-out and overexpression lines defective in polar PIN localization or using variable chemicals interfering with specific pathways involved in this process. To better understand the mechanisms regulating polar PIN localization and maintenance, and possibly characterize unknown players involved in those processes, we took the advantage of chemical genomics approach. We selected two chemicals, which interfere with polar PIN localization. Through characterization of these two small molecules we expected to reveal unknown pathways regulating polarity of PIN proteins.

PIN proteins transport auxin not only between cells, but also intracellularly. Opposite auxin fluxes between ER membranes presumably contribute to maintain auxin homeostasis and regulate availability of auxin for signaling and transport. PIN8 protein, localized to the ER membranes, transport auxin in opposite direction to other PIN proteins. Sequence alignment between PIN proteins revealed two domains characteristic for PIN8. The aim of this project was to determine whether the two motifs specific for PIN8 play a role in mediating directionality of auxin fluxes.

Chapter 1

Introduction.
Polar delivery in plants; commonalities and differences to animal epithelial cells

Urszula Kania[a,b], Matyáš Fendrych[b] and Jiří Friml[a,b]

[a]Institute of Science and Technology Austria (IST Austria), 3400 Klosterneuburg, Austria
[b]Department of Plant Systems Biology, VIB and Department of Plant Biotechnology and Genetics, Ghent University, 9052 Gent, Belgium

ABSTRACT

Although plant and animal cells use a similar core mechanism to deliver proteins to the plasma membrane, their different life style, body organization and specific cell structures resulted in the acquisition of regulatory mechanisms that vary in the two kingdoms. In particular, cell polarity regulators do not seem to be conserved, because genes encoding key components are absent in plant genomes. In plants, the broad knowledge on polarity derives from the study of auxin transporters, the PIN-FORMED proteins, in the model plant *Arabidopsis thaliana.* In animals much information is provided from the study of polarity in epithelial cells that exhibit basolateral and luminal apical polarities, separated by tight junctions. In this review, we summarize the similarities and differences of the polarization mechanisms between plants and animals and survey the main genetic approaches that have been used to characterize new genes involved in polarity establishment in plants, including the frequently utilized forward and reverse genetics screens, as well as a novel chemical genetics approach that is expected to overcome the limitation of classical genetics methods.

AUTHOR CONTRIBUTIONS

U.K., wrote the article, M.F. and J.F. revised and corrected the article.

Adapted from: **Kania U, Fendrych M and Friml J** (2014) Polar delivery in plants; commonalities and differences to animal epithelial cells. *Open Biol.* **4:** 140017.

INTRODUCTION

Establishment and maintenance of cell polarity are one of the most fundamental topics in cell biology. Differences in cell polarization among different cell types enable them to form cell sheets that carry out the same function and result in the formation of various tissues and organs. At the cellular level, polarity can be described as an asymmetrical distribution of molecules, proteins, organelles or cytoskeletal strands along a particular axis (Grebe et al., 2001). Such organization of intracellular structures plays a crucial role during cell differentiation, proliferation, morphogenesis, intercellular communication and cell signaling. Cell polarity is of crucial importance in unicellular organisms that, thanks to asymmetrically distributed molecules inside the cells, are able not only to proliferate and move, but also to specify distinct cell sites to fulfill a different function. A canonical example of such an organism is the green alga *Acetabularia* that develops structures resembling organs of higher plants, such as rhizoids, stalks and cups (Mine et al., 2008). In multicellular organisms, polarity plays an additional role in the communication between cells that is necessary for their cooperation and function as a whole organ. Although in both plants and animals, cell polarity determines the integrity of the organism, in most animal cells, polarity is, once established, retained throughout the life span, whereas in plants, due to their sessile life style, relocation of the plasma membrane (PM)-localized proteins between different polar domains plays an additional role in responding to the ever-changing environmental stimuli and in developmental plasticity. The mechanism that allows plants to align along the gravity vector involves the relocation of the PIN-FORMED3 (PIN3) auxin efflux carriers in columella root cells and endodermal hypocotyl cells to redirect the auxin flow (Friml et al., 2002a; Rakusová et al., 2011). Different life strategies between plants and animals are reflected in their distinctive development: whereas most animals shape their adult body plan already during embryogenesis, plants continue to develop their body architecture postembryonically and are able to rearrange it in response to environmental conditions.

In plants, virtually all developmental processes, such as embryogenesis, organogenesis, vascular tissue formation or regeneration, require the establishment or rearrangement of the polarity. Many aspects of this developmental flexibility are mediated by the plant hormone auxin that acts as a polarizing cue (Berleth and Sachs, 2001; Leyser, 2011; Sauer et al., 2006). Through an asymmetric distribution between cells and the formation of local maxima and minima, auxin controls many developmental processes, such as embryogenesis (Friml et al., 2003; Schlereth et al., 2010), organogenesis (Benková et al., 2003; Heisler et al., 2005; Reinhardt et al., 2003; Sorefan et al., 2009), tropic growth (Chen et al., 1998; Friml et al., 2002a; Luschnig et al., 1998; Müller et al., 1998; Utsuno et al., 1998), vascular tissue formation (Scarpella et al., 2006), root meristem maintenance (Blilou

et al., 2005; Friml et al., 2002b; Sabatini et al., 1999) and apical hook formation (Zádníková et al., 2010). An auxin concentration gradient in a tissue can be created by its localized synthesis or metabolism, but predominantly by polar auxin transport (PAT). PAT depends on polarly localized auxin influx and efflux carriers that guide the auxin flow direction (Grunewald and Friml, 2010). Auxin efflux is carried out by a family of PIN proteins (Petrásek et al., 2006), most of which (PIN1, PIN2, PIN3, PIN4 and PIN7) are polarly localized on the PM, depending on PIN protein, cell type, and developmental stage (Vieten et al., 2007). Already during embryogenesis, the localization of PIN1, PIN4 and PIN7 directs the auxin accumulation toward distinct parts of the developing embryo and results in the specification of the main apical-basal plant axis. After the first division of the zygote, auxin accumulates in the proembryo, which specifies the apical pole. At the globular stage, auxin starts to accumulate in the hypophysis where the future root pole will be established (Friml et al., 2003). Besides PIN proteins, auxin transport is also facilitated by other components, such as AUXIN-RESISTANT1/LIKE AUX1 (AUX1/LAX) and MULTIDRUG RESISTANCE/PHOSPHOGLYCOPROTEIN/ATP-BINDING CASSETTE OF B-TYPE (MDR/PGP/ABCB), which are influx and efflux carriers, respectively (Zazímalová et al., 2010). The localization of these proteins depends on the cell type in which they are expressed; for example, in the protophloem, AUX1/LAX proteins are located on the apical part of the cells, whereas in the shoot apical meristem, they localize similarly as the PIN1 proteins on the basal part of the cells (Swarup et al., 2001). The ABCB auxin transporters, ABCB1/PGP1, ABCB4/PGP4 and ABCB19/PGP19, are mainly distributed equally at the PM; however, in root epidermal cells, ABCB4/PGP4 displays a more polarized basal or apical localization (Terasaka et al., 2005). Unraveling the mechanisms of the polarization process at the cellular level is crucial for understanding how single cells are able to organize themselves in a polarized manner to form the tissues and organs of living organisms.

1. COMPARISON OF VESICULAR TRAFFICKING AND PROTEIN LOCALIZATION FACTORS BETWEEN POLARIZED CELLS OF PLANTS AND ANIMALS

Eukaryotic cells share common cellular components that are involved in cell polarization, such as the endomembrane system, cytoskeleton, extracellular matrix/cell wall, and molecular regulators of polarity (such as Rab GTPases). Nevertheless, the independent evolution of multicellularity in plants and animals resulted in the origin of specific executors and structures, such as cell walls in plants or tight junctions in animals, associated with the establishment and maintenance of polarity. In the animal system, the most remarkable polarity determinants (partitioning defective (PAR) and the Scribble and Crumbs complexes) serve as components to multiple effector pathways, including cytoskeleton formation, cell-cell junctions and cell membrane and cortex organization, ensuring formation and maintenance

of polar domains as a consequence (Chen et al., 2010; Humbert et al., 2006; Lu and Bilder, 2005; Tepass et al., 2001; Wells et al., 2006). Plants have established their own polarization manner based on the activity of the Rho-like small G proteins, designated RAC/ROP GTPases (Yang and Lavagi, 2012) that are domain identity proteins. ROP GTPases are master molecular switches controlling cell polarization by regulating vesicle trafficking, interacting with cytoskeleton or working as domain identity proteins. Additionally, PIN proteins are important factors that induce their own polarity: they are auxin transporters, not regulatory proteins, and they need a polarized vesicular transport. Furthermore, the polar domains are differently organized in plants and animals (Figure 1). In plant epidermal cells, four polar domains have been identified: the apical, basal, outer lateral and inner lateral, whereas in animal epithelial cells, only basolateral and apical domains can be distinguished separated by the so-called tight junctions (Kleine-Vehn and Friml, 2008).

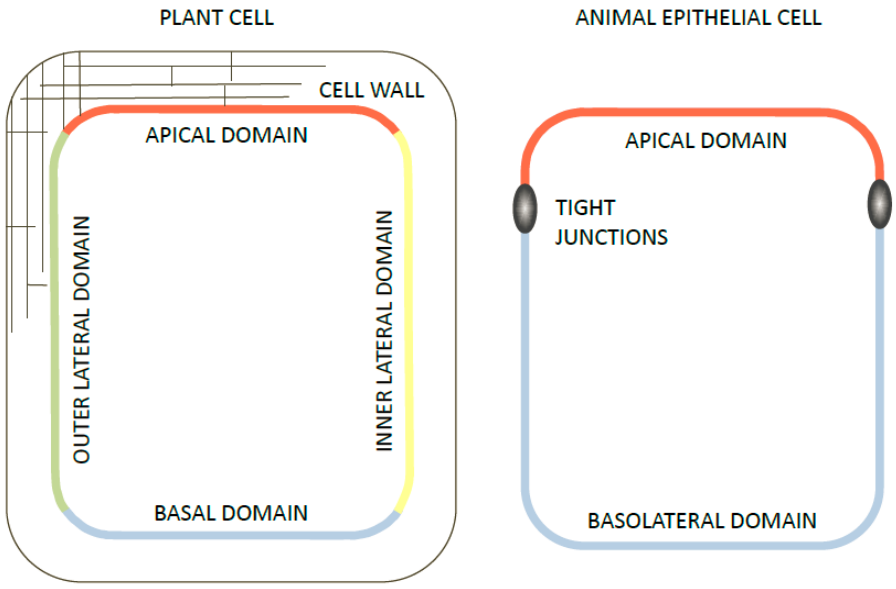

Figure 1. Schematic representation of polar domains in the plant epidermal and animal epithelial cells.
Plant epidermal cells exhibit four polar domains: apical, basal, inner lateral and outer lateral and are surrounded by cell walls. Animal epithelial cells exhibit apical and basolateral domains separated by tight junctions.

1.1 Conserved trafficking cellular machinery and organelles

In both plants and animals, polarly localized proteins follow the secretory pathway from the endoplasmic reticulum (ER), through the *cis*- and *trans*-Golgi stacks, to the PM (Peer, 2011). Proteins are transported between the intracellular compartments in vesicles that are formed by three classes of protein complexes: the coatomer protein complex II (COPII) guides the anterograde transport from the ER to the Golgi apparatus; the coatomer protein complex I (COPI) is crucial for retrograde transport from the Golgi apparatus to the ER and the intra-Golgi stacks (Beck et al., 2009; Popoff et al., 2011); and the adaptor protein (AP) clathrin

complex encapsulates proteins during the transport between PM, Golgi apparatus and endosomes (Paul and Frigerio, 2007).

Sorting and polar targeting of newly synthetized proteins to the PM are better examined in animal systems. For a long time, only three main routes had been described for the secretion of polar proteins after exiting the *trans*-Golgi network (TGN). Proteins could be targeted directly to the apical polar and basolateral domains or, in some cases, apically localized proteins could follow an indirect route and go first to the basolateral domain from where they were transcytosed to the apical side (Bonilha et al., 1997; Mostov et al., 2003). The direct targeting to the polar domains was identified in the 1980s by biochemical and morphological studies that investigated the localization of different viral proteins in epithelial cells. After coexisting at the TGN, the influenza virus hemagglutinin and the vesicular stomatitis virus G protein were targeted directly to the apical or basolateral PM domains, respectively (Fuller et al., 1985; Misek et al., 1984; Pfeiffer et al., 1985). Recently, new experiments have demonstrated that the secretory pathway of some proteins can be more complex, encompassing the so-called recycling endosomes (REs) on the way from the Golgi apparatus to the PM. Although in animals the trafficking of newly synthetized, polarly localized proteins is well characterized, in plants this process is still unclear. In *Arabidopsis* cells, proteins are probably secreted in a polar manner (Łangowski et al., manuscript in preparation). The transcytosis of PIN proteins in plants has been shown (Kleine-Vehn et al., 2008a, 2008b) but it remains unclear whether this process assists the polar delivery in general or serves only for the repolarization after signals, such as gravity (Kleine-Vehn et al., 2010).

Besides the involvement of polar secretion in the cellular polarization, establishment and maintenance of the distinct polar domain is also regulated, both in plants and animals, by the constant polar recycling of the PM proteins. In epithelial cells, internalized proteins from the apical and basolateral domains localize to the apical and basolateral early endosomes, respectively, from where they can be recycled back to the PM, or targeted to the common recycling endosome that plays multiple roles in the protein-sorting pathway where common trafficking pathways intersect, such as recycling, secretion and transcytosis. Additionally, an apical recycling route encompasses the apical recycling endosome that is involved in basal-to-apical transcytosis and transport of newly synthesized proteins (Gonzalez and Rodriguez-Boulan, 2009). In plants, PIN proteins are internalized from the PM to the TGN/early endosome (EE) compartments and can further follow either the recycling route to the PM via hypothetical compartments, the REs (Figure 2), or the degradation route to the vacuole via prevacuolar compartments that correspond to late endosomes in plants (Grunewald and Friml, 2010; Robinson et al., 2008).

Polar cargoes derived both from secretory and endocytic pathways have to be sorted to the destination site. In epithelial cells, sorting of secreted proteins occurs mainly at the TGN, whereas REs sort mainly recycling proteins (Treyer and Müsch, 2013) (Figure 3A and 3B). In contrast, in plants, the TGN/EE is the compartment in which secretory and endocytic routes merge (Dettmer et al., 2006; Viotti et al., 2010). Exocytosis is mediated by evolutionarily conserved complex, the exocyst, which consist of eight subunits (Sec3, Sec5, Sec6, Sec8, Sec10, Sec15, Exo70, and Exo84). In plants and animals, exocyst is responsible for vesicle tethering to the PM (Drdová et al., 2013; Hála et al., 2008; Liu and Guo, 2012; Ory and Gasman, 2011). Constant trafficking of PM proteins is required for their proper polar localization. Although the trafficking mechanisms between plants and animals are similar, there are some main differences at the molecular level. The cellular trafficking machinery is better described in epithelial system. Different types of sorting endosomes are distinguished in epithelial cells, whereas in plant the main sorting station is EE/TGN. Also, more polarly localized proteins were identified in epithelial cells, allowing a better insight into dissecting the trafficking routes. However, in plant cells, a lot of important information is still missing, such as the sorting mechanism of *de novo* synthetized PIN proteins.

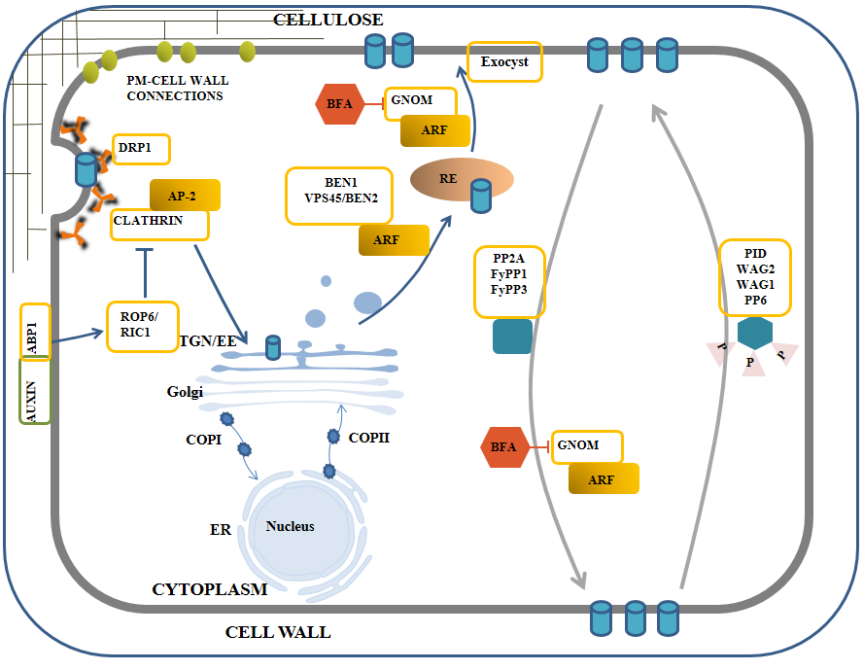

Figure 2. Intracellular trafficking and cellular requirements for polarization of PIN proteins.
Auxin binding to its receptor ABP1 inhibits CME through ROP6/RIC1 signaling. PIN proteins require the DRP1 function for CME. Clathrin interacts with AP-2 to form clathrin-coated vesicles. They are internalized to the TGN/EE and then follow the pathway to the RE that is regulated by BEN1 and VPS45/BEN2 ARF-GEFs. Exocyst tether vesicles to the PM. Recycling of PIN proteins from the RE to the PM is regulated by a GNOM-dependent mechanism. Control of apical and basal PIN targeting depends on the phosphorylation status of PIN proteins. PIN proteins are directed to the apical domain through phosphorylation by PID/WAG1/WAG2/PP6 kinases, whereas they are guided to the basal domain by

dephosphorylation by means of PP2A/FyPP1/FyPP3 phosphatases. Basal targeting of PIN cargoes is controlled by GNOM.

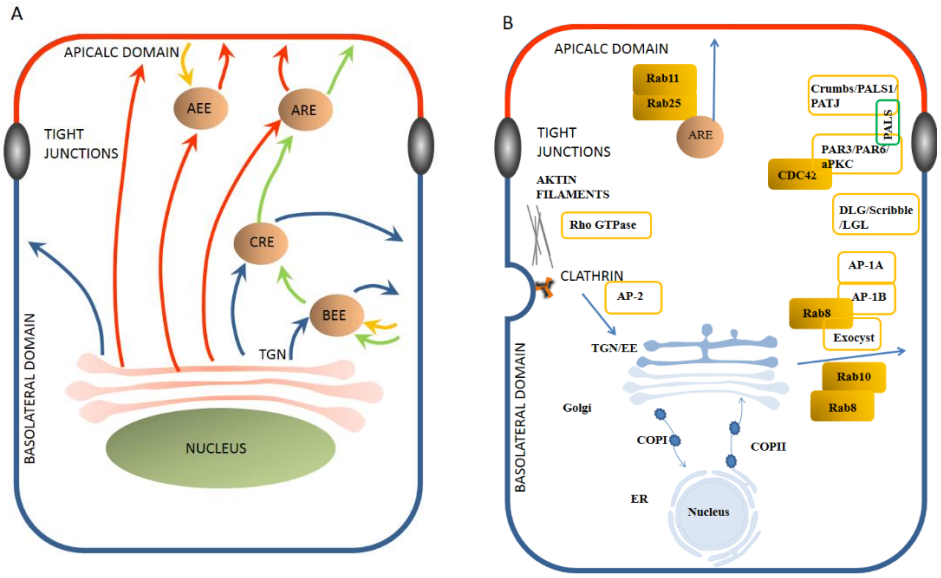

Figure 3. Schematic representation of intracellular trafficking in epithelial cells.
(A) Proteins from TGN to the apical domain can be targeted directly, through apical early endosome (AEE), apical recycling endosome (ARE), common recycling endosome (CRE) followed by ARE or can go first to the basolateral domain from where they are transcytosed to the apical domain. Proteins from TGN to the basolateral domain can be targeted directly, through CRE or basolateral early endosome (BEE).
(B) COPI and COPII guides the protein transport between Golgi and ER. Clathrin interacts with AP-2 in CME. AP-1A and AP-1B interact with clathrin and sort proteins to the basolateral domain. Two signalling complexes PAR and Crumbs mediate tight junctions establishment and formation of the apical domain. Scribble complex regulate the identity of the basolateral domain. The PAR, Crumbs and Scribble mutually regulate the localization and activity of eachother. CDC42 interacts with PAR3/PAR6/APKC and maintains tight junctions. Rho GTPases stimulate actin polymerization through which deliver proteins to the PM. Rab8 interacts with AP-1A, AP-1B and exocyst complex and mediate protein delivery to the basolateral PM. Rab10 together with Rab8 mediate cargo trafficking to the basolateral domain. Rab25 and Rab11 control the apical recycling.

1.2 Clathrin adaptor complexes

Endocytosis and exocytosis are highly dynamic processes (Ketelaar et al., 2008) that are key determinants of the PM integrity and that regulate transport and signaling at the cell surface. Clathrin-mediated endocytosis (CME) has been shown to be involved in the recycling of polarly localized proteins in plants and animals (Dhonukshe et al., 2007; McMahon and Boucrot, 2011). Protein endocytosis from the PM to the endosomal compartment is initiated by recognition of the cargo-sorting signals by the adaptor protein-2 (AP-2) complex that recruits clathrin to form clathrin-coated vesicles. The AP-2 complex can recognize two specific peptide motifs in the cytoplasmic domain of transmembrane proteins, the tyrosine-based and the dileucine-based motifs, as well as posttranslational modifications, such as phosphorylation and ubiquitination (Ohno et al., 1998). Recently, the role of AP-2 in endocytosis has been shown in plants as well (Kim et al., 2013a; Rubbo et al., 2013).

From the five existing adaptor protein complexes, the AP-2 complex is implicated in CME (Kim et al., 2013a; McMahon and Boucrot, 2011; Rubbo et al., 2013). As CME is the main endocytic route involved in the transport of PM components known in plants, it has a great influence on the polarization of PM proteins. However, in mammalian cells, also clathrin-independent mechanisms of endocytosis are known that regulate the PM composition. In contrast, other clathrin-dependent trafficking pathways have a tremendous impact on the polarization events. Analysis of clathrin knockdown mutants in Madin-Darby canine kidney (MDCK) cells has revealed that clathrin-mediated vesicle transport plays an essential role for the basolateral polarity without effect on the apical polarity (Deborde et al., 2008). Three of the adaptor protein complexes (AP-1, AP-2 and AP-3) have binding sites for clathrin (Bonifacino and Traub, 2003), but the AP-3 function in polarized cell sorting has not been studied yet. The AP-1A and AP-1B complexes sort the proteins to the basolateral domain of epithelial cells, by recognizing the sorting signals and coating the proteins into clathrin vesicles (Gravotta et al., 2012). The AP-1B complex occurs specifically in epithelial cells and differs from the ubiquitously expressed AP-1A complex in the μ1B subunit that is closely related to the μ1A (Ohno et al., 1999). The sorting signals for basolateral PM proteins are tyrosine and dileucine motifs that are similar to those recognized in CME (Hunziker and Fumey, 1994; Matter et al., 1992). Another sorting signal, a single leucine motif, has been characterized in the stem cell transmembrane growth factor, which is important specifically for basolateral sorting, but not for endocytosis (Wehrle-Haller and Imhof, 2001). Additionally, the AP-4 complex that does not interact with clathrin can recognize different basolateral sorting signals to mediate transport in epithelial cells, as confirmed by depletion of the μ4 adaptin that results in missorting of some basolateral proteins to the apical domain (Simmen et al., 2002).

Whereas CME was well characterized in mammals and yeast, the genetic characterization of the clathrin involvement in this process has been identified only recently in plants. A first insight into the role of clathrin in CME was gained by immunolocalization of clathrin at different stage of vesicle formation (Dhonukshe et al., 2007). CME was best described for PIN proteins as an important factor for their polar localization. When endocytosis is blocked by chemical inhibitors, PIN proteins at the PM spread laterally. Live-cell imaging and computational approaches revealed that laterally diffused PIN proteins that escaped from polar domains are internalized by clathrin-dependent endocytosis and via exocytosis are delivered back to the polar domain center by superpolar recycling (Kleine-Vehn et al., 2011). Characterization of the clathrin heavy chain 2 (*chc2*) mutants and dominant-negative CHC1 (*HUB*) showed defects in the bulk endocytosis and the recycling machinery of PIN proteins, with a defective polar targeting as a consequence (Kitakura et al., 2011). Furthermore, mutations in different subunits of the AP-2 complex, such as the σ

adaptin (*ap2σ*) or the μ adaptin (*ap2m*), result in impaired endocytosis and disruption of the polar PIN1-GFP localization during embryogenesis or of the PIN2-GFP localization in the male reproductive organ development (Fan et al., 2013; Kim et al., 2013b). Deficient PIN localization together with other developmental defects in clathrin and AP-2 mutants, such as reduced vegetative growth or impaired vascular patterns, which are reminiscent of defects in auxin signaling and transport, hint at an important role of CME in the polarization process. Another group of proteins involved in the CME process required for fission of clathrin-coated vesicles in mammals are dynamin-related proteins (DRPs). Although their function is not very well characterized in plants, DRP1A has been shown to interact with PIN proteins during CME at the cell plate. Examination of the *drp1* mutant phenotype confirmed the importance of these proteins for proper PIN1 distribution in dividing cells and of their role in auxin-mediated development (Mravec et al., 2011). Additionally, AP-1 is involved in intracellular protein sorting at the TGN/EE in the interphase and in protein delivery to the cell plate during cytokinesis (Park et al., 2013; Teh et al., 2013; Wang et al., 2013). AP-3 has been suggested to act in the transport from the Golgi apparatus to the plant vacuoles, but its function is still poorly defined (Feraru et al., 2010; Zwiewka et al., 2011) and its role in polarity has not been shown yet. Clathrin, together with the AP-2 complex, plays an important role in polarity maintenance, both in plants and animals. However, in plants, CME serves as a main pathway for internalization and recycling of PM proteins, whereas in animals it is involved mostly in the regulation of basolateral trafficking. Additional important role in basolateral cargo delivery in epithelial cells plays the AP-1 complex. In plants, other AP complexes have to be examined further to evaluate their role in polarization events.

1.3 Small GTPases

Small GTPases are a group of hydrolase enzymes implicated in a broad range of cellular signaling events. Of the many genes that code for GTPases and their regulators in plants and animals, some subfamilies are involved in polarization events, such as the Rho, Rab and ADP-Ribosylation Factor (ARF) GTPases. They regulate the vesicular trafficking between intracellular compartments by recruiting coat protein complexes to the vesicle formation sites, organizing the cytoskeleton, and docking vesicles to the destination membranes. GTPase proteins constitutively cycle between their active GTP-bound and inactive GDP-bound conformations. Their activation is mediated by the Guanine Exchange Factor (GEF) that stimulates the GDP-to-GTP substitution and the deactivation process by GTPase-Activating Proteins (GAPs) that promote the GTP hydrolysis and the return of Rho, ARF or Rab proteins to the GDP-bound form (Nielsen et al., 2008). Additionally, the Rho protein has another regulator, the Rho GDP Dissociation Inhibitor (RhoGDI). During evolution, the Rho superfamily diverged into subgroups: characteristic for mammals and filamentous fungi, Rho,

Rac and the cell division control protein CDC42; for yeast, CDC42 and Rho, and the plant-specific Rho Of Plants (ROP) (Nagawa et al., 2010). In metazoans and fungi, Rho and CDC42 are considered the major polarity organizers. In budding yeasts, a preexisting budding scar provides a landmark for the formation of the next daughter cell, but CDC42 can polarize cells even in the absence of polarizing cues. CDC42 activated by its exchange factor polarizes actin filaments toward itself to the new bud formation site, enhancing the activated CDC42 accumulation to the same site and depletion from other cell sites (Wedlich-Soldner et al., 2003). In animal cells, CDC42 is necessary to polarize PAR proteins, it interacts with the PAR3/PAR6/aPKC polarity complex, and maintains tight junctions (Joberty et al., 2000; Lin et al., 2000). In general, in animals and yeasts, Rho GTPases influence the actin filament formation and regulate vesicle transport by actin polymerization targeting to the PM domains, where they deliver the proteins (Ridley, 2006). In the mammalian system, the secretory and endocytic pathways are regulated by the Rab family of small GTPases that plays a role in the different steps of membrane trafficking, i.e. budding, delivery, tethering and fusion (Grosshans et al., 2006), but only a few of them might have a specific function in the basolateral and apical trafficking. The small GTPase Rab8 regulates the basolateral cargo delivery by interacting with the AP-1B complex and the exocyst-tethering complex, which is implicated with basolateral cargo delivery (Ang et al., 2003). Besides basolateral polarization, Rab8 is also involved in apical protein localization in intestinal cells (Sato et al., 2007) and in *de novo* generation of the apical domain and lumen (Bryant et al., 2010). Another Rab GTPase, Rab10, together with Rab8, mediate cargo trafficking from the TGN to the basolateral surface of newly synthetized proteins (Schuck et al., 2007), whereas Rab25 and Rab11 control the apical recycling in epithelial cells (Wang et al., 2000). Different Rho and Rab proteins mark polar PM domains and regulate polar exocytosis by interaction with the exocyst complex. The first small GTPase found to interact with the exocyst was Sec4 in yeast (Guo et al., 1999). In epithelial cells, basolateral exocytosis is controlled by Rab8, Rab10, CDC42 and RalA, whereas Rab8, Rab11 and Rabin8 (Rab8GEF) drive the transport to the cilium in the apical domain (Kang and Folsch, 2009). Another small GTPase, ARF6, regulates the CME in the apical and basolateral domains (Altschuler et al., 1999) that, besides its function in endocytosis, plays also an important role in actin cytoskeleton rearrangements.

Recent experiments have improved the knowledge on the involvement of ROP GTPases and their interactors in polarity establishment in plants. In some cell types, such as trichoblasts, the localization of ROP GTPases to specific membrane domains is determined by auxin. A local auxin gradient induces the ROP accumulation on the rootward end of trichoblasts, marking the future root hair growth position (Fischer et al., 2006). In pollen tubes, highly polarized growth that occurs at the very tube tip is governed by ROP1 that

oscillates between an active and inactive form to maintain the optimal level for efficient tube elongation. Globally, RhoGDI and RhoGAP inhibit ROP1 to prevent lateral propagation from the apical cap. Furthermore, ROP1 influences the apical actin microfilament formation that drives the polar exocytosis of ROP activators and inhibitors, generating positive and negative feedback-regulatory mechanisms, respectively (Yang and Lavagi, 2012). Furthermore, ROP6 and its downstream ROP-INTERACTIVE CRIB MOTIF-CONTAINING PROTEIN 1 (RIC1) effector are involved in CME of PIN proteins in roots, where they recruit clathrin to the PM. This process is regulated by auxin through the Auxin-Binding Protein 1 (ABP1) that acts upstream of ROP6/RIC1 (Chen et al., 2012). Recently, the PM-localized transmembrane kinase (TMK) receptor-like kinases has been demonstrated to interact with the ABP1 protein at the cell surface and to activate ROP GTPases (Xu et al., 2014), which have been shown to be master regulators of the formation of interdigitated pavement cells where the locally activated ROP4 and ROP6 are responsible for lobe and indentation formation (Bloch and Yalovsky, 2013). The interactor of the activated *ROP* gene, ICR1, mediates the interaction of ROP-Sec3 at the PM and is necessary to recruit PIN proteins to the polar domains (Hazak et al., 2010).

Endocytosis of PIN proteins is not only mediated by clathrin (Chen et al., 2011; Dhonukshe et al., 2007), but is also dependent on the GNOM (GN or also known as EMBRYO DEFECTIVE30 [EMB30] or VASCULAR NETWORK7 [VAN7]) and GNOM-like1 (GNL1) ARF-GEFs (Naramoto et al., 2010; Teh and Moore, 2007), together with the Rab GTPase ARA7 (Dhonukshe et al., 2008). The PIN1 proteins that are directed to the recycling route are controlled by the GNOM-regulated ARF GTPase (Geldner et al., 2003). GNOM consists of a Sec7 domain recognized by the fungal toxin Brefeldin A (BFA) that inhibits GNOM-dependent exocytosis, resulting in the accumulation of internalized proteins in so-called BFA compartments, together with the TGN, and in the depletion of PIN proteins from the PM (Geldner et al., 2003). After a prolonged incubation with BFA or a genetic interference with GNOM, PIN1 proteins from the basal domain are gradually transported to the apical cell side, whereas apically localized PIN2 proteins in the epidermis are BFA insensitive, indicating the importance of GNOM in the basal PIN localization (Kleine-Vehn et al., 2008a). In addition to its role in the intracellular trafficking, GNOM is involved in the endocytosis process, together with another ARF-GEF, namely GNL1, and ARF-GAP, namely Vascular Network Defective 3 (VAN3). Mutant analysis and localization of these factors at the PM confirmed the significant role of the ARF GTPase machinery in the endocytic process (Naramoto et al., 2010; Teh and Moore, 2007). Besides the GBF class of ARF-GEFs that includes GNOM and GNL1, another class of BFA-Inhibited Guanine nucleotide exchange (BIG) proteins is also involved in intracellular trafficking, although it is still not well characterized. One member of this class, i.e. BFA-visualized endocytic trafficking defective 1

(BEN1)/BIG5/MIN7, has been found to be involved in BFA-induced internalization of basally localized PIN proteins: PIN1-GFP in the stele and PIN2 in cortex cells (Tanaka et al., 2009). BEN1, together with BEN2/VPS45, functions in early endosomal trafficking, which is required for polar PIN localization (Tanaka et al., 2013). Besides ARF and ROP GTPases, also other small GTPases, such as Rab GTPases, play a role in the regulation of vesicle trafficking and polar PIN localization. BFA-visualized exocytic trafficking defective5 (BEX5)/RabA1b is associated with trafficking and proper PIN polarization. BEX5 is localized to the TGN/EE compartment and is implicated in exocytosis and transcytosis processes of PIN proteins (Feraru et al., 2012). Small GTPases are crucial for many steps in endomembrane vesicle trafficking, such as vesicle formation, movement, tethering and fusion. However, due to the divergence of the GTPases in evolution, they regulate distinct stages in vesicle trafficking and have a different impact on cell polarization processes in plants and animals.

1.4 Phosphorylation

Protein phosphorylation is a posttranslational modification that occurs on serine, threonine or tyrosine residues and that is catalyzed by kinase enzymes. The reverse process of phosphate groups removal is mediated by phosphatases. Besides other roles, the phosphorylation status of proteins in plants and animals serves as an intrinsic cue for polar cargo delivery.

In mammalian cells, phosphorylation plays an important role in polar cargo delivery to the PM. Two main kinases are involved in this process: the serine/threonine kinase LKB1/PAR4 that is activated by the bile acid taurocholate and, in turn, triggers the second AMP-activated protein kinase (AMPK). LKB1 additionally activates 11 AMP-related kinases, including the four mammalian PAR1 paralogs (Lizcano et al., 2004). LKB1 has been described first as a polarity determinant in a genetic screen for mutants defective in cell divisions of early *Caenorhabditis elegans* embryos that were designated *partitioning defective* (*par*) (Kemphues et al., 1988). After fertilization, the first asymmetrical cell division of the zygote is crucial for proper establishment of the polarity axis in the future embryo. In most of the *par* mutants, the first cell division is symmetrical, leading to the synchronous division of the daughter cells, with severe defects in cell specification as a consequence. Each of the six PAR proteins identified so far is distributed in a characteristic manner after the first asymmetric cell division, indicating that their role is crucial for the formation of anterior-posterior cell polarity (Goldstein and Macara, 2007). That PIN protein sorting to the apical or basal domains relies on its phosphorylation status (Dhonukshe et al., 2010; Friml et al., 2004; Huang et al., 2010; Kleine-Vehn et al., 2009; Zhang et al., 2010) could be demonstrated after study of the localization of distinct PIN proteins in the same cell type. In root epidermal cells, the ectopically expressed *PIN1* was located on the basal cell side, in

contrast to the apically localized PIN2, hinting at sequence-based determinants for polar PIN localization (Wisniewska et al., 2006). Sequence analysis and *in vitro* phosphorylation assays revealed that phosphorylation of PIN1 by PINOID (PID) kinase occurs in the central hydrophilic loop (Michniewicz et al., 2007) on several serine residues (Huang et al., 2010; Zhang et al., 2010). An antagonistic function of the serine/threonine PID kinase and Protein Phosphatase 2A (PP2A) in the polar PIN trafficking was demonstrated by a genetic study of *pp2a* and *pid* mutants in embryo and root development. PID phosphorylates PIN proteins to direct them to the apical domain, whereas PP2A counteracts the PID activity and dephosphorylates PIN proteins, targeting them to the basal cell side (Michniewicz et al., 2007). Close analysis of the *pid* mutant phenotype with defective apical polarization revealed that the apical PIN2 localization was intact in root epidermal cells (Sukumar et al., 2009), implying that additional kinases are present that redundantly regulate the phosphorylation status of PIN proteins. WAVY ROOT GROWTH1 (WAG1) and WAG2 kinases that belong to the AGC-3 kinases, phosphorylate PIN proteins, together with PID, predominantly at the PM, where from they are directed to the apical recycling pathway after endocytosis (Dhonukshe et al., 2010). Mutations in *pid*, *wag1* or *wag2* lead to root meristem collapse and agravitropic growth (Dai et al., 2012). Another kinase involved in the phosphorylation of PIN proteins is D6 Protein Kinase (D6PK). D6PK colocalizes with PIN proteins on the basal membrane of the stele, cortex and lateral root cap cells. The *d6pk* mutant was shown to be defective in auxin transport, but its exact role remains unclear (Zourelidou et al., 2009).

PP2A phosphatase with its multiple regulatory (A and B) and catalytic (C) subunits produces various holoenzymes with distinct functions and properties. Analysis of the loss-of-function mutants of three PP2AA isoforms revealed abnormal cotyledon phenotypes and aberrations in early embryo developmental stages (Michniewicz et al., 2007; Zhou et al., 2004) that resembled embryos with defects in auxin transport (Friml et al., 2003) and the *pin1* and *pid* mutant phenotypes, implying a role for the regulatory A subunit in basal PIN localization. Three isoforms of the regulatory A subunit gene family together with the catalytic subunits Phytochrome-associated serine/threonine protein phosphatase1 (FyPP1), its homolog FyPP2, and SAPS DOMAIN-LIKE (SAL) proteins, physically interact to form the PP6 heterotrimeric holoenzyme complex (Dai et al., 2012). Genetic interference in *FyPP* genes by mutations or their dominant-negative versions results in an altered PIN phosphorylation level that causes a basal-to-apical shift of PIN1 in stele cells and of PIN2 in cortex cells (Dai et al., 2012). Recent data also indicated that the catalytic subunits of the PP2A subfamily II, PP2A-C3 and PP2A-C4, redundantly regulate embryo patterning and root development and affect the PIN1 protein polarity (Ballesteros et al., 2013). In plants and animals, the protein phosphorylation status plays a crucial role in their localization to the proper polar PM domains. However different kinases and phosphatases are involved in the

phosphorylation process: the LKB1/PAR4 and AMPK kinases in animal cells and the PID, WAG1, WAG2 and D6PK kinases, together with the PP2A phosphatase and PP6 complex, in plant cells.

1.5 Cytoskeleton involvement in cell polarity

Actin filaments and microtubules are polar polymers oriented along the polarity axis and consist of actin subunits and tubulin heterodimers, respectively. The polarity of cytoskeletal structures results from the unidirectional association of the subunits that can polymerize and depolymerize in a fast manner, depending on changing polarity signals (Li and Gundersen, 2008). Trafficking of vesicles and polar deposition to the PM takes place along the cytoskeleton. The cortical cytoskeleton serves also as a scaffold structure that determines the animal cell shape, whereas the plant cell shape relies on cell wall and turgor pressure. Treatment of actin and microtubules with depolymerizing chemicals revealed that the cytoskeleton targets polarly localized proteins, such as PIN proteins (Kleine-Vehn et al., 2008b).

In epithelial cells, the actin cytoskeleton plays a role in the vesicle assembly at the Golgi and endosomes and in the vesicle transport across the cytoplasm. Actin, together with actin-associated proteins (such as spectrin, ankyrin and myosin), and the actin-regulatory protein CDC42 that is considered a main polarity regulator in most eukaryotes, regulate the vesicle exit from the TGN to the basolateral domain. CDC42 is necessary for the polymerization of actin cables in a polarized orientation and, subsequently, in directional transport. Interruption of the CDC42 function by knockout mutation leads to a reduced transport from the Golgi apparatus to the basolateral domain and an increased trafficking to the apical domain (Müsch et al., 2001). Additionally, actin depolymerization results in transcytosis of the cargo vesicles from the basolateral EEs directly to the apical surface, omitting the REs (Sheff et al., 2002). In many epithelial cells, the microtubular orientation designates the apical-basal cue of the cell: microtubule minus-ends face the apical and plus-ends the basal domain. Microtubules together with microtubule motors, are also involved in the vesicular sorting/transport from the TGN and endosomes to the apical PM (Allan et al., 2002).

The impact of actin on differentially localized PIN proteins in distinct cell types was checked after actin interference with Latrunculin B. The experiment revealed an essential role for the actin filaments in both apical and basal cargo deliveries, but the apical targeting seemed to be more sensitive to actin disintegration (Kleine-Vehn et al., 2008b). Microtubules are essential both in plants and animals during cell division as well as in the interphase to maintain the general cell polarity. Disruption of the microtubule organization interferes not only with the general vesicle trafficking with cellular shape loss as a consequence, but also

specifically with the polar PIN trafficking. After microtubules had been depolymerized with oryzalin, basally localized PIN proteins were mislocalized and shifted preferentially to the apical domain, whereas their apical localization was largely unaffected, indicating that, in contrast to actin filaments, an intact microtubule organization is needed for basal PIN trafficking (Kleine-Vehn et al., 2008b). Additionally, the same cargo can be transported by two different pathways, depending on the cell cycle phase. PIN1 trafficking in the interphase between PM and endosomes depends on actin filaments, whereas delivery to the cell plate during cytokinesis depends on microtubules (Geldner et al., 2001). In summary, both the actin and microtubule cytoskeleton are crucial for establishment and maintenance of cargoes at the polar domains, but further analysis is needed to dissect their role for specific cargos and their regulation.

1.6 Specific non-conserved polarity components: tight junction, Casparian stripes and cell wall

In addition to similar components of the basic cellular machinery and the involvement of the cytoskeleton and clathrin adaptor complexes in the establishment and maintenance of polarity, there are also other structures that are specific only either for animals, such as tight junctions that serve as physical borders between apical and basolateral polar domains, or for plants, such as cell walls. A structure comparable to the tight junctions exists in plants as well, but is present exclusively in the endodermis, namely the Casparian strips that are belts made of specialized cell wall material that acts as an extracellular diffusion barrier (Roppolo et al., 2011).

In polarized epithelial cells, basolateral and apical domains are separated by tight junctions that form a mechanical barrier against diffusion events and regulate paracellular permeability and, as a consequence, they help maintain the unidirectional transport of macromolecules across the epithelial cells. Tight junctions consist of transmembrane and peripheral membrane proteins that interact with the cytoskeleton and form a protein complex involved in polarity and proliferation control through signaling transduction pathways. The tight junctions consist of a few main families of transmembrane proteins: occludin, claudins, E-cadherins, and junctional adhesion molecules (Shin et al., 2006), among which E-cadherin is a crucial protein in cell-cell adhesion and cell polarization and is required for the tight junction orientation and lumen positioning. These proteins also promote basolateral cargo delivery to the cell-cell adhesion sites and lateral membrane domains (Nejsum and Nelson, 2007). Two evolutionarily conserved protein complexes, PAR and Crumbs, take part in the organization of the tight junctions and are involved in polarity establishment and maintenance in epithelial cells. The Crumbs/Proteins Associated with Lin Seven1 (PALS1)/PALS-associated tight junction protein (PATJ) module is linked via PALS to the

PAR3/PAR6/atypical Protein Kinase C (aPKC) module that helps in the establishment of tight junctions and contributes to the formation of the apical domain, whereas the DISCS LARGE (DLG)/Scribble/LETHAL GIANT LARVAE (LGL) module functions at the basolateral domain (St Johnston and Ahringer, 2010).

Until recently, no data had been provided for the connection between polarity maintenance of PIN proteins and the cell wall integrity. Such a link was suggested after the characterization of the *regulator of PIN polarity3* (*repp3*) mutant, which is affected in the ectopically expressed *PIN1* gene. The mutation responsible for the phenotype was localized in the gene coding for the CELLULOSE SYNTHASE CATALYTIC SUBUNIT3/CONSTITUTIVE EXPRESSION OF VEGETATIVE STORAGE PROTEIN1 (VSP1)/ISOXABEN RESISTANT1/ECTOPIC LIGNIN1 (CESA3/CEV1/IXR1/ELI1) (Feraru et al., 2011). CESA3 is part of the cellulose synthase complex that is localized at the PM and is responsible for the synthesis of the β-1,4 glucans, the building blocks for cellulose microfibrils (Desprez et al., 2007). Moreover, chemical disintegration of the cell wall and plasmolysis experiments revealed that proteins localized in the polar domains are attached to the extracellular matrix in a cellulose-dependent manner, preventing lateral protein diffusion (Feraru et al., 2011). The data obtained from the genetic analysis of the *repp3* mutant and a pharmacologic study also indicated that the cell wall is implicated in the process of PIN polarity maintenance (Figure 4) (Feraru et al., 2011).

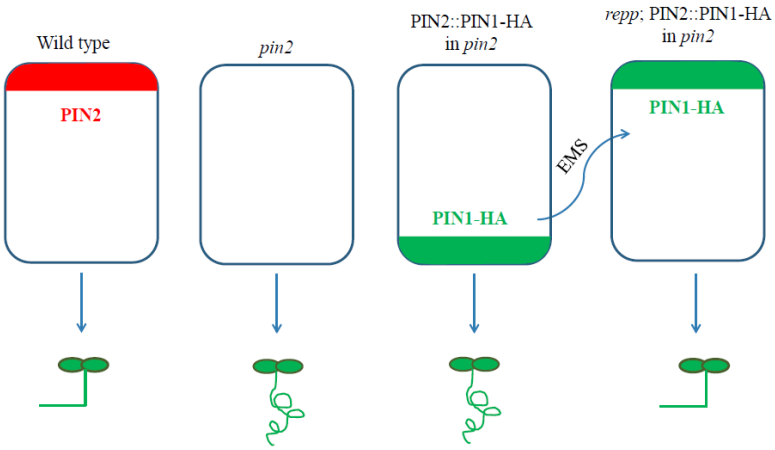

Figure 4. Design of a specific screen for PIN polarity components.
PIN2 proteins localize to the apical side of epidermal cells in the gravitropic wild-type line. In the *pin2* mutant, PIN2 proteins do not occur, provoking the agravitropic phenotype. PIN1-HA is mislocalized in the epidermis to the basal cell side in the PIN2::PIN1-HA;*pin2* line, resulting in an agravitropic phenotype. Mutations in the putative PIN polarity regulators (*repp*) are predicted to restore the apical localization of PIN1 and, hence, the gravitropic phenotype.

2. GENETIC APPROACHES TO DISSECT POLARITY IN PLANTS

To gain more insight into the process of polarity establishment and maintenance, it is important to characterize all proteins involved in these signaling cascades. Different methods

are applied to find novel genes active in this process. One of such methods is the forward genetic screen, in which mutants with the desired phenotypes are mapped to find the causative mutation. In the reverse genetic approach, the gene function and its action in various processes are assigned by analyzing the phenotypic changes after perturbation of the gene activity. Mutagenesis induction in the *Arabidopsis* genome can be achieved by using different biological and chemical agents, of which ethyl methanesulfonate (EMS) causes predominantly single-base pair substitutions.

2.1 Identification of polarity-defective mutants by morphological phenotypes

Several polarity-linked mutants were found in genetic screens based on morphological phenotypes, such as the *gnom* mutant with impaired basal PIN trafficking, the *pid* mutant with affected apical PIN distribution, and the *macchi-bou 4/enhancer of pinoid/naked pins in yuc mutants 1* (*mab4/enp/npy1*) with preserved PIN proteins at the PM in the polar domains. The *gnom* mutant was first discovered in a screen for mutants defective in pattern formation in *Arabidopsis* seedlings (Mayer et al., 1991). The loss-of-function *gnom* mutant displays severe phenotypes, including lack of roots, fused cotyledons, defects in vascular patterning, and defective formation of the embryo axis (Mayer et al., 1993). Further analysis of GNOM function hinted at a role in embryo axis formation (Steinmann et al., 1999) and postembryonic development of *Arabidopsis* (Geldner et al., 2004). All the phenotypes of *gnom* mutants can be mimicked by application of a high dosage of auxin or polar auxin transport inhibitors, demonstrating the connection between GNOM and auxin transport. Further characterization of GNOM revealed that its action mechanism is the regulation of the basal PIN localization and that it is a crucial component in this process.

Another mutant with a key function in the polar PIN localization is *pid* (Christensen et al., 2000) that has been isolated in a screen for mutants defective in inflorescence meristem formation. Besides the defects in floral organ development, the *pid* mutant is also impaired in cotyledon and leaf growth (Bennett et al., 1995). The defective bud formation in the *pid* mutant is similar to the *pin1* phenotype and the phenotype induced by the polar auxin transport inhibitors, indicating that both mutations play a role in the polar auxin transport (Okada et al., 1991). Furthermore, characterization of loss-of-function and gain-of-function PID lines revealed that PID is implicated in the polar PIN localization (Friml et al., 2004).

Genetic analysis of the *laterne* mutant that displays a complete deletion of cotyledons pointed toward two phenotype-causing mutations: one in the *PID* gene and another one in the *MAB4/ENP* gene (Treml et al., 2005). Through a detailed analysis of the *MAB4/ENP* and other members of the *MAB4/ENP* subfamily, its polar localization at the PM and function in retaining of PIN proteins at the PM were validated (Furutani et al., 2007, 2011).

2.2 Fluorescent marker-based forward genetic screen

An EMS-treated population of transgenic *Arabidopsis* plants with the PIN1-GFP marker was used in a forward genetic screen to identify new mutants defective in the accumulation and/or internalization of PIN1::PIN1-GFP into BFA compartments (Tanaka et al., 2009, 2013). Mutants were screened using a fluorescence microscope to identify the desired subcellular phenotype. Three mutants were characterized and designated *ben1*, *ben2* and *ben3* (from BFA visualized endocytic trafficking defective). They were defective in agglomeration of internalized PM proteins, but showed a different sensitivity to the aggregation of endosomes and the Golgi apparatus, hinting at their distinct role in intracellular trafficking. *ben1* has been identified as an ARF-GEF component from the BIG subfamily of early endosomal trafficking AtMIN7/BIG5 with a defect in polar PIN1 localization, whereas *ben2* codes for the SEC1/Munc18 family protein BEN2/VPS45, a universal constituent of membrane fusion in eukaryotic cells (Tanaka et al., 2009, 2013). The BEN2 localization in the early endosomal pathway differs from that of BEN1 and mutation in the *BEN2* gene modify the intracellular trafficking of PIN proteins.

2.3 Reverse genetic screen

Whereas the aim of forward genetics is to find the genetic basis of phenotypic features, reverse genetics looks for phenotypes that result from gene modifications. In reverse genetics, specific genes are disrupted to find their function by comparing the mutated gene phenotypes with the wild-type organisms. Different approaches are used in *A. thaliana* reverse genetics, such as gene silencing with RNAi or artificial microRNAs, which specifically target the gene of interest, or T-DNA and transposon insertional mutagenesis and targeting-induced local lesions in genomes (TILLING), which randomly perturb the gene activity. Recently, new tools for targeted mutagenesis have been introduced in plants which use sequence-specific nucleases, such as zinc finger nucleases (ZFNs), meganucleases, and transcription activator-like effector nucleases (TALENs) (Voytas, 2013). In mammalian cells, the Rab5 protein plays a pivotal role in the internalization of PM-localized proteins. In plants, two genes homologous to Rab5, designated Ara7 and Rha1, are involved in endocytosis as well. Mutations in either gene do not display any phenotype, but the double mutant *ara7rha1* and the knockout mutant of its activator Rab5-GEF AtVPS9a, is embryo lethal. Characterization of the dominant-negative version of Ara7 (*DN-Ara7*), which is an inactive Ara7 form, specified its role in endocytosis and in PIN polarity establishment (Dhonukshe et al., 2008).

Genetic interference with the clathrin heavy chain (CHC) by overexpression of its C-terminal part led to the dominant-negative effect noticeable by impaired PIN internalization and defective plant development and auxin distribution (Dhonukshe et al., 2007; Kitakura et

al., 2011). Further characterization of the loss-of-function *chc* mutant confirmed the previous observation of the involvement of clathrin in endocytosis.

2.4 Specific screens for PIN polarity components

Screening of mutants using the microscope by direct observation of the cellular PIN localization is very laborious and time consuming. To overcome these difficulties, it was necessary to translate the problem of polarity at the cellular level to a macroscopically visible phenotype that would be fast and easy to screen. Examination of the gravitropic response of the mutagenized transgenic PIN2::PIN1-HA line in the *pin2* mutant background provided the solution. In wild-type plants, the apical localization of PIN2 in the root epidermis directs the auxin flow from the root tip to the top parts of the root, enabling root growth toward the gravity vector. In the PIN2::PIN1-HA line, the PIN1 proteins localize predominantly at the basal side of epidermal cells and, thus, do not rescue the agravitropic phenotype of the *pin2* mutant. Weak polarity mutants are mostly defective in PIN1 localization and exhibit a basal-to-apical polarity shift; hence, in polarity-defective mutants, the basal PIN1 proteins in the epidermis were hypothesized to be targeted to the apical domain, as macroscopically observed by the gravitropic growth restoration. Screening for mutants that respond to the gravity vector enabled the identification of the *repp3* mutant as a new candidate for the polar PIN localization (Feraru et al., 2011).

2.5 Chemical genetic screen and chemical biology

Classical genetic approaches have greatly contributed to our understanding of polarity in plants. However, the plant genomes are genetically redundant, meaning that a cellular function can be encoded by more than one gene and, in the case of a mutation, the redundant gene can take over the function of the inactive one. As a result, some genes important for polarity might have been omitted in the classical genetic screens. Another limitation of classical screens is that mutations in genes that are crucial for polarity establishment and maintenance, which are the essential features of all living organisms, might be lethal. Biologically active small molecules can overcome these limitations because they can be applied at different stages of plant development and at different concentrations, with a broad range of phenotypes as a result. Some small molecules can also target one specific protein, whereas others can affect entire protein families when a conserved region is targeted, thereby overcoming gene redundancy. Chemical genetic screens have already been used to dissect chemicals affecting cell wall synthesis (Desprez et al., 2007; Scheible et al., 2001), molecules inhibiting auxin signaling or transport (Armstrong et al., 2004; Rojas-Pierce et al., 2007; Sungur et al., 2007; Surpin et al., 2005), molecules inhibiting brassinosteroids synthesis (Asami et al., 2003), or affecting the endomembrane system (Zouhar et al., 2004). The endosidin1 (ES1) small molecule induced the selective

accumulation of the auxin transporters PIN2 and AUX1 and the brassinosteroid receptor BRI1, but not other PM proteins, such as PIN1 and PIN7, providing a new tool to investigate recycling pathways (Robert et al., 2008). Huge libraries of small molecules have been used in high-throughput screens as a novel tool to dissect the polarity process, although from the very beginning plant polarity research was conducted with small molecules, such as auxin analogs, antagonists, and transport inhibitors. The synthetic auxin naphthalene-1-acetic acid was utilized in a forward genetic screen that helped characterize the *AUXIN RESISTANT1* (*AXR1*) loci involved in the TIR1 and SKP1/CULLIN1/F-BOX PROTEIN (SCR^{TIR1})/AUXIN SIGNALING F BOX (AFB)-based auxin signaling pathway. Other substances, such as BFA or wortmannin are commonly used in plant research to interfere with specific trafficking routes. Wortmannin induces the accumulation of PIN2 on its way to the vacuole by affecting phosphatidylinositol 3-kinase (Jaillais et al., 2006). Other chemicals, such as 1-*N*-naphthylphthalamic acid (NPA) or 2,3,5-triiodobenzoic acid, (TIBA) inhibit the polar auxin transport (Keitt and Baker, 1966) and interfere with the auxin trafficking transporters, the PIN proteins and PGPs, possibly by targeting the actin cytoskeleton (Tanaka et al., 2009), but the exact mechanism has still to be determined.

To assess the mechanism of polar targeting in plants, libraries of small molecules can be screened for modifiers of the PIN polar localization by means of an innovative chemical genomics approach. In a first round, a high-throughput screen was carried out based on the ability of small molecules to inhibit pollen germination in tobacco (*Nicotiana* sp.) or interfere with polarized tube growth. Potential inhibitors of pollen germination were selected and tested on their effect on the polar PIN localization (Drakakaki et al., 2011). By this approach, a set of bioactive chemicals affecting the basal PIN localization or PIN trafficking is selected and characterized. To further identify targets and affected pathways of the small molecules, the genetic resistance or hypersensitivity to the chosen molecule in *Arabidopsis* has to be screened. Although a chemical genetic screen is more laborious than a classical one because even two screens have to be performed – one to find biologically active molecules affecting the desired pathways and another to find the target protein of the chemical – it is nevertheless expected that it will be an instrumental new method to identify novel regulators of polarity in plants.

3. SUMMARY

The generation of polarity involves a complex machinery of interacting factors, including ROP GTPases, the cytoskeleton, vesicular trafficking, mechanical tensions (not described here), the extracellular matrix, and environmental signals. In animal epithelial cells, the main polarization factors are PAR proteins that are involved in the establishment of the antero-posterior axis of the developing embryo. They localize polarly in the cells and mutually

regulate their polarity. Additionally, CDC42 plays a role in polarity establishment by interacting with the PAR6 protein and is implicated in the association of the PAR3/PAR6/aPKC complex with the cell cortex. In plants, ROP GTPases can be considered as main factors responsible for the polarization processes that influence the local polarization of actin and microtubules. ROP GTPases accumulate at the PM landmarks, such as the growing pollen tube tip. The active GTPase sites trigger the local polarization of actin and microtubules that serve as roads along which the vesicles can be transported to the place of destination.

4. ACKNOWLEDGEMENTS

We thank Martine De Cock and Annick Bleys for help in preparing the manuscript.
This work was supported by a grant from the Research Foundation-Flanders (Odysseus).

REFERENCES

Allan, V.J., Thompson, H.M., and McNiven, M.A. (2002). Motoring around the Golgi. Nat. Cell Biol. *4*, E236–E242.

Altschuler, Y., Liu, S., Katz, L., Tang, K., Hardy, S., Brodsky, F., Apodaca, G., and Mostov, K. (1999). ADP-ribosylation factor 6 and endocytosis at the apical surface of Madin-Darby canine kidney cells. J. Cell Biol. *147*, 7–12.

Ang, A.L., Fölsch, H., Koivisto, U.-M., Pypaert, M., and Mellman, I. (2003). The Rab8 GTPase selectively regulates AP-1B-dependent basolateral transport in polarized Madin-Darby canine kidney cells. J. Cell Biol. *163*, 339–350.

Armstrong, J.I., Yuan, S., Dale, J.M., Tanner, V.N., and Theologis, A. (2004). Identification of inhibitors of auxin transcriptional activation by means of chemical genetics in *Arabidopsis*. Proc. Natl. Acad. Sci. U. S. A. *101*, 14978–14983.

Asami, T., Nakano, T., Nakashita, H., Sekimata, K., Shimada, Y., and Yoshida, S. (2003). The Influence of Chemical Genetics on Plant Science: Shedding Light on Functions and Mechanism of Action of Brassinosteroids Using Biosynthesis Inhibitors. J. Plant Growth Regul. *22*, 336–349.

Ballesteros, I., Domínguez, T., Sauer, M., Paredes, P., Duprat, A., Rojo, E., Sanmartín, M., and Sánchez-Serrano, J.J. (2013). Specialized functions of the PP2A subfamily II catalytic subunits PP2A-C3 and PP2A-C4 in the distribution of auxin fluxes and development in *Arabidopsis*. Plant J. Cell Mol. Biol. *73*, 862–872.

Beck, R., Rawet, M., Ravet, M., Wieland, F.T., and Cassel, D. (2009). The COPI system: molecular mechanisms and function. FEBS Lett. *583*, 2701–2709.

Benková, E., Michniewicz, M., Sauer, M., Teichmann, T., Seifertová, D., Jürgens, G., and Friml, J. (2003). Local, efflux-dependent auxin gradients as a common module for plant organ formation. Cell *115*, 591–602.

Bennett, S.R.M., Alvarez, J., Bossinger, G., and Smyth, D.R. (1995). Morphogenesis in pinoid mutants of *Arabidopsis thaliana*. Plant J. *8*, 505–520.

Berleth, T., and Sachs, T. (2001). Plant morphogenesis: long-distance coordination and local patterning. Curr. Opin. Plant Biol. *4*, 57–62.

Blilou, I., Xu, J., Wildwater, M., Willemsen, V., Paponov, I., Friml, J., Heidstra, R., Aida, M., Palme, K., and Scheres, B. (2005). The PIN auxin efflux facilitator network controls growth and patterning in *Arabidopsis* roots. Nature *433*, 39–44.

Bloch, D., and Yalovsky, S. (2013). Cell polarity signaling. Curr. Opin. Plant Biol. *16*, 734–742.

Bonifacino, J.S., and Traub, L.M. (2003). Signals for Sorting of Transmembrane Proteins to Endosomes and Lysosomes *. Annu. Rev. Biochem. *72*, 395–447.

Bonilha, V.L., Marmorstein, A.D., Cohen-Gould, L., and Rodriguez-Boulan, E. (1997). Apical sorting of influenza hemagglutinin by transcytosis in retinal pigment epithelium. J. Cell Sci. *110 (Pt 15)*, 1717–1727.

Bryant, D.M., Datta, A., Rodríguez-Fraticelli, A.E., Peränen, J., Martín-Belmonte, F., and Mostov, K.E. (2010). A molecular network for de novo generation of the apical surface and lumen. Nat. Cell Biol. *12*, 1035–1045.

Chen, C.-L., Gajewski, K.M., Hamaratoglu, F., Bossuyt, W., Sansores-Garcia, L., Tao, C., and Halder, G. (2010). The apical-basal cell polarity determinant Crumbs regulates Hippo signaling in Drosophila. Proc. Natl. Acad. Sci. U. S. A. *107*, 15810–15815.

Chen, R., Hilson, P., Sedbrook, J., Rosen, E., Caspar, T., and Masson, P.H. (1998). The *Arabidopsis thaliana* AGRAVITROPIC 1 gene encodes a component of the polar-auxin-transport efflux carrier. Proc. Natl. Acad. Sci. U. S. A. *95*, 15112–15117.

Chen, X., Irani, N.G., and Friml, J. (2011). Clathrin-mediated endocytosis: the gateway into plant cells. Curr. Opin. Plant Biol. *14*, 674–682.

Chen, X., Naramoto, S., Robert, S., Tejos, R., Löfke, C., Lin, D., Yang, Z., and Friml, J. (2012). ABP1 and ROP6 GTPase signaling regulate clathrin-mediated endocytosis in *Arabidopsis* roots. Curr. Biol. CB *22*, 1326–1332.

Christensen, S.K., Dagenais, N., Chory, J., and Weigel, D. (2000). Regulation of auxin response by the protein kinase PINOID. Cell *100*, 469–478.

Dai, M., Zhang, C., Kania, U., Chen, F., Xue, Q., McCray, T., Li, G., Qin, G., Wakeley, M., Terzaghi, W., et al. (2012). A PP6-type phosphatase holoenzyme directly regulates PIN phosphorylation and auxin efflux in *Arabidopsis*. Plant Cell *24*, 2497–2514.

Deborde, S., Perret, E., Gravotta, D., Deora, A., Salvarezza, S., Schreiner, R., and Rodriguez-Boulan, E. (2008). Clathrin is a key regulator of basolateral polarity. Nature *452*, 719–723.

Desprez, T., Juraniec, M., Crowell, E.F., Jouy, H., Pochylova, Z., Parcy, F., Höfte, H., Gonneau, M., and Vernhettes, S. (2007). Organization of cellulose synthase complexes involved in primary cell wall synthesis in *Arabidopsis thaliana*. Proc. Natl. Acad. Sci. U. S. A. *104*, 15572–15577.

Dettmer, J., Hong-Hermesdorf, A., Stierhof, Y.-D., and Schumacher, K. (2006). Vacuolar H+-ATPase activity is required for endocytic and secretory trafficking in *Arabidopsis*. Plant Cell *18*, 715–730.

Dhonukshe, P., Aniento, F., Hwang, I., Robinson, D.G., Mravec, J., Stierhof, Y.-D., and Friml, J. (2007). Clathrin-mediated constitutive endocytosis of PIN auxin efflux carriers in *Arabidopsis*. Curr. Biol. CB *17*, 520–527.

Dhonukshe, P., Tanaka, H., Goh, T., Ebine, K., Mähönen, A.P., Prasad, K., Blilou, I., Geldner, N., Xu, J., Uemura, T., et al. (2008). Generation of cell polarity in plants links endocytosis, auxin distribution and cell fate decisions. Nature *456*, 962–966.

Dhonukshe, P., Huang, F., Galvan-Ampudia, C.S., Mähönen, A.P., Kleine-Vehn, J., Xu, J., Quint, A., Prasad, K., Friml, J., Scheres, B., et al. (2010). Plasma membrane-bound AGC3 kinases phosphorylate PIN auxin carriers at TPRXS(N/S) motifs to direct apical PIN recycling. Dev. Camb. Engl. *137*, 3245–3255.

Drakakaki, G., Robert, S., Szatmari, A.-M., Brown, M.Q., Nagawa, S., Van Damme, D., Leonard, M., Yang, Z., Girke, T., Schmid, S.L., et al. (2011). Clusters of bioactive compounds target dynamic endomembrane networks in vivo. Proc. Natl. Acad. Sci. U. S. A. *108*, 17850–17855.

Drdová, E.J., Synek, L., Pečenková, T., Hála, M., Kulich, I., Fowler, J.E., Murphy, A.S., and Zárský, V. (2013). The exocyst complex contributes to PIN auxin efflux carrier recycling and polar auxin transport in *Arabidopsis*. Plant J. Cell Mol. Biol. *73*, 709–719.

Fan, L., Hao, H., Xue, Y., Zhang, L., Song, K., Ding, Z., Botella, M.A., Wang, H., and Lin, J. (2013). Dynamic analysis of *Arabidopsis* AP2 σ subunit reveals a key role in clathrin-mediated endocytosis and plant development. Dev. Camb. Engl. *140*, 3826–3837.

Feraru, E., Paciorek, T., Feraru, M.I., Zwiewka, M., De Groodt, R., De Rycke, R., Kleine-Vehn, J., and Friml, J. (2010). The AP-3 β adaptin mediates the biogenesis and function of lytic vacuoles in *Arabidopsis*. Plant Cell *22*, 2812–2824.

Feraru, E., Feraru, M.I., Kleine-Vehn, J., Martinière, A., Mouille, G., Vanneste, S., Vernhettes, S., Runions, J., and Friml, J. (2011). PIN polarity maintenance by the cell wall in *Arabidopsis*. Curr. Biol. CB *21*, 338–343.

Feraru, E., Feraru, M.I., Asaoka, R., Paciorek, T., De Rycke, R., Tanaka, H., Nakano, A., and Friml, J. (2012). BEX5/RabA1b regulates trans-Golgi network-to-plasma membrane protein trafficking in *Arabidopsis*. Plant Cell *24*, 3074–3086.

Fischer, U., Ikeda, Y., Ljung, K., Serralbo, O., Singh, M., Heidstra, R., Palme, K., Scheres, B., and Grebe, M. (2006). Vectorial information for *Arabidopsis* planar polarity is mediated by combined AUX1, EIN2, and GNOM activity. Curr. Biol. CB *16*, 2143–2149.

Friml, J., Wiśniewska, J., Benková, E., Mendgen, K., and Palme, K. (2002a). Lateral relocation of auxin efflux regulator PIN3 mediates tropism in *Arabidopsis*. Nature *415*, 806–809.

Friml, J., Benková, E., Blilou, I., Wisniewska, J., Hamann, T., Ljung, K., Woody, S., Sandberg, G., Scheres, B., Jürgens, G., et al. (2002b). AtPIN4 mediates sink-driven auxin gradients and root patterning in *Arabidopsis*. Cell *108*, 661–673.

Friml, J., Vieten, A., Sauer, M., Weijers, D., Schwarz, H., Hamann, T., Offringa, R., and Jürgens, G. (2003). Efflux-dependent auxin gradients establish the apical-basal axis of *Arabidopsis*. Nature *426*, 147–153.

Friml, J., Yang, X., Michniewicz, M., Weijers, D., Quint, A., Tietz, O., Benjamins, R., Ouwerkerk, P.B.F., Ljung, K., Sandberg, G., et al. (2004). A PINOID-dependent binary switch in apical-basal PIN polar targeting directs auxin efflux. Science *306*, 862–865.

Fuller, S.D., Bravo, R., and Simons, K. (1985). An enzymatic assay reveals that proteins destined for the apical or basolateral domains of an epithelial cell line share the same late Golgi compartments. EMBO J. *4*, 297–307.

Furutani, M., Kajiwara, T., Kato, T., Treml, B.S., Stockum, C., Torres-Ruiz, R.A., and Tasaka, M. (2007). The gene MACCHI-BOU 4/ENHANCER OF PINOID encodes a NPH3-like protein and reveals similarities between organogenesis and phototropism at the molecular level. Dev. Camb. Engl. *134*, 3849–3859.

Furutani, M., Sakamoto, N., Yoshida, S., Kajiwara, T., Robert, H.S., Friml, J., and Tasaka, M. (2011). Polar-localized NPH3-like proteins regulate polarity and endocytosis of PIN-FORMED auxin efflux carriers. Development *138*, 2069–2078.

Geldner, N., Friml, J., Stierhof, Y.D., Jürgens, G., and Palme, K. (2001). Auxin transport inhibitors block PIN1 cycling and vesicle trafficking. Nature *413*, 425–428.

Geldner, N., Anders, N., Wolters, H., Keicher, J., Kornberger, W., Muller, P., Delbarre, A., Ueda, T., Nakano, A., and Jürgens, G. (2003). The *Arabidopsis* GNOM ARF-GEF mediates endosomal recycling, auxin transport, and auxin-dependent plant growth. Cell *112*, 219–230.

Geldner, N., Richter, S., Vieten, A., Marquardt, S., Torres-Ruiz, R.A., Mayer, U., and Jürgens, G. (2004). Partial loss-of-function alleles reveal a role for GNOM in auxin transport-related, post-embryonic development of *Arabidopsis*. Dev. Camb. Engl. *131*, 389–400.

Goldstein, B., and Macara, I.G. (2007). The PAR proteins: fundamental players in animal cell polarization. Dev. Cell *13*, 609–622.

Gonzalez, A., and Rodriguez-Boulan, E. (2009). Clathrin and AP1B: key roles in basolateral trafficking through trans-endosomal routes. FEBS Lett. *583*, 3784–3795.

Gravotta, D., Carvajal-Gonzalez, J.M., Mattera, R., Deborde, S., Banfelder, J.R., Bonifacino, J.S., and Rodriguez-Boulan, E. (2012). The clathrin adaptor AP-1A mediates basolateral polarity. Dev. Cell *22*, 811–823.

Grebe, M., Xu, J., and Scheres, B. (2001). Cell axiality and polarity in plants--adding pieces to the puzzle. Curr. Opin. Plant Biol. *4*, 520–526.

Grosshans, B.L., Ortiz, D., and Novick, P. (2006). Rabs and their effectors: achieving specificity in membrane traffic. Proc. Natl. Acad. Sci. U. S. A. *103*, 11821–11827.

Grunewald, W., and Friml, J. (2010). The march of the PINs: developmental plasticity by dynamic polar targeting in plant cells. EMBO J. *29*, 2700–2714.

Guo, W., Roth, D., Walch-Solimena, C., and Novick, P. (1999). The exocyst is an effector for Sec4p, targeting secretory vesicles to sites of exocytosis. EMBO J. *18*, 1071–1080.

Hála, M., Cole, R., Synek, L., Drdová, E., Pečenková, T., Nordheim, A., Lamkemeyer, T., Madlung, J., Hochholdinger, F., Fowler, J.E., et al. (2008). An Exocyst Complex Functions in Plant Cell Growth in *Arabidopsis* and Tobacco. Plant Cell Online *20*, 1330–1345.

Hazak, O., Bloch, D., Poraty, L., Sternberg, H., Zhang, J., Friml, J., and Yalovsky, S. (2010). A rho scaffold integrates the secretory system with feedback mechanisms in regulation of auxin distribution. PLoS Biol. *8*, e1000282.

Heisler, M.G., Ohno, C., Das, P., Sieber, P., Reddy, G.V., Long, J.A., and Meyerowitz, E.M. (2005). Patterns of auxin transport and gene expression during primordium development revealed by live imaging of the *Arabidopsis* inflorescence meristem. Curr. Biol. CB *15*, 1899–1911.

Huang, F., Zago, M.K., Abas, L., van Marion, A., Galván-Ampudia, C.S., and Offringa, R. (2010). Phosphorylation of conserved PIN motifs directs *Arabidopsis* PIN1 polarity and auxin transport. Plant Cell *22*, 1129–1142.

Humbert, P.O., Dow, L.E., and Russell, S.M. (2006). The Scribble and Par complexes in polarity and migration: friends or foes? Trends Cell Biol. *16*, 622–630.

Hunziker, W., and Fumey, C. (1994). A di-leucine motif mediates endocytosis and basolateral sorting of macrophage IgG Fc receptors in MDCK cells. EMBO J. *13*, 2963–2969.

Jaillais, Y., Fobis-Loisy, I., Miège, C., Rollin, C., and Gaude, T. (2006). AtSNX1 defines an endosome for auxin-carrier trafficking in *Arabidopsis*. Nature *443*, 106–109.

Joberty, G., Petersen, C., Gao, L., and Macara, I.G. (2000). The cell-polarity protein Par6 links Par3 and atypical protein kinase C to Cdc42. Nat. Cell Biol. *2*, 531–539.

Kang, R.S., and Folsch, H. (2009). An old dog learns new tricks: novel functions of the exocyst complex in polarized epithelia in animals. F1000 Biol. Rep. *1*.

Keitt, G.W., and Baker, R.A. (1966). Auxin Activity of Substituted Benzoic Acids and Their Effect on Polar Auxin Transport. Plant Physiol. *41*, 1561–1569.

Kemphues, K.J., Priess, J.R., Morton, D.G., and Cheng, N.S. (1988). Identification of genes required for cytoplasmic localization in early C. elegans embryos. Cell *52*, 311–320.

Ketelaar, T., Galway, M. e., Mulder, B. m., and Emons, A. m. c. (2008). Rates of exocytosis and endocytosis in *Arabidopsis* root hairs and pollen tubes. J. Microsc. *231*, 265–273.

Kim, I., Pan, W., Jones, S.A., Zhang, Y., Zhuang, X., and Wu, D. (2013a). Clathrin and AP2 are required for PtdIns(4,5)P2-mediated formation of LRP6 signalosomes. J. Cell Biol. *200*, 419–428.

Kim, S.Y., Xu, Z.-Y., Song, K., Kim, D.H., Kang, H., Reichardt, I., Sohn, E.J., Friml, J., Juergens, G., and Hwang, I. (2013b). Adaptor protein complex 2-mediated endocytosis is crucial for male reproductive organ development in *Arabidopsis*. Plant Cell *25*, 2970–2985.

Kitakura, S., Vanneste, S., Robert, S., Löfke, C., Teichmann, T., Tanaka, H., and Friml, J. (2011). Clathrin mediates endocytosis and polar distribution of PIN auxin transporters in *Arabidopsis*. Plant Cell *23*, 1920–1931.

Kleine-Vehn, J., and Friml, J. (2008). Polar targeting and endocytic recycling in auxin-dependent plant development. Annu. Rev. Cell Dev. Biol. *24*, 447–473.

Kleine-Vehn, J., Dhonukshe, P., Sauer, M., Brewer, P.B., Wiśniewska, J., Paciorek, T., Benková, E., and Friml, J. (2008a). ARF GEF-dependent transcytosis and polar delivery of PIN auxin carriers in *Arabidopsis*. Curr. Biol. CB *18*, 526–531.

Kleine-Vehn, J., Langowski, L., Wisniewska, J., Dhonukshe, P., Brewer, P.B., and Friml, J. (2008b). Cellular and molecular requirements for polar PIN targeting and transcytosis in plants. Mol. Plant *1*, 1056–1066.

Kleine-Vehn, J., Huang, F., Naramoto, S., Zhang, J., Michniewicz, M., Offringa, R., and Friml, J. (2009). PIN auxin efflux carrier polarity is regulated by PINOID kinase-mediated recruitment into GNOM-independent trafficking in *Arabidopsis*. Plant Cell *21*, 3839–3849.

Kleine-Vehn, J., Ding, Z., Jones, A.R., Tasaka, M., Morita, M.T., and Friml, J. (2010). Gravity-induced PIN transcytosis for polarization of auxin fluxes in gravity-sensing root cells. Proc. Natl. Acad. Sci. U. S. A. *107*, 22344–22349.

Kleine-Vehn, J., Wabnik, K., Martinière, A., Łangowski, Ł., Willig, K., Naramoto, S., Leitner, J., Tanaka, H., Jakobs, S., Robert, S., et al. (2011). Recycling, clustering, and endocytosis jointly maintain PIN auxin carrier polarity at the plasma membrane. Mol. Syst. Biol. *7*, 540.

Leyser, O. (2011). Auxin, self-organisation, and the colonial nature of plants. Curr. Biol. CB *21*, R331–R337.

Li, R., and Gundersen, G.G. (2008). Beyond polymer polarity: how the cytoskeleton builds a polarized cell. Nat. Rev. Mol. Cell Biol. *9*, 860–873.

Lin, D., Edwards, A.S., Fawcett, J.P., Mbamalu, G., Scott, J.D., and Pawson, T. (2000). A mammalian PAR-3-PAR-6 complex implicated in Cdc42/Rac1 and aPKC signalling and cell polarity. Nat. Cell Biol. *2*, 540–547.

Liu, J., and Guo, W. (2012). The exocyst complex in exocytosis and cell migration. Protoplasma *249*, 587–597.

Lizcano, J.M., Göransson, O., Toth, R., Deak, M., Morrice, N.A., Boudeau, J., Hawley, S.A., Udd, L., Mäkelä, T.P., Hardie, D.G., et al. (2004). LKB1 is a master kinase that activates 13 kinases of the AMPK subfamily, including MARK/PAR-1. EMBO J. *23*, 833–843.

Lu, H., and Bilder, D. (2005). Endocytic control of epithelial polarity and proliferation in Drosophila. Nat. Cell Biol. *7*, 1232–1239.

Luschnig, C., Gaxiola, R.A., Grisafi, P., and Fink, G.R. (1998). EIR1, a root-specific protein involved in auxin transport, is required for gravitropism in *Arabidopsis thaliana*. Genes Dev. *12*, 2175–2187.

Matter, K., Hunziker, W., and Mellman, I. (1992). Basolateral sorting of LDL receptor in MDCK cells: the cytoplasmic domain contains two tyrosine-dependent targeting determinants. Cell *71*, 741–753.

Mayer, U., Ruiz, R.A.T., Berleth, T., Miseéra, S., and Juürgens, G. (1991). Mutations affecting body organization in the *Arabidopsis* embryo. Nature *353*, 402–407.

Mayer, U., Buttner, G., and Jurgens, G. (1993). Apical-basal pattern formation in the *Arabidopsis* embryo: studies on the role of the gnom gene. Development *117*, 149–162.

McMahon, H.T., and Boucrot, E. (2011). Molecular mechanism and physiological functions of clathrin-mediated endocytosis. Nat. Rev. Mol. Cell Biol. *12*, 517–533.

Michniewicz, M., Zago, M.K., Abas, L., Weijers, D., Schweighofer, A., Meskiene, I., Heisler, M.G., Ohno, C., Zhang, J., Huang, F., et al. (2007). Antagonistic regulation of PIN phosphorylation by PP2A and PINOID directs auxin flux. Cell *130*, 1044–1056.

Mine, I., Menzel, D., and Okuda, K. (2008). Morphogenesis in giant-celled algae. Int. Rev. Cell Mol. Biol. *266*, 37–83.

Misek, D.E., Bard, E., and Rodriguez-Boulan, E. (1984). Biogenesis of epithelial cell polarity: intracellular sorting and vectorial exocytosis of an apical plasma membrane glycoprotein. Cell *39*, 537–546.

Mostov, K., Su, T., and ter Beest, M. (2003). Polarized epithelial membrane traffic: conservation and plasticity. Nat. Cell Biol. *5*, 287–293.

Mravec, J., Petrášek, J., Li, N., Boeren, S., Karlova, R., Kitakura, S., Pařezová, M., Naramoto, S., Nodzyński, T., Dhonukshe, P., et al. (2011). Cell plate restricted association of DRP1A and PIN proteins is required for cell polarity establishment in *Arabidopsis*. Curr. Biol. CB *21*, 1055–1060.

Müller, A., Guan, C., Gälweiler, L., Tänzler, P., Huijser, P., Marchant, A., Parry, G., Bennett, M., Wisman, E., and Palme, K. (1998). AtPIN2 defines a locus of *Arabidopsis* for root gravitropism control. EMBO J. *17*, 6903–6911.

Müsch, A., Cohen, D., Kreitzer, G., and Rodriguez-Boulan, E. (2001). cdc42 regulates the exit of apical and basolateral proteins from the trans-Golgi network. EMBO J. *20*, 2171–2179.

Nagawa, S., Xu, T., and Yang, Z. (2010). RHO GTPase in plants: Conservation and invention of regulators and effectors. Small GTPases *1*, 78–88.

Naramoto, S., Kleine-Vehn, J., Robert, S., Fujimoto, M., Dainobu, T., Paciorek, T., Ueda, T., Nakano, A., Van Montagu, M.C.E., Fukuda, H., et al. (2010). ADP-ribosylation factor machinery mediates endocytosis in plant cells. Proc. Natl. Acad. Sci. U. S. A. *107*, 21890–21895.

Nejsum, L.N., and Nelson, W.J. (2007). A molecular mechanism directly linking E-cadherin adhesion to initiation of epithelial cell surface polarity. J. Cell Biol. *178*, 323–335.

Nielsen, E., Cheung, A.Y., and Ueda, T. (2008). The Regulatory RAB and ARF GTPases for Vesicular Trafficking. Plant Physiol. *147*, 1516–1526.

Ohno, H., Aguilar, R.C., Yeh, D., Taura, D., Saito, T., and Bonifacino, J.S. (1998). The Medium Subunits of Adaptor Complexes Recognize Distinct but Overlapping Sets of Tyrosine-based Sorting Signals. J. Biol. Chem. *273*, 25915–25921.

Ohno, H., Tomemori, T., Nakatsu, F., Okazaki, Y., Aguilar, R.C., Foelsch, H., Mellman, I., Saito, T., Shirasawa, T., and Bonifacino, J.S. (1999). Mu1B, a novel adaptor medium chain expressed in polarized epithelial cells. FEBS Lett. *449*, 215–220.

Okada, K., Ueda, J., Komaki, M.K., Bell, C.J., and Shimura, Y. (1991). Requirement of the Auxin Polar Transport System in Early Stages of *Arabidopsi*s Floral Bud Formation. Plant Cell *3*, 677–684.

Ory, S., and Gasman, S. (2011). Rho GTPases and exocytosis: what are the molecular links? Semin. Cell Dev. Biol. *22*, 27–32.

Park, M., Song, K., Reichardt, I., Kim, H., Mayer, U., Stierhof, Y.-D., Hwang, I., and Jürgens, G. (2013). *Arabidopsis* μ-adaptin subunit AP1M of adaptor protein complex 1 mediates late secretory and vacuolar traffic and is required for growth. Proc. Natl. Acad. Sci. *110*, 10318–10323.

Paul, M.J., and Frigerio, L. (2007). Coated vesicles in plant cells. Semin. Cell Dev. Biol. *18*, 471–478.

Peer, W.A. (2011). Plasma Membrane Protein Trafficking. In The Plant Plasma Membrane, A.S. Murphy, B. Schulz, and W. Peer, eds. (Springer Berlin Heidelberg), pp. 31–56.

Petrásek, J., Mravec, J., Bouchard, R., Blakeslee, J.J., Abas, M., Seifertová, D., Wisniewska, J., Tadele, Z., Kubes, M., Covanová, M., et al. (2006). PIN proteins perform a rate-limiting function in cellular auxin efflux. Science *312*, 914–918.

Pfeiffer, S., Fuller, S.D., and Simons, K. (1985). Intracellular sorting and basolateral appearance of the G protein of vesicular stomatitis virus in Madin-Darby canine kidney cells. J. Cell Biol. *101*, 470–476.

Popoff, V., Adolf, F., Brügger, B., and Wieland, F. (2011). COPI budding within the Golgi stack. Cold Spring Harb. Perspect. Biol. *3*, a005231.

Rakusová, H., Gallego-Bartolomé, J., Vanstraelen, M., Robert, H.S., Alabadí, D., Blázquez, M.A., Benková, E., and Friml, J. (2011). Polarization of PIN3-dependent auxin transport for hypocotyl gravitropic response in *Arabidopsis thaliana*. Plant J. Cell Mol. Biol. *67*, 817–826.

Reinhardt, D., Pesce, E.-R., Stieger, P., Mandel, T., Baltensperger, K., Bennett, M., Traas, J., Friml, J., and Kuhlemeier, C. (2003). Regulation of phyllotaxis by polar auxin transport. Nature *426*, 255–260.

Ridley, A.J. (2006). Rho GTPases and actin dynamics in membrane protrusions and vesicle trafficking. Trends Cell Biol. *16*, 522–529.

Robert, S., Chary, S.N., Drakakaki, G., Li, S., Yang, Z., Raikhel, N.V., and Hicks, G.R. (2008). Endosidin1 defines a compartment involved in endocytosis of the brassinosteroid receptor BRI1 and the auxin transporters PIN2 and AUX1. Proc. Natl. Acad. Sci. U. S. A. *105*, 8464–8469.

Robinson, D.G., Jiang, L., and Schumacher, K. (2008). The endosomal system of plants: charting new and familiar territories. Plant Physiol. *147*, 1482–1492.

Rojas-Pierce, M., Titapiwatanakun, B., Sohn, E.J., Fang, F., Larive, C.K., Blakeslee, J., Cheng, Y., Cutler, S.R., Cuttler, S., Peer, W.A., et al. (2007). *Arabidopsis* P-glycoprotein19 participates in the inhibition of gravitropism by gravacin. Chem. Biol. *14*, 1366–1376.

Roppolo, D., De Rybel, B., Tendon, V.D., Pfister, A., Alassimone, J., Vermeer, J.E.M., Yamazaki, M., Stierhof, Y.-D., Beeckman, T., and Geldner, N. (2011). A novel protein family mediates Casparian strip formation in the endodermis. Nature *473*, 380–383.

Rubbo, S.D., Irani, N.G., Kim, S.Y., Xu, Z.-Y., Gadeyne, A., Dejonghe, W., Vanhoutte, I., Persiau, G., Eeckhout, D., Simon, S., et al. (2013). The Clathrin Adaptor Complex AP-2 Mediates Endocytosis of BRASSINOSTEROID INSENSITIVE1 in *Arabidopsis*. Plant Cell Online tpc.113.114058.

Sabatini, S., Beis, D., Wolkenfelt, H., Murfett, J., Guilfoyle, T., Malamy, J., Benfey, P., Leyser, O., Bechtold, N., Weisbeek, P., et al. (1999). An auxin-dependent distal organizer of pattern and polarity in the *Arabidopsis* root. Cell *99*, 463–472.

Sato, T., Mushiake, S., Kato, Y., Sato, K., Sato, M., Takeda, N., Ozono, K., Miki, K., Kubo, Y., Tsuji, A., et al. (2007). The Rab8 GTPase regulates apical protein localization in intestinal cells. Nature *448*, 366–369.

Sauer, M., Balla, J., Luschnig, C., Wisniewska, J., Reinöhl, V., Friml, J., and Benková, E. (2006). Canalization of auxin flow by Aux/IAA-ARF-dependent feedback regulation of PIN polarity. Genes Dev. *20*, 2902–2911.

Scarpella, E., Marcos, D., Friml, J., and Berleth, T. (2006). Control of leaf vascular patterning by polar auxin transport. Genes Dev. *20*, 1015–1027.

Scheible, W.-R., Eshed, R., Richmond, T., Delmer, D., and Somerville, C. (2001). Modifications of cellulose synthase confer resistance to isoxaben and thiazolidinone herbicides in *Arabidopsis ixr1* mutants. Proc. Natl. Acad. Sci. *98*, 10079–10084.

Schlereth, A., Möller, B., Liu, W., Kientz, M., Flipse, J., Rademacher, E.H., Schmid, M., Jürgens, G., and Weijers, D. (2010). MONOPTEROS controls embryonic root initiation by regulating a mobile transcription factor. Nature *464*, 913–916.

Schuck, S., Gerl, M.J., Ang, A., Manninen, A., Keller, P., Mellman, I., and Simons, K. (2007). Rab10 is involved in basolateral transport in polarized Madin-Darby canine kidney cells. Traffic Cph. Den. *8*, 47–60.

Sheff, D.R., Kroschewski, R., and Mellman, I. (2002). Actin dependence of polarized receptor recycling in Madin-Darby canine kidney cell endosomes. Mol. Biol. Cell *13*, 262–275.

Shin, K., Fogg, V.C., and Margolis, B. (2006). Tight junctions and cell polarity. Annu. Rev. Cell Dev. Biol. *22*, 207–235.

Simmen, T., Höning, S., Icking, A., Tikkanen, R., and Hunziker, W. (2002). AP-4 binds basolateral signals and participates in basolateral sorting in epithelial MDCK cells. Nat. Cell Biol. *4*, 154–159.

Sorefan, K., Girin, T., Liljegren, S.J., Ljung, K., Robles, P., Galván-Ampudia, C.S., Offringa, R., Friml, J., Yanofsky, M.F., and Østergaard, L. (2009). A regulated auxin minimum is required for seed dispersal in *Arabidopsis*. Nature *459*, 583–586.

Steinmann, T., Geldner, N., Grebe, M., Mangold, S., Jackson, C.L., Paris, S., Gälweiler, L., Palme, K., and Jürgens, G. (1999). Coordinated polar localization of auxin efflux carrier PIN1 by GNOM ARF GEF. Science *286*, 316–318.

St Johnston, D., and Ahringer, J. (2010). Cell polarity in eggs and epithelia: parallels and diversity. Cell *141*, 757–774.

Sukumar, P., Edwards, K.S., Rahman, A., Delong, A., and Muday, G.K. (2009). PINOID kinase regulates root gravitropism through modulation of PIN2-dependent basipetal auxin transport in *Arabidopsis*. Plant Physiol. *150*, 722–735.

Sungur, C., Miller, S., Bergholz, J., Hoye, R.C., Brisbois, R.G., and Overvoorde, P. (2007). The small molecule 2-furylacrylic acid inhibits auxin-mediated responses in *Arabidopsis thaliana*. Plant Cell Physiol. *48*, 1693–1701.

Surpin, M., Rojas-Pierce, M., Carter, C., Hicks, G.R., Vasquez, J., and Raikhel, N.V. (2005). The power of chemical genomics to study the link between endomembrane system components and the gravitropic response. Proc. Natl. Acad. Sci. U. S. A. *102*, 4902–4907.

Swarup, R., Friml, J., Marchant, A., Ljung, K., Sandberg, G., Palme, K., and Bennett, M. (2001). Localization of the auxin permease AUX1 suggests two functionally distinct hormone transport pathways operate in the *Arabidopsis* root apex. Genes Dev. *15*, 2648–2653.

Tanaka, H., Kitakura, S., De Rycke, R., De Groodt, R., and Friml, J. (2009). Fluorescence imaging-based screen identifies ARF GEF component of early endosomal trafficking. Curr. Biol. CB *19*, 391–397.

Tanaka, H., Kitakura, S., Rakusová, H., Uemura, T., Feraru, M.I., De Rycke, R., Robert, S., Kakimoto, T., and Friml, J. (2013). Cell Polarity and Patterning by PIN Trafficking through Early Endosomal Compartments in *Arabidopsis thaliana*. PLoS Genet *9*, e1003540.

Teh, O.-K., and Moore, I. (2007). An ARF-GEF acting at the Golgi and in selective endocytosis in polarized plant cells. Nature *448*, 493–496.

Teh, O.-K., Shimono, Y., Shirakawa, M., Fukao, Y., Tamura, K., Shimada, T., and Hara-Nishimura, I. (2013). The AP-1 μ Adaptin is Required for KNOLLE Localization at the Cell Plate to Mediate Cytokinesis in *Arabidopsis*. Plant Cell Physiol. *54*, 838–847.

Tepass, U., Tanentzapf, G., Ward, R., and Fehon, R. (2001). Epithelial cell polarity and cell junctions in Drosophila. Annu. Rev. Genet. *35*, 747–784.

Terasaka, K., Blakeslee, J.J., Titapiwatanakun, B., Peer, W.A., Bandyopadhyay, A., Makam, S.N., Lee, O.R., Richards, E.L., Murphy, A.S., Sato, F., et al. (2005). PGP4, an ATP binding cassette P-glycoprotein, catalyzes auxin transport in *Arabidopsis thaliana* roots. Plant Cell *17*, 2922–2939.

Treml, B.S., Winderl, S., Radykewicz, R., Herz, M., Schweizer, G., Hutzler, P., Glawischnig, E., and Ruiz, R.A.T. (2005). The gene ENHANCER OF PINOID controls cotyledon development in the *Arabidopsis* embryo. Dev. Camb. Engl. *132*, 4063–4074.

Treyer, A., and Müsch, A. (2013). Hepatocyte polarity. Compr. Physiol. *3*, 243–287.

Utsuno, K., Shikanai, T., Yamada, Y., and Hashimoto, T. (1998). Agr, an Agravitropic locus of *Arabidopsis thaliana*, encodes a novel membrane-protein family member. Plant Cell Physiol. *39*, 1111–1118.

Vieten, A., Sauer, M., Brewer, P.B., and Friml, J. (2007). Molecular and cellular aspects of auxin-transport-mediated development. Trends Plant Sci. *12*, 160–168.

Viotti, C., Bubeck, J., Stierhof, Y.-D., Krebs, M., Langhans, M., van den Berg, W., van Dongen, W., Richter, S., Geldner, N., Takano, J., et al. (2010). Endocytic and secretory traffic in *Arabidopsis* merge in the trans-Golgi network/early endosome, an independent and highly dynamic organelle. Plant Cell *22*, 1344–1357.

Voytas, D.F. (2013). Plant Genome Engineering with Sequence-Specific Nucleases. Annu. Rev. Plant Biol. *64*, 327–350.

Wang, J.-G., Li, S., Zhao, X.-Y., Zhou, L.-Z., Huang, G.-Q., Feng, C., and Zhang, Y. (2013). HAPLESS13, the *Arabidopsis* μ1 Adaptin, Is Essential for Protein Sorting at the trans-Golgi Network/Early Endosome. Plant Physiol. *162*, 1897–1910.

Wang, X., Kumar, R., Navarre, J., Casanova, J.E., and Goldenring, J.R. (2000). Regulation of vesicle trafficking in madin-darby canine kidney cells by Rab11a and Rab25. J. Biol. Chem. *275*, 29138–29146.

Wedlich-Soldner, R., Altschuler, S., Wu, L., and Li, R. (2003). Spontaneous cell polarization through actomyosin-based delivery of the Cdc42 GTPase. Science *299*, 1231–1235.

Wehrle-Haller, B., and Imhof, B.A. (2001). Stem cell factor presentation to c-Kit. Identification of a basolateral targeting domain. J. Biol. Chem. *276*, 12667–12674.

Wells, C.D., Fawcett, J.P., Traweger, A., Yamanaka, Y., Goudreault, M., Elder, K., Kulkarni, S., Gish, G., Virag, C., Lim, C., et al. (2006). A Rich1/Amot complex regulates the Cdc42 GTPase and apical-polarity proteins in epithelial cells. Cell *125*, 535–548.

Wiśniewska, J., Xu, J., Seifertová, D., Brewer, P.B., Ruzicka, K., Blilou, I., Rouquié, D., Benková, E., Scheres, B., and Friml, J. (2006). Polar PIN localization directs auxin flow in plants. Science *312*, 883.

Xu, J., and Scheres, B. (2005). Dissection of *Arabidopsis* ADP-RIBOSYLATION FACTOR 1 function in epidermal cell polarity. Plant Cell *17*, 525–536.

Xu, T., Dai, N., Chen, J., Nagawa, S., Cao, M., Li, H., Zhou, Z., Chen, X., Rycke, R.D., Rakusová, H., et al. (2014). Cell Surface ABP1-TMK Auxin-Sensing Complex Activates ROP GTPase Signaling. Science *343*, 1025–1028.

Yang, Z., and Lavagi, I. (2012). Spatial control of plasma membrane domains: ROP GTPase-based symmetry breaking. Curr. Opin. Plant Biol. *15*, 601–607.

Zádníková, P., Petrásek, J., Marhavy, P., Raz, V., Vandenbussche, F., Ding, Z., Schwarzerová, K., Morita, M.T., Tasaka, M., Hejátko, J., et al. (2010). Role of PIN-mediated auxin efflux in apical hook development of *Arabidopsis thaliana*. Dev. Camb. Engl. *137*, 607–617.

Zazímalová, E., Murphy, A.S., Yang, H., Hoyerová, K., and Hosek, P. (2010). Auxin transporters--why so many? Cold Spring Harb. Perspect. Biol. *2*, a001552.

Zhang, J., Nodzynski, T., Pencík, A., Rolcík, J., and Friml, J. (2010). PIN phosphorylation is sufficient to mediate PIN polarity and direct auxin transport. Proc. Natl. Acad. Sci. U. S. A. *107*, 918–922.

Zhou, H.-W., Nussbaumer, C., Chao, Y., and DeLong, A. (2004). Disparate roles for the regulatory A subunit isoforms in *Arabidopsis* protein phosphatase 2A. Plant Cell *16*, 709–722.

Zouhar, J., Hicks, G.R., and Raikhel, N.V. (2004). Sorting inhibitors (Sortins): Chemical compounds to study vacuolar sorting in *Arabidopsis*. Proc. Natl. Acad. Sci. U. S. A. *101*, 9497–9501.

Zourelidou, M., Müller, I., Willige, B.C., Nill, C., Jikumaru, Y., Li, H., and Schwechheimer, C. (2009). The polarly localized D6 PROTEIN KINASE is required for efficient auxin transport in *Arabidopsis thaliana*. Dev. Camb. Engl. *136*, 627–636.

Zwiewka, M., Feraru, E., Möller, B., Hwang, I., Feraru, M.I., Kleine-Vehn, J., Weijers, D., and Friml, J. (2011). The AP-3 adaptor complex is required for vacuolar function in *Arabidopsis*. Cell Res. *21*, 1711–1722.

Chapter 2

Endosidin 4 inhibits SEC7 domain-mediated ARF1 activation and interferes with subcellular trafficking and basal PIN polarity in *Arabidopsis thaliana*

Urszula Kania,[a,b] Stéphanie Robert,[b,c] Riet De Rycke,[b] Peter Grones,[a,b,c] Glenn R. Hicks,[d] and Jiří Friml[a]

[a]Institute of Science and Technology Austria, 3400 Klosterneuburg, Austria
[b]Department of Plant Systems Biology, VIB and Department of Plant Biotechnology and Bioinformatics, Ghent University, 9052 Gent, Belgium
[c]Umeå Plant Science Centre (UPSC), Department of Forest Genetics and Plant Physiology, Swedish University of Agricultural Sciences, 90183 Umeå, Sweden
[d]Center for Plant Cell Biology and Department of Botany and Plant Sciences, University of California, Riverside, CA 92521, USA

ABSTRACT

Subcellular cargo trafficking in plant cells is tightly regulated by the vesicle budding machinery mediated by the ADP-ribosylation factor guanine nucleotide exchange factors (ARF GEFs). ARF GEFs have been shown to play crucial roles in a multitude of processes, including endocytosis, vacuolar trafficking, recycling, secretion, and polar trafficking, illustrating the pronounced developmental importance of this gene family. Here, we identified a small molecule endosidin 4 (ES4) from a chemical genomic screen as a compound affecting the basal polar localization of the PIN-FORMED1 auxin transporter. ES4 acts additively with the ARF GEF inhibitor brefeldin A and has a broad spectrum of effects on intracellular trafficking, including endocytosis, exocytosis, and vacuolar targeting. Genetic analysis revealed that mutants defective in ARF GEFs were the most sensitive to ES4. Additionally, in a forward genetic screen for mutants resistant to ES4, we identified a mutant encoding the ARF GEF-regulated δ subunit of coat protein I (COPI) vesicles. ES4 interfered with the localization of the ARF1 GTPases, but not of their mutant variants activated independently of ARF GEFs. Screening of yeast trafficking mutant strains confirmed the SEC7 domain-containing ARF GEFs as targets of the ES4 action. These observations collectively identified ES4 as a previously unknown chemical tool that interferes with ARF GEF-mediated processes, also acting on brefeldin A-resistant ARF GEFs.

AUTHOR CONTRIBUTIONS

U.K., S.R., G.R.H, and J.F. conceived the project. R.D.R. conducted TEM experiments. U.K. and P.G. conducted root growth experiments. U.K. performed the majority of the experiments and analyzed the data. U.K. wrote the article J.F., S.R., G.R.H. revised and corrected the manuscript. All authors revised the article.

INTRODUCTION

In plants, polarity at the cellular and tissue level is manifested and linked by the directional transport of the plant signaling molecule auxin, which mediates various developmental responses (Grunewald and Friml, 2010). The polar localization of PIN-FORMED (PIN) auxin transporters on the plasma membrane (PM) determines the directionality of auxin transport, contributes to the establishment of a differential auxin distribution within tissues, and coordinates tissue polarization (Petrášek et al., 2006; Wiśniewska et al., 2006). The PM-localized PIN proteins (PIN1, PIN2, PIN3, PIN4, and PIN7) are located at different cell sides, depending on PIN identity, cell type, and developmental context (Kleine-Vehn and Friml, 2008). PIN polarity establishment is regulated by many factors, including phosphorylation, cell wall and PM sterol composition, feedback of auxin and other hormones, and intracellular vesicle trafficking, including secretion, endocytosis, and degradation (Grunewald and Friml, 2010).

To maintain their polar distribution, PIN proteins undergo constant cycles of endocytosis and recycling between PM and endosomes. Recycling of PIN proteins to the basal side is predominantly regulated by the ADP-ribosylation factor guanine nucleotide exchange factor (ARF GEF) GNOM (Geldner et al., 2003). PIN protein cycling can be visualized by application of brefeldin A (BFA), an inhibitor of some ARF GEFs, including GNOM, that impedes PIN1 exocytosis and results in its accumulation intracellularly in BFA compartments (Geldner et al., 2001). Inhibition of PIN recycling by BFA or in *gnom* mutants results in polarity loss and, after prolonged treatments, induces transcytosis of PIN proteins from the basal to the apical cell side (Kleine-Vehn et al., 2008a). Also in the *gnom*^{R5} mutant, a basal-to-lateral shift of PIN1 was observed that is reminiscent to that induced by BFA treatment (Kleine-Vehn et al., 2008b). Another ARF GEF involved in retrograde trafficking of the endoplasmic reticulum (ER)-localized cargos from the Golgi apparatus to the ER is the BFA-resistant GNOM-LIKE 1 (GNL1) (Richter et al., 2007; Teh and Moore, 2007). GNOM and GNL1 display distinct, but overlapping, functions in intracellular trafficking (Richter et al., 2007; Doyle et al., 2015). They work together at the Golgi, regulating retrograde coat protein I (COPI)-dependent vesicle transport from the Golgi to the ER (Richter et al., 2007). Additionally, they are involved in selective endocytosis (Teh and Moore, 2007; Naramoto et al., 2010), but only GNOM is implicated in protein recycling. Another ARF GEF, BFA-VISUALIZED ENDOCYTIC TRAFFICKING DEFECTIVE1 (BEN1), mediates early endosomal trafficking (Tanaka et al., 2009, 2014). The *ben1* mutant is defective in polarity, BFA sensitivity, and growth. The functionally redundant ARF GEFs, BIG1, BIG2, BIG3, and BIG4, mediate the late secretory pathway and transport newly synthesized and recycled proteins to the cell division plane during cytokinesis (Richter et al., 2014).

Other proteins involved in vesicle transport and PIN polar trafficking are ARF GTPases, the direct targets of ARF GEFs. ARF proteins cycle constantly between their active GTP-bound and inactive GDP-bound states. Inactive ARF GDPs localize to the cytosol. Following activation to the GTP-bound state, ARFs bind to the membranes where they are responsible for recruiting cytosolic coat proteins (COPI, COPII, and clathrin) to the specific sites of vesicle budding at the Golgi apparatus, *trans*-Golgi network (TGN), and endosomal compartments (Serafini et al., 1991: Bonifacino and Lippincott-Schwartz, 2003). ARF1 was shown to be involved in retrograde trafficking from the Golgi apparatus to the ER and from the TGN to the endosome (Dascher and Balch, 1994; Ooi et al., 1998; Goldberg, 1999; Poon et al., 1999; Jackson and Casanova, 2000), regulating the sequence-specific vacuolar sorting route to the lytic vacuoles (Pimpl et al., 2003) and dynamin-independent endocytosis (Kumari and Mayor, 2008). In plants, ARF1 localizes to the TGN and Golgi stacks (Robinson et al., 2011), is implicated in ER-to-Golgi and cargo-dependent Golgi-to-PM transport (Lee et al., 2002; Takeuchi et al., 2002), and is involved in epidermal PIN2 cell polarity (Xu and Scheres, 2005) and PIN recycling to the PM (Tanaka et al., 2014).

Forward genetic methods had been used to identify mutants defective in PIN localization or trafficking (Feraru et al., 2011; Tanaka et al., 2009, 2013; Zwiewka and Friml, 2012), but genetic approaches are insufficient to study complexity of the dynamic vesicular trafficking due to gene lethality and redundancy. One approach that can overcome these problems and assess the polar targeting mechanism in plants is chemical genomics. Small molecules can interfere with intracellular trafficking in a dose-dependent manner, resulting in severe phenotypes. Recently, chemical libraries were screened on free-living tobacco (*Nicotiana tabacum*) pollen to select small molecules that interfered with the endomembrane trafficking system. Out of 46,418 tested chemicals, 360 were selected as inhibitors of pollen germination and growth (Robert et al., 2008; Drakakaki et al., 2011). Further analysis with different marker lines helped to cluster the chemicals based on the intracellularly induced phenotypes (Drakakaki et al., 2011). One of the clusters consisted of molecules affecting the polar localization of PIN1 proteins in *PIN2:PIN1-GFP;pin2*, but not in the wild-type *PIN2:PIN2-GFP* (Drakakaki et al., 2011). From this set of molecules, we selected the basal PIN polarity-influencing endosidin 4 (ES4). Characterization of its morphological and intracellular effects revealed that ES4 inhibits ARF1/ARF GEF-dependent pathways. Additionally, from an ethyl methanesulfonate (EMS) screen, we identified an ES4-resistant mutant with a mutation in a δ-COPI subunit. Characterization of ES4 can contribute to our understanding of the connectivity between vesicular trafficking and control of polarized growth in plants.

RESULTS

Identification of the ES4 compound Affecting PIN1 Polarity in the *PIN2:PIN1-HA;pin2* Line

In wild-type plants, PIN2 localizes to the apical side of epidermal cells, directing auxin from the root tip toward the upper parts of the root. PIN2-mediated auxin transport is required for asymmetric auxin translocation following gravistimulation and, thus, for root growth toward the gravity vector (Müller et al., 1998; Abas et al., 2006; Baster et al., 2013). In the *PIN2:PIN1-HA;pin2* line, the absence of PIN2 results in agravitropic root growth. The ectopic localization of PIN1 (normally localized on the basal side of stele cells) in basal or both apical and basal sides of epidermal cells does not rescue the agravitropic *pin2* phenotype in this line (Wiśniewska et al., 2006). We reasoned that PIN1 apicalization would facilitate the auxin flow and result in gravity rescue. From clusters of chemicals able to apicalize PIN1 proteins in epidermal cells of the *PIN2:PIN1-GFP;pin2* line (Drakakaki et al., 2011) we analyzed a set of 11 molecules in term of their effect on the PIN1 localization and gravity response restoration. Three-day-old seedlings were grown on medium supplemented with chemicals for another 2 days. The PIN1-HA localization was verified by immunolocalization with anti-HA antibodies (Supplemental Figure 1A). Plants sense the gravity vector and modulate their growth accordingly. Turning a plate with vertically grown seedlings by 90° (gravistimulation) allowed us to analyze gravitropic responses of roots. The effect of chemicals on the gravity response was tested by gravistimulation of seedlings grown on medium supplemented with chemicals (Supplemental Figure 1B). Among the tested molecules, besides ES6, which is the subject of other studies, ES4 (Figure 1A) displayed the strongest effect in increasing apical localization of PIN1 and rescuing gravitropic defect and was therefore selected for further analysis. ES4 increased prominently the number of epidermal cells with apically localized PIN1 (Figures 1B to 1D) and partially rescued the response to gravitropic stimuli (Figures 1E to 1G) of *PIN2:PIN1-HA;pin2*. The impact of ES4 on the polar localization of PIN1 and PIN2 was also investigated in wild-type plants. Prominent changes in polar localization were observed only for ectopically expressed *PIN1* in *PIN2:PIN1-HA;pin2*, but not for natively expressed *PIN2* in wild-type plants, which localized at the apical side of epidermal cells (Supplemental Figures 2A and 2B). The weak polarity mutants have a preferentially disrupted basal polar localization, leading to the basal-to-apical switch in the PIN localization (Kleine-Vehn et al., 2008b), pointing to a more robust control of the apical than of the basal polar proteins. We examined the effect of ES4 on native basally localized PIN1 and PIN2 in stele and cortex, respectively. In the cortex, a dual expression of *PIN2* occurs: in the young cortex cells, PIN2 localizes on the basal cell side, whereas in the older

cells, away from the root tip, the PIN2 polarity switches its localization to the apical cell side (Kleine-Vehn et al., 2008b).

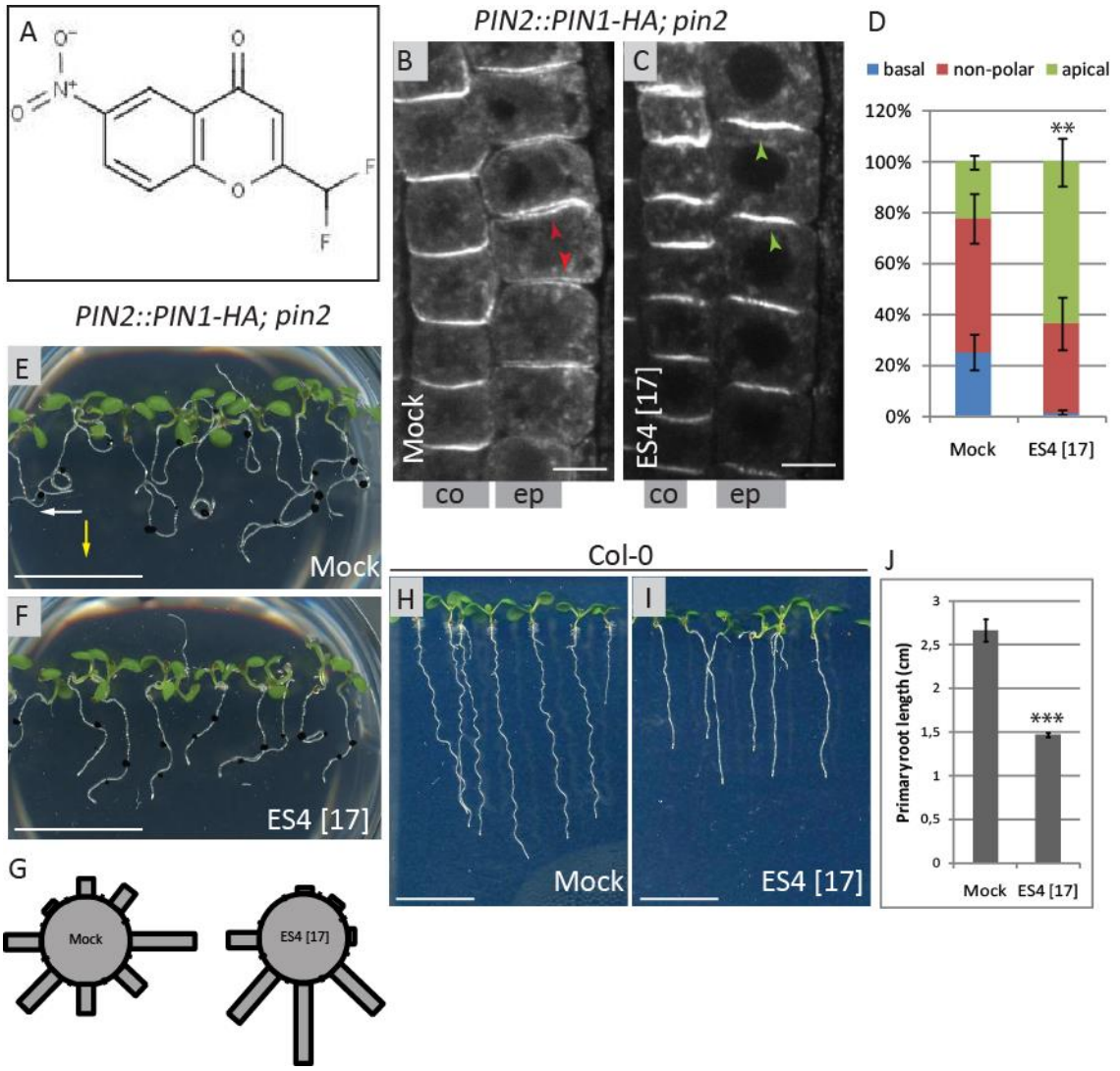

Figure 1. Identification of the ES4 compound.
(A) Chemical structure of ES4.
(B) to **(D)** Immunolocalization of PIN1-HA in epidermal (ep) and cortex (co) cells. After mock treatment **(B),** *PIN2:PIN1-HA;pin2* shows a predominantly basal and nonpolar PIN1-HA localization (red arrowheads), whereas after ES4 treatment (17 µM; 48 h), the localization of PIN1-HA is predominantly apical in epidermal cells (green arrowheads) **(C)**. Evaluation of PIN1-HA localization in epidermal cells **(D)** indicates that after ES4 treatment, 63% of the *PIN2:PIN1-HA;pin2* epidermal cells display a predominantly PIN2-like localization of PIN1-HA at the apical side, contrasting to mock-treated *PIN2:PIN1-HA;pin2* that has a predominantly nonpolar and basal PIN1-HA localization. In three independent experiments, 308 and 325 epidermal cells were analyzed in total for the mock and ES4 treatments, respectively. Data are means ± standard error (SE) of three experiments. Student's *t* test, ***P* < 0.01. Bars = 10 µm.
(E) to **(G)** Response of 48 h gravistimulated 7-day-old seedlings and quantification of the root gravitropic response. The white and yellow arrows mark gravity vectors after the first and second gravistimulation, respectively. The black dots on the roots represent the localization of the root tips at the time of the plate turning. In contrast to mock **(E)**, *PIN2::PIN1-HA;pin2* grown on 17 µM ES4 **(F)** shows a positive gravitropic response. Gravistimulated roots were assigned to one of the eight 45° sectors on a gravitropism diagram **(G)**. The length of the

bars in the diagram represents the percentage of seedlings assigned to the respective sector. In four independent experiments, at least 41 roots were analyzed for each treatment in total. Bars = 1 cm.
(H) to **(J)** Root length sensitivity to ES4 and quantification. Seven-day-old Col-0 seedlings grown on media supplemented with 17 µM of ES4 had shorter primary root length **(I)** than the mock control **(H)**. In three independent experiments, at least 48 roots were analyzed for each treatment in total **(J)**. Data are means ± SE of three experiments. Error bars represent SE. Student's *t* test, ***$P < 0.001$. Bars = 1 cm.

After ES4 treatment, both PIN1 and PIN2 signals became weaker. However, neither the PIN1 basal localization in the stele of wild-type plants, nor the PIN2 basal localization in young cortex cells was affected (Supplemental Figures 2A to 2E). Accordingly, ES4 did not affect the normal gravitropic response of gravistimulated Col-0 wild-type roots (Supplemental Figures 2F to 2H). Next, we checked the phenotypic effects of ES4 on primary root growth, hypocotyl growth, and lateral root density of the Col-0 wild-type. At the concentration of 17 µM, the primary root length was nearly reduced by 50% (Figures 1H to 1J), the hypocotyl length of dark-grown *Arabidopsis* seedlings by 25% (Supplemental Figures 2I to 2K), cotyledons of dark-grown seedlings were open without apical hook (Supplemental Figures 2I to 2K, insets), and lateral root density decreased (Supplemental Figure 2L). To test whether ES4 influenced auxin accumulation, we used the auxin-responsive promoter *DR5:GUS*. Treatment for 48 h at a 17 µM concentration had no visible effect when compared to the control (Supplemental Figures 2M and 2N).

ES4 Affects Endocytic Trafficking and Multiple Intracellular Compartments

PM-localized PIN1 proteins undergo constitutive cycling between PM and endosomes (Geldner et al., 2001). In the presence of the recycling inhibitor BFA, internalized PIN1 proteins accumulate in BFA-induced intracellular agglomerations, called BFA bodies (Geldner et al., 2001). In comparison to mock treatment, ES4 decreased the number of PIN1-labeled BFA bodies depending on the concentration, even by 93% at 83 µM (Figures 2A to 2C; Supplemental Figures 3A to 3D). The observed effect was not specific for the polar PIN1, but was also visible for the apolarly localized PM marker PIP2-GFP. After treatment with 17 µM ES4, the number of PIP2-labeled BFA bodies significantly decreased (Supplemental Figures 3E to 3G), whereas the number of PIN1-labeled BFA bodies was only slightly reduced at the same concentration, possibly suggesting that PIP2 is more sensitive to ES4 than PIN1. To test whether the reduced number of BFA bodies after ES4 treatment resulted from inhibited endocytosis by ES4, we examined the uptake of the endocytosis tracer FM4-64 (Ueda et al., 2001). At 17 µM ES4, the internalization of FM4-64 was not affected, but the morphology of the endosomes differed (Supplemental Figures 3H to 3J). At higher concentration (83 µM), the uptake of FM4-64 was reduced, hinting at endocytosis inhibition by ES4 (Figures 2D to 2F).

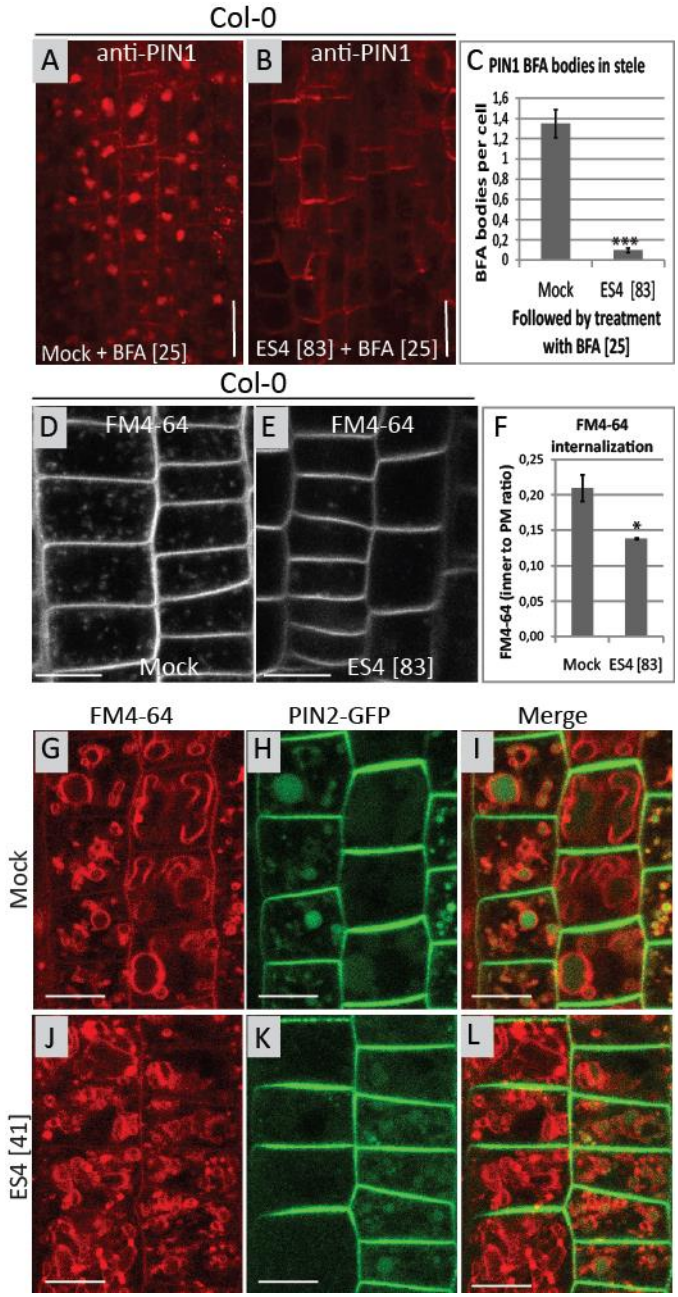

Figure 2. Effect of ES4 on intracellular trafficking.

(A) to **(C)** Immunolocalization of PIN1 (red signal) in Col-0 stele cells and mean number of BFA bodies per cell. Five-day-old seedlings were pretreated for 30 min with mock or 83 µM ES4 before 25 µM BFA was added for an additional 90 min. Compared to mock **(A)**, almost no BFA bodies were visible after ES4 **(B)**. The number of BFA bodies in the stele was counted for 10 cells in each root. In four independent experiments, 41 roots were analyzed for each treatment in total. Data are means ± SE of four experiments. Mann-Whitney *U* test, ***$P < 0.001$. Bars = 10 µm.

(D) to **(F)** Uptake of endocytic tracer dye FM4-64 (2 µM) after 10 min. Five-day-old Col-0 seedlings were pretreated for 2 h with mock **(D)** or 83 µM ES4 **(E)**. Decreased uptake of FM4-64 in epidermal cells was observed after ES4 treatment **(E)** compared with the mock **(D)**. FM4-64 uptake was quantified by dividing the mean grey value of the fluorescent signal inside the cell to the adjacent PM signal **(F)**. In three independent experiments, at least 21 roots were analyzed for each treatment in total. Data are means ± SE of three experiments. Student's *t* test, *$P < 0.05$. Bars = 10 µm.

(G) to **(L)** Intracellular localization of PIN2-GFP pretreated for 2 h with mock (**[G]** to **[I]**) or 41 µM ES4 (**[J]** to **[L]**) and stained with 8 µM of FM4-64 followed by a 4 h treatment in the dark on the growth medium supplemented with mock or ES4, respectively. After the ES4 treatment, aberrant vacuolar targeting of FM4-64 was observed with decreased labeling of the tonoplast and intracellular agglomerations of the signal after ES4 **(J),** whereas in the control, a clear tonoplast labeling was visible **(G)**. The vacuolar accumulation of PIN2-GFP after ES4 [**(K)** and **(L)**] decreased when compared to the control [**(H)** and **(I)**]. Bars = 10 µm.

Additionally, the ES4 effect on exocytosis was tested by BFA washout in the presence of ES4. Washing removes the BFA inhibitory effect on exocytosis, restores vesicle trafficking to the PM and results in disappearance of BFA bodies (Geldner et al., 2001). After treatment with 25 µM BFA followed by washout with 41 µM ES4, the number of BFA bodies was slightly higher than that of the washout with mock medium, indicating a mild effect of ES4 on exocytic trafficking (Supplemental Figure 3K to 3N). Recycling of PIN1 to the PM is inhibited by 25 µM BFA, whereas 50 µM BFA additionally inhibits the degradation pathway to the vacuoles, resulting in formation of enlarged BFA bodies (Kleine-Vehn et al., 2008c). Washout of 50 µM BFA with ES4 increased the number of BFA bodies when compared to the mock washout (Supplemental Figures 3O to 3R). This observation suggests that ES4, besides its effect on recycling, affects also the vacuolar trafficking pathway. Therefore, we examined the localization of FM4-64 and PIN2-GFP after treatment in the dark, knowing that dark treatment stabilizes GFP proteins in the lytic vacuoles (Tamura et al., 2003). After FM4-64 uptake, followed by 4 h of mock treatment in the dark, the FM4-64 dye reached almost completely the tonoplast and the PIN2-GFP signal was detected in the vacuoles, whereas after ES4 treatment at 41 µM, the morphology of tonoplasts was changed when compared to the control. Vacuoles appeared more fragmented, tonoplast labeling was less pronounced, the PIN2-GFP signal was less visible at the PM and small agglomerates of the FM4-64 signal, not present in the mock treatment, occurred (Figures 2G to 2L). Additionally, the vacuolar PIN2-GFP signal was less abundant after ES4, although the ratio of intracellular PIN2-GFP signal versus the PM signal was comparable with that of the control, indicating that PIN2 was internalized from the PM, but was affected in reaching the vacuole (Supplemental Figure 3S). Furthermore, analysis of the ultrastructure by electron microscopy after ES4 treatment revealed enlarged and a slightly increased number of prevacuolar compartment/multivesicular bodies (PVC/MVBs) per cell (Figures 3A to 3D). Transport to the lytic vacuoles in *Arabidopsis* is mediated by MVBs that mature from the TGN/early endosome (EE) (Scheuring et al., 2011). Enlarged MVBs, together with the altered FM4-64 staining of tonoplasts, indicate that ES4 affects the vacuolar trafficking pathway. To better examine the ES4 impact on intracellular compartments, we tested different marker lines: *BRASSINOSTEROID INSENSITIVE 1 (BRI1)-GFP* (PM and endosomes), *CLATHRIN LIGHT CHAIN 2 (CLC2)-GFP* (PM and TGN), *GNL1-yellow fluorescent protein* (*YFP*) (Golgi and

TGN/EE), *GNOM-GFP*, *SIALYLTRANSFERASE (N-ST)-GFP* (Golgi) and *VACUOLAR H^+-ATPase SUBUNIT A1 (VHAa1)-GFP* (TGN/EE) (Figures 3E to 3L; Supplemental Figures 3T to 3W).

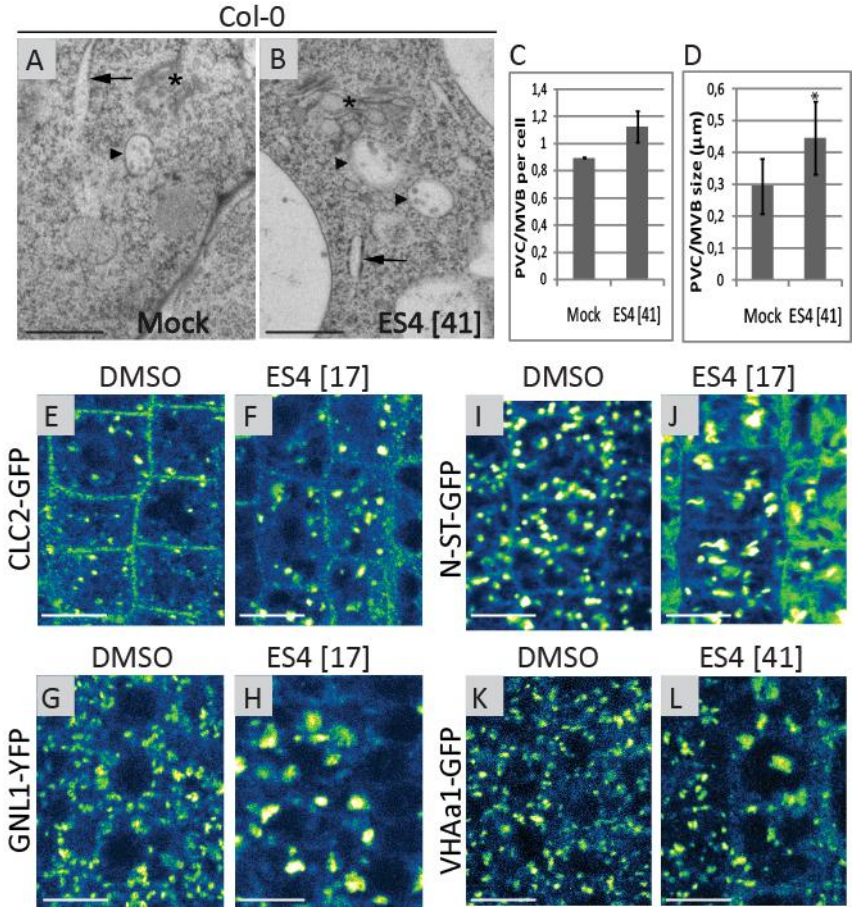

Figure 3. Effect of ES4 on intracellular compartments.
(A) to **(D)** Transmission electron microscopy images of MVBs after 2 h mock and 41 µM ES4 treatment and quantification of number and size of MVBs [**(C)** and **(D)**]. After ES4 treatment, the size of MVBs increased when compared to the control **(D)** whereas there was no significant difference in MVBs number per cell between treatments ($P > 0.05$, by Mann-Whitney *U* test) **(C)**. Quantity of PVC/MVBs was calculated for 39 cells for mock and 46 cells for ES4 **(C)** and the size of the PVC/MVBs was measured for 12 cells for mock and 21 cells for ES4 in one experiment **(D)**. Asterisks indicate Golgi apparatus, arrows, rough ER, and arrowheads, PVC/MVBs. Data are means ± standard deviation (SD) of indicated cells number. Student's *t* test, $*P < 0.05$. Bars = 0.5 µm.
(E) to **(L)** Intracellular localization of CLC-GFP [**(E)** and **(F)**], GNL1-YFP [**(G)** and **(H)**], N-ST-GFP [**(I)** and **(J)**], and VHAa1-GFP [**(K)** and **(L)**] after mock [**(E)**, **(G)**, **(I)** and **(K)**] and 17 µM [**(F)**, **(H)** and **(J)**] or 41 µM **(L)** ES4 treatment. After 2 h of ES4 treatment, all markers displayed an intracellular signal accumulation when compared to the controls. Bars = 10 µm.

At the concentration of 17 µM ES4 intracellular signal agglomerations were observed for almost all tested marker lines, except *VHAa1*. The lowest active concentration of ES4 for this marker, which induced signal agglomeration, was 41 µM. Thus, ES4, to a different extent depending on the concentration, affects many intracellular trafficking routes, including endocytosis, recycling, and vacuolar transport pathway.

To determine essential structural determinants of ES4 bioactivity the structure activity relationship (SAR) was performed. Five chemicals with chemical structure similar to ES4 (Supplemental Figure 4A) were tested for their ability to restore gravitropic growth of *PIN2:PIN1-HA; pin2* seedlings (Supplemental Figure 4B to 4I) and for effects on intracellular agglomeration of GNL1 and SYNTAXIN OF PLANTS 61 (Syp61) markers (Supplemental Figures 4J to 4V). The chemical derivatives differed in modifications of the difluoro, nitro and carbonyl groups and the presence of chlorine on the bicyclic chroman-4-one core. None of the tested molecules affected agravitropic root growth of *PIN2:PIN1-HA; pin2* seedlings or induced intracellular makers' accumulation as observed after ES4 treatment. These results indicate that all groups present on the bicyclic core are important for ES4 activity.

Forward Genetic Screen for Mutants Resistant to ES4 Identifies *ES4-resistant 1* (*es4r1)*

With the aim of identifying targets of ES4, we performed a forward genetic screen for mutants resistant to the compound. The effect of ES4 on shortening of the root length was a macroscopically easily observed phenotype, convenient to use in a screen. Therefore, we screened M2 EMS-mutagenized PIN1-GFP populations grown on ES4 for mutants with roots longer than those of the wild-type control (Figures 4A to 4F and 4J). The M3 generation of selected candidates was rescreened based on the root length. Confirmed candidates with longer roots were additionally tested for the effect of ES4 on the formation of BFA bodies at 83 µM, a concentration that inhibits this process in wild-type plants (Figures 4L to 4O). From 4,600 M1 families, we identified 10 *es4r* mutants displaying elongated roots together with the formation of BFA bodies after ES4 treatment. Under standard growth conditions, the *es4r1* mutant, which had the most pronounced resistance to ES4, did not differ in primary root growth (Figures 4A, 4D, and 4J), hypocotyl length, and number of lateral roots when compared to the wild-type (Supplemental Figures 5A to 5D), confirming the specificity of this mutation for ES4 effects. When grown on ES4, the root length of the wild type was nearly 50% reduced, but only 28% of the *es4r1* (Figure 4K). Additionally, reduction of the *es4r1* hypocotyl length induced by ES4 was smaller than the wild-type hypocotyl length under the same conditions (Supplemental Figure 5C). We identified the *es4r1* mutant that was resistant to the ES4 effects on growth, morphology and cellular processes.

Es4r1 Encodes δ Subunit of COPI Coatomer

The *es4r1* mutant, with the strongest resistance, was mapped to a 121-kb interval on chromosome 5 by using *es4r1* recombinants derived from the F2 progenies of a cross between *es4r1* (Columbia background) and Landsberg *erecta*. The F1 heterozygous plants grown on ES4 exhibited intermediate growth and the F2 progenies displayed segregation of the root length from short through medium to long, suggesting that this mutation is semi-dominant. Map-based cloning and sequencing revealed a proline^{365}-to-leucine^{365} amino acid

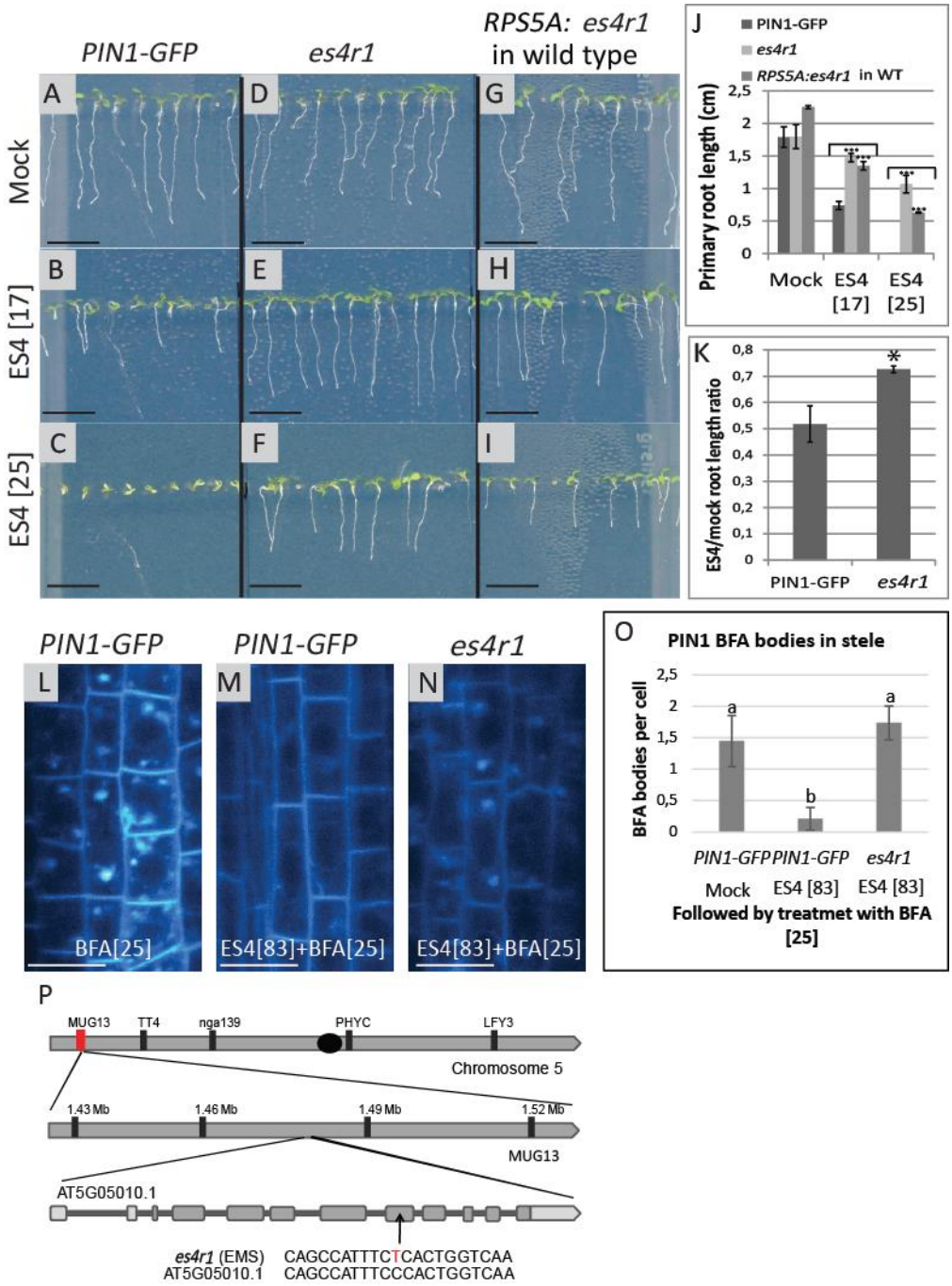

Figure 4. Identification of the *es4r1* mutant from the screen.
(A) to **(J)** Root length sensitivity to ES4 of the wild type, *es4r1*, and *RPS5A:es4r1* in the wild-type background grown for 7 days in a 16-h light/8-h dark photoperiod on media supplemented with mock [**(A)**, **(D)** and **(G)**] and 17 μM [**(B)**, **(E)** and **(H)**] or 25 μM [**(C)**, **(F)** and **(I)**] ES4. There was no significant difference in mock treated root length between PIN1-GFP and *es4r1* (*P* > 0.05, by Student's t test) **(J)**. Primary root length of *es4r1* grown on ES4 was longer [**(D)** and **(F)**] than that of the wild-type control [**(B)** and **(C)**], indicating its resistance to ES4. *RPS5A:es4r1* in a wild-type background, when grown on ES4, had an intermediate root length [**(H)** and **(I)**] between the sensitive short roots of the wild type [**(B)** and **(C)**] and the resistant long roots of *es4r1* [**(E)** and **(F)**]. The partial resistance of RPS5A:*es4r1* in the wild type results from the existence of a nonmutated copy of a gene from a wild-type background that is sensitive to ES4. Quantification of primary root length in

two independent experiments with 27-76 roots analyzed for each treatment in total **(J)**. Data are means ± SE of two experiments. Student's *t* test, ***$P < 0.001$. Bars = 1 cm.
(K) Ratio of root lengths grown on 17 µM ES4 to those grown on mock in three independent experiments for 29-44 roots per treatment per line. Data are means ± SE of three experiments. Student's *t* test, *$P < 0.05$. Bars = 1 cm.
(L) to **(O)** Live imaging of 5-day-old PIN1-GFP and *es4r1* in PIN1-GFP background seedlings and mean number of BFA bodies per cell. After 2 h of 25 µM BFA treatment, regular PIN1-GFP-labeled BFA bodies were observed in the wild type **(L)**. The *es4r1* mutant shows resistance to ES4, as demonstrated by the formation of BFA bodies **(N)**, whereas in the wild type almost no BFA bodies were detected **(M)**. The number of BFA bodies in the stele was counted for 10 cells in each root. In one experiment, 7 roots were analyzed for each treatment. Data are means ± SE of indicated roots number. ANOVA, $P < 0.05$. Bars = 10 µm.
(P) Scheme of *Es4*-coding locus and organization. The position of the *es4r1* allele (continuous line) and the point mutation (red letter) are depicted.

substitution in the open-reading frame of the gene described as a clathrin adaptor complexes medium subunit family protein that codes for the δ subunit of the COPI coatomer (δ-COPI) (Figure 4P). The mutation was found in the µ homology domain (MHD) that, besides *δ-COPI*, also occurs in µ subunits of adaptor protein (AP) complexes and proteins of the stonin and muniscin families. Those proteins are endocytic adaptors that bind to transmembrane cargos through MHD (Jung et al., 2007; Reider et al., 2009). COPI vesicles are formed on the ER and Golgi membranes and are associated with transport between these organelles. Formation of COPI involves activation of the ARF1 protein by ARF GEF regulators (Wieland and Harter, 1999) that recruit COPI coatomer and AP1 proteins to the vesicle formation sites (Scales et al., 1999). The COPI coatomer is a protein complex composed of seven subunits (α-, β-, β'-, γ-, δ-, ε-, and ζ-COPI) (Waters et al., 1991).

In publicly available mutant libraries, we did not identify any loss-of-function mutants in δ-COPI, consistent with the lethal phenotypes of the corresponding mutants from yeast (*Saccharomyces cerevisiae*) (Faulstich et al., 1996), *Drosophila melanogaster* (http://flybase.org, Flybase ID: FBal0096846), and *Caenorhabditis elegans* (http://www.wormbase.org/db, Wormbase RNAi ID:WBRNAi00033328 and WBRNAi0007611). To confirm that the *es4r1* resistance to ES4 was caused by the semi-dominant mutation in the *δ-COPI* gene, we introduced the mutated version of the gene under the constitutively strong *RPS5A* promoter into the wild-type background. Indeed, wild-type plants transformed with *RPS5A:es4r1* displayed a partial, but clear, resistance to ES4 in terms of root length (Figures 4G to 4J) although the resistance phenotype of *RPS5A:es4r1* compared to that of the original *es4r1* mutant was less pronounced. Perhaps it is that the overexpression is not tissue specific so it may have a detrimental effect on development compared to a *PIN* promoter construct in *es4r1*. Additionally, *RPS5A:es4r1* transformants after an 83-µM ES4 treatment were also resistant in terms of inhibition of formation of BFA bodies as observed for the original *es4r1* mutant (Supplemental Figures 5E to 5I). These

data confirm that the proline^{365}-to-leucine^{365} *δ-COPI* mutation is responsible for the ES4 resistance. Thus, identification of *es4r1* defective in δ-COPI revealed a possible ES4 action in ARF1 and ARF GEF-mediated vesicle formation.

ES4 Targets ARF GEF-Dependent Processes

Identification of the *es4r1* mutant defective in δ-COPI suggested ARF GEF-related processes as an ES4 mode of action. To gain further insight into the mechanism of the ES4 action, we tested the sensitivity of different PIN trafficking mutants to ES4 by measuring their root length after growth on media supplemented or not with chemicals (Figure 5A). Among all tested mutants, the *gnl1-2*, *gnl1-3*, and *ben1-2* mutants defective in different ARF GEFs displayed the highest sensitivity to ES4 (Figure 5B). Mutation in another ARF GEF, GNOM, known for its important function in PIN protein trafficking, resulted in agravitropic, short roots that made the analysis after ES4 treatment more difficult.

However, sensitivity of both GNOM mutants, *gnomR5* and *van7*, to ES4 was similar to the wild-type. In contrast, *35S::PID-21*, overexpressing PINOID (PID) kinase, which phosphorylates PIN proteins and promotes their apical cell side localization, showed a slight resistance to ES4 (Figure 5A). The PID kinase-mediated apical PIN polarity has been shown to be independent from GNOM trafficking (Kleine-Vehn et al., 2009), whereas ES4 affects preferentially the basal PIN cargo, without affecting the apical PIN proteins, thus explaining the partial ES4 resistance of this line. Other trafficking-related or auxin-related mutants, such as *roots curl in NPA* (*rcn1*), *auxin resistant* (*axr*), *35S:PIN1*, *clathrin heavy chain* (*chc*), *sorting nexin 1* (*snx1*), *vti12,* and *big3* did not change their sensitivity to ES4. These observations strengthen the link between the ES4 action and the ARF GEF-dependent processes.

BFA is a well-characterized inhibitor of the SEC7 domain-containing ARF GEFs. Similar to ES4, BFA affects more strongly *gnl1* than the wild type (Supplemental Figures 6A and 6B). Moreover, the combined treatment with BFA and ES4 completely inhibited germination in the *gnl1* mutants when compared to single treatments with BFA or ES4. In BFA-treated *gnl1*, both ARF GEFs, GNOM and GNL1, are inactive, strengthening growth inhibition (Richter et al., 2007; Teh and Moore, 2007). GNOM can functionally substitute GNL1 in the Golgi-ER-dependent pathway, but not vice versa (Richter et al., 2007). Accordingly, after the BFA treatment, the BFA-sensitive GNOM cannot substitute GNL1 anymore in the *gnl1* mutant, resulting in largely reduced primary root growth. Similarly, the *ben1* mutant is also hypersensitive to both BFA (Tanaka et al., 2013) and ES4. In contrast, the *big3* mutant, in which an ARF GEF from the BIG family is affected, displayed an ES4 sensitivity similar to that of the wild type (Figure 5A). BIG3, together with BIG1, BIG2, and BIG4, play a redundant function in regulating post-Golgi trafficking (Richter et al., 2014).

Among the four BIG proteins, BIG3 is the only one resistant to BFA; hence, BFA treatment of *big3* results in a more pronounced plant growth inhibition (Richter et al., 2014).

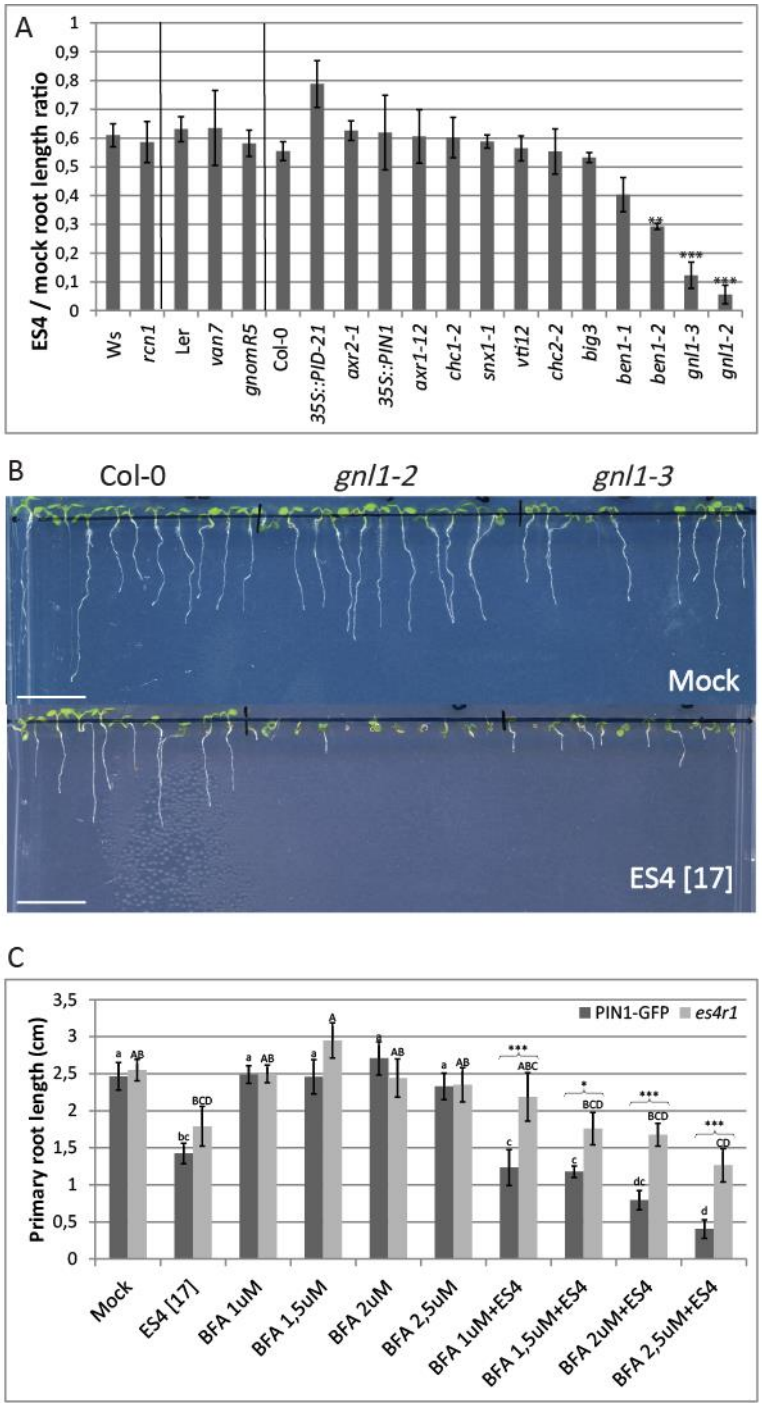

Figure 5. Identification of ES4-sensitive trafficking mutants.
(A) Quantification of root length sensitivity of the wild type (Ws, L*er*, and Col-0) and mutants (*rcn1*, *van7*, *gnom*^{R5}, 35S:PID21, *axr2-1*, *35S:PIN1*, *axr1-12*, *chc1-2*, *snx1-1*, *vti12*, *chc2-2*, *big3*, *ben1-1*, *ben1-2*, *gnl1-3*, and *gnl1-2*). Seedlings were grown for 7 days on growth medium supplemented with mock and 17 µM ES4. Ratio of root lengths grown on ES4 to those grown on mock was calculated. The highest ES4 sensitivity was revealed for *gnl1-2* and *gnl1-3* mutants. In three independent experiments, 20-69 roots measured per treatment

per line. Data are means ± SE of three experiments. Student's *t* test, ***P* < 0.01, ****P* < 0.001.
(B) Representative image of the ES4 sensitivity of *gnl1* mutants. Wild-type, *gnl1-2,* and *gnl1-3* seedlings were grown for 7 days on growth medium supplemented with 17 µM ES4. *gnl1* demonstrated a highly reduced root length when compared to the control, indicating its ES4 sensitivity. Bars = 10 µm.
(C) Root length sensitivity of PIN1-GFP and *es4r1* to ES4 and BFA. Seven-day-old seedlings were grown on medium supplemented with mock, 17 µM ES4, BFA (1 µM, 1.5 µM, 2 µM, and 2.5 µM), and ES4 together with BFA. BFA together with ES4 has an additive effect on root length reduction. In one experiments, 10-22 roots were analyzed for each treatment. Data are means ± SE of indicated roots number. Different letters indicate statistically significant differences between the treatments (ANOVA, *P* < 0.05). Asterisks indicate statistically significant differences between the genotypes (Student's *t* test, **P* < 0.05, ****P* < 0.001).

To characterize the effects of ES4 and BFA, we tested the sensitivity of the wild type and *es4r1* mutant to a range of BFA concentrations in combination with ES4 (Figure 5C). ES4 inhibited root growth of *PIN1-GFP* and, to a lesser extent, of *es4r1*. BFA in concentrations varying between 0.5 µM to 2.5 µM did not visibly reduce root growth of the tested lines. However, when BFA and ES4 were combined, the root length of the wild type was shorter than when grown separately on each of the chemicals, indicating their additive effect. Importantly, *es4r1* was strongly resistant to the combined effect of ES4 and BFA. The results demonstrate that ES4, similarly to BFA, affects the SEC7 domain-containing ARF GEFs, but given the additive effects, presumably by distinct mechanisms.

ES4 Interferes with ARF1 Activation

Previous experiments suggested that ES4 might act on different ARF GEFs. The direct role of ARF GEFs is to activate ARF1 proteins by catalyzing the exchange from GDP to GTP. Activated, GTP-bound, ARFs recruit coat proteins from the cytosol to the membranes and initiate the vesicle formation and transport processes (Beck et al., 2009).

We tested the impact of ES4 on the wild-type (*ARF1*^{WT}), GTP-locked (*ARF1*^{Q71L}), and GDP-locked (*ARF*^{T31N}) forms of ARF1 (Xu and Scheres, 2005) in transgenic *Arabidopsis* plants. The expression of these constructs was driven by the *Arabidopsis* heat shock-inducible promoter of the *HSP18.2* gene and proteins were tagged with fluorescent proteins (XFPs). For activation, the lines were incubated for 2 h at 37°C, followed by chemical treatments for 2 h at room temperature. ARF1^{WT} localized to the Golgi structures and endocytic organelles (Xu and Scheres, 2005) (Figure 6A). After treatment with 17 µM ES4, the GFP labeling was agglomerated and partially localized to the cytosol (Figure 6B), whereas a higher (41 µM) concentration led to an almost complete cytosolic fluorescence signal (Figure 6C).

Similar cytosolic localization and no organellar labeling were observed for an inactive GDP-locked ARF^{T31N} form (Xu and Scheres, 2005) (Supplemental Figures 7A and 7B). On the contrary, the GTP-locked ARF1^{Q71L} form was more associated with membranes than the wild-

type ARF1^{WT} form (Figures 6A and 6D). Importantly, the GTP-locked ARF1^{Q71L} was resistant to the ES4 treatment and, in contrast to the ES4-treated ARF1^{WT}, the cytosolic fluorescent signal did not increase (Figures 6E and 6F).

These results are entirely consistent with the ES4 impact on the ARF GEFs that are required for ARF1^{WT} activation and their binding to the membranes. The permanently activated GTP-bound and already membrane-bound ARF1^{Q71L} does not require the ARF GEF function and therefore, is unaffected by the ES4 treatment, whereas the GDP-locked ARF^{T31N} form shows a localization similar to that of the ES4-treated ARF1^{WT} wild-type form, namely an inactive, cytosolic localization.

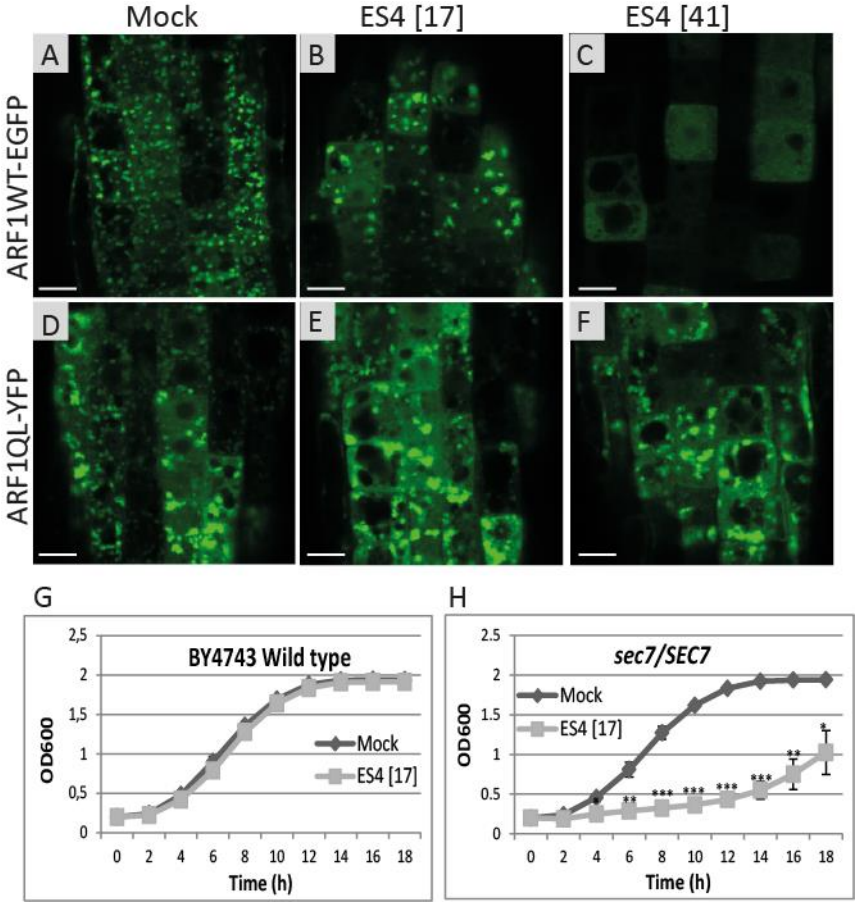

Figure 6. Effect of ES4 on ARF1-GFP marker and *sec7* yeast deletion mutant.
(A) to **(F)** Intracellular localization of ARF1^{WT}-GFP and ARF1^{Q71L}-YFP. Five-day-old seedlings were induced by heat shock at 37°C for 2 h and treated with mock, 17 µM, and 41 µM ES4. In wild-type seedlings, partial cytosolic localization and agglomerated intracellular signal were visible for 17 µM ES4 **(B)** or localized mostly to the cytoplasm for 41 µM **(C)** when compared to the mock treatment with regular intracellular signal **(A)**. A similar intracellular localization of agglomerated signals was visible for ARF1^{Q71L}-YFP after ES4 treatments [**(E)** and **(F)**] and after mock treatment **(D)**. After ES4 treatment, ARF1^{Q71L}-YFP did not localize to the cytosol **(F)** as the ARF1^{WT}-GFP **(C)**, indicating its probable ES4 resistance. Bars = 10 µm.
(G) to **(H)** ES4 sensitivity of heterozygous deletion strains of yeast. Growth of wild-type **(G)** and *sec7/SEC7* **(H)** strain as a function of time (h) in the yeast extract peptone dextrose

(YPD) liquid culture under mock and 17 µM ES4. Growth curves were done in triplicate and OD_{600} was measured by means of a Microplate Reader (BioTek). Growth curves represent means ± SE of three experiments. Student's *t* test, **P* < 0.05, ***P* < 0.01, ***P > 0.001.

ES4 Targets Evolutionarily Conserved SEC7-containing ARF GEFs

We have established that in *Arabidopsis* ES4 inhibits ARF GEF function and interferes with the ARF GEF-mediated activation of ARF1 GTPases. As these ARF GEFs are evolutionarily conserved, we tested the effect of ES4 in yeast. Many proteins in plants and yeast share some conserved sequences, enabling one to search for or confirm a known target from plants also in yeast. We performed a yeast growth assay on a set of heterozygous yeast deletion strains, including COPI coatomer subunits and ARF GEFs (Supplemental Table 1). Treatment of heterozygous yeast strains has been reported to trigger drug-induced haploinsufficiency, meaning that a deletion of one gene copy in diploid cells results in an increased sensitivity to the applied chemical (Giaever et al., 1999; Baetz et al., 2004). To determine the sensitivity of yeast to ES4, the wild-type diploid yeast strain (BY4743) was grown in a liquid culture with a range of ES4 concentrations (Supplemental Figure 8A). At a concentration 41 µM, ES4 severely inhibited yeast growth, whereas at 17 µM, the concentration used for *Arabidopsis* experiments, slightly reduced yeast growth and, therefore, was chosen for the growth assays of heterozygous deletion strains. From the tested deletion strains (Figures 6G and 6H; Supplemental Figures 8B to 8H), the only mutant that displayed a severely increased ES4 sensitivity was a *sec7*/SEC7 ARG GEF (Figures 6G and 6H). SEC7p is the major ARF GEF in yeasts and is required for the membrane traffic from the ER to and through the Golgi and from TGN (Franzusoff et al., 1991; Deitz et al., 2000; Richardson et al., 2012). Like other ARF GEFs, it contains a highly conserved SEC7 domain that had first been identified in this protein and took its name from it (Achstetter et al., 1988). A line deficient in another GEF, SEC12, that activates another GTPase (Sar1), but not from the ARF class, was not affected by ES4 (Supplemental Figure 8H). ES4 had also no effect on the deletion strains of the COPI subunits α-COPI (RET1), β-COPI (SEC26), β'-COPI (SEC27), γ-COPI (SEC21), δ-COPI (RET2), and ζ-COPI (RET3). Two other major ARF GEF proteins involved in the ER-Golgi secretory pathway in yeast, GEA1p and GEA2p, play redundant functions in ARF1 activation at the early Golgi compartments to regulate COPI-mediated vesicle formation (Peyroche et al., 1996, 2001). Complete knockout of GEA1p protein showed an ES4 sensitivity comparable to that of the wild type (Supplemental Figures 8I and 8J), due to the second redundant GEA2p. The obtained results were in line with the observations from *Arabidopsis* and confirmed that also in yeast, ES4 affects specifically the SEC7-domain-containing ARF GEFs, but no other similar regulators.

DISCUSSION

ES4 is a Compound Interfering specifically with ARF GEF-Dependent Trafficking

Here, we identified and characterized a chemical compound that affects endomembrane trafficking, particularly the ARF/ARF GEF-dependent pathway. ES4 works in a dose-dependent manner, slowing down or inhibiting multiple trafficking processes, including endocytosis, recycling, and trafficking to the vacuole. ES4 treatment changes basal polarity of ectopically expressed PIN1 in the *PIN2:PIN1;pin2* line, without visibly affecting the native PIN1 and PIN2 in the wild type. This impact is in accordance with previous findings (Kleine-Vehn et al., 2008b), showing that the ectopic basal PIN1 polarity in epidermis is easily perturbed by trafficking defects; ES4 does not specifically affect the PIN protein trafficking, but that of other PM proteins as well. Defects at the cellular level are mirrored in macroscopically observed phenotypes, including inhibited primary roots and hypocotyl growth and decrease in lateral root density, revealing that ES4 is a developmentally important inhibitor of a broad range of trafficking processes. The number of independent experimental approaches strongly indicates that ES4 specifically acts on ARF GEFs: (i) the highest ES4 sensitivity occurs in the *gnl1* and *ben1* mutants defective in different ARF GEFs; (ii) ES4, together with the known ARF GEF inhibitor BFA, has similar and additive effects on growth, suggesting a common pathway as target of both ES4 and BFA; (iii) ES4 affects the subcellular localization of the ARF GEF substrates - the ARF1 proteins that are responsible for coat protein recruitment to the membranes and initiation of vesicle formation for endomembrane trafficking; (iv) the wild type version of ARF1 is sensitive but the GTP-locked ARF1^{Q71L} that does not require functional ARF GEFs for its activation, is resistant to ES4; and (v) ES4 application to the yeast deletion mutants has identified *sec7*/SEC7p, which is defective in the major ARF GEF-regulating subcellular trafficking in yeast (Wolf et al., 1998), as the most ES4 sensitive. Defects in ARF1 activity triggered by ES4 are fully consistent with the observed ES4-induced agglomerations of membrane proteins and all other trafficking defects, including enlarged PVC/MVBs and defects in vacuolar trafficking, because transient assays in tobacco cells showed the ARF1 involvement in transport to the lytic vacuole (Pimpl et al., 2003). All these results strongly suggest that ES4, similarly to BFA, inhibits ARF GEF-dependent pathways, most probably the SEC7 domain-containing ARF GEFs.

Years of experimentation helped us to better understand the BFA mode of action and established BFA as an important tool in dissecting endomembrane trafficking pathways. Especially important was the discovery of its target, the SEC7 domain of ARF GEFs (Peyroche et al., 1999). ES4 is an extra chemical with an impact distinct from that of BFA, but targeting the same process. It has a clear potential to become an important tool to dissect different roles of ARF/ARF GEF-dependent trafficking pathways, including those in

polar targeting. Herein, the GTP- and GDP-locked versions of ARF1 helped us understand the effect of ES4 in intracellular trafficking. Analysis of the *bex1* mutant, encoding ARF1A1C demonstrated its importance in PIN recycling and auxin-dependent developmental responses (Tanaka et al., 2014). Although the combination of genetic and cell biological approaches conclusively mapped the ES4 action on ARF GEF-mediated processes, future work should focus on defining the precise molecular target of ES4. Already at the present stage of knowledge, ES4 enables the targeted manipulation of ARF GEF-mediated processes, circumventing the obstacles of the BFA-insensitive ARF GEF versions.

ES4 confirms a role in ARF GEF-Dependent Trafficking in basal PIN polarity

Two of the characterized ARF GEF mutants, *gnom* and *ben1*, displayed defects in basal trafficking of the PIN1 proteins, indicating a role for GNOM and BEN1 in the regulation of this process (Kleine-Vehn et al., 2008a; Tanaka et al., 2009, 2013). In the partial loss-of-function *gnomR5* mutant, the basal-to-apical shift of PIN1 in the stele and of PIN2 in the cortex was demonstrated, whereas in the *ben1* mutant, the lateral PIN1 signal was relatively strong. We identified ES4 as a compound causing the basal-to-apical shift of ectopically expressed *PIN1*. The subsequent genetic and microscopical analyses established that ES4 affects different ARF GEF-mediated processes, confirming the involvement of ARF GEFs in trafficking of basal PIN cargos. Additionally, we detected a mutant, defective in the δ-COPI coatomer subunit that was resistant to ES4 in terms of root length, hypocotyl length, and formation of BFA bodies. The COPI vesicles are mainly involved in retrograde transport between Golgi and ER. Although some of the subunits of COPI coatomer were shown to play a role also in other trafficking pathways (Whitney et al., 1995; Aniento et al., 1996; Gu et al., 1997; Gabriely et al., 2007; Razi et al., 2009), so far, δ-COPI subunit has only been associated with Golgi-to-ER trafficking. For a long time, GNOM has been suggested to localize at the endosomal compartments, presumably at its recycling part (Geldner et al., 2003). However, recent studies showed that GNOM predominantly localizes to the Golgi apparatus and that, only after BFA treatment, it translocates to the TGN/EE (Naramoto et al., 2014). Colocalization studies of GNL1 and GNOM revealed their close, but not overlapping, localization at the same Golgi stacks. Defects in secretion of polysaccharides and secGFP in *gnom* and *gnl1* mutants, respectively, hint at a role in transport regulation of different cargos (Shevell et al., 2000; Teh and Moore, 2007). Immunogold labeling of plant coatomer localized all COPI subunits only on the Golgi stacks or in their close vicinity (Pimpl et al., 2000). Interestingly, fluorescently labeled GNOM and GNL1 localize to ring-like structures (Naramoto et al., 2014), similarly to COPI with its ring-like distribution at the Golgi (Pimpl et al., 2000). These observations link the localization of δ-COPI and ARF GEFs at the Golgi and hint at a possible role in basal PIN polar targeting from this compartment.

Further research has to be conducted to elucidate the δ-COPI involvement in intracellular trafficking in plants and its possible role in polar trafficking. The δ-COPI mutant, together with ES4, can contribute to our understanding of coatomer involvement in vesicle trafficking and its interaction with ARF1.

METHODS

Plant Material and Growth Conditions

Seeds of *Arabidopsis thaliana* (L.) Heyhn. were stratified for 2 days in the dark at 4°C and grown vertically at 21°C under continuous light on 0.8% agar half-strength Murashige and Skoog (½MS) medium (Duchefa) with 1% sucrose (pH 5.9). The *Arabidopsis* lines *PIN2:PIN1-HA;eir1-1/pin2* (Wiśniewska et al., 2006); *DR5:GUS* (Ulmasov et al., 1997); *N-ST-GFP* (Batoko et al., 2000); *35S:PID21* (Benjamins et al., 2001); *BRI1:BRI1-GFP* (Russinova et al., 2004); *CLC2:CLC2-GFP* (Konopka and Bednarek, 2008); *VHA-a1:VHA-a1-GFP* (Dettmer et al., 2006); *PIN1:PIN1-GFP* (Benková et al., 2003); *35S:GFP-PIP2a* (Cutler et al., 2000); *PIN2:PIN2-GFP* (Xu and Scheres, 2005); *GNOM:GNOM-GFP* (Geldner et al., 2003); *GNL1:GNL1-YFP* (Richter et al., 2007); *SYP61:SYP61-CFP* (Robert et al., 2008) ; *HSP:ARF1^{WT}-EGFP* and *HSP:ARF1^{Q71L}-EYFP* (Xu and Scheres, 2005); *axr2-1* (Wilson et al., 1990); *ben1-1* and *ben1-2* (SALK_013761) (Tanaka et al., 2009); *big3* (SALK_044617) (Richter et al., 2014); *rcn1* (Garbers et al., 1996); *gnl1-2* and *gnl1-3* (Teh and Moore, 2007); *gnom^{R5}* (Geldner et al., 2004); *van7* (Koizumi et al., 2000); *snx1-1* (Jaillais et al., 2006); *chc1-2* (SALK_103252) and *chc2-2* (SALK_028826) (Kitakura et al., 2011); and *vti12* (Surpin et al., 2003) have been described previously. Columbia (Col-0) accession was used for immunolocalization, transmission electron microscopy, FM4-64 uptake, and as wild-type control in seedling growth experiments, except for growth of *rcn1* and *gnom^{R5}* and *van7* for which the Wassilewskija (Ws) and Landsberg *erecta* (L*er*) accessions were used, respectively.

Chemical Treatments

Chemical numbers in Supplemental Figures 1A and 2A are the Chembridge IDs. Stock solutions of BFA (Sigma-Aldrich), ES4 (Chembridge ID 6938485) and FM4-64 (Invitrogen) were prepared in dimethylsulfoxide (DMSO) and diluted in liquid ½MS (or growth) medium for treatments with the indicated concentrations and times. Equal volumes of solvents were used as mock treatments for controls. For germination and growth of seedlings on ES4 and BFA, seeds were sown directly onto ES4/BFA/ES4+BFA-supplemented growth medium. For polar localization and *DR5:GUS* experiment, 3-day-old seedlings were transferred for 48 h from solid growth medium to solid media complemented with ES4. For shorter treatment (4 h) of *DR5:GUS*, 5-day-old seedlings were mounted in liquid medium complemented with

ES4. After treatment, seedlings were stained overnight at 37°C in darkness in GUS staining buffer [100 mM Na-phosphate buffer (pH 7), 0.1% Triton X-100, 10 mM EDTA (pH 8), and 2 mM of each $K_3FeIII(CN)_6$ and $K_4FeII(CN)_6$] containing X-Gluc to visualize GUS activity. X-Gluc was added at a final concentration of 1 mg/ml from a freshly prepared 10-mg/ml stock dissolved in DMSO. For BFA treatments, 5-day-old seedlings were pretreated for 30 min with ES4 before addition of 25 µM BFA to the treatment for a further 90 min. For BFA washouts, 5-day-old seedlings were treated with 25 µM or 50 µM BFA for 2 h followed by 30 min of wash treatment. For FM4-64 uptake experiments, 5-day-old seedlings were transferred directly after 2 h of treatment to 2 µM FM4-64 in the treatment medium on ice for 5 min, followed by two washes in treatment medium on ice. Endocytosis was started by removing seedlings from the ice-cold conditions. For visualization of the vacuolar GFP labeling, 5-day-old seedlings were transferred directly after 2 h of treatment with 41 µM ES4 to 8 µM FM4-64 in treatment medium on ice for 5 min, followed by two washes in treatment medium on ice and transferred to 41-µM ES4-supplemented growth medium and incubated vertically in darkness for 4 h. For live imaging and transmission electron microscopy, 5-day-old seedlings were mounted for 2 h in their treatment medium. For induction of *HSP:ARF1* expression, plates were incubated at 37°C for 2 h followed by ES4 treatment for 2 h at room temperature.

Forward Genetic Screen

Seven-day-old EMS-mutagenized *PIN1:PIN1-GFP* seedlings (progenies of 4,600 M1) grown on 25 µM ES4 were scored for individuals with roots longer than those of the wild-type control. From 447 candidates, 96 were confirmed with long roots in the next generation from which 10 *es4* mutants had long roots and formed BFA bodies upon ES4 treatment.

Mapping

es4r1 was mapped on the short arm of chromosome 5 between MUK11 (1.409 Mb) and K2A11-*Mse*I (1.530 Mb) (SSLP and CAPS markers). *es4r1* displayed a C-to-T point mutation that causes an amino acid substitution at position 1834: proline to leucine. For the information about the Col-0/L*er* polymorphisms, we used the collection of SNPs and INDELs provided by Monsanto Arabidopsis Polymorphism and L*er* Sequence Collection (Cereon Genomics) and TAIR (http://www.arabidopsis.org).

Genotyping

To genotype *es4r1*, we used the foward primer 5'-CATCCCAACATCAACCGAG and the reverse primer 5'-AACACCATCTCCACCTTGACCACTG and digested the PCR product with *Dde*I.

Generation of the *RPS5A*:*es4r1* Construct and Transformation

δ-COPI genomic DNA (AT5G05010) was amplified by PCR from the *es4r1* mutant isolated from the EMS screen with the following primers: forward 5'-ggggacaagtttgtacaaaaaagcaggctccatggtattgacttttgttctatg and reverse 5'-ggggaccactttgtacaagaaagctgggtctcatatgacttgatagttctgg and cloned into the pDONR221 Gateway donor vector (Karimi et al., 2002). The *RPS5A* promoter from the pDONRP4-P1/RPS5A donor vector (kind gift of W. Grunewald) and δ-COPI were transferred to the pK7m24GW.3 Gateway destination vector (Karimi et al., 2002) by LR Clonase II (Invitrogen). The obtained construct was transformed to the *Agrobacterium tumefaciens* strain C58C1 and introduced into *Arabidopsis* accession Col-0 with the floral dip method (Clough and Bent, 1998). Transformants were selected on kanamycin-containing plates.

Immunolocalization

Whole-mount immunolocalization on 5-day-old seedlings of *Arabidopsis* was done with the InSituProrobot (Intavis, Germany) according to the described protocol (Sauer et al., 2006). Primary antibodies and final dilutions were: rabbit anti-PIN1 (Paciorek et al., 2005) 1:1000; rabbit anti-PIN2 (generously provided by C. Luschnig) 1:1000; mouse anti-HA (AbCam/HA.C5) 1:500. Secondary antibodies and final dilutions were: Cy3 anti-rabbit (Sigma-Aldrich) 1:600 and Alexa488 anti-mouse (Invitrogen) 1:600.

TEM on Roots

Root tips of 5-day-old Col-0 seedlings untreated and treated for 2 h with 41 µM ES4 were excised and processed as described (Tanaka et al., 2009).

Yeast Strains and Media

The diploid heterozygous and homozygous *gea1* deletion mutants generated by the International Deletion Consortium (Winzeler et al., 1999) were obtained from EUROSCARF. BY4743 and BY4742 were used as the diploid wild-type control for the diploid heterozygous and the *gea1* homozygous deletion mutants, respectively. Yeasts were grown on standard rich medium [yeast extract/peptone/dextrose (YPD)] with and without ES4. For growth rate analysis and ES4 sensitivity, BY4743 cells were grown in 1 ml liquid YPD medium in 50-ml Falcon tubes for 4 h at 28°C with shaking at 200 rpm to an OD_{600} of approximately 1. After 4 h, 2 µl of the liquid cell culture was transferred into 96-well plates containing 198 µl of liquid YPD with mock treatment or with different concentrations of ES4 (17 µM, 21 µM, 28 µM, and 41 µM) at final OD_{600} of approximately 0.1 and was grown overnight at 28°C with shaking in a H1 Microplate Reader (BioTek). The deletion mutants were grown at 17 µM ES4 and with the mock treatment as described for the wild type.

Quantitative and Statistical Analyses

For PIN polarity quantification in the cortex, the ratio of the cell numbers with basal PIN2 and the total number of cortical cells was calculated from the confocal laser scanning microscopy (CLSM) images of the root apical meristem. For polarity in epidermal cells of *PIN2:PIN1*, the ratio of the cell numbers with basal, both basal and apical, or apical PIN localization was compared to the total number of epidermal cells from the CLSM images of the root apical meristem. For analysis of the gravitropic response, 5-day-old seedlings grown vertically in light were gravistimulated by a 90° rotation (Col-0). *PIN2:PIN1-HA* seedlings were gravistimulated twice, at the 5-day-old stage and 24 h after the first gravistimulation. The bending angle was measured with the Java-based ImageJ application (http://rsb.info.nih.gov/ij/) 48 h after the first gravistimulation. All gravitropically stimulated roots were assigned to one of the eight 45° sectors on a gravitropism diagram. The length of the bars in the diagram represents the percentage of seedlings assigned to the respective sector. Wild-type root lengths and hypocotyl lengths were measured with the ImageJ software. For the mutant root lengths, the ratio was calculated of the root length of seedlings grown on ES4 and that of seedlings grown on mock media with the ImageJ application. For quantification of FM4-64 and PIN2-GFP internalization, the ratio of the mean pixel intensity of the internal cell fluorescence and the mean pixel intensity of the adjacent PM fluorescence was obtained by ImageJ. The size of the PVC/MVBs was calculated by the ImageJ software. For the yeast growth assay, we analyzed the growth curves of 12 strains (including wild types), each grown with mock treatment or in the presence of 17 μM of ES4. OD_{600} of the cell density was determined every 2 h for nine time points. Three or two replications per strain per experiment for ES4 or mock treatment were done, respectively. The statistical significances of differences of data were quantified with Student's *t*-tests, Mann-Whitney *U* test and ANOVA.

Image Analysis

Imaging was done on a LSM 710 (Zeiss), LSM 700 (Zeiss) and Leica SP2 confocal laser scanning microscopes.

Accession Numbers

Sequence data from this article can be found in the Arabidopsis Genome Initiative or GenBank/EMBL databases under the following accession numbers: PIN1 (At1g73590), PIN2 (At5G57090), PIP2a (At3G53420), VHAa1 (At2g28520), CLC2 (At2G40060), N-ST (AJ243198), BEN1 (At3G43300), SYP61 (AF355754), GNL1 (At5G39500), ARF1 (At2g47170), δ-COPI (At5g05010), GNOM(At1g13980), BRI1 (At4g39400), PID (At2g34650), CHC1 (At3g11130), CHC2 (At3g08530), SNX1 (At5g06140), VTI12 (At1g26670), RCN1 (At1g25490), AXR2 (At3g23050), and BIG3 (At1g01960).

ACKNOWLEDGMENTS

We thank Wim Grunewald for the unpublished pDONRP4-P1/RPS5A construct, Wilson Ardiles-Diaz and Carina Braeckman for sequencing and plant transformation, respectively, Fernando Aniento, Sebastian Bednarek, Maciek Adamowski, Matyás Fendrych, Elena Feraru, and Mugurel I. Feraru for helpful discussions and suggestions, Siamsa Doyle for critical reading of the manuscript and helpful comments and suggestions and Martine De Cock for help in preparing it. This work was supported by the Odysseus program of the Research Foundation-Flanders and the Körber Stiftung.

REFERENCES

Abas, L., Benjamins, R., Malenica, N., Paciorek, T., Wiśniewska, J., Moulinier-Anzola, J.C., Sieberer, T., Friml, J., and Luschnig, C. (2006). Intracellular trafficking and proteolysis of the *Arabidopsis* auxin-efflux facilitator PIN2 are involved in root gravitropism. Nat. Cell Biol. 8: 249-256.

Achstetter, T., Franzusoff, A., Field, C., and Schekman, R. (1988). *SEC7* encodes an unusual, high molecular weight protein required for membrane traffic from the yeast Golgi apparatus. J. Biol. Chem. 263: 11711-11717.

Aniento, F., Gu, F., Parton, R.G., and Gruenberg, J. (1996). An endosomal βCOP is involved in the pH-dependent formation of transport vesicles destined for late endosomes. J. Cell Biol. 133: 29-41.

Baetz, K., McHardy, L., Gable, K., Tarling, T., Rebérioux, D., Bryan, J., Andersen, R.J., Dunn, T., Hieter, P., and Roberge, M. (2004). Yeast genome-wide drug-induced haploinsufficiency screen to determine drug mode of action. Proc. Natl. Acad. Sci. USA 101: 4525-4530.

Baster, P., Robert, S., Kleine-Vehn, J., Vanneste, S., Kania, U., Grunewald, W., De Rybel, B., Beeckman, T., and Friml, J. (2013). $SCF^{TIR1/AFB}$-auxin signalling regulates PIN vacuolar trafficking and auxin fluxes during root gravitropism. EMBO J. 32: 260-274.

Batoko, H., Zheng, H.-Q., Hawes, C., and Moore, I. (2000). A Rab1 GTPase is required for transport between the endoplasmic reticulum and Golgi apparatus and for normal Golgi movement in plants. Plant Cell 12: 2201-2217.

Beck, R., Rawet, M., Ravet, M., Wieland, F.T., and Cassel, D. (2009). The COPI system: molecular mechanisms and function. FEBS Lett. 583: 2701–2709.

Benjamins, R., Quint, A., Weijers, D., Hooykaas, P., and Offringa, R. (2001). The PINOID protein kinase regulates organ development in *Arabidopsis* by enhancing polar auxin transport. Development 128: 4057-4067.

Benková, E., Michniewicz, M., Sauer, M., Teichmann, T., Seifertová, D., Jürgens, G., and Friml, J. (2003). Local, efflux-dependent auxin gradients as a common module for plant organ formation. Cell 115: 591–602.

Bonifacino, J.S., and Lippincott-Schwartz, J. (2003). Coat proteins: shaping membrane transport. Nat. Rev. Mol. Cell Biol. 4: 409-414.

Clough, S.J., and Bent, A.F. (1998). Floral dip: a simplified method for *Agrobacterium*-mediated transformation of *Arabidopsis thaliana*. Plant J. 16: 735-743.

Cutler, S.R., Ehrhardt, D.W., Griffitts, J.S., and Somerville, C.R. (2000). Random GFP::cDNA fusions enable visualization of subcellular structures in cells of *Arabidopsis* at a high frequency. Proc. Natl. Acad. Sci. USA 97: 3718-3723.

Dascher, C., and Balch, W.E. (1994). Dominant inhibitory mutants of ARF1 block endoplasmic reticulum to Golgi transport and trigger disassembly of the Golgi apparatus. J. Biol. Chem. 269: 1437-1448.

Deitz, S.B., Rambourg, A., Képès, F., and Franzusoff, A. (2000). SEC7p directs the transitions required for yeast Golgi biogenesis. Traffic 1: 172-183.

Dettmer, J., Hong-Hermesdorf, A., Stierhof, Y.-D., and Schumacher, K. (2006). Vacuolar H^+-ATPase activity is required for endocytic and secretory trafficking in *Arabidopsis*. Plant Cell 18: 715–730.

Doyle, S.M., Haeger, A., Vain, T., Rigal, A., Viotti, C., Łangowska, M., Ma, Q., Friml, J., Raikhel, N.V., Hicks, G.R., and Robert, S. (2015). An early secretory pathway mediated by GNOM-LIKE 1 and GNOM is essential for basal polarity establishment in *Arabidopsis thaliana*. Proc. Natl. Acad. Sci. USA 112: E806–E815.

Drakakaki, G., Robert, S., Szatmari, A.-M., Brown, M.Q., Nagawa, S., Van Damme, D., Leonard, M., Yang, Z., Girke, T., Schmid, S.L., Russinova, E., Friml, J., Raikhel, N.V., and Hicks, G.R. (2011). Clusters of bioactive compounds target dynamic endomembrane networks in vivo. Proc. Natl. Acad. Sci. USA 108: 17850-17855.

Faulstich, D., Auerbach, S., Orci, L., Ravazzola, M., Wegehingel, S., Lottspeich, F., Stenbeck, G., Harter, C., Wieland, F.T., and Tschochner, H. (1996). Architecture of coatomer: molecular characterization of δ-COP and protein interactions within the complex. J. Cell Biol. 135: 53-61.

Feraru, E., Feraru, M.I., Kleine-Vehn, J., Martinière, A., Mouille, G., Vanneste, S., Vernhettes, S., Runions, J., and Friml, J. (2011). PIN polarity maintenance by the cell wall in *Arabidopsis*. Curr. Biol. 21: 338–343.

Franzusoff, A., Redding, K., Crosby, J., Fuller, R.S., and Schekman, R. (1991). Localization of components involved in protein transport and processing through the yeast Golgi apparatus. J. Cell Biol. 112: 27-37.

Gabriely, G., Kama, R., and Gerst, J.E. (2007). Involvement of specific COPI subunits in protein sorting from the late endosome to the vacuole in yeast. Mol. Cell. Biol. 27: 526-540.

Garbers, C., DeLong, A., Deruére, J., Bernasconi, P., and Söll, D. (1996). A mutation in protein phosphatase 2A regulatory subunit A affects auxin transport in *Arabidopsis*. EMBO J. 15: 2115-2124.

Geldner, N., Anders, N., Wolters, H., Keicher, J., Kornberger, W., Muller, P., Delbarre, A., Ueda, T., Nakano, A., and Jürgens, G. (2003). The *Arabidopsis* GNOM ARF-GEF mediates endosomal recycling, auxin transport, and auxin-dependent plant growth. Cell 112: 219–230.

Geldner, N., Friml, J., Stierhof, Y.-D., Jürgens, G., and Palme, K. (2001). Auxin transport inhibitors block PIN1 cycling and vesicle trafficking. Nature 413: 425–428.

Geldner, N., Richter, S., Vieten, A., Marquardt, S., Torres-Ruiz, R.A., Mayer, U., and Jürgens, G. (2004). Partial loss-of-function alleles reveal a role for *GNOM* in auxin transport-related, post-embryonic development of *Arabidopsis*. Development 131: 389–400.

Giaever, G., Shoemaker, D.D., Jones, T.W., Liang, H., Winzeler, E.A., Astromoff, A., and Davis, R.W. (1999). Genomic profiling of drug sensitivities via induced haploinsufficiency. Nat. Genet. 21: 278-283.

Goldberg, J. (1999). Structural and functional analysis of the ARF1-ARFGAP complex reveals a role for coatomer in GTP hydrolysis. Cell 96: 893-902.

Grunewald, W., and Friml, J. (2010). The march of the PINs: developmental plasticity by dynamic polar targeting in plant cells. EMBO J. 29: 2700–2714.

Gu, F., Aniento, F., Parton, R.G., and Gruenberg, J. (1997). Functional dissection of COP-I subunits in the biogenesis of multivesicular endosomes. J. Cell Biol. 139: 1183-1195.

Jackson, C.L., and Casanova, J.E. (2000). Turning on ARF: the SEC7 family of guanine-nucleotide-exchange factors. Trends Cell Biol. 10: 60-67.

Jaillais, Y., Fobis-Loisy, I., Miège, C., Rollin, C., and Gaude, T. (2006). AtSNX1 defines an endosome for auxin-carrier trafficking in *Arabidopsis*. Nature 443: 106–109.

Jung, N., Wienisch, M., Gu, M., Rand, J.B., Müller, S.L., Krause, G., Jorgensen, E.M., Klingauf, J., Haucke, V. (2007) Molecular basis of synaptic vesicle cargo recognition by the endocytic sorting adaptor stonin 2. J Cell Biol. 179: 1497-510.

Karimi, M., Inzé, D., and Depicker, A. (2002). GATEWAY™ vectors for *Agrobacterium*-mediated plant transformation. Trends Plant Sci. 7: 193-195.

Kitakura, S., Vanneste, S., Robert, S., Löfke, C., Teichmann, T., Tanaka, H., and Friml, J. (2011). Clathrin mediates endocytosis and polar distribution of PIN auxin transporters in *Arabidopsis*. Plant Cell 23: 1920–1931.

Kleine-Vehn, J., and Friml, J. (2008). Polar targeting and endocytic recycling in auxin-dependent plant development. Annu. Rev. Cell Dev. Biol. 24: 447–473.

Kleine-Vehn, J., Dhonukshe, P., Sauer, M., Brewer, P.B., Wiśniewska, J., Paciorek, T., Benková, E., and Friml, J. (2008a). ARF GEF-dependent transcytosis and polar delivery of PIN auxin carriers in *Arabidopsis*. Curr. Biol. 18: 526–531.

Kleine-Vehn, J., Huang, F., Naramoto, S., Zhang, J., Michniewicz, M., Offringa, R., and Friml, J. (2009). PIN auxin efflux carrier polarity is regulated by PINOID kinase-mediated recruitment into GNOM-independent trafficking in *Arabidopsis*. Plant Cell 21: 3839–3849.

Kleine-Vehn, J., Łangowski, Ł., Wiśniewska, J., Dhonukshe, P., Brewer, P.B., and Friml, J. (2008b). Cellular and molecular requirements for polar PIN targeting and transcytosis in plants. Mol. Plant 1: 1056–1066.

Kleine-Vehn, J., Leitner, J., Zwiewka, M., Sauer, M., Abas, L., Luschnig, C., and Friml, J. (2008c). Differential degradation of PIN2 auxin efflux carrier by retromer-dependent vacuolar targeting. Proc. Natl. Acad. Sci. USA 105: 17812-17817.

Koizumi, K., Sugiyama, M., and Fukuda, H. (2000). A series of novel mutants of *Arabidopsis thaliana* that are defective in the formation of continuous vascular network: calling the auxin signal flow canalization hypothesis into question. Development 127: 3197-3204.

Konopka, C.A., and Bednarek, S.Y. (2008). Variable-angle epifluorescence microscopy: a new way to look at protein dynamics in the plant cell cortex. Plant J. 53: 186-196.

Kumari, S., and Mayor, S. (2008). ARF1 is directly involved in dynamin-independent endocytosis. Nat. Cell Biol. 10: 30-41.

Lee, M.H., Min, M.K., Lee, Y.J., Jin, J.B., Shin, D.H., Kim, D.H., Lee, K.-H., and Hwang, I. (2002). ADP-ribosylation factor 1 of *Arabidopsis* plays a critical role in intracellular

trafficking and maintenance of endoplasmic reticulum morphology in *Arabidopsis*. Plant Physiol. 129: 1507-1520.

Müller, A., Guan, C., Gälweiler, L., Tänzler, P., Huijser, P., Marchant, A., Parry, G., Bennett, M., Wisman, E., and Palme, K. (1998). *AtPIN2* defines a locus of *Arabidopsis* for root gravitropism control. EMBO J. 17: 6903-6911.

Naramoto, S., Otegui, M.S., Kutsuna, N., de Rycke, R., Dainobu, T., Karampelias, M., Fujimoto, M., Feraru, E., Miki, D., Fukuda, H., Nakano, A., and Friml, J. (2014). Insights into the localization and function of the membrane trafficking regulator GNOM ARF-GEF at the Golgi apparatus in *Arabidopsis*. Plant Cell 26: 3062-3076.

Ooi, C.E., Dell'Angelica, E.C., and Bonifacino, J.S. (1998). ADP-ribosylation factor 1 (ARF1) regulates recruitment of the AP-3 adaptor complex to membranes. J. Cell Biol. 142: 391-402.

Paciorek, T., Zažímalová, E., Ruthardt, N., Petrášek, J., Stierhof, Y.-D., Kleine-Vehn, J., Morris, D.A., Emans, N., Jürgens, G., Geldner, N., and Friml, J. (2005). Auxin inhibits endocytosis and promotes its own efflux from cells. Nature 435: 1251-1256.

Petrášek, J., Mravec, J., Bouchard, R., Blakeslee, J.J., Abas, M., Seifertová, D., Wiśniewska, J., Tadele, Z., Kubeš, M., Čovanová, M., et al. (2006). PIN proteins perform a rate-limiting function in cellular auxin efflux. Science 312: 914-918.

Peyroche, A., Antonny, B., Robineau, S., Acker, J., Cherfils, J., and Jackson, C.L. (1999). Brefeldin A acts to stabilize an abortive ARF-GDP-SEC7 domain protein complex: involvement of specific residues of the SEC7 domain. Mol. Cell 3: 275-285.

Peyroche, A., Courbeyrette, R., Rambourg, A., and Jackson, C.L. (2001). The ARF exchange factors Gea1p and Gea2p regulate Golgi structure and function in yeast. J. Cell Sci. 114: 2241-2253.

Peyroche, A., Paris, S., and Jackson, C.L. (1996). Nucleotide exchange on ARF mediated by yeast Gea1 protein. Nature 384: 479-481.

Pimpl, P., Hanton, S.L., Taylor, J.P., Pinto-daSilva, L.L., and Denecke, J. (2003). The GTPase ARF1p controls the sequence-specific vacuolar sorting route to the lytic vacuole. Plant Cell 15: 1242-1256.

Pimpl, P., Movafeghi, A., Coughlan, S., Denecke, J., Hillmer, S., and Robinson, D.G. (2000). In situ localization and in vitro induction of plant COPI-coated vesicles. Plant Cell 12: 2219-2235.

Poon, P.P., Cassel, D., Spang, A., Rotman, M., Pick, E., Singer, R.A., and Johnston, G.C. (1999). Retrograde transport from the yeast Golgi is mediated by two ARF GAP proteins with overlapping function. EMBO J. 18: 555-564.

Razi, M., Chan, E.Y.W., and Tooze, S.A. (2009). Early endosomes and endosomal coatomer are required for autophagy. J. Cell Biol. 185: 305-321.

Reider, A., Barker, S.L., Mishra, S.K., Im, Y.J., Maldonado-Báez, L., Hurley J.H., Traub L.M., Wendland, B. (2009). Syp1 is a conserved endocytic adaptor that contains domains involved in cargo selection and membrane tubulation. EMBO J. 28: 3103-16.

Richardson, B.C., McDonold, C.M., and Fromme, J.C. (2012). The SEC7 Arf-GEF is recruited to the *trans*-Golgi network by positive feedback. Dev. Cell 22: 799-810.

Richter, S., Geldner, N., Schrader, J., Wolters, H., Stierhof, Y.-D., Rios, G., Koncz, C., Robinson, D.G., and Jürgens, G. (2007). Functional diversification of closely related ARF-GEFs in protein secretion and recycling. Nature 448: 488-492.

Richter, S., Kientz, M., Brumm, S., Nielsen, M.E., Park, M., Gavidia, R., Krause, C., Voss, U., Beckmann, H., Mayer, U., Stierhof, Y.-D., and Jürgens, G. (2014). Delivery of endocytosed proteins to the cell-division plane requires change of pathway from recycling to secretion. eLife 3: e02131.

Robert, S., Chary, S.N., Drakakaki, G., Li, S., Yang, Z., Raikhel, N.V., and Hicks, G.R. (2008). Endosidin1 defines a compartment involved in endocytosis of the brassinosteroid receptor BRI1 and the auxin transporters PIN2 and AUX1. Proc. Natl. Acad. Sci. USA 105: 8464-8469.

Robinson, D.G., Scheuring, D., Naramoto, S., and Friml, J. (2011). ARF1 localizes to the Golgi and the *trans*-Golgi network. Plant Cell 23: 846-850.

Russinova, E., Borst, J.-W., Kwaaitaal, M., Caño-Delgado, A., Yin, Y., Chory, J., and de Vries, S.C. (2004). Heterodimerization and endocytosis of *Arabidopsis* brassinosteroid receptors BRI1 and AtSERK3 (BAK1). Plant Cell 16: 3216-3229.

Sauer, M., Paciorek, T., Benková, E., and Friml, J. (2006). Immunocytochemical techniques for whole mount *in situ* protein localization in plants. Nat. Protocols 1: 98-103.

Scales, S.J., Gomez, M., and Kreis, T.E. (1999). Coat proteins regulating membrane traffic. Int. Rev. Cytol. 195: 67-144.

Scheuring, D., Viotti, C., Krüger, F., Künzl, F., Sturm, S., Bubeck, J., Hillmer, S., Frigerio, L., Robinson, D.G., Pimpl, P., and Schumacher, K. (2011). Multivesicular bodies mature from the *trans*-Golgi network/early endosome in *Arabidopsis*. Plant Cell 23: 3463-3481.

Serafini, T., Orci, L., Amherdt, M., Brunner, M., Kahn, R.A., and Rothman, J.E. (1991). ADP-ribosylation factor is a subunit of the coat of Golgi-derived COP-coated vesicles: a novel role for a GTP-binding protein. Cell 67: 239-253.

Shevell, D.E., Kunkel, T., and Chua, N.-H. (2000). Cell wall alterations in the *Arabidopsis emb30* mutant. Plant Cell 12: 2047-2059.

Surpin, M., Zheng, H., Morita, M.T., Saito, C., Avila, E., Blakeslee, J.J., Bandyopadhyay, A., Kovaleva, V., Carter, D., Murphy, A., Tasaka, M., and Raikhel, N. (2003). The VTI family of SNARE proteins is necessary for plant viability and mediates different protein transport pathways. Plant Cell 15: 2885-2899.

Takeuchi, M., Ueda, T., Yahara, N., and Nakano, A. (2002). Arf1 GTPase plays roles in the protein traffic between the endoplasmic reticulum and the Golgi apparatus in tobacco and *Arabidopsis* cultured cells. Plant J. 31: 499-515.

Tamura, K., Shimada, T., Ono, E., Tanaka, Y., Nagatani, A., Higashi, S.-i., Watanabe, M., Nishimura, M., and Hara-Nishimura, I. (2003). Why green fluorescent fusion proteins have not been observed in the vacuoles of higher plants. Plant J. 35: 545-555.

Tanaka, H., Kitakura, S., De Rycke, R., De Groodt, R., and Friml, J. (2009). Fluorescence imaging-based screen identifies ARF GEF component of early endosomal trafficking. Curr. Biol. 19: 391–397.

Tanaka, H., Kitakura, S., Rakusová, H., Uemura, T., Feraru, M.I., De Rycke, R., Robert, S., Kakimoto, T., and Friml, J. (2013). Cell polarity and patterning by PIN trafficking through early endosomal compartments in *Arabidopsis thaliana*. PLoS Genet 9: e1003540.

Tanaka, H., Nodzyński, T., Kitakura, S., Feraru, M.I., Sasabe, M., Ishikawa, T., Kleine-Vehn, J., Kakimoto, T., and Friml, J. (2014). BEX1/ARF1A1C is required for BFA-sensitive recycling of PIN auxin transporters and auxin-mediated development in *Arabidopsis*. Plant Cell Physiol. 55: 737-749.

Teh, O.-k., and Moore, I. (2007). An ARF-GEF acting at the Golgi and in selective endocytosis in polarized plant cells. Nature 448: 493–496.

Ueda, T., Yamaguchi, M., Uchimiyia, H., and Nakano, A. (2001). Ara6, a plant-unique novel type Rab GTPase, functions in the endocytic pathway of *Arabidopsis thaliana*. EMBO J. 20: 4730-4741.

Ulmasov, T., Murfett, J., Hagen, G., and Guilfoyle, T.J. (1997). Aux/IAA proteins repress expression of reporter genes containing natural and highly active synthetic auxin response elements. Plant Cell 9: 1963-1971.

Waters, M.G., Serafini, T., and Rothman, J.E. (1991). 'Coatomer': a cytosolic protein complex containing subunits of non-clathrin-coated Golgi transport vesicles. Nature 349: 248-251.

Whitney, J.A., Gomez, M., Sheff, D., Kreis, T.E., and Mellman, I. (1995). Cytoplasmic coat proteins involved in endosome function. Cell 83: 703-713.

Wieland, F., and Harter, C. (1999). Mechanisms of vesicle formation: insights from the COP system. Curr. Opin. Cell Biol. 11: 440-446.

Wilson, A.K., Pickett, F.B., Turner, J.C., and Estelle, M. (1990). A dominant mutation in *Arabidopsis* confers resistance to auxin, ethylene and abscisic acid. Mol. Gen. Genet. 222: 377-383.

Winzeler., E.A., Shoemaker, D.D., Astromoff, A., Liang, H., Anderson, K., Andre, B., Bangham, R., Benito, R., Boeke, J.D., Bussey, H., et al. (1999). Functional characterization of the *S. cerevisiae* genome by gene deletion and parallel analysis. Science 285: 901-906.

Wiśniewska, J., Xu, J., Seifertová, D., Brewer, P.B., Růžička, K., Blilou, I., Rouquié, D., Benková, E., Scheres, B., and Friml, J. (2006).). Polar PIN localization directs auxin flow in plants. Science 312: 883-883.

Wolf, J., Nicks, M., Deitz, S., van Tuinen, E., and Franzusoff, A. (1998). An N-end rule destabilization mutant reveals pre-Golgi requirements for SEC7p in yeast membrane traffic. Biochem. Biophys. Res. Commun. 243: 191-198.

Xu, J., and Scheres, B. (2005). Dissection of *Arabidopsis* ADP-RIBOSYLATION FACTOR 1 function in epidermal cell polarity. Plant Cell 17: 525-536.

Zwiewka, M., and Friml, J. (2012). Fluorescence imaging-based forward genetic screens to identify trafficking regulators in plants. Front. Plant Sci. 3: 97.

SUPPLEMENTARY INFORMATION

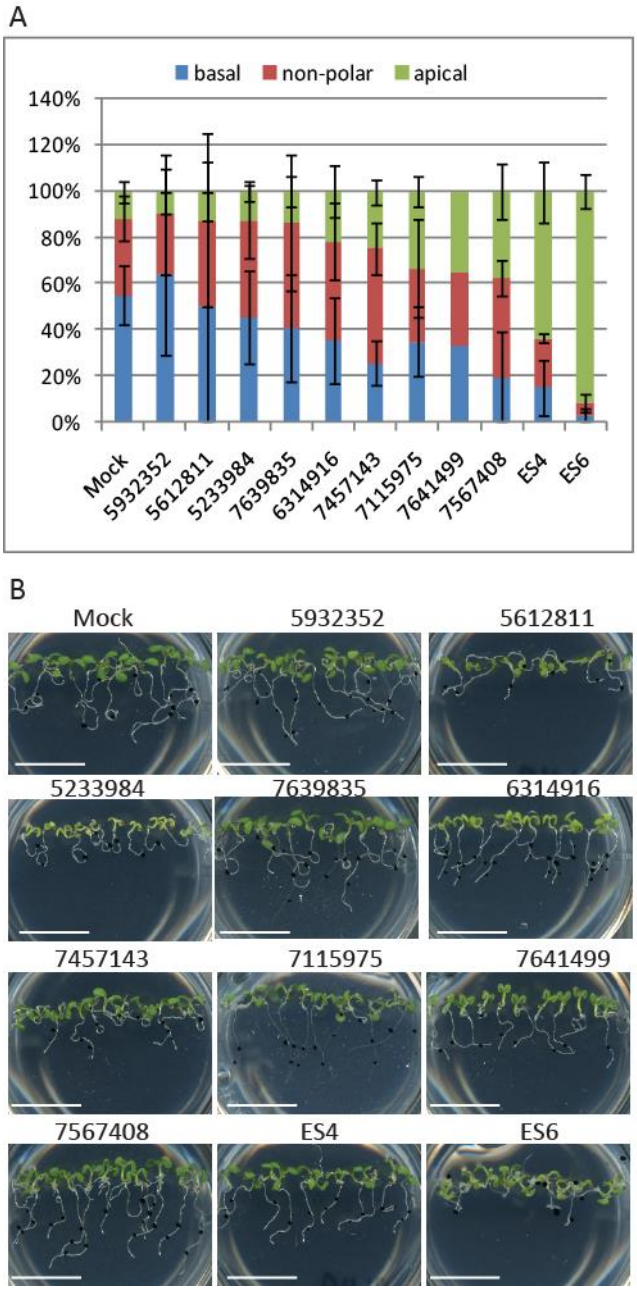

Supplemental Figure 1. Chemical screen of a set of 11 small molecules implicated in polarity changes.
(A) Evaluation of the PIN1-HA localization in *PIN2:PIN1-HA;pin2* epidermal cells after chemical treatments followed by immunolocalization. Three-day-old *PIN2:PIN1-HA;pin2* seedlings were transferred on growth medium supplemented with mock or a set of 11 chemicals and grown vertically for 48 h. Eight of the chemicals were diluted in a growth medium at 1:200 from a stock concentration of 10 mg/ml; ES4 was used at 17 µM and ES6 at 6 µM. The *PIN2:PIN1-HA;pin2* line showed predominantly a basal and nonpolar PIN1-HA localization. Among the 11 tested compounds, ES6 and ES4 had the most prominent effect on PIN1-HA apicalization in epidermal cells. Two to four independent experiments were done for each chemical and one experiment for the ID7641499 small molecule. Error bars represent SE. Chemical numbers are the Chembridge IDs.

(B) Response of 7-day-old *PIN2::PIN1-HA;pin2* seedlings gravistimulated for 48 h. Seedlings were grown on medium supplemented with mock or a set of 11 chemicals, of which eight were diluted in a growth medium at 1:200 from a stock concentration of 10 mg/ml. ES4 was used at 17 µM and ES6 at 6 µM. The most prominent gravitropic response was observed for seedlings grown on ES4 when compared to the agravitropic root growth on the mock treatment. Bars = 1 cm.

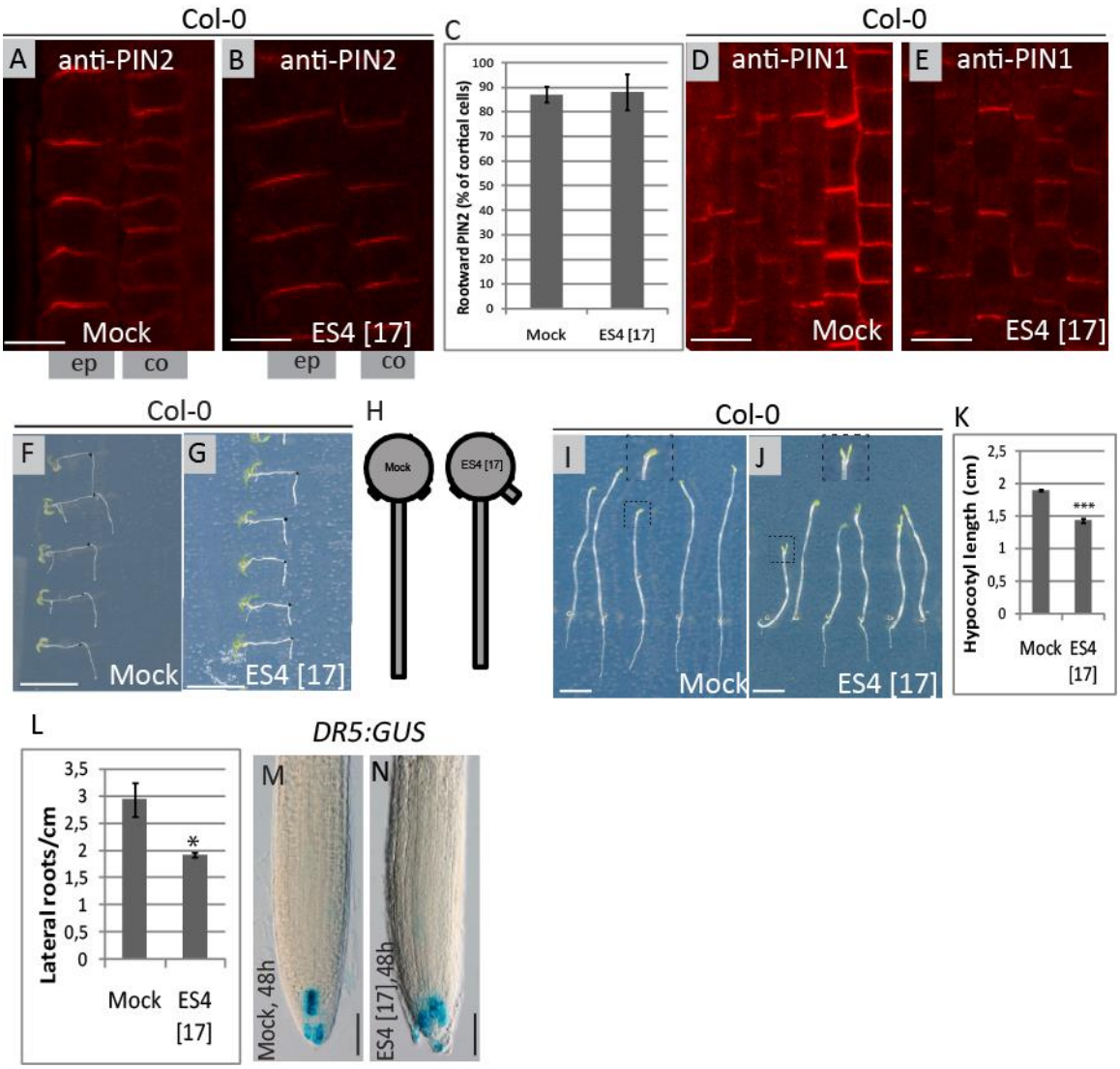

Supplemental Figure 2. Characterization of the ES4 effect.

(A) to **(E)** Immunolocalization of PIN2 in epidermal (ep) and cortex (co) cells [**(A)** and **(B)**] and PIN1 in the stele [**(D)** and **(E)**] of 5-day-old Col-0 seedlings and quantification of basal PIN2 in cortical cells **(C)**. Three-day-old seedlings were transferred on medium supplemented with mock or 17 µM ES4 and grown for 48 h. After mock treatment, PIN2 shows an apical localization in the epidermis and older cortex cells and a basal localization in young cortex cells **(A)**, whereas PIN1 is localized basally in the stele. No changes in PIN2 and PIN1 localizations were observed after the ES4 treatment [**(B)** and **(E)**]. Evaluation of PIN2 localization **(C)** shows no significant changes in the polar localization between ES4 and mock-treated samples ($P > 0.05$, by Student's t test). In four independent experiments, at least 26 roots were analyzed per treatment in total. Error bars represent SE. Bars = 10 µm.

(F) to **(H)** Response of 7-day-old Col-0 seedlings gravistimulated for 48 h and quantification of the root gravitropic response. Seedlings were grown on medium supplemented with mock or 17 µM of ES4. After 5 days, plates were turned 90° for another 48 h. Seedlings grown on 17 µM ES4 **(F)** showed positive gravitropic responses as observed for the control **(G)**. Gravistimulated roots were assigned to one of the eight 45° sectors on a gravitropism diagram **(H)**. Percentage of seedlings assigned to the respective sector. Three independent experiments were done with at least 72 roots analyzed per treatment in total. Bars = 1cm.

(I) to **(K)** Hypocotyl length sensitivity of 7-day-old Col-0 seedlings grown in the dark on medium supplemented with mock or 17 µM of ES4 and quantification **(K)**. Hypocotyls grown on ES4 had open and shorter cotyledons **(J)** than the control with closed cotyledons formed

in the apical hook **(I)**. Insets, magnified cotyledons. In three independent experiments, at least 24 hypocotyls were analyzed for each assay. Error bars represent SE. Student's *t*-test, ***$P < 0.001$. Bars = 0.5 cm.
(L) Quantification of lateral roots density in 11-day-old Col-0 seedlings grown on medium supplemented with mock or 17 µM of ES4. Three independent experiments were done with 20 roots analyzed for each assay. Error bars represent SE. Student's *t*-test, *$P < 0.05$.
(M) and **(N)** GUS staining of 5-day-old *DR5:GUS* seedlings. Three-day-old seedlings were transferred on growth medium supplemented with mock **(M)** or 17 µM ES4 **(N)** and grown for 48 h. Bars = 100 µm.

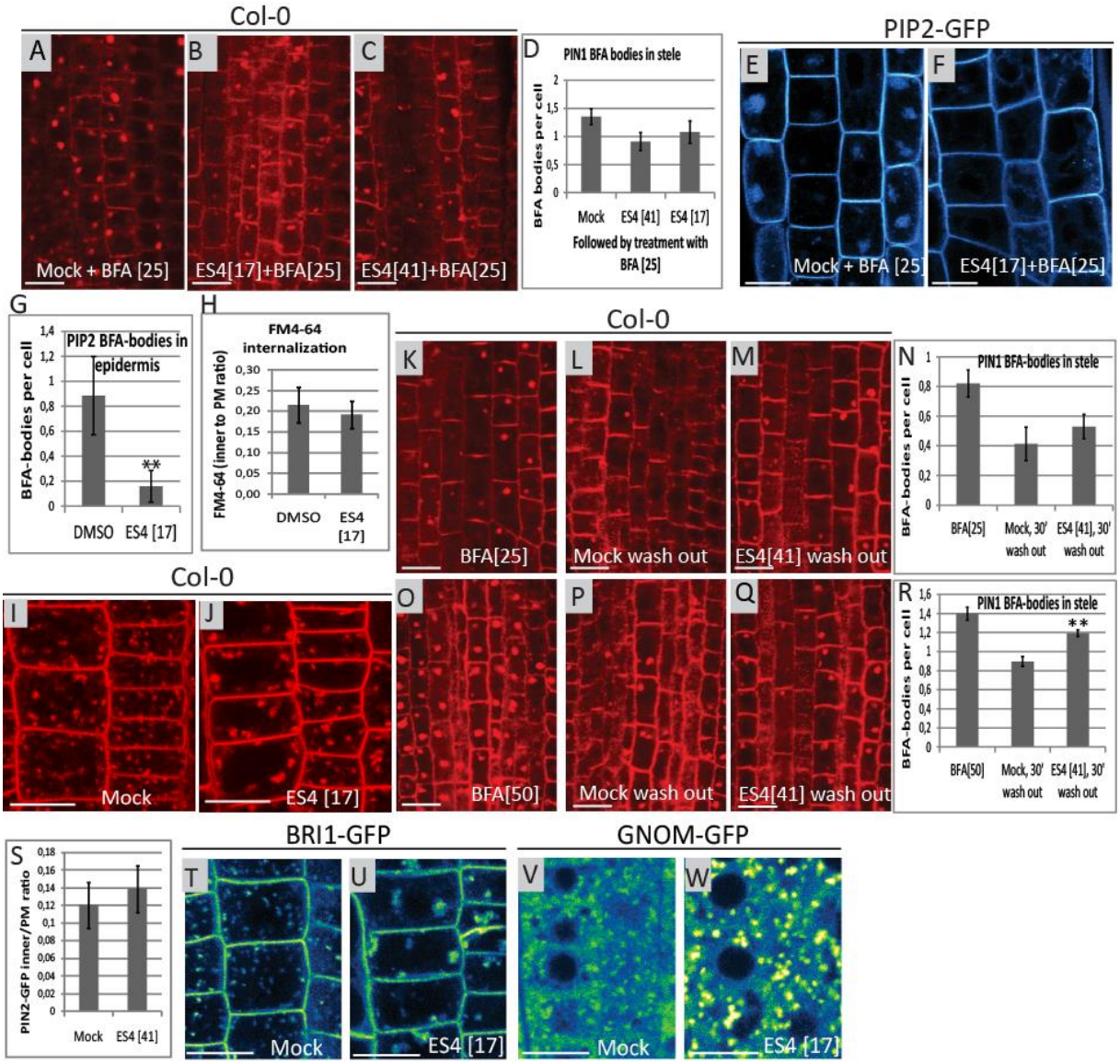

Supplemental Figure 3. Effect of ES4 on intracellular trafficking and compartments.
(A) to **(D)** Immunolocalization of PIN1 (red signal) in the stele and number of BFA bodies per cell. Seedlings were pretreated for 30 min. with 17 µM or 41 µM ES4 before addition of 25 µM BFA for an additional 90 min. Compared to mock **(A)**, the number of BFA bodies was not significantly reduced after ES4 treatment ($P > 0.05$, by Mann-Whitney *U* test) [**(B)** and **(C)**]. Quantification of BFA bodies in the stele was counted for 10 cells in each root. In four independent experiments, 20 (for 17 µM) or 41 (for 41 µM) roots were analyzed in total. Error bars represent SE. Bars = 10 µm.
(E) to **(G)** Life imaging of PIP2-GFP **(E** and **F)** and number of PIP2-labeled BFA bodies **(G)**. Five-day-old seedlings were pretreated for 30 min. with mock or 17 µM ES4 before addition of 25 µM BFA for an additional 90 min. Compared to mock **(E)**, the number of BFA bodies had decreased after ES4 treatment **(F)**. Bars = 10 µm.
(H) to **(J)** Uptake of endocytic tracer dye FM4-64 (2 µM) after 10 min. Five-day-old Col-0 seedlings were pretreated for 2 h with mock **(I)** or 17 µM ES4 **(J)**. No difference in uptake of FM4-64 was observed after ES4 treatment **(J)** compared with the mock **(I)** ($P > 0.05$, by Student's *t* test). FM4-64 uptake was quantified by dividing the mean grey value of the fluorescent signal inside the cell to the adjacent PM signal **(H)**. Six independent experiments were done with at least 23 roots analyzed for each treatment in total. Error bars represent SE. Bars = 10 µm.

(K) to **(R)** Immunolocalization of PIN1 (red signal) in the stele [**(K)** to **(M)** and **(O)** to **(Q)**] and number of BFA bodies per cell after wash-out with ES4. Five-day-old seedlings were treated for 2 h with 25 µM **(K)** or 50 µM BFA **(O),** followed by 30 min of wash-out with medium complemented with mock [**(L)** and **(P)**] or 41 µM ES4 [**(M)** and **(Q)**]. Three independent experiments were done with 5-49 cells analyzed for each root and for 16-23 roots for each treatment in total. Error bars represent SE. Mann-Whithey *U* test, ***P* < 0.01. Bars = 10 µm.
(S) Ratio of the intracellular to the PM PIN2-GFP signal. Seedlings were treated as described (Figure 2G to 2L). For each root, 32-63 cells were analyzed and 15 roots for each treatment. There was no significant difference between mock and ES4 treatments (*P* > 0.05, by Student's *t* test). Error bars represent SD.
(T) to **(W)** Intracellular localization of BRI1-GFP [**(T)** and **(U)**] and GNOM-GFP [**(V)** and **(W)**] after mock [**(T)** and **(V)**] and 17 µM [**(U)** and **(W)**] ES4. After 2 h of ES4 treatment, all markers displayed an intracellular signal accumulation when compared to the controls. Bars = 10 µm.

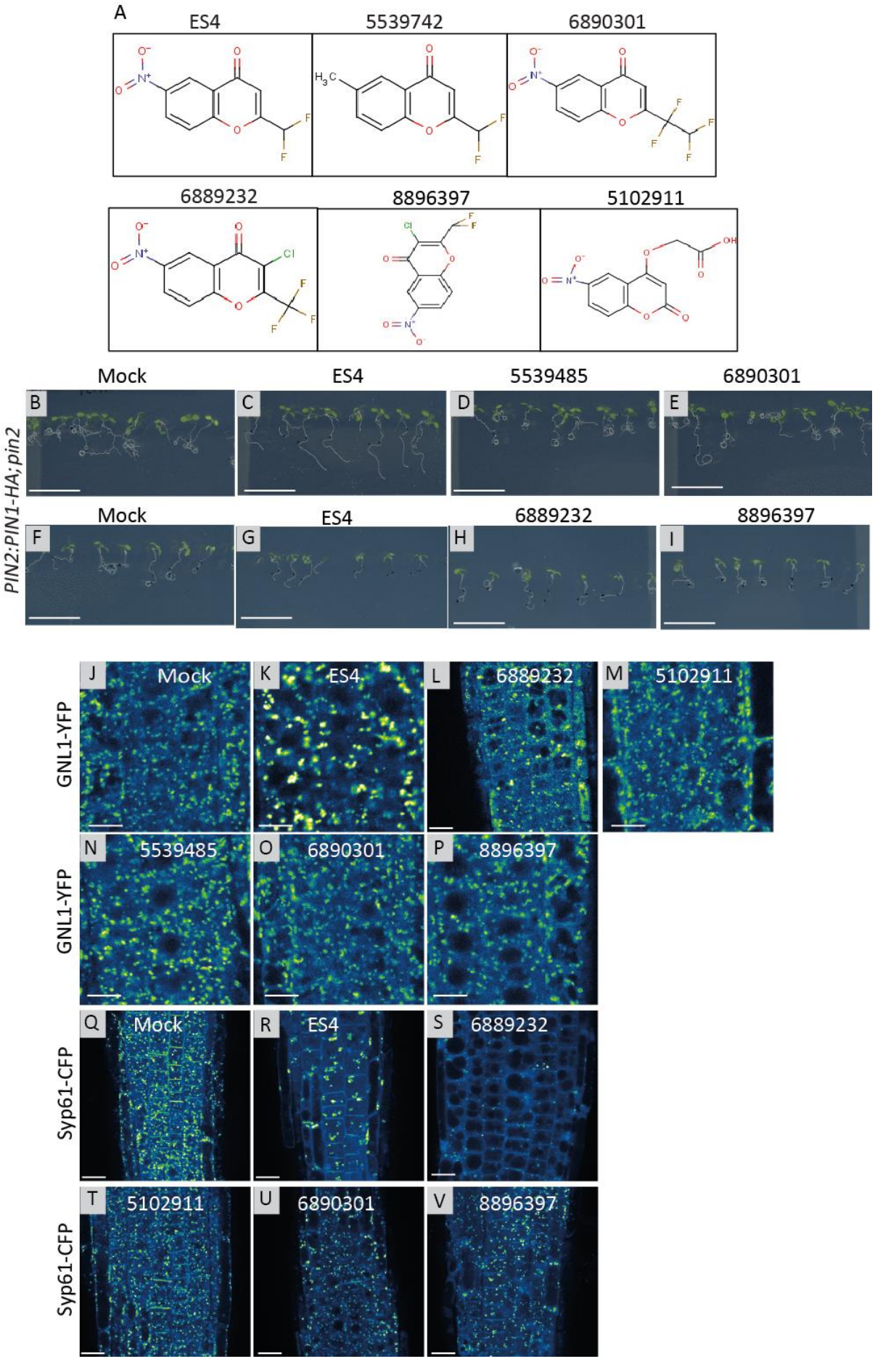
A
ES4
5539742
6890301
6889232
8896397
5102911
Mock
ES4
5539485
6890301
PIN2:PIN1-HA;pin2
Mock
ES4
6889232
8896397
GNL1-YFP
Mock
ES4
6889232
5102911
GNL1-YFP
5539485
6890301
8896397
Syp61-CFP
Mock
ES4
6889232
Syp61-CFP
5102911
6890301
8896397

Supplemental Figure 4. Search for ES4 bioactive analogue.

(A) Chemical structures of ES4, 5539742, 6890301, 6889232, 8896397 and 5102911.

(B) to **(I)** Response of 10-day-old **(B)** to **(E)** or 8-day-old **(F)** to **(I)** gravistimulated *PIN2:PIN1-HA;pin2* seedlings. Seedlings were gravistimulated twice, at the 6-day-old stage and 24 h later. Seedlings were grown on medium supplemented with mock or a set of five chemicals, of which four were diluted in a growth medium at 1:2400 from a stock concentration of 10 mg/ml. ES4 was used at 17 µM. None of the four chemicals showed rescue of *PIN2:PIN1-HA;pin2* agravitropic root growth when compared to the root growth on the ES4. Bars = 1 cm.

(J) to **(V)** Intracellular localization of GNL1-YFP [**(J)** to **(P)**] and Syp61-CFP [**(Q)** to **(V)**] after mock [**(J)** and **(Q)**], 17 µM [**(K)** and **(R)**] ES4, 6889232 [**(L)** and **(S)**], 5102911 [**(M)** and **(T)**], 5539485 **(N)**, 6890301 [**(O)** and **(U)**] and 8896397 [**(P)** and **(V)**] treatment. After 2 h of chemicals treatment, only ES4 induced an intracellular signal accumulation of both markers, when compared to the controls. Bars = 10 µm.

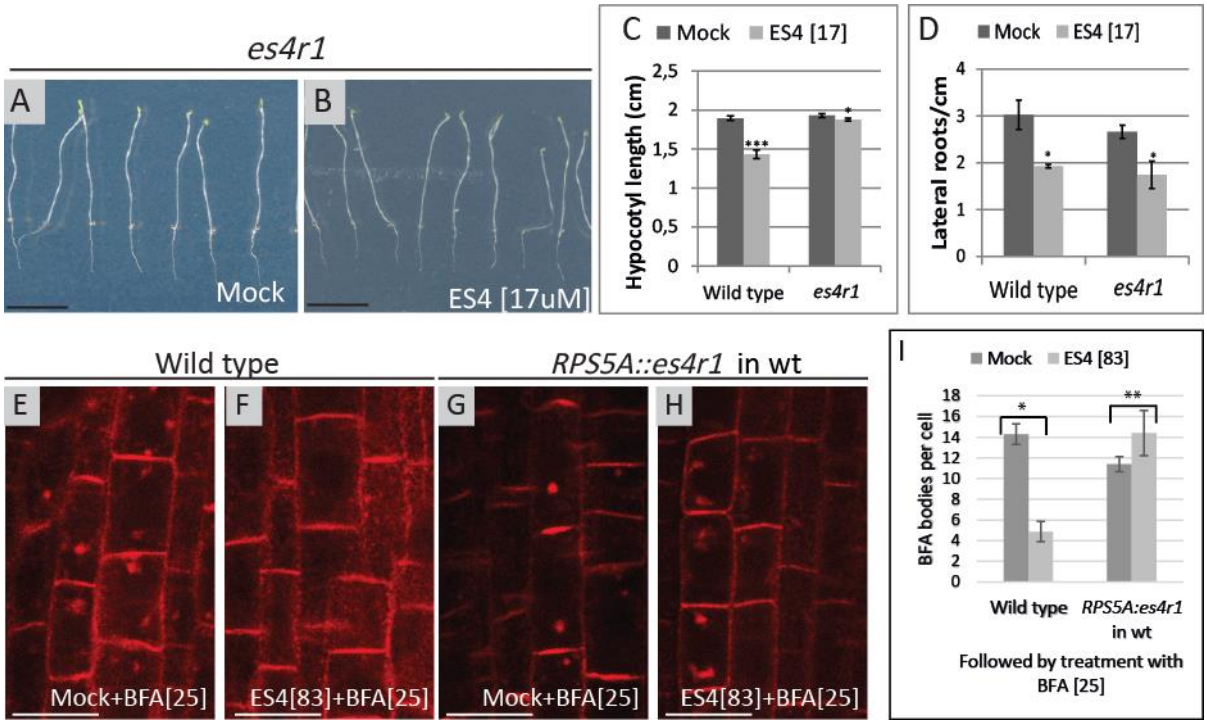

Supplemental Figure 5. Characterization of the *es4r1* sensitivity to ES4.
(A) to **(C)** Hypocotyl length sensitivity of 7-day-old *es4r1* seedlings grown in the dark on medium supplemented with mock **(A)** or 17 µM ES4 **(B)** and quantification **(C)** and comparison with the results obtained for wild type. The lengths of the hypocotyls grown on ES4 **(A)** was slightly shorter than those of the control **(B)**. Three independent experiments were done with 30 hypocotyls analyzed per treatment per experiment. Error bars represent SE. Student's *t*-test, **P* < 0.05, ****P* < 0.001. Bars = 1 cm.
(D) Quantification of lateral root densities in 11-day-old *es4r1* seedlings grown on medium supplemented with mock or 17 µM ES4 and comparison with the results obtained for wild type. In three independent experiments, 20 roots were analyzed per treatment per experiment. Error bars represent SE. Student's *t*-test, **P* < 0.05.
(E) to **(I)** Immunolocalization of PIN1 (red signal) in stele cells of Col-0 [**(E)** and **(F)**] and *RPS5A:es4r1* in Col-0 background. Five-day-old seedlings were pretreated for 30 min with mock [**(E)** and **(G)**] or 83 µM ES4 [**(F)** and **(H)**] before addition of 25 µM BFA for an additional 90 min. BFA bodies were observed in *RPS5A:es4r1* in a Col-0 background after ES4 treatment **(H)** when compared to the mock treatment in which almost no BFA bodies were visible **(F)**. The number of BFA bodies in the stele was counted for 10 cells in each root **(I)**. In one experiment, 5-7 roots were analyzed for each treatment. Error bars represent SE. Mann-Whitney *U* test, **P* < 0.05, ***P* < 0.01. Bars = 10 µm.

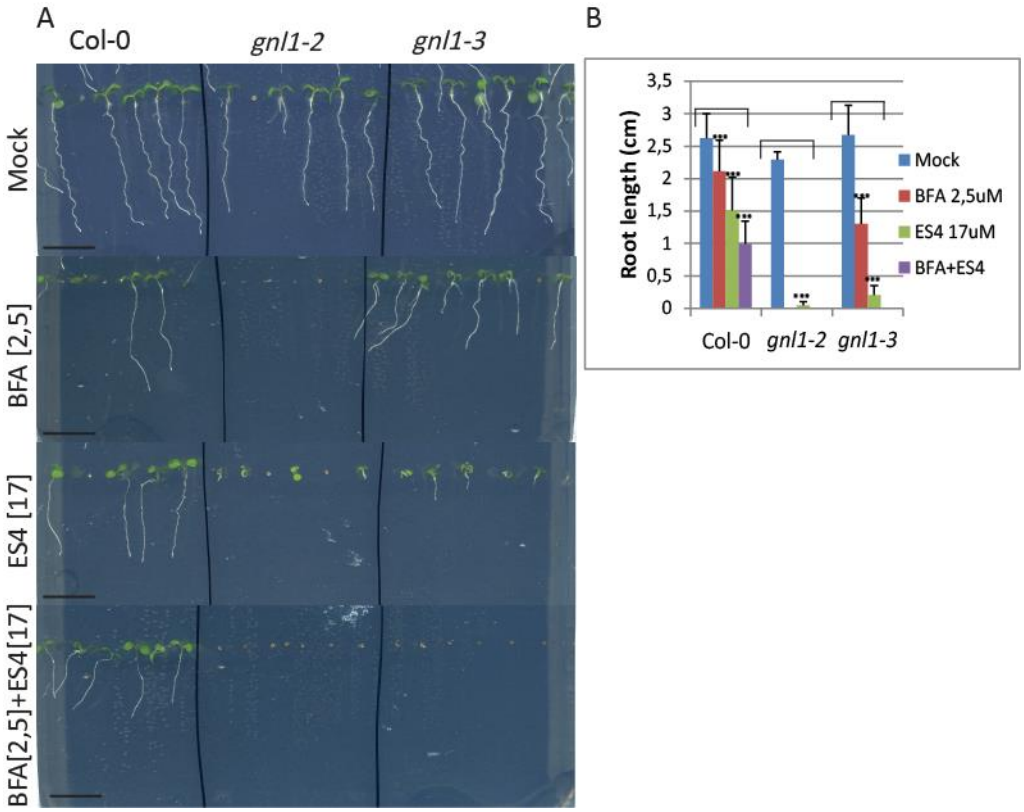

Supplemental Figure 6. Characterization of ES4 and BFA sensitivities of ARF GEFs.
(A) and **(B)** Root length sensitivities of 7-day-old Col-0, *gnl1-2* and *gnl1-3* seedlings grown on medium supplemented with mock, 2.5 µM BFA, 17 µM ES4 or 2.5 µM BFA plus 17 µM ES4. One experiment was done with at least 13 roots analyzed per treatment. Error bars represent SD. Student's *t*- test, ***$P < 0.001$. Bars = 10 µm.

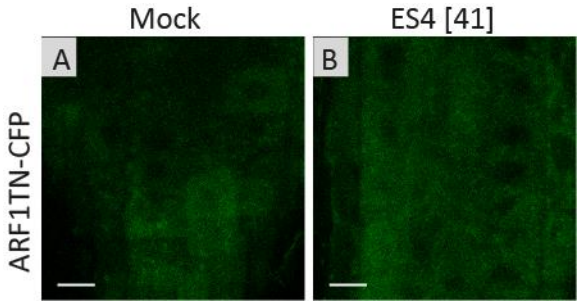

Supplemental Figure 7. Effect of ES4 on ARF1^{T31N}-CFP marker.
(A) and **(B)** Intracellular localization of ARF1^{T31N}-CFP. Five-day-old seedlings were induced by heat shock at 37°C for 2 h and treated with mock and 41 µM ES4. In mock and ES4-treated samples, the localization was only cytosolic. Bars = 10 µm.

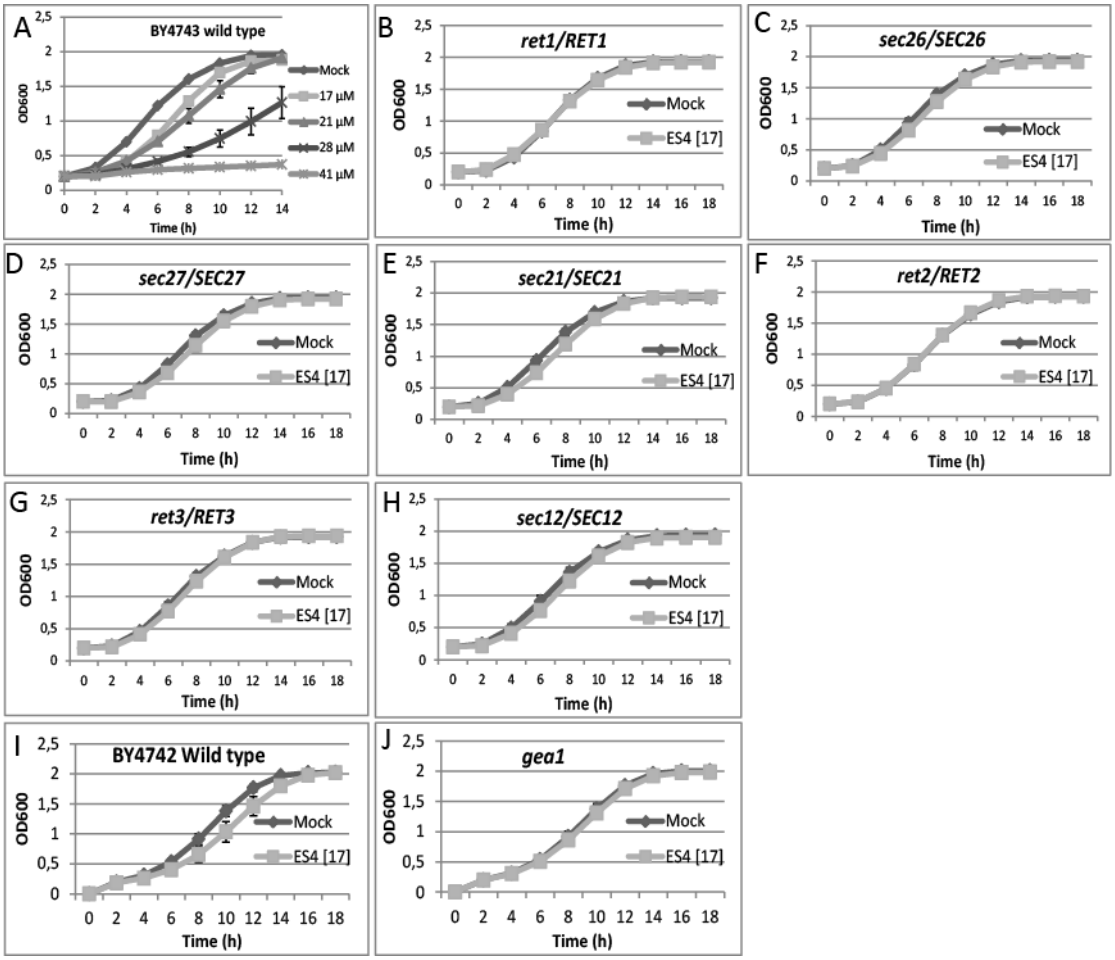

Supplemental Figure 8. ES4 sensitivity of deletion yeast strains.
(A) to **(H)** Growth of wild-type (BY4743) **(A),** *ret1/RET1* **(B)**, *sec26/SEC26* **(C)**, *sec27/SEC27* **(D)**, *sec21/SEC21* **(E)**, *ret2/RET2* **(F)**, *ret3/RET3* **(G)**, *sec12/SEC12* **(H)**, wild-type (BY4742) **(I),** and *gea1/gea1* **(J)** strains in function of time (hours). Strains were grown in YPD liquid medium with or without ES4 treatment as indicated. Growth curves were obtained with a H1 Microplate Reader (BioTek) and represent the average of three independent experiments. There was no significant differences between mock and ES4 treatments ($P > 0.05$, by Student's *t* test).

ORF	Name	Encoded protein
YDL145C	*RET1*	alfa-COPI
YDR238C	*SEC26*	beta-COPI
YGL137W	*SEC27*	beta'-COPI
YNL287W	*SEC21*	gamma-COPI
YFR051C	*RET2*	delta-COPI
YPL010W	*RET3*	teta-COPI
YDR170C	*SEC7*	ARFGEF
YNR026C	*SEC12*	GEF

Supplemental Table 1. Heterozygous deletion strains used in the growth assay.

Chapter 3

Endosidin 6, a novel inhibitor of cell wall biosynthesis affects polarity and development in *Arabidopsis*

Urszula Kania,[a,b] Stéphanie Robert,[a,c] Samantha Vernhettes,[d] Grégory Mouille,[d] and Jiří Friml[a]

[a]Institute of Science and Technology Austria, 3400 Klosterneuburg, Austria

[b]Department of Plant Systems Biology, VIB and Department of Plant Biotechnology and Bioinformatics, Ghent University, 9052 Gent, Belgium

[c]Umeå Plant Science Centre (UPSC), Department of Forest Genetics and Plant Physiology, Swedish University of Agricultural Sciences, 90183 Umeå, Sweden

[d]Laboratoire de Biologie Cellulaire, Institut National de la Recherche Agronomique, 78026 Versailles cedex, France

ABSTRACT

Polarity is fundamental feature of living organisms, enabling cellular function and multicellular development. In plants, polarly localized PIN proteins transport auxin in a cell-to-cell manner and help to establish differential auxin distribution. In plant tissue, these so called auxin gradients are required for many developmental processes and responses to the environment. One of the known components involved in maintenance of polar PIN localization is the cell wall. Here we identified in a chemical genomic screen a small molecule endosidin 6 (ES6), which interferes with the basal localization of PIN-FORMED1 (PIN1) proteins. Plant treatments with ES6 induced phenotypes similar to the cellulose defective mutants, including radial swelling of the roots; depletion of CELLULOSE SYNTHASEs (CESAs) markers from the plasma membrane; formation of MICROTUBULE ASSOCIATED CELLULOSE SYNTHASE COMPARTMENTS (MASCs); and changed composition of the cell wall. These observations identified ES6 as a new tool inhibiting cellulose synthase and interfering with cell wall composition.

AUTHOR CONTRIBUTIONS

U.K., S.R., and J.F. conceived the project. S.V. conducted confocal microscopy experiments visualising MASCs. G.M. measured primary cell wall sucrose composition. U.K. performed the majority of the experiments and analysed the data. U.K. wrote the manuscript. J.F. revised and corrected the manuscript.

INTRODUCTION

Polar localization of the PIN auxin efflux carriers is crucial for directional transport of auxin, which is involved in many developmental processes (Grunewald and Friml, 2010). Different factors are involved in establishment of PIN polarity, including intracellular vesicle trafficking (reviewed in Luschnig and Vert, 2014), plasma membrane composition (Carland et al., 2010; Men et al., 2008; Willemsen et al., 2003), cytoskeleton (Geldner et al., 2001; Kleine-Vehn et al., 2006) and phosphorylation (Huang et al., 2010; Zhang et al., 2010). It has been shown that cell wall also plays a role in maintaining polarity of PIN proteins (Feraru et al., 2011). The plant cell wall is a rigid structure that provides structural support and protection for cells. It connects neighboring cells together, prevents them from moving, and influences their localization in the tissue. However, it is not only the mechanical structure which strengthens the body of plants, but it is also important in the dynamic response to intracellular and environmental signals. Loosening and rearrangements of the cell wall is required for cell elongation and is initiated by auxin (reviewed in Perrot-Rechenmann, 2010). Identification of *regulator of PIN polarity* (*repp3*) mutant, defective in cell wall formation and polar PIN localization, revealed connections between polar PIN domains at the plasma membrane and the cell wall (Feraru et al., 2011). Disruption of cell wall by genetic, pharmacological, or mechanical interference breaks the connections and consequently leads to lateralization and complete loss of PIN polarity (Feraru et al., 2011). Additionally it has been shown that isoxaben, a known chemical that inhibits cellulose synthesis, reduces the thickness of the cell wall and leads to localization of PIN1-GFP to the corners of the meristematic cells (Hamant et al., 2011; Heisler et al., 2010). Connection between cell polarity and cell wall is represented in rapid and highly polarized growth of root hairs and pollen tubes. They are formed through tip elongation of cells, which require deposition of new cell wall material at the precise end of the growing cell. Growth of root hairs is similar to growth of pollen tubes requiring action of Rho of Plants (ROP)-GTPases, formation of tip-focused Ca^{2+} gradient, and vesicle delivery to the apical region (Gu and Nielsen, 2013). Consequently, many mutants defective in cellulose synthesis, one of the components of the cell wall next to the hemicelluloses and pectins, display defects in root hair formation (Caño-Delgado et al., 2000; Gu and Nielsen, 2013).

Herein, we took advantage of chemical genomics approach to identify components involved in polar PIN localization and maintenance. Recently a chemical genomic screen was performed on a library of chemicals to select small molecules interfering with intracellular trafficking (Drakakaki et al., 2011). The first selection was based on the ability of small molecules to inhibit or affect highly polarized growth of pollen tubes. In the second screen, chemicals affecting localization of fluorescently labelled proteins were chosen and

classified according to the induced phenotype. One of the chemical clusters contained molecules interrupting ectopic polar localization of PIN1 in the *PIN2:PIN1-GFP;pin2* line (Drakakaki et al., 2011). From those chemicals, we characterized endosidin 6, which we found is a specific inhibitor of cellulose synthase localization and interferes with cell wall composition.

RESULTS

Identification of the Endosidin 6 Compound Affecting Polarity of *PIN2:PIN1-HA*

From the cluster of chemicals interfering with the ectopic, predominantly basal (rootward), PIN1 localization in *PIN2:PIN1-GFP;pin2* line (Drakakaki et al., 2011; Wiśniewska et al., 2006) we analyzed a set of 11 molecules in term of their effect on the PIN1 localization (Figure 1A). To select those with the strongest effect leading to the basal-to-apical switch of PIN1 in *PIN2:PIN1-HA; pin2*, seedlings were grown for 48h on medium supplemented with small molecules and an immunolocalization with anti-PIN1 antibody was performed. Endosidin 6 (Figure 1B) was identified as the most effective small molecule, inducing apicalization of ectopically expressed PIN1 in about 82% of analyzed epidermal cells at the concentration of 6 μM (Figure 1C to 1E).

Additionally we analyzed PIN2 polarity in the cortex cells of wild-type seedlings after 48 h of 6 μM ES6 treatment. Since PIN2 displays dual localization in the cortex cells, basal in young cells, and apical in older cortex cells that are more distant from the root tip (Kleine-Vehn et al., 2008), it is a sensitive system to test factors for their effects on PIN polarity. Thus, some factors might induce basal-to-apical shift of PIN2 in the young cortex cells, while having no obvious effect on PIN polar localization in other tissues. However, despite ES6 clearly have effect on the polarity of ectopically expressed PIN1 in epidermis, it did not visibly affect the polar localization of PIN2 in cortex cells (Supplemental Figure 1A).

Next we tested the effect of ES6 on the expression of *DR5:GUS'* auxin response reporter (Figure 1F to 1I). A less pronounced auxin response maximum in the root meristem (Sabatini et al., 1999) and visibly induced DR5 activity in the whole root tip, and in particular in the elongation zone, was observed already after treatment with 4 h of 6 μM ES6. This suggests increased auxin flow away from the root tip consistent with more apicalized PIN proteins as a result of the ES6 treatment. Thus, it is possible that despite no visible changes in PIN polarities being detected on the level of individual cells, the ES6-mediated partial apicalization occurs in the wild-type, leading to the ectopically increased auxin response in the elongation zone.

To determine essential structural determinants of ES6 bioactivity the structure activity relationship was performed (SAR). Two chemicals with chemical structure similar to the ES6

(Supplemental Figure 2A) were tested for their ability to restore gravitropic growth of *PIN2:PIN1-HA; pin2* seedlings (Supplemental Figure 2B to 2E) and effects on intracellular agglomeration of CESA3 marker (Supplemental Figures 2F to 2I). These two chemicals differed in modifications of the phenolic and the bicyclic rings. 7813952 molecule generated similar phenotype changes as ES6, including less curly root growth, depletion of marker signal from the PM and its intracellular accumulation. These results indicate, that the bicyclic structure is important for ES6 activity and 7813952 is a bioactive molecule.

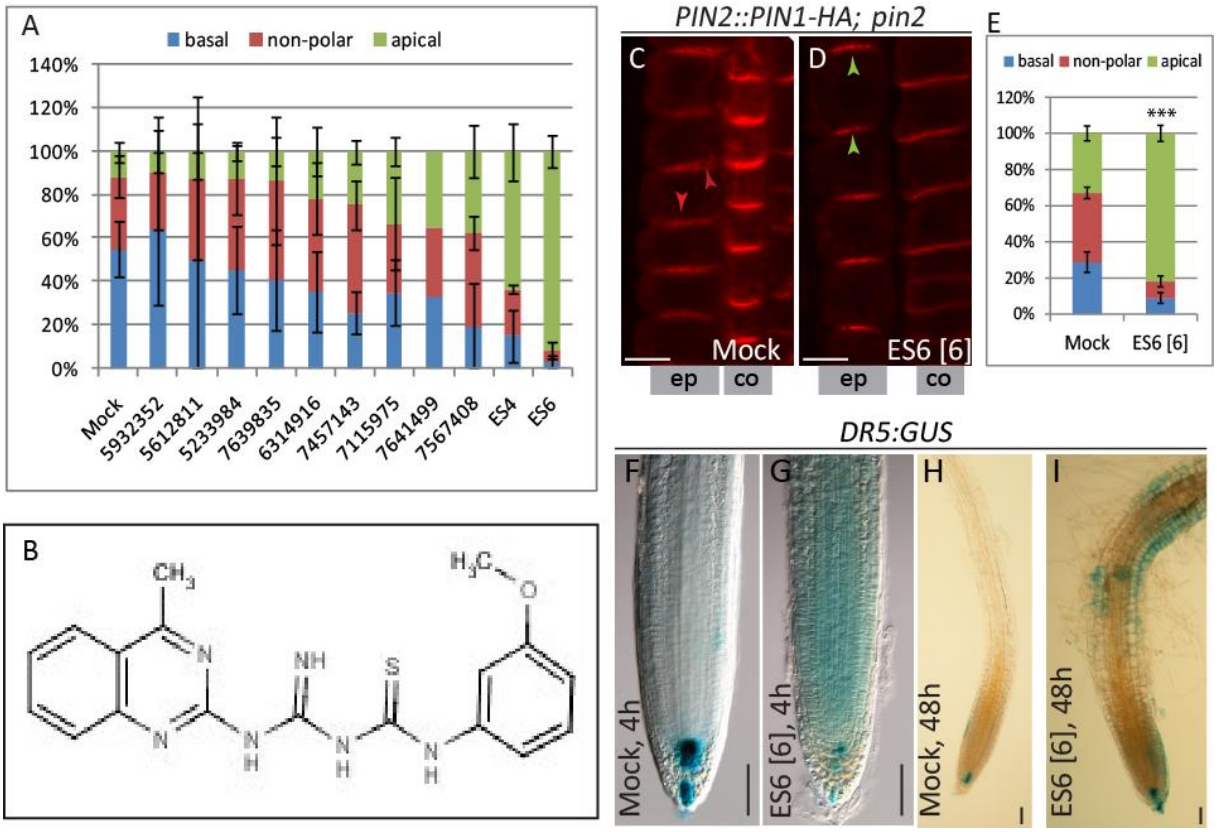

Figure 1. Identification of ES6 chemical.
(A) Evaluation of the PIN1-HA localization in *PIN2:PIN1-HA;pin2* epidermal cells after chemical treatments followed by immunolocalization. Three-day-old *PIN2:PIN1-HA;pin2* seedlings were transferred on growth medium supplemented with mock or a set of 11 chemicals and grown vertically for 48 h. Eight of the chemicals were diluted in a growth medium at 1:200 from a stock concentration of 10 mg/ml; ES4 was used at 17 µM and ES6 at 6 µM. The *PIN2:PIN1-HA;pin2* line showed predominantly a basal and nonpolar PIN1-HA localization. Among the 11 tested compounds, ES6 had the most prominent effect on PIN1-HA apicalization in epidermal cells. Two to four independent experiments were done for each chemical and one experiment for the ID7641499 small molecule. Data are means ± SE of two to four experiments. Error bars represent SE. Chemical numbers are the Chembridge IDs.
(B) Chemical structure of ES6.
(C) to **(E)** Immunolocalization of PIN1-HA in epidermal (ep) and cortex (co) cells. After mock treatment **(C)** PIN2:PIN1-HA;*pin2* shows predominantly basal and nonpolar PIN1-HA localization (red arrowheads), whereas after ES6 treatment **(D)** (6 µM; 48 h) shows predominantly apical PIN1-HA in epidermal cells (green arrowheads). Evaluation of PIN1-HA

localization in epidermal cells **(E)** indicates that after ES6 treatment, 82% of PIN2:PIN1-HA;*pin2* epidermal cells display a predominantly PIN2-like localization of PIN1-HA at the apical side, contrasting to mock-treated PIN2:PIN1-HA;*pin2*, that has a predominantly nonpolar and basal PIN1-HA localization. In eight independent experiments, at least 70 roots were analyzed in total for the mock and ES6 treatments. Data are means ± standard error (SE) of eight experiments. Student's *t* test, ***P < 0.001. Bars = 10 µm.
(F) to **(I)** GUS staining of five-day-old DR5:GUS seedlings. Five-day-old seedlings were mounted in liquid medium supplemented with mock **(F)** or 6 µM ES6 **(G)** for 4 h; or three-day-old seedlings were transferred on growth medium supplemented with mock **(H)** or 6 µM ES6 **(I)** and grown for another 48 h. Induced GUS staining was observed in ES6 treated seedlings [**(G)** and **(I)**] when compare to mock [**(F)** and **(H)**] treatment. Bars = 10 µm.

Endosidin 6 effects on plant growth and development

Next we analyzed the ES6 effect on the gravity response of *PIN2:PIN1-HA; pin2*. In wild-type plants PIN2 is localized at the apical (shootward) side of epidermal root cells that enables auxin transport from the root tip towards the elongation zone. Ectopically localized PIN1 proteins on the basal side of epidermal cells in *PIN2:PIN1-HA; pin2* are not able to transport auxin away from the root tip, which results in their agravitropic root growth (Wiśniewska et al., 2006). We expected that the basal-to-apical shift of PIN1, induced by chemical treatment restores the gravitropic response in *PIN2:PIN1-HA; pin2.* After five days of growth on 0.5 or 1.4 µM ES6, vertically located plates were turned by 90° (gravistimulation) (Supplemental Figure 1B to 1E). Although ES6 was very effective in inducing the apical PIN1 localization, (see above) it did not rescue the gravity response of *PIN2:PIN1-HA; pin2* (Supplemental Figure 1B to 1D). In addition, application of 1.4 µM ES6 to the growth medium did not change the root gravity response in the wild-type (Supplemental Figure 1F to 1H).

Next we examined morphological responses of wild-type seedlings grown on 1.4 µM ES6, including primary root, lateral root, hypocotyl and root hair growth. Primary roots of ES6-treated seedlings were significantly shorter compared to the control (Figure 2A to 2C) and they showed an increased number of lateral roots in 11-day-old seedlings (Supplemental Figure 1I). Seedlings grown in the dark on 1.4 µM ES6 displayed shorter and thicker hypocotyls with open cotyledons, in contrast to the control seedlings with elongated hypocotyls and closed cotyledons forming an apical hook (Figure 2D to 2F). Additionally we observed an increased number of longer root hairs and root swelling induced by ES6 treatment (Figure 1I; 2G and 2H).

Similar phenotypes have been observed in cellulose synthase mutants, *cesa1*, *cesa3* and *cesa6*, displaying shorter root growth, radial swelling, increased root hair growth and density (Caño-Delgado et al., 2000). The same phenotypic effects can also be induced by isoxaben, a chemical which interferes with cellulose synthase activities (Desprez et al., 2002; Park et al., 2011; Scheible et al., 2001). Additionally *cesa* mutants display defects in pollen germination and pollen tube growth (Persson et al., 2007). A similar effect on tobacco pollen

has been observed for ES6, which was selected in the chemical screen as an inhibitor of pollen tube germination (Drakakaki et al., 2011). Notably, isoxaben treatment or *cesa* mutations also lead to basal-to-apical PIN1 polarity switch (Feraru et al., 2011) as induced by ES6. All these observations suggest that ES6 may interfere with some aspects of cellulose synthesis.

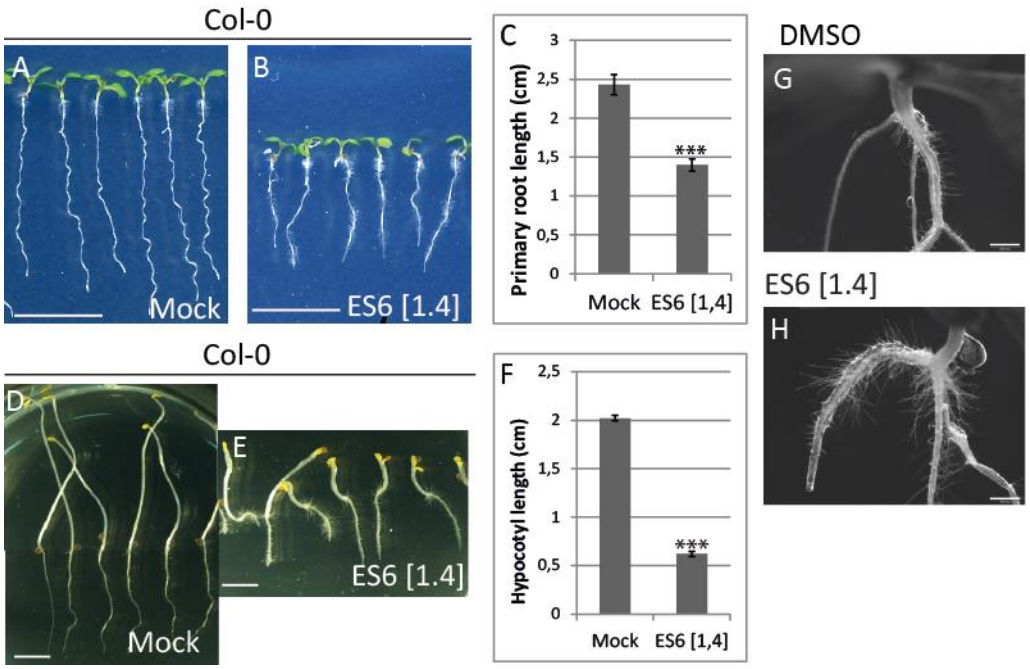

Figure 2. Morphological effects induced by ES6.
(A) to **(C)** Root length sensitivity to ES6 and quantification. Seven-day-old Col-0 seedlings grown on media supplemented with 6 μM ES6 had shorter primary root length **(B)** than the mock control **(A)**. In four independent experiments, at least 58 roots analyzed for each treatment in total **(C)**. Data are means ± SE of four experiments. Student's *t* test, ***P < 0.001. Bars = 1cm.
(D) to **(F)** Hypocotyl length sensitivity of seven-day-old Col-0 seedlings grown in the dark on medium supplemented with mock or 1.4 μM ES6 and quantification **(F)**. Hypocotyls grown on ES6 demonstrated reduced hypocotyls length **(E)** compared to the control **(D)**. In three independent experiments, at least 112 hypocotyls were analyzed for each treatment in total. Data are means ± SE of three experiments. Student's *t*-test, ***P < 0.001. Bars = 0.5 cm.
(G) to **(H)** Root hair growth in 11 day old Col-0 seedlings grown on mock or 1.4 μM ES6. Seedlings grown on ES6 **(H)** displayed denser and longer root hairs than that of the wild type control **(G)**. Bars = 500 μm.

Effects of Endosidin 6 on Intracellular Trafficking and Intracellular Compartments

To gain further insight in the mode of ES6 action we examined its effect on intracellular trafficking of various subcellular markers. First we tested whether ES6 affect endocytic or exocytic trafficking pathways. We used a fungal toxin brefeldin A (BFA), a known inhibitor of the ADP-ribosylation factor small GTPases (ARF-GEFs). PIN1 proteins cycle constantly between plasma membrane (PM) and intracellular compartments. This continuous trafficking

can be visualized by application of BFA, which inhibits PIN1 recycling and results in its accumulation in intracellular compartments called BFA-bodies (Geldner et al., 2001). An immunolocalization experiment with PIN1 antibodies on the wild-type seedlings treated with 6 µM ES6 for 30 min. followed by co-treatment with ES6 and 25 or 50 µM BFA did not show any difference in number of BFA-bodies per cell. This suggested that ES6 has no effect on the endocytosis of PIN1 (Supplemental Figure 3A to 3F). To examine the potential influence of ES6 on exocytosis, wild-type seedlings were treated with 25 or 50 µM BFA followed by wash-out with 6 µM ES6. Compared to the mock wash-out, the number of BFA-bodies did not significantly differ. This indicated that the exocytosis process was not affected by ES6 (Supplemental Figure 3G to 3N). Next we analyzed 5-day-old marker lines after 2 h treatment with 6 µM ES6, including CESA3 and CESA6 (cellulose markers), ARA7 (prevacuolar compartment / multivesicular bodies), CLATHRIN LIGHT CHAIN 2 (CLC2) (PM and trans-Golgi network (TGN)), MICROTUBULE ASSOCIATED PROTEIN 4 (MAP4) (microtubules), SIALYLTRANSFERASE (N-ST) (Golgi) and SYNTAXIN OF PLANTS 61 (Syp61) (TGN). Localization of fluorescent signal was not changed for ARA7, CLC2, MAP4, N-ST and Syp61 (Supplemental Figure 3O to 3X). However, the cellulose markers CESA3 and CESA6 were visibly affected (Figure 3A to 3D). CESAs in the roots are localized mainly at the lateral side of the cells and intracellularly at the TGN. After ES6 treatment, the lateral localization disappeared and bigger agglomerations of GFP-labelled proteins were observed intracellularly (Figure 3B and 3D). These results, together with the effect of ES6 on the hypocotyl and root hair growth, indicate that ES6 might affect cell wall formation.

Endosidin 6 Induce Formation of MASCs and Affects Cellulose Content of Primary Cell Wall

Next we tested the effect of ES6 on the formation of MASCs. In the elongated hypocotyls CELLULOSE SYNTHASE COMPLEXEs (CSCs) localize to the PM, Golgi bodies, VHAa1/GFP-CESA3-containing compartments and MASCs. Internalization of CSCs into the MASCs can be induced by treatment with the cellulose synthesis inhibitor CGA 325’615 or osmotic stress (Crowell et al., 2009). MASCs were identified by their fluctuating velocities and linear trajectories whereas Golgi bodies and the VHAa1/GFP-CESA3-containing compartments are characterized by rapid and non-linear movements. Additionally, movement and formation of MASCs depends on the dynamic cortical microtubule array (Crowell et al., 2009). 5-day-old seedlings expressing GFP-CESA3 together with microtubule marker mCherry:MICROTUBULE BINDING DOMAIN (MBD) were treated for 5 h with mock and 6 µM ES6 (Figure 3E to 3J). Compared to the mock control displaying bidirectional movement of CESA3 particles (Figure 3K),

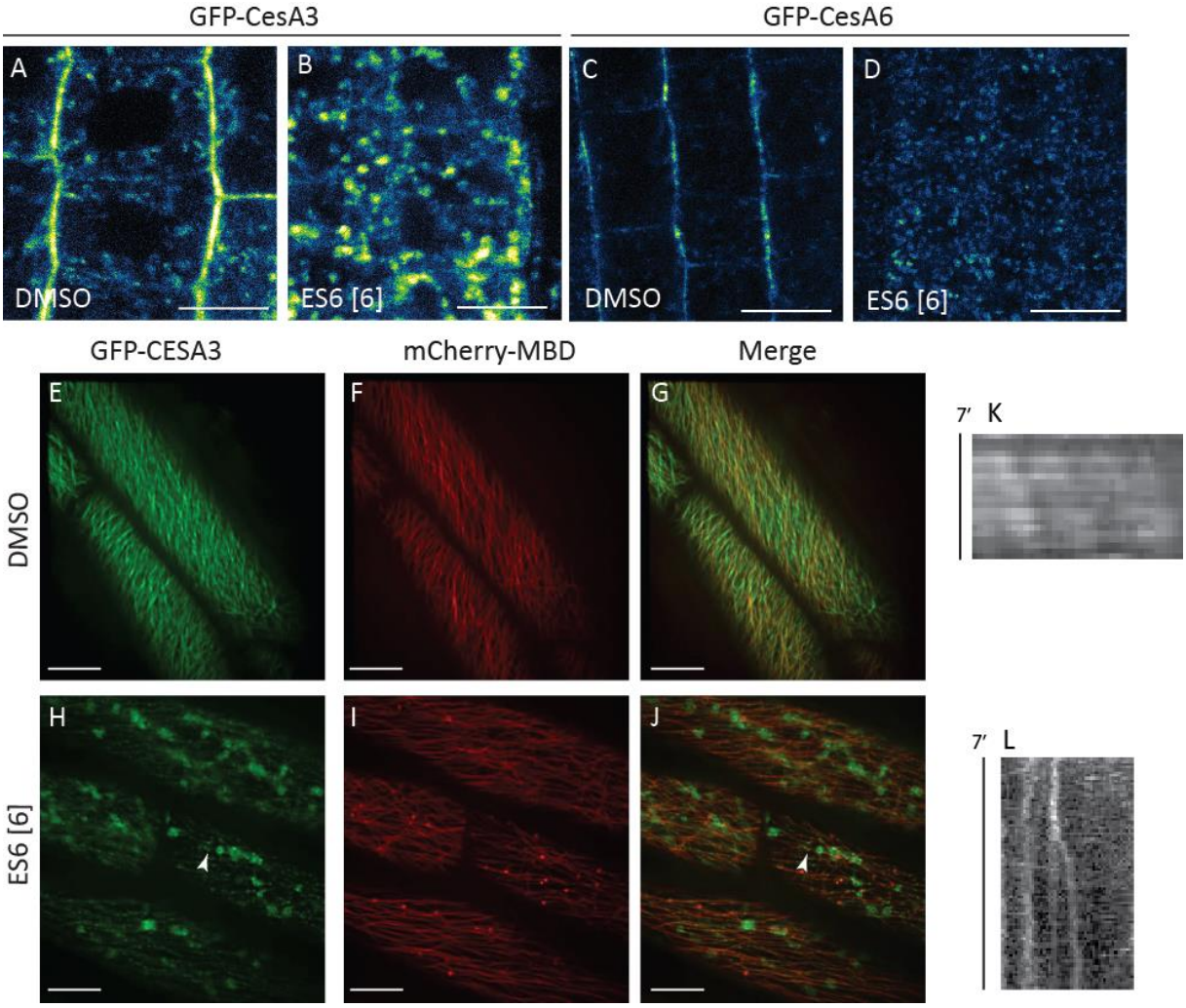

Figure 3. ES6 affects cellulose synthase complex.
(A) to **(D)** Intracellular localization of GFP-CesA3 and GFP-CesA6 in roots of five-day-old seedlings after mock [**(A)** and **(C)**] and 6 µM ES6 [**(B)** and **(D)**] treatment. After 2 h of ES6 treatment, both markers displayed reduced signal at the lateral PM an intracellular signal accumulation when compared to the controls. Bars = 10 µm.
(E) to **(J)** Intracellular distribution of GFP-CASA3 [**(E)** and **(H)**] and mCherry-MBD [**(F)** and **(I)**] in the five-day-old seedlings after 5 h of mock [**(E)** to **(G)**] and 6 µM ES6 [**(H)** to **(J)**] treatment in epidermal root cells. White arrows indicate GFP-CESA3 labelled MASC particles. Bars = 10 µm.
(K) and **(L)** Representative kymographs for treatment with mock **(K)** and 6 µM ES6 **(L)**. Time is represented along the vertical axis, and a 7 min scale bar is shown at left (for information on interpreting kymographs see Crowell et al., 2009). CSC movement is steady and bidirectional **(K)**. Erratic movements of CSC indicates presence of MASCs **(L)**.

ES6 treated seedlings presented discrete, small, bright particles labeled with GFP-CESA3 associated with cortical microtubules having erratic movement of GFP-CESA3 complexes (Figure 3L). Such fluctuating velocities indicate presence of MASCs. Formation of MASCs were also observed in GFP-CESA1 and GFP-CESA6 (Supplemental Figure 4A to 4H) indicating that ES6 is not CESA3 specific but affects the whole cellulose synthase complex. Next we compared cell wall composition of 5-day-old wild-type seedlings grown in the dark

on mock, 1.4 µM ES6 and 2 nM of established cellulose synthesis inhibitor isoxaben (Figure 4A). The hemicellulose (fucose, arabinose, rhamnose, galactose, glucose, xylose and mannose) and cellulose (glucose and xylose) assay was performed separately for hypocotyls and roots dissected from the same seedlings. The primary cell wall in plants is composed of three main polysaccharides: cellulose, hemicelluloses (mainly xyloglucan) and pectins (Cosgrove, 2005). The backbone of cellulose and hemicelluloses is comprised of β-1,4-linked glucan polymers. The hemicelluloses glucan polymers are highly modified with chains of xylose, galactose and fucose sugars. Inhibition of cellulose synthesis by chemical inhibitors like isoxaben leads to change in polysaccharide content of extracellular matrix an accumulation of lignin and callose (Desprez et al., 2002; His et al., 2001).

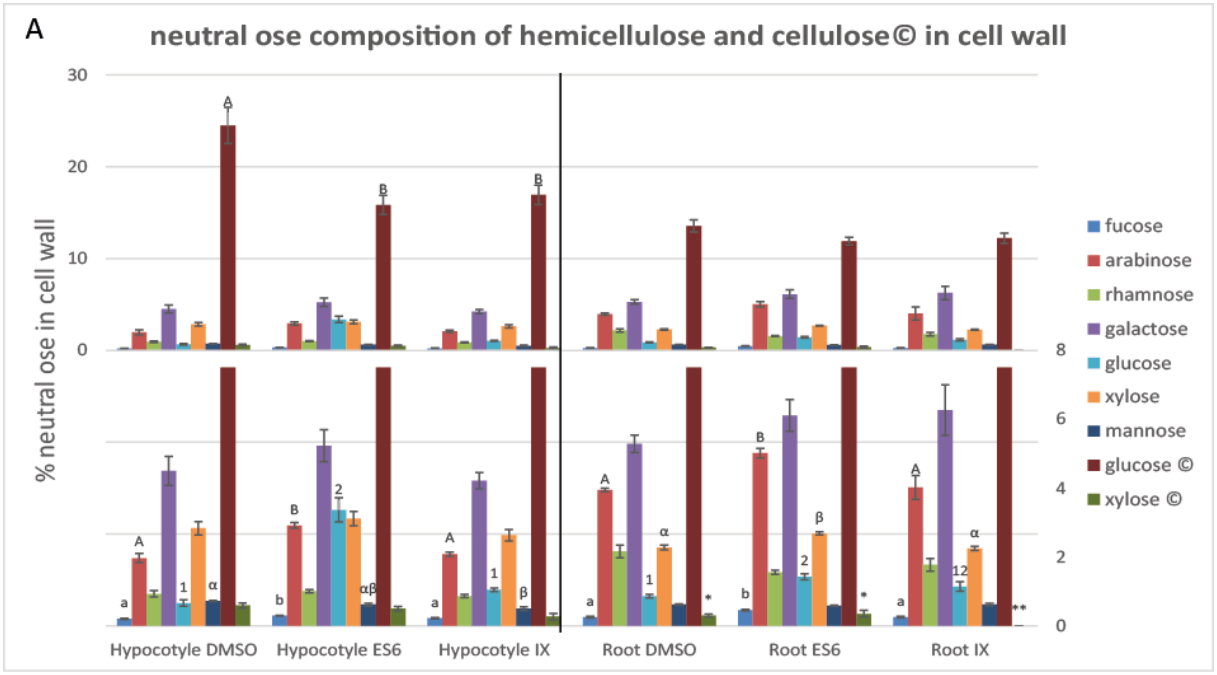

Figure 4. Effects of ES6 and isoxaben on cell wall sucrose composition.
(A) Neutral ose composition of hemicelluloses and cellulose in the cell wall. Five-day-old Col-0 seedlings grown on mock, 1.4 µM ES6 or 2 nm isoxaben (IX) supplemented medium in the dark. In three independent experiments, 100 mg of hypocotyl tissue plus corresponding roots was collected from each treatment. Different letters, numbers and number of asterisks indicate statistically significant differences between the treatments (ANOVA, $P < 0.05$). Upper and lower panels present the same data in different scales. Data are means ± standard deviation (SD) of three experiments.

ES6 and isoxaben treatment decrease the mannose and cellulosic glucose content of the dark grown hypocotyls (Figure 4A). Additionally, in the ES6-treated hypocotyls, the fucose, arabinose and hemicellulosic glucose content was increased, whereas in isoxaben-treated plants no change compared to mock was observed. Also in roots of ES6-treated seedlings fucose, arabinose and hemicellulosic glucose and xylose content was elevated when

compared to the mock and isoxaben-treated seedlings. Cellulosic xylose was decreased in roots of isoxaben-treated seedlings. The results suggests that ES6 targets cell wall biosynthesis but does not act exactly the same way as isoxaben, perhaps not directly on the CESA complex. Furthermore we tested different cellulose defective mutants, *je5*, *35S:THE1*, *eli1-1*, *prc1-1*, *rsw1-10* and *repp3*, for their sensitivity to ES6 (Supplemental Figure 4I). Seedlings were grown for 7 days on medium supplemented with 1.4 µM ES6. *eli1-1*, *prc1-1*, *rsw1-10* and *repp3* roots appeared to be slightly more sensitive when grown on ES6. However, such difference could be caused by reduced root length of mutants grown on mock and poor germination of *repp3*, which made it more difficult to measure. Such an explanation can be supported by the fact, that je5, another allel of CESA3 next to repp3, displays similar sensitivity to ES6 as the wild-type.

rcn1 mutant resistant to Endosidin 6 effect

To further dissect what intracellular trafficking pathways might be affected by ES6, we compared the root growth of 7-day-old wild-type and different trafficking mutants seedlings (*rcn1*, *van7*, *gnom*^{R5}, *axr2-1, vti12, chc1-2*, *big3*, *35S:PIN1*, *chc2-2*, *gnl1-3*, *ben1-2, 35S:PID21*, *gnl1-2*, *pin2*, *ben1-1* and *pid wag1 wag2*) (Figure 5A) on mock and 1.4 µM ES6. When compared to mock, none of those mutants showed increased sensitivity to ES6 as compared to the wild-type. On the other hand, the root growth of the *ROOT CURLING ON NPA (rcn1)* mutant displayed the highest resistance to ES6. *rcn1* is defective in A1 subunit of PROTEIN PHOSPHATASE 2 (PP2AA1), which, in addition to other roles, is involved in dephosphorylation of PIN proteins and basal PIN targeting (Michniewicz et al., 2007). PP2AA acts antagonistically to the PINOID (PID) kinase, which phosphorylate PIN proteins and mediate apical PIN targeting (Michniewicz et al., 2007; Zhang et al., 2010; Huang et al., 2010). AGC3 kinases mutant *pid wag1 wag2*, displayed slightly increased sensitivity to ES6, however, the difference was not statistically significant. Few other trafficking mutants (*vti12*, *chc1-2*, *big3*, *chc2-2*) or auxin signaling mutant *axr2-1* and PIN1 overexpression line revealed slight reduction of ES6 sensitivity when compared to the wild-type. Since *rcn1* was the only strongly ES6-resistant mutant, we analyzed other phosphatases loss-of-function and overexpression lines. We compared the root growth of 7-day-old seedlings on mock and 1.4 µM ES6 of *pp2aa3-2*, *F1OE*, *sac3 sac4 sac5*, *sal1*, *fypp3* (*f3)*, *fypp1* (*f1)*, *sal1OE* and *35S:SAC2* (Figure 5B). *F1OE*, *sal1*, *f3*, *f1* and *sa1OE pp2aa3* are lines defective in PP6-type phosphatase holoenzyme (Dai et al., 2012), whereas SUPPRESOR OF ACTIN (SAC) phosphatases mediate vacuolar trafficking and morphogenesis (Nováková et al., 2014). Among all tested lines no statistically significant difference in sensitivity to ES6 was detected when compare to the control. Additionally hypocotyl growth of *35S:SAC2*, *sac3 sac4 sac5* and *rcn1* was tested (Figure 5C). 7-day-old seedlings were grown on medium supplemented

with mock and 1.4 µM ES6. Compared to mock, only *rcn1* displayed increased resistance to ES6 treatment. Those results suggests that PP2AA1 is specifically affected by ES6 among other phosphatases.

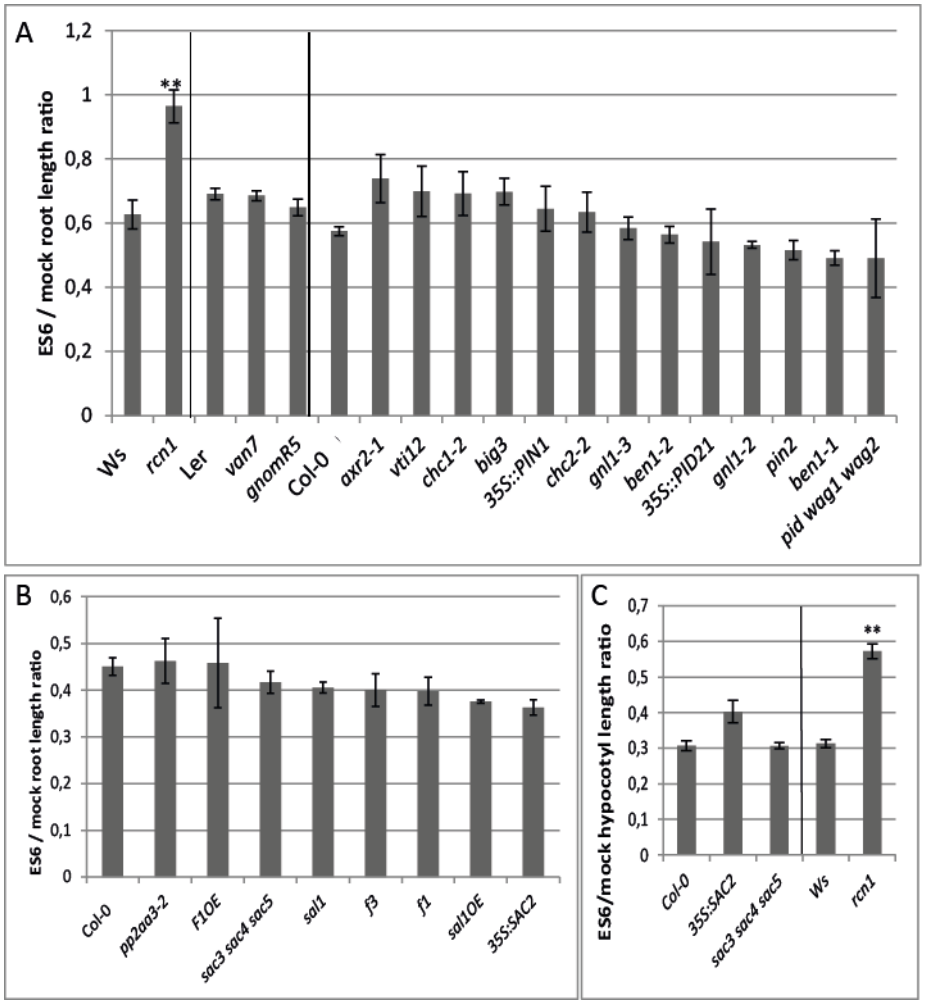

Figure 5. Identification of ES6 resistant mutants.
(A) Quantification of root length sensitivity of wild type (Ws, L*er*, and Col-0) and mutant (*rcn1*, *van7*, *gnom*^{R5}, *axr2-1, vti12, chc1-2*, *big3*, *35S:PIN1*, *chc2-2*, *gnl1-3*, *ben1-2, 35S:PID21*, *gnl1-2*, *pin2*, *ben1-1* and *pid wag1 wag2*) lines. Seedlings were grown for seven days on growth medium supplemented with mock and 1.4 µM ES6. Ratio of root lengths grown on ES6 to those grown on mock was calculated. The highest ES6 resistance was revealed by *rcn1* mutants. In four independent experiments, 32-88 roots were measured per each line per treatment. Data are means ± SE of four experiments. Student's *t* test, ***P* < 0.01.
(B) Quantification of root length sensitivity of wild type (Ws and Col-0) and mutant (*rcn1*, *F3DN*, *F1DN*, *rcnL2-2*, *F1OE*, *sac3sac4sac5*, *sal1*, *f3*, *f1*, *sal1OE* and *35S:SAC2*) lines. Seedlings were grown for seven days on growth medium supplemented with mock and 1.4 µM ES6. Ratio of root lengths grown on ES6 to those grown on mock was calculated. In two independent experiments, 20-61 roots were measured per each line and each treatment. Data are means ± SE of two experiments. There were no statistically significant differences between wild type and mutant lines (Student's *t* test, *P* > 0.05).
(C) Quantification of hypocotyl sensitivity of wild type (Col-0) and mutant (*pp2aa3-2*, *F1OE*, *sac3sac4sac5*, *sal1*, *f3*, *f1*, *sal1OE* and *35S:SAC2*) lines. Seedlings were grown in the dark for seven days on growth medium supplemented with mock and 1.4 µM ES6. Ratio of hypocotyl lengths grown on ES6 to those grown on mock was calculated. In three

independent experiments at least 70 roots were measured per each line and each treatment in total. Data are means ± SE of three experiments. Student's *t* test, $^{**}P < 0.01$.

DISCUSSION

ES6 as a New Inhibitor of the Cell Wall Biosynthesis

Here we identified and characterized endosidin 6, small molecule, which specifically affects cell wall structure. Wild-type seedlings treated with ES6 displayed variable morphological defects, including decreased root and hypocotyl length, induced root hair length and density and higher number of lateral roots - phenotypes associated with cell wall defects. Cellulose deficient mutants exhibit denser root hairs, swelling of the roots, changed cellulose content as well as polarity defects (Caño-Delgado et al., 2000; Gu and Nielsen, 2013; Feraru et al., 2011). Further experiments confirmed specific effect of ES6 on cell wall organization. Various intracellular trafficking processes including endo- and exocytosis were also not significantly affected by ES6. Among all tested subcellular markers only cellulose synthesis CESAs localization were affected by ES6 treatment. Similar effects on CESAs localization were observed after treatment with inhibitors of cellulose biosynthesis, CGA and isoxaben, which induced clearance of CESA-GFP signal from plasma membranes (Crowell et al., 2009; Paredez et al., 2006). Additionally, ES6 changed the cellulose and hemicellulose composition of the cell wall. Analysis of the sugar composition in hypocotyls and roots revealed elevated or decreased level of different components when compared to mock and isoxaben treatment. Isoxaben specifically inhibits radioactive glucose incorporation into the acid insoluble cellulosic cell wall fraction of *Arabidopsis* (Heim et al., 1990a). ES6, besides decreased cellulosic glucose, had also changed fucose, arabinose, glucose, xylose and mannose levels. Two isoxaben resistant loci, IXR1 and IXR2 encoding for CESA3 and CESA6, respectively, have been described in *Arabidopsis* (Desprez et al., 2002; Heim et al., 1989, 1990b; Scheible et al., 2001). Among tested cellulose deficient mutants, none of them displayed resistance to ES6. Since isoxaben was shown to affect cellulose synthesis complex and some of the *cesas* mutants showed resistance to its effect, it might suggest that ES6 affects CSC complex by other mechanisms. Phenotypic defects induced by ES6 specifically resemble those of *cesas* mutants, which display root hair formation, whereas other cell wall mutants have no root hairs. It might be due to the fact that CESAs were not detected in the area of growing root tips and other proteins, like *CELLULOSE* SYNTHASE (CESA)-LIKE PROTEIN (CLSD3) localize to the polar plasma membrane domain in root hairs (Park et al., 2011). It might indicate that observed cell wall defects are due to the ES6 effect on CSC complex.

Cell Wall Plays a Role in Apical-Basal Cell Polarity

ES6 induced basal-to-apical shift of ectopically expressed PIN1 protein in *PIN2:PIN1-HA;pin2* line but had no strong effect on natively expressed PIN1 in stele nor PIN2 in epidermis or cortex.

So far the connection between PIN polarity localization and cell wall has been revealed by characterization of polarity defective *repp3* mutant. It is defective in cellulose synthesis, resistant to isoxaben and with basal-to-apical shift of PIN1 localization in epidermis (Feraru et al., 2011). It also rescued the gravity response of agravitropic *PIN2PIN1-HA;pin2*, whereas ES6 was not able to do so. Additionally, it has been shown that defects in cell wall influence mobility of proteins at the plasma membrane (Martinière et al., 2012). Ectopically expressed PIN1 do not show clear basal localization in the epidermal cells of *PIN2PIN1-HA;pin2*, but rather non-polar localization. It suggests that the proteins are not as stable as native PIN proteins, and, as such are easier to perturb.

Auxin also has an effect on cell wall rearrangements. It induces cell wall loosening, leading to cell expansion (reviewed in Perrot-Rechenman, 2010) and induces growth of root hairs (Lee and Cho, 2006). Decreased auxin level was suppressing the swollen roots of cellulose deficient roots (Steinwand et al., 2014). We demonstrated, that ES6 induced accumulation of auxin, visualized by *DR5:GUS* reporter system. However, it has to further examine if ES6 has a direct effect on CSC or the cell wall defects is induced by auxin accumulation.

ES6 effect on PP2AA1

Among all tested mutants only *rcn1* showed resistance to the ES6 effect in terms of root and hypocotyl growth. *rcn1* is defective in A1 subunit of PP2A phosphatases, which were reported to play role in apical-basal targeting of PIN proteins (Michniewicz et al., 2007). It has been shown that double *pp2aa1,3* mutant displays altered, apical localization of PIN1 proteins in stele, PIN2 in cortex and PIN4 in all expression domain (Michniewicz et al., 2007). Defects in protein phosphatases exhibit also defects in auxin transport, gravity responses and lateral root growth (Rashotte et al., 2001). Additionally, *rcn1* displays increased auxin content (Fisher et al., 1996). Effects on lateral root growth and auxin response were also observed after ES6 treatment. The effect of phosphatases on cell wall composition is not well examined. It has been shown, that *rcn1* mutant was selected as defective in responses to auxin transport inhibitor NAPHTHYLPHTHALAMIC ACID (NPA), exhibited by root curling and hypocotyl elongation (Garbers et al., 1996). Interestingly, some cellulose biosynthetic mutants, which show resistance to isoxaben and other cellulose biosynthetic inhibitor thaxtomin A, display enhanced tolerance to NPA (Tegg et al., 2013). At the same time root growth response of these mutants, ISOXABEN RESISTANT (*ixr1-1*) and THAXTOMIN RESISTANT (*txr1-1*), was not affected by synthetic auxins or another auxin transport inhibitor

2,3,5-TRIIODOBENZOIC ACID (TIBA) (Tegg et al., 2013). It is also known, that changes in CESA phosphorylation affects mobility of the proteins and reduce anisotropic cell growth (Chen et al., 2010; Bischoff et al., 2011). Additionally, PP2A is involved in regulating microtubule dynamics (Camilleri et al., 2002). PP2A phosphatase might act in CESA phosphorylation signaling. It is possible, that ES6 alters phosphorylation sites of CSCs which influence its trafficking, activity, or association with microtubules. However, it is not excluded, that ES6 affects the two pathways, cellulose biosynthesis and PP2A, independently.

These data indicate a connection between PP2AA1 and cell wall biosynthesis, although the mechanism is not clear and has to be further examined. ES6 appears as a promising additional tool to elucidate the connection between polarity, phosphatases and cell wall function.

METHODS

Plant Material and Growth Conditions

Seeds of *Arabidopsis thaliana* were stratified for 2 days in the dark at 4°C and grown vertically at 21°C under continuous light conditions, under long-day conditions in Figure 5B (16 / 8 h of light/dark), or in the dark when indicated on 0.8% agar 0.5x Murashige and Skoog (MS) medium (Duchefa) with 1% sucrose (pH 5.9). The *Arabidopsis* lines: *PIN2:PIN1-HA;eir1-1/pin2* (Wiśniewska et al., 2006); *DR5:GUS* (Ulmasov et al., 1997); *N-ST-GFP* (Batoko et al., 2000); *CLC2:CLC2-GFP* (Konopka and Bednarek, 2008); *PIN1:PIN1-GFP* and *35S:PIN1* (Benková et al., 2003); *CESA3:GFP-CESA3, CESA1:GFP-CESA1* and *CESA6:GFP-CESA6* (Desprez et al., 2007); *ARA7-GFP:ARA7* (Ueda et al., 2004); *SYP61:SYP61-CFP* (Robert et al., 2008); *35S:GFP-MAP4* (Marc et al., 1998); *GFP-CESA3/mRFP-MBD* (Crowell et al., 2009); *35S:PID21* (Benjamins et al., 2001); *axr2-1* (Wilson et al., 1990); *ben1-1* and *ben1-2* (SALK_013761) (Tanaka et al., 2009); *big3* (SALK_044617) (Richter et al., 2014); *rcn1* (Garbers et al., 1996); *gnl1-2, gnl1-3* (Teh and Moore, 2007); *gnom*^{R5} (Geldner et al., 2004); *van7* (Koizumi et al., 2000); *chc1-2* (SALK_103252) and *chc2-2* (SALK_028826) (Kitakura et al., 2011); *vti12* (Surpin et al., 2003); *pin2* (*eir1-1*) (Luschnig et al., 1998); *pid wag1 wag2* (Dhonukshe et al., 2010); *F1OE* (*35S:YFP-FyPP1*), *sal1* (SALK_035181), *f3* (or *fypp3,* CS877364), *f1* (or *fypp1,* CS874166) and *sal1OE* (Dai et al., 2012); *35S:SAC2* and *sac3 sac4 sac5* (Nováková et al., 2014); *pp2aa3-2* (SALK_099550) (Zhou et al., 2004); *35S:THE1-GFP* (Hématy et al., 2007); *je5*^{cesa3} (Fagard et al., 2000); *eli1-1*^{cesa3} (Caño-Delgado et al., 2003); *prc1-1*^{cesa6} (Desnos et al., 1996); *rsw1-10*^{cesa1} (Arioli et al., 1998) and *repp3*^{cesa3} (Feraru et al., 2011) have been described previously. Columbia (Col-0) ecotype was used for immunolocalization, cell wall content analysis, and as wild-type control in seedling growth experiments, except for growth

of *rcn1* for which Wassilewskija (Ws) ecotype was used and *gnom*^{R5} and *van7* for which Landsberg *erecta* (L*er*) ecotypes was used.

Chemical Treatments

Stock solutions of BFA (Sigma-Aldrich), ES6 (Chembridge ID 7697233), isoxaben (Sigma) were made in dimethylsulfoxide (DMSO) and diluted in liquid 0.5x MS medium (or growth medium where indicated) for treatments of the indicated concentrations and times. Equal volumes of solvent were used as mock treatments for controls. For germination and growth of seedlings on ES6 and isoxaben, seeds were sown directly onto ES6/isoxaben-supplemented growth medium. For root length and hypocotyl measurements mutants and overexpression lines were grown for 7 days. For lateral roots calculation Col-0 was grown for 11 days. For polar localization and *DR5:GUS* experiment 3-day-old seedlings were transferred for 48 h from solid growth medium to solid medium supplemented with ES6. For shorter treatment (8 h) of *DR5:GUS*, 5-day-old seedlings were mounted in liquid medium complemented with ES6. After treatment seedlings were stained overnight at 37°C in darkness in GUS staining buffer [100 mM Na-phosphate buffer (pH 7), 0.1% Triton X-100, 10 mM EDTA (pH 8) and 2mM of each $K_3FeIII(CN)_6$ and $K_4FeII(CN)_6$] containing X-Gluc to visualize GUS activity. X-Gluc was added to a final concentration of 1 mg/ml from a 10 mg/ml stock dissolved in DMSO, which was freshly prepared. For BFA treatments, 5-day-old seedlings were pre-treated for 30 min with ES6 before adding 25 µM BFA to the treatment for a further 90 min. For BFA washouts, 5-day-old seedlings were treated with 25 or 50 µM BFA for 2 hours followed by 30 min treatment wash. For live imaging 5-day-old seedlings were mounted for 2 h (5 h for visualization of MASCs) in their treatment medium.

Immunolocalization

Whole-mount immunolocalization on *Arabidopsis* 5-day-old seedlings was performed with the InSituProrobot (Intavis, Germany) according to the described protocol (Sauer et al., 2006). Primary antibodies and final dilutions were: rabbit anti-PIN1 (Paciorek et al., 2005) 1:1000; rabbit anti-PIN2 (generously provided by C. Luschnig) 1:1000; mouse anti-HA (AbCam/HA.C5) 1:500. Secondary antibodies and final dilutions were: Cy3 anti-rabbit (Sigma) 1:600 and Alexa488 anti-mouse (Invitrogen) 1:600.

Quantitative and Statistical Analyses

For PIN polarity quantification in the cortex, the ratio of the cell numbers with basal PIN2 and the total number of cortical cells was calculated from the confocal laser scanning microscopy (CLSM) images of the root apical meristem. For polarity in epidermal cells of *PIN2:PIN1*, the ratio of the cell numbers with basal, both basal and apical or apical PIN localization was compared to the total number of epidermal cells from the CLSM images of root apical

meristem. For analysis of gravitropic response, 5-day-old seedlings grown vertically in light were gravistimulated by a 90° rotation. The bending angle was measured with the Java-based ImageJ application (http://rsb.info.nih.gov/ij/) software 48 h after gravistimulation. All gravitropically stimulated roots were assigned to one of the eight 45° sectors on a gravitropism diagram. The length of the bars in the diagram represents the percentage of seedlings assigned to the respective sector. Wild-type root lengths and hypocotyl lengths were measured with ImageJ software. For the mutant root lengths, the ratio was calculated of the root lengths of seedlings grown on ES6 and that of seedlings grown on mock media with the ImageJ application. The statistical significances of differences of data were quantified with Student's *t*-tests, Mann-Whitney *U* test and ANOVA.

Image Analysis

The imaging was performed on a Zeiss LSM 710, Zeiss LSM 700 and Leica SP2 confocal laser scanning microscopes.

Cellulose quantification

The analyses of polysaccharides were performed on an alcohol insoluble material prepared as follow. Hundred mg (FW) of grounded 4-days-old dark-grown seedlings were washed twice in 4 volumes of absolute ethanol for 15 min at 80°C, then rinsed twice in 2 volumes of acetone at room temperature for 10 min and left to dry under a fume hood overnight at room temperature. Non-crystalline polysaccharides were hydrolysed in 2.5 M TriFluoroAcetic acid for 1.5 h at 100 °C as described previously in (Harholt et al., 2006). To determine the cellulose content, the residual pellet obtained was rinsed twice with ten volumes of water and hydrolysed with H_2SO_4 as described in (Updegraff, 1969). The released glucose was diluted 500 times and then quantified using an HPAEC-PAD chromatography as described in (Harholt et al., 2006).

REFERENCES

Arioli, T., Peng, L., Betzner, A.S., Burn, J., Wittke, W., Herth, W., Camilleri, C., Höfte, H., Plazinski, J., Birch, R., et al. (1998). Molecular Analysis of Cellulose Biosynthesis in *Arabidopsis*. Science *279*, 717–720.

Batoko, H., Zheng, H.Q., Hawes, C., and Moore, I. (2000). A rab1 GTPase is required for transport between the endoplasmic reticulum and golgi apparatus and for normal golgi movement in plants. Plant Cell *12*, 2201–2218.

Benjamins, R., Quint, A., Weijers, D., Hooykaas, P., and Offringa, R. (2001). The PINOID protein kinase regulates organ development in *Arabidopsis* by enhancing polar auxin transport. Dev. Camb. Engl. *128*, 4057–4067.

Benková, E., Michniewicz, M., Sauer, M., Teichmann, T., Seifertová, D., Jürgens, G., and Friml, J. (2003). Local, efflux-dependent auxin gradients as a common module for plant organ formation. Cell *115*, 591–602.

Bischoff, V., Desprez, T., Mouille, G., Vernhettes, S., Gonneau, M., and Höfte, H. (2011). Phytochrome Regulation of Cellulose Synthesis in *Arabidopsis*. Curr. Biol. *21*, 1822–1827.

Camilleri, C., Azimzadeh, J., Pastuglia, M., Bellini, C., Grandjean, O., and Bouchez, D. (2002). The *Arabidopsis* TONNEAU2 Gene Encodes a Putative Novel Protein Phosphatase 2A Regulatory Subunit Essential for the Control of the Cortical Cytoskeleton. Plant Cell *14*, 833–845.

Caño-Delgado, A., Penfield, S., Smith, C., Catley, M., and Bevan, M. (2003). Reduced cellulose synthesis invokes lignification and defense responses in *Arabidopsis thaliana*. Plant J. *34*, 351–362.

Caño-Delgado, A.I., Metzlaff, K., and Bevan, M.W. (2000). The eli1 mutation reveals a link between cell expansion and secondary cell wall formation in *Arabidopsis thaliana*. Dev. Camb. Engl. *127*, 3395–3405.

Carland, F., Fujioka, S., and Nelson, T. (2010). The sterol methyltransferases SMT1, SMT2, and SMT3 influence *Arabidopsis* development through nonbrassinosteroid products. Plant Physiol. *153*, 741–756.

Chen, S., Ehrhardt, D.W., and Somerville, C.R. (2010). Mutations of cellulose synthase (CESA1) phosphorylation sites modulate anisotropic cell expansion and bidirectional mobility of cellulose synthase. Proc. Natl. Acad. Sci. U. S. A. *107*, 17188–17193.

Cosgrove, D.J. (2005). Growth of the plant cell wall. Nat. Rev. Mol. Cell Biol. *6*, 850–861.

Crowell, E.F., Bischoff, V., Desprez, T., Rolland, A., Stierhof, Y.-D., Schumacher, K., Gonneau, M., Höfte, H., and Vernhettes, S. (2009). Pausing of Golgi bodies on microtubules regulates secretion of cellulose synthase complexes in *Arabidopsis*. Plant Cell *21*, 1141–1154.

Dai, M., Zhang, C., Kania, U., Chen, F., Xue, Q., McCray, T., Li, G., Qin, G., Wakeley, M., Terzaghi, W., et al. (2012). A PP6-type phosphatase holoenzyme directly regulates PIN phosphorylation and auxin efflux in *Arabidopsis*. Plant Cell *24*, 2497–2514.

Desnos, T., Orbović, V., Bellini, C., Kronenberger, J., Caboche, M., Traas, J., and Höfte, H. (1996). Procuste1 mutants identify two distinct genetic pathways controlling hypocotyl

cell elongation, respectively in dark- and light-grown *Arabidopsis* seedlings. Dev. Camb. Engl. *122*, 683–693.

Desprez, T., Vernhettes, S., Fagard, M., Refregier, G., Desnos, T., Aletti, E., Py, N., Pelletier, S., and Hofte, H. (2002). Resistance against Herbicide Isoxaben and Cellulose Deficiency Caused by Distinct Mutations in Same Cellulose Synthase Isoform CESA6. Plant Physiol. *128*, 482–490.

Desprez, T., Juraniec, M., Crowell, E.F., Jouy, H., Pochylova, Z., Parcy, F., Höfte, H., Gonneau, M., and Vernhettes, S. (2007). Organization of cellulose synthase complexes involved in primary cell wall synthesis in *Arabidopsis thaliana*. Proc. Natl. Acad. Sci. U. S. A. *104*, 15572–15577.

Dhonukshe, P., Huang, F., Galvan-Ampudia, C.S., Mähönen, A.P., Kleine-Vehn, J., Xu, J., Quint, A., Prasad, K., Friml, J., Scheres, B., et al. (2010). Plasma membrane-bound AGC3 kinases phosphorylate PIN auxin carriers at TPRXS(N/S) motifs to direct apical PIN recycling. Dev. Camb. Engl. *137*, 3245–3255.

Drakakaki, G., Robert, S., Szatmari, A.-M., Brown, M.Q., Nagawa, S., Van Damme, D., Leonard, M., Yang, Z., Girke, T., Schmid, S.L., et al. (2011). Clusters of bioactive compounds target dynamic endomembrane networks in vivo. Proc. Natl. Acad. Sci. U. S. A. *108*, 17850–17855.

Fagard, M., Desnos, T., Desprez, T., Goubet, F., Refregier, G., Mouille, G., McCann, M., Rayon, C., Vernhettes, S., and Höfte, H. (2000). PROCUSTE1 encodes a cellulose synthase required for normal cell elongation specifically in roots and dark-grown hypocotyls of *Arabidopsis*. Plant Cell *12*, 2409–2424.

Feraru, E., Feraru, M.I., Kleine-Vehn, J., Martinière, A., Mouille, G., Vanneste, S., Vernhettes, S., Runions, J., and Friml, J. (2011). PIN polarity maintenance by the cell wall in *Arabidopsis*. Curr. Biol. CB *21*, 338–343.

Fisher, R.H., Barton, M.K., Cohen, J.D., and Cooke, T.J. (1996). Hormonal Studies of fass, an *Arabidopsis* Mutant That Is Altered in Organ Elongation. Plant Physiol. *110*, 1109–1121.

Garbers, C., DeLong, A., Deruére, J., Bernasconi, P., and Söll, D. (1996). A mutation in protein phosphatase 2A regulatory subunit A affects auxin transport in *Arabidopsis*. EMBO J. *15*, 2115–2124.

Geldner, N., Friml, J., Stierhof, Y.D., Jürgens, G., and Palme, K. (2001). Auxin transport inhibitors block PIN1 cycling and vesicle trafficking. Nature *413*, 425–428.

Geldner, N., Richter, S., Vieten, A., Marquardt, S., Torres-Ruiz, R.A., Mayer, U., and Jürgens, G. (2004). Partial loss-of-function alleles reveal a role for GNOM in auxin transport-related, post-embryonic development of *Arabidopsis*. Dev. Camb. Engl. *131*, 389–400.

Grunewald, W., and Friml, J. (2010). The march of the PINs: developmental plasticity by dynamic polar targeting in plant cells. EMBO J. *29*, 2700–2714.

Gu, F., and Nielsen, E. (2013). Targeting and regulation of cell wall synthesis during tip growth in plants. J. Integr. Plant Biol. *55*, 835–846.

Hamant, O., Meyerowitz, E.M., and Traas, J. (2011). Is cell polarity under mechanical control in plants? Plant Signal. Behav. *6*, 137–139.

Harholt, J., Jensen, J.K., Sørensen, S.O., Orfila, C., Pauly, M., and Scheller, H.V. (2006). ARABINAN DEFICIENT 1 is a putative arabinosyltransferase involved in biosynthesis of pectic arabinan in *Arabidopsis*. Plant Physiol. *140*, 49–58.

Heim, D.R., Roberts, J.L., Pike, P.D., and Larrinua, I.M. (1989). Mutation of a Locus of *Arabidopsis thaliana* Confers Resistance to the Herbicide Isoxaben. Plant Physiol. *90*, 146–150.

Heim, D.R., Skomp, J.R., Tschabold, E.E., and Larrinua, I.M. (1990a). Isoxaben Inhibits the Synthesis of Acid Insoluble Cell Wall Materials In *Arabidopsis thaliana*. Plant Physiol. *93*, 695–700.

Heim, D.R., Roberts, J.L., Pike, P.D., and Larrinua, I.M. (1990b). A Second Locus, Ixr B1 in *Arabidopsis thaliana*, that Confers Resistance to the Herbicide Isoxaben. Plant Physiol. *92*, 858–861.

Heisler, M.G., Hamant, O., Krupinski, P., Uyttewaal, M., Ohno, C., Jönsson, H., Traas, J., and Meyerowitz, E.M. (2010). Alignment between PIN1 polarity and microtubule orientation in the shoot apical meristem reveals a tight coupling between morphogenesis and auxin transport. PLoS Biol. *8*, e1000516.

Hématy, K., Sado, P.-E., Van Tuinen, A., Rochange, S., Desnos, T., Balzergue, S., Pelletier, S., Renou, J.-P., and Höfte, H. (2007). A receptor-like kinase mediates the response of *Arabidopsis* cells to the inhibition of cellulose synthesis. Curr. Biol. CB *17*, 922–931.

His, I., Driouich, A., Nicol, F., Jauneau, A., and Höfte, H. (2001). Altered pectin composition in primary cell walls of korrigan, a dwarf mutant of *Arabidopsis* deficient in a membrane-bound endo-1,4-beta-glucanase. Planta *212*, 348–358.

Huang, F., Zago, M.K., Abas, L., van Marion, A., Galván-Ampudia, C.S., and Offringa, R. (2010). Phosphorylation of conserved PIN motifs directs *Arabidopsis* PIN1 polarity and auxin transport. Plant Cell *22*, 1129–1142.

Kitakura, S., Vanneste, S., Robert, S., Löfke, C., Teichmann, T., Tanaka, H., and Friml, J. (2011). Clathrin mediates endocytosis and polar distribution of PIN auxin transporters in *Arabidopsis*. Plant Cell *23*, 1920–1931.

Kleine-Vehn, J., Dhonukshe, P., Swarup, R., Bennett, M., and Friml, J. (2006). Subcellular trafficking of the *Arabidopsis* auxin influx carrier AUX1 uses a novel pathway distinct from PIN1. Plant Cell *18*, 3171–3181.

Kleine-Vehn, J., Dhonukshe, P., Sauer, M., Brewer, P.B., Wiśniewska, J., Paciorek, T., Benková, E., and Friml, J. (2008). ARF GEF-dependent transcytosis and polar delivery of PIN auxin carriers in *Arabidopsis*. Curr. Biol. CB *18*, 526–531.

Koizumi, K., Sugiyama, M., and Fukuda, H. (2000). A series of novel mutants of *Arabidopsis thaliana* that are defective in the formation of continuous vascular network: calling the auxin signal flow canalization hypothesis into question. Dev. Camb. Engl. *127*, 3197–3204.

Konopka, C.A., and Bednarek, S.Y. (2008). Variable-angle epifluorescence microscopy: a new way to look at protein dynamics in the plant cell cortex. Plant J. Cell Mol. Biol. *53*, 186–196.

Lee, S.H., and Cho, H.-T. (2006). PINOID Positively Regulates Auxin Efflux in *Arabidopsis* Root Hair Cells and Tobacco Cells. Plant Cell *18*, 1604–1616.

Luschnig, C., and Vert, G. (2014). The dynamics of plant plasma membrane proteins: PINs and beyond. Dev. Camb. Engl. *141*, 2924–2938.

Luschnig, C., Gaxiola, R.A., Grisafi, P., and Fink, G.R. (1998). EIR1, a root-specific protein involved in auxin transport, is required for gravitropism in *Arabidopsis thaliana*. Genes Dev. *12*, 2175–2187.

Marc, J., Granger, C.L., Brincat, J., Fisher, D.D., Kao, T., McCubbin, A.G., and Cyr, R.J. (1998). A GFP-MAP4 reporter gene for visualizing cortical microtubule rearrangements in living epidermal cells. Plant Cell *10*, 1927–1940.

Martinière, A., Lavagi, I., Nageswaran, G., Rolfe, D.J., Maneta-Peyret, L., Luu, D.-T., Botchway, S.W., Webb, S.E.D., Mongrand, S., Maurel, C., et al. (2012). Cell wall constrains lateral diffusion of plant plasma-membrane proteins. Proc. Natl. Acad. Sci. U. S. A. *109*, 12805–12810.

Men, S., Boutté, Y., Ikeda, Y., Li, X., Palme, K., Stierhof, Y.D., Hartmann, M.A., Moritz, T., and Grebe, M. (2008). Sterol-dependent endocytosis mediates post-cytokinetic acquisition of PIN2 auxin efflux carrier polarity. Nat. Cell Biol. *10*, 237–244.

Michniewicz, M., Zago, M.K., Abas, L., Weijers, D., Schweighofer, A., Meskiene, I., Heisler, M.G., Ohno, C., Zhang, J., Huang, F., et al. (2007). Antagonistic regulation of PIN phosphorylation by PP2A and PINOID directs auxin flux. Cell *130*, 1044–1056.

Nováková, P., Hirsch, S., Feraru, E., Tejos, R., van Wijk, R., Viaene, T., Heilmann, M., Lerche, J., De Rycke, R., Feraru, M.I., et al. (2014). SAC phosphoinositide phosphatases at the tonoplast mediate vacuolar function in *Arabidopsis*. Proc. Natl. Acad. Sci. U. S. A. *111*, 2818–2823.

Paciorek, T., Zazímalová, E., Ruthardt, N., Petrásek, J., Stierhof, Y.D., Kleine-Vehn, J., Morris, D.A., Emans, N., Jürgens, G., Geldner, N., et al. (2005). Auxin inhibits endocytosis and promotes its own efflux from cells. Nature *435*, 1251–1256.

Paredez, A.R., Somerville, C.R., and Ehrhardt, D.W. (2006). Visualization of Cellulose Synthase Demonstrates Functional Association with Microtubules. Science *312*, 1491–1495.

Park, S., Szumlanski, A.L., Gu, F., Guo, F., and Nielsen, E. (2011). A role for CSLD3 during cell-wall synthesis in apical plasma membranes of tip-growing root-hair cells. Nat. Cell Biol. *13*, 973–980.

Perrot-Rechenmann, C. (2010). Cellular Responses to Auxin: Division versus Expansion. Cold Spring Harb. Perspect. Biol. *2*.

Persson, S., Paredez, A., Carroll, A., Palsdottir, H., Doblin, M., Poindexter, P., Khitrov, N., Auer, M., and Somerville, C.R. (2007). Genetic evidence for three unique components in primary cell-wall cellulose synthase complexes in *Arabidopsis*. Proc. Natl. Acad. Sci. U. S. A. *104*, 15566–15571.

Rashotte, A.M., DeLong, A., and Muday, G.K. (2001). Genetic and chemical reductions in protein phosphatase activity alter auxin transport, gravity response, and lateral root growth. Plant Cell *13*, 1683–1697.

Richter, S., Kientz, M., Brumm, S., Nielsen, M.E., Park, M., Gavidia, R., Krause, C., Voss, U., Beckmann, H., Mayer, U., et al. (2014). Delivery of endocytosed proteins to the cell-division plane requires change of pathway from recycling to secretion. eLife *3*, e02131.

Robert, S., Chary, S.N., Drakakaki, G., Li, S., Yang, Z., Raikhel, N.V., and Hicks, G.R. (2008). Endosidin1 defines a compartment involved in endocytosis of the brassinosteroid receptor BRI1 and the auxin transporters PIN2 and AUX1. Proc. Natl. Acad. Sci. U. S. A. *105*, 8464–8469.

Sauer, M., Paciorek, T., Benková, E., and Friml, J. (2006). Immunocytochemical techniques for whole-mount in situ protein localization in plants. Nat. Protoc. *1*, 98–103.

Scheible, W.-R., Eshed, R., Richmond, T., Delmer, D., and Somerville, C. (2001). Modifications of cellulose synthase confer resistance to isoxaben and thiazolidinone herbicides in *Arabidopsis ixr1* mutants. Proc. Natl. Acad. Sci. *98*, 10079–10084.

Steinwand, B.J., Xu, S., Polko, J.K., Doctor, S.M., Westafer, M., and Kieber, J.J. (2014). Alterations in auxin homeostasis suppress defects in cell wall function. PloS One *9*, e98193.

Surpin, M., Zheng, H., Morita, M.T., Saito, C., Avila, E., Blakeslee, J.J., Bandyopadhyay, A., Kovaleva, V., Carter, D., Murphy, A., et al. (2003). The VTI family of SNARE proteins is necessary for plant viability and mediates different protein transport pathways. Plant Cell *15*, 2885–2899.

Tanaka, H., Kitakura, S., De Rycke, R., De Groodt, R., and Friml, J. (2009). Fluorescence imaging-based screen identifies ARF GEF component of early endosomal trafficking. Curr. Biol. CB *19*, 391–397.

Tegg, R.S., Shabala, S.N., Cuin, T.A., Davies, N.W., and Wilson, C.R. (2013). Enhanced resistance to the cellulose biosynthetic inhibitors, thaxtomin A and isoxaben in *Arabidopsis thaliana* mutants, also provides specific co-resistance to the auxin transport inhibitor, 1-NPA. BMC Plant Biol. *13*, 76.

Teh, O.-K., and Moore, I. (2007). An ARF-GEF acting at the Golgi and in selective endocytosis in polarized plant cells. Nature *448*, 493–496.

Ueda, T., Uemura, T., Sato, M.H., and Nakano, A. (2004). Functional differentiation of endosomes in *Arabidopsis* cells. Plant J. Cell Mol. Biol. *40*, 783–789.

Ulmasov, T., Murfett, J., Hagen, G., and Guilfoyle, T.J. (1997). Aux/IAA proteins repress expression of reporter genes containing natural and highly active synthetic auxin response elements. Plant Cell *9*, 1963–1971.

Updegraff, D.M. (1969). Semimicro determination of cellulose inbiological materials. Anal. Biochem. *32*, 420–424.

Willemsen, V., Friml, J., Grebe, M., van den Toorn, A., Palme, K., and Scheres, B. (2003). Cell polarity and PIN protein positioning in *Arabidopsis* require STEROL METHYLTRANSFERASE1 function. Plant Cell *15*, 612–625.

Wilson, A.K., Pickett, F.B., Turner, J.C., and Estelle, M. (1990). A dominant mutation in Arabidopsis confers resistance to auxin, ethylene and abscisic acid. Mol. Gen. Genet. MGG *222*, 377–383.

Wiśniewska, J., Xu, J., Seifertová, D., Brewer, P.B., Ruzicka, K., Blilou, I., Rouquié, D., Benková, E., Scheres, B., and Friml, J. (2006). Polar PIN localization directs auxin flow in plants. Science *312*, 883.

Zhang, J., Nodzynski, T., Pencík, A., Rolcík, J., and Friml, J. (2010). PIN phosphorylation is sufficient to mediate PIN polarity and direct auxin transport. Proc. Natl. Acad. Sci. U. S. A. *107*, 918–922.

Zhou, H.-W., Nussbaumer, C., Chao, Y., and DeLong, A. (2004). Disparate roles for the regulatory A subunit isoforms in *Arabidopsis* protein phosphatase 2A. Plant Cell *16*, 709–722.

SUPPLEMENTARY INFORMATION

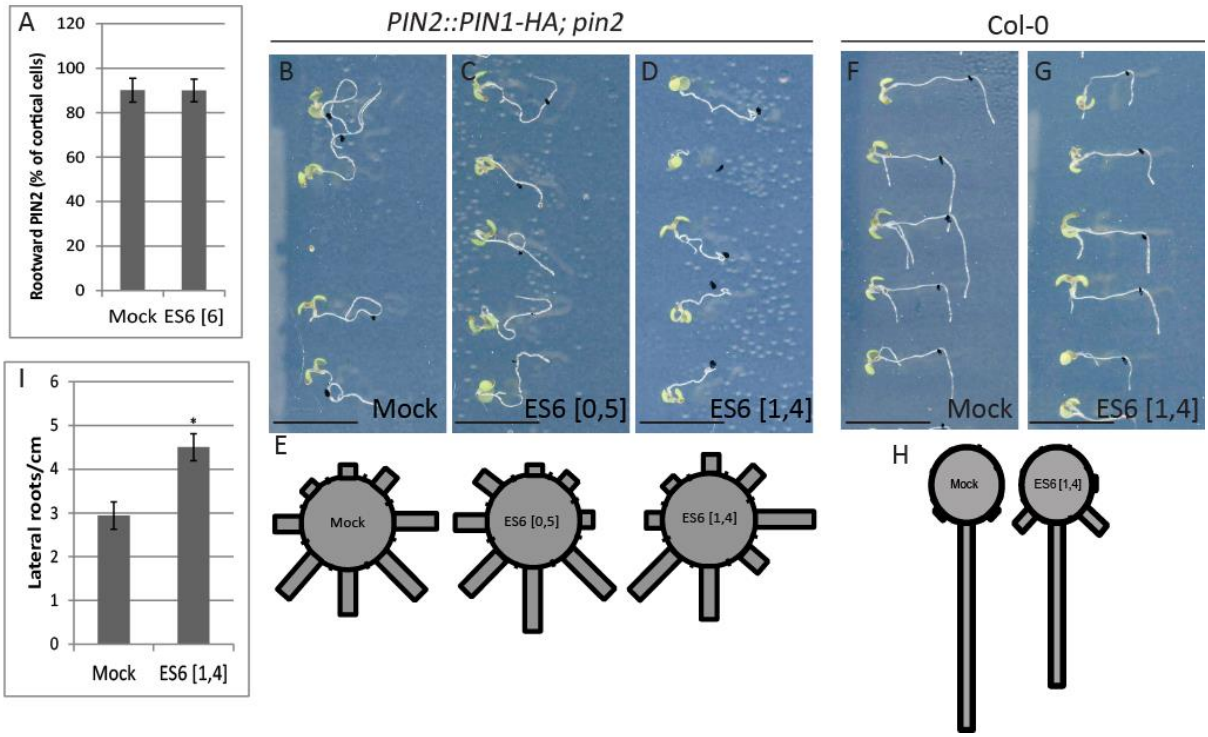

Supplemental Figure 1. Characterization of ES6 effects.
(A) Quantification of rootward PIN2 in cortical cells of five-day-old Col-0 seedlings. Three-day-old seedlings were transferred on medium supplemented with mock or 6 µM ES6 and grown for 48 h. After mock treatment PIN2 shows apical localization in epidermis and older cortex cells, and basal localization in young cortex cells. No change in PIN2 and localization was observed after ES6 treatment. In three independent experiments, 16 roots were analyzed per treatment in total. There was no statistically significant difference between treatments (Student's *t* test, $P > 0.05$). Data are means ± SE of three experiments.
(B) to **(H)** Response of seven-day-old seedlings gravistimulated for 48 h and quantification of the root gravitropic response. PIN2:PIN1-HA;*pin2* seedlings [**(B)** to **(D)**] were grown on medium supplemented with mock **(B)**, 0.5 **(C)** or 1.4 µM ES6 **(D)** and Col-0 [**(F)** and **(G)**] on medium supplemented with mock **(F)** and 1.4 µM ES6 **(G)**. After five days plates were turned 90° for another 48 h. PIN2:PIN1-HA;*pin2* did not show positive gravitropic response to neither mock **(B)** nor ES6 [**(C)** and **(D)**]. Col-0 seedlings on both mock **(F)** and 1.4 µM ES6 **(G)** showed positive gravitropic response. Gravistimulated roots were assigned to one of the eight 45° sectors on a gravitropism diagram [**(E)** and **(H)**]. The length of the bars in the diagram represents the percentage of seedlings assigned to the respective sector. In three independent experiments, at least 54 roots were analyzed for each treatment in total. Bars = 1cm.
(I) Quantification of lateral roots density in Col-0 eleven-day-old seedlings grown on medium supplemented with mock or 1.4 µM ES6. In three independent experiments, 60 roots were analyzed for each treatment in total. Data are means ± SE of three experiments. Student's *t* test, $*P < 0.05$.

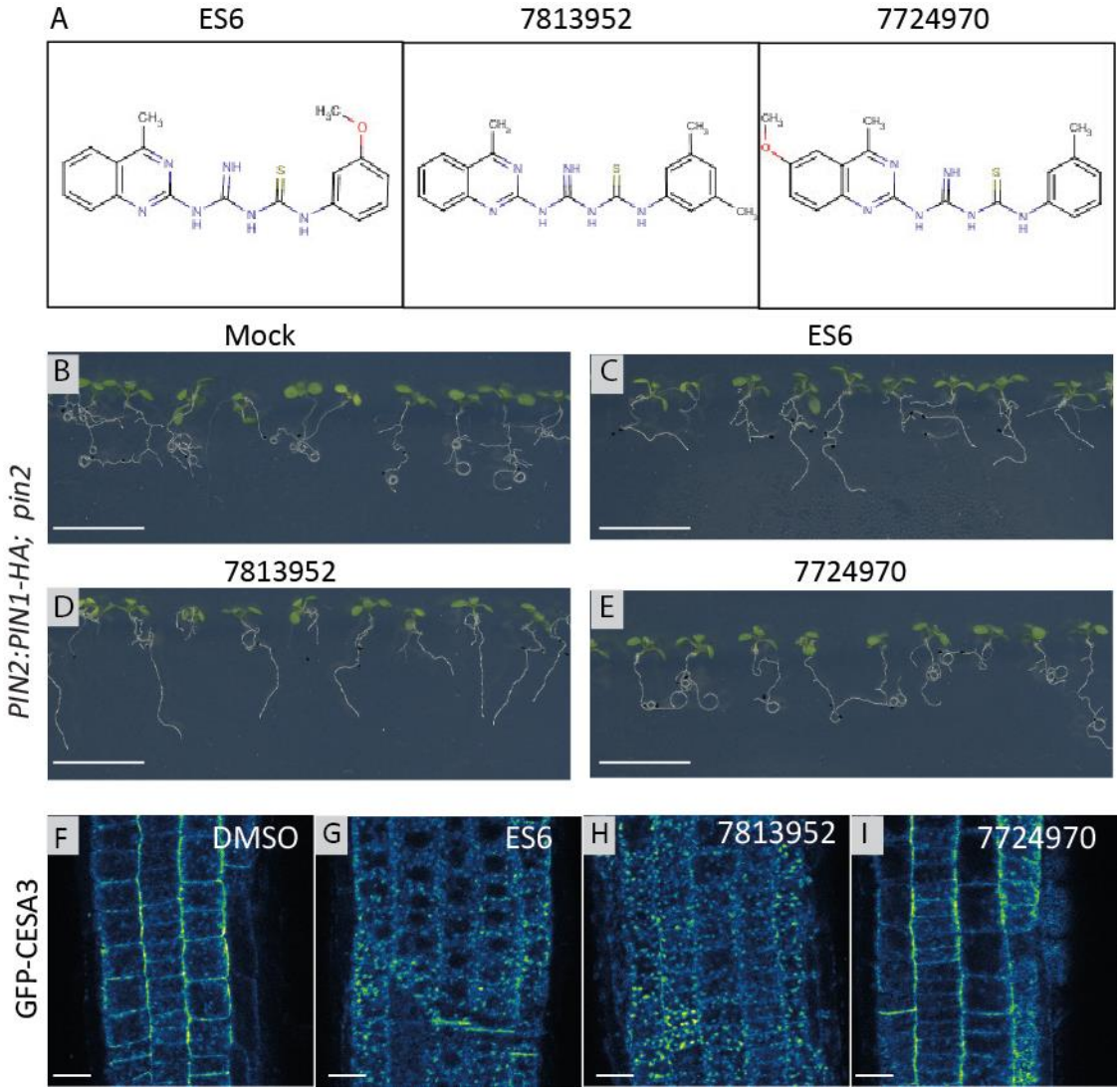

Supplemental Figure 2. Identification of ES6 bioactive analogue.

(A) Chemical structures of ES6, 7813952 and 7724970.

(B) to **(E)** Response of 10-day-old gravistimulated *PIN2:PIN1-HA;pin2* seedlings. Seedlings were gravistimulated twice, at the 6-day-old stage and 24 h later. Seedlings were grown on medium supplemented with mock or a set of three chemicals, of which two were diluted in a growth medium at 1:20000 from a stock concentration of 10 mg/ml. ES6 was used at 1.4 µM. Treatment with 7813952 resulted in less curly roots when compared to the mock control. Similar phenotype was observed for ES6 treated roots. Bars = 1 cm.

(F) to **(I)** Intracellular localization of GFP-CESA3 after 2 h of mock **(F)**, 6 µM ES6 **(G)**, 7813952 **(H)** and 7724970 **(I)** treatment. The 7813952 and 7724970 were diluted at 1:4800 from a stock concentration of 10 mg/ml. The 7813952 induced signal depletion from PM and its intracellular accumulation similar to that observed for ES6 treated seedlings. Bars = 10 µm.

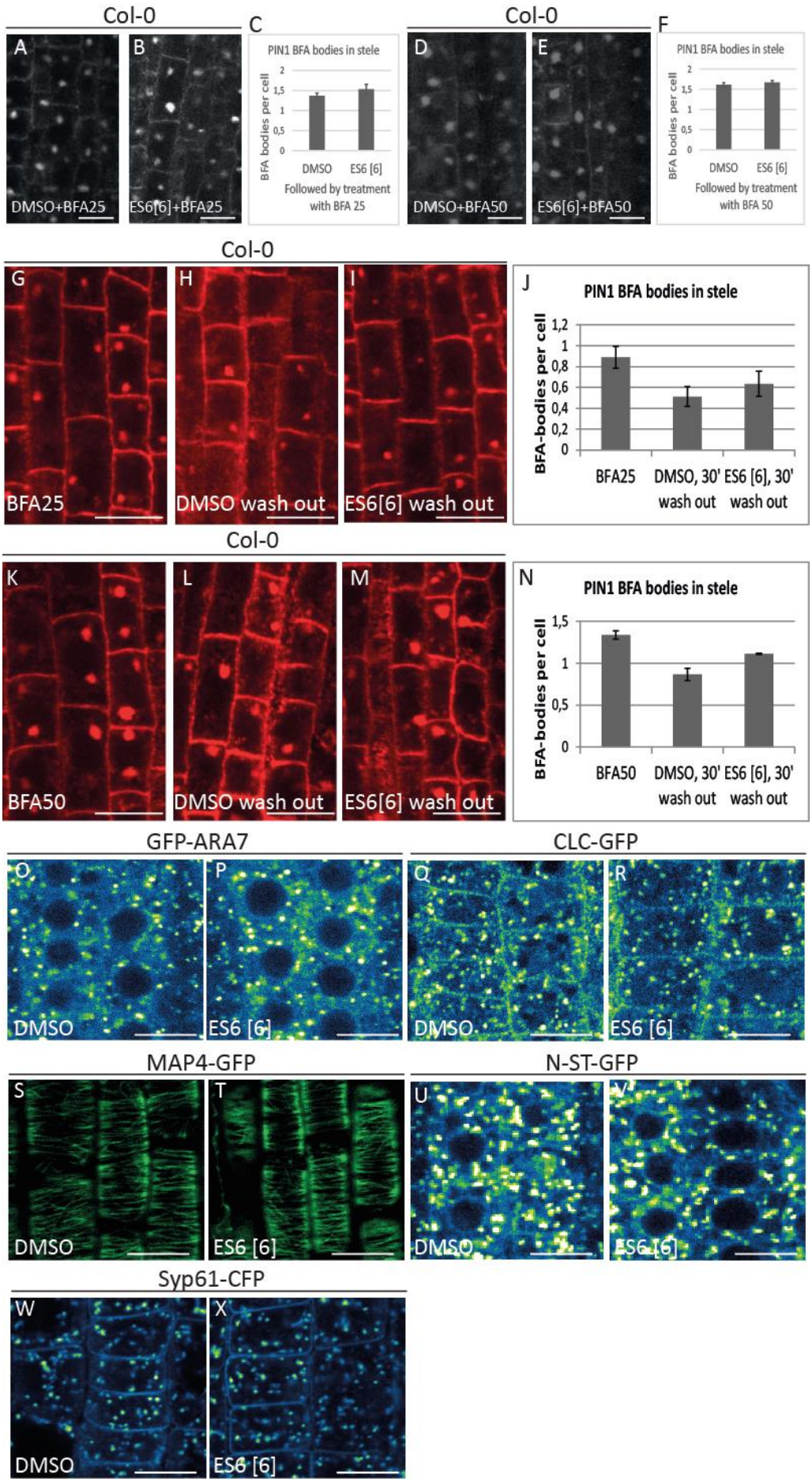
Col-0
A
B
C
PIN1 BFA bodies in stele
BFA bodies per cell
2
1,5
1
0,5
0
DMSO
ES6 [6]
Followed by treatment with BFA 25
DMSO+BFA25
ES6[6]+BFA25
Col-0
D
E
F
PIN1 BFA bodies in stele
BFA bodies per cell
DMSO
ES6 [6]
Followed by treatment with BFA 50
DMSO+BFA50
ES6[6]+BFA50
Col-0
G
H
I
J
PIN1 BFA bodies in stele
BFA-bodies per cell
1,2
1
0,8
0,6
0,4
0,2
0
BFA25
DMSO, 30' wash out
ES6 [6], 30' wash out
BFA25
DMSO wash out
ES6[6] wash out
Col-0
K
L
M
N
PIN1 BFA bodies in stele
BFA-bodies per cell
1,5
1
0,5
0
BFA50
DMSO, 30' wash out
ES6 [6], 30' wash out
BFA50
DMSO wash out
ES6[6] wash out
GFP-ARA7
O
P
DMSO
ES6 [6]
CLC-GFP
Q
R
DMSO
ES6 [6]
MAP4-GFP
S
T
DMSO
ES6 [6]
N-ST-GFP
U
V
DMSO
ES6 [6]
Syp61-CFP
W
X
DMSO
ES6 [6]

Supplemental Figure 3. Effects of ES6 on intracellular trafficking and compartments.
(A) to **(F)** Immunolocalization of PIN1 in Col-0 stele cells and mean number of BFA bodies per cell. Five-day-old seedlings were pre-treated for 30 min. with mock [**(A)** and **(D)**] or 6 µM ES6 [**(B)** and **(E)**] before 25 µM [**(A)** to **(C)**] or 50 µM BFA [**(D)** to **(F)**] was added for additional 90 min. The number of BFA bodies in the stele was counted for 10 cells in each root. In three independent experiments, 19-23 roots were analyzed for each treatment in total. There was no statistically significant difference between mock and ES6 treatment (Mann-Whitney *U* test, $P > 0.05$). Data are means ± SE of three experiments. Bars = 10 µm.
(G) to **(N)** Immunolocalization of PIN1 (red signal) in stele and quantification of BFA-bodies after wash-out with ES6. Five-day-old seedlings were treated for 2 h with 25 µM **(G)** or 50 µM of BFA **(K)** followed by 30 min. wash-out with medium complemented with mock [**(H)** and **(L)**] or 6 µM of ES6 [**(I)** and **(M)**]. In two independent experiments, 219-513 cells were analyzed for each treatment in total. There was no statistically significant difference between mock and ES6 wash-out (Mann-Whitney *U* test, $P > 0.05$). Data are means ± SE of two experiments. Bars = 10 µm.
(O) to **(X)** Intracellular localization of five-day-old ARA7-GFP [**(O)** and **(P)**], CLC-GFP [**(Q)** and **(R)**], MAP4-GFP [**(S)** and **(T)**], N-ST-GFP[**(U)** and **(V)**] and Syp61-CFP [**(W)** and **(X)**]marker lines after 2 h of mock and 6 µM ES6 treatment. There was no visible difference between mock and ES6 treatments in all tested markers. Bars = 10 µm.

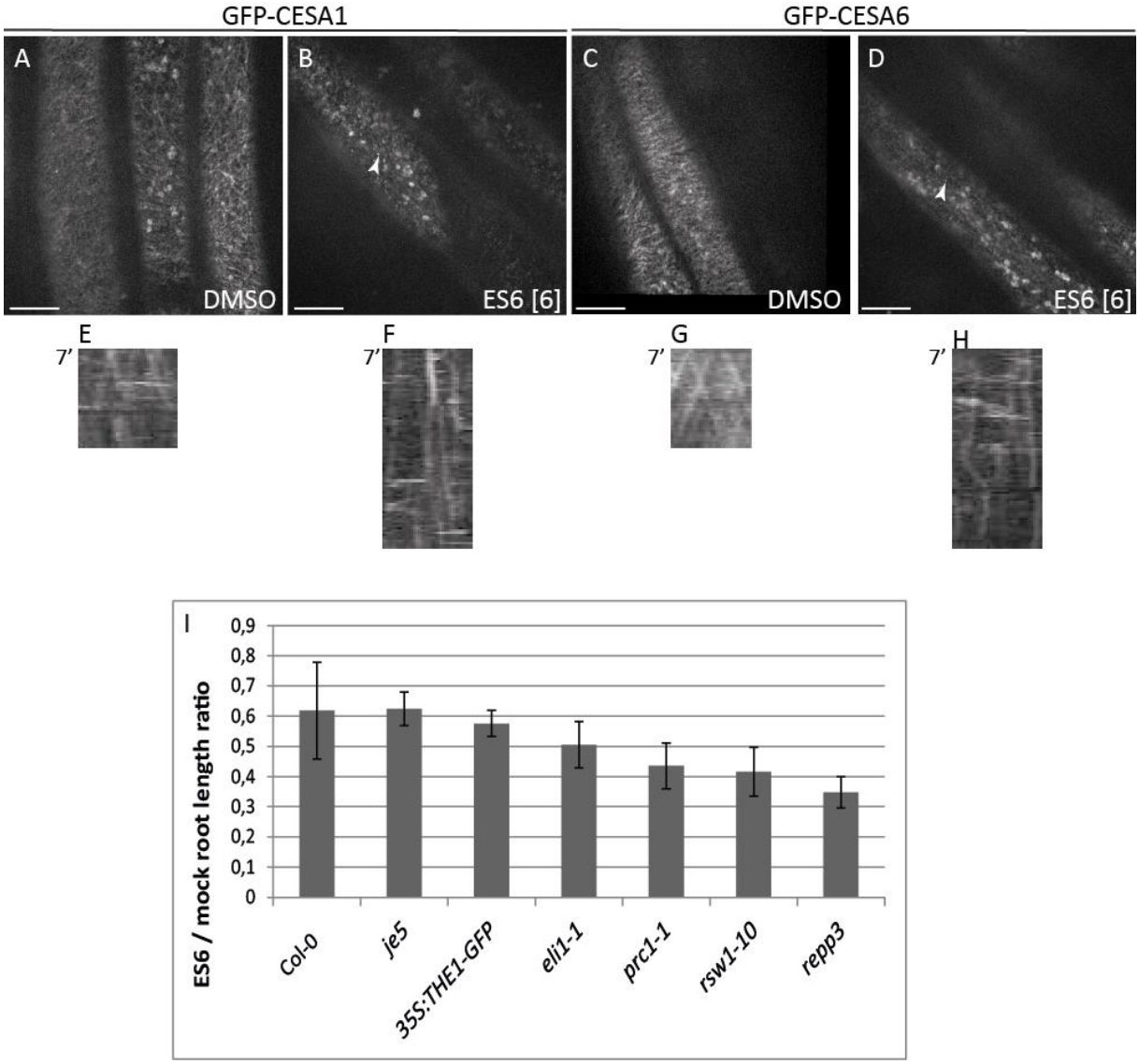

Supplemental Figure 4. Effects of ES6 on intracellular compartments and identification of ES6 sensitive mutants.

(A) to **(D)** Maximum projected z-stacks showing intracellular distribution of GFP-CASA1 [**(A)** and **(B)**] and GFP-CESA6 [**(C)** and **(D)**] in the five-day-old seedlings after 5 h of mock [**(A)** and **(C)**] and 6 µM ES6 [**(B)** and **(D)**] treatment in epidermal root cells. White arrows indicate GFP-CESA labelled MASC particles. Bars = 10 µm.

(E) to **(H)** Representative kymographs for treatment with mock [**(A)** and **(C)**] and 6 µM ES6 [**(B)** and **(D)**]. Time is represented along the vertical axis, and a 7 min scale bar is shown at left. CSC movement is steady and bidirectional [**(E)** and **(G)**]. Erratic movements of CSC indicates presence of MASCs [**(F)** and **(H)**].

(I) Quantification of root length sensitivity of wild type Col-0 and mutant (*je5*, *35S:THE-GFP*, *eli1-1*, *pre1-1*, *rsw1-1* and *repp3*) lines. Seedlings were grown for seven days on growth medium supplemented with mock and 1.4 µM ES6. Ratio of root lengths grown on ES6 to those grown on mock was calculated. In two independent experiments 10-25 roots were measured per each line and each treatment. There was no statistically significant difference between Col-0 and mutant lines (Student's *t* test, $P > 0.05$). Data are means ± SE of two experiments.

Chapter 4

Opposite auxin fluxes

Urszula Kania,[a,b] Zhaojun Ding,[c] Markus Geisler,[d] and Jiří Friml[a]

[a]Institute of Science and Technology Austria, 3400 Klosterneuburg, Austria
[b]Department of Plant Systems Biology, VIB and Department of Plant Biotechnology and Bioinformatics, Ghent University, 9052 Gent, Belgium
[c]The Key Laboratory of Plant Cell Engineering and Germplasm Innovation, Ministry of Education, School of Life Science, Shandong University, Jinan, Shandong 250 100, PR China
[d]University of Fribourg, Department of Biology- Plant Biology, Rue Albert-Gockel 3, PER04, CH-1700 Fribourg, Switzerland

ABSTRACT

PIN5 and PIN8 auxin transporters are localized to the endoplasmic reticulum (ER) membranes where they regulate auxin transport between cytosol and ER lumen. Previous studies suggest that PIN5 transports auxin from the cytosol to the ER lumen, whereas PIN8 may direct auxin flux in the opposite direction from the ER to the cytosol. To address the molecular properties and roles of PIN5 and PIN8 in determining the auxin flow directions across ER membranes, sequence based analysis of plasma membrane (PM) and ER-localized PIN proteins was conducted. The results revealed two domains specific for PIN8 proteins. To test whether these two motifs are important for the direction of auxin transport we generated a set of constructs designed for both auxin transport assays in heterologous yeast and tobacco protoplasts systems as well as for generating transgenic plants. The designed constructs contained modified PIN1 and PIN2 proteins with various configurations of the two PIN8 specific domains. Functional analysis of these constructs by genetic and biochemical approaches will provide new information about the possible role of these two motifs in controlling auxin fluxes.

AUTHOR CONTRIBUTIONS

Z.D., M.G. and J.F. conceived the project. M.G. performed auxin transport assay in yeasts, CLUSTAL X sequence alignment and proposed PIN sites for mutagenesis. Z.D. generated constructs indicated in the tables. U.K. generated constructs for auxin transport assays in yeasts and protoplasts and for plant transformation. U.K. transformed plants with the constructs. U.K. wrote the manuscript. J.F. revised and corrected the manuscript.

INTRODUCTION

Auxin is an important hormone regulating many aspects of plant development including embryogenesis (Friml et al., 2003), organogenesis (Benková et al., 2003), vascular tissue differentiation (Cheng et al., 2006; Scarpella et al., 2006) and tropic responses (Friml et al., 2002; Marchant et al., 1999). A variety of developmental responses in plants are associated with differential auxin distribution in the tissues. Such an unequal distribution of auxin, sometimes called auxin gradient, is established in tissues through PIN mediated polar auxin transport (PAT) (Petrásek et al., 2006). PM polarly localized PIN proteins mediate auxin efflux from the cells and in result auxin flow across the tissues. Besides PIN auxin efflux carriers, PM-localized AUXIN RESISTANT1/ LIKE AUX1 (AUX1/LAX) family proteins are responsible for auxin flowing into cells (Swarup et al., 2008; Yang et al., 2006). In some tissue types, like protophloem and shoot apical meristem, AUX1 displays asymmetric localization (Reinhardt et al., 2003; Swarup et al., 2001). In addition to the PM-localized PIN proteins, cellular auxin level is regulated by ER-localized PIN5, PIN6, and PIN8 mediating intracellular auxin transport between the cytosol and the ER (Bosco et al., 2012; Ding et al., 2012; Mravec et al., 2009; Sawchuk et al., 2013). Also recently characterized PIN-LIKES (PILS) were shown to regulate intracellular auxin accumulation and metabolism (Barbez et al., 2012). Characterization of PIN5 indicates its role in auxin transport at the ER, presumably transporting auxin from the cytosol to the lumen of the ER and reducing the amount of auxin available for the intercellular auxin transport and TIR1-dependant auxin signaling in the nucleus (Dharmasiri et al., 2005; Kepinski and Leyser, 2005). PIN8 is expressed in *Arabidopsis* male gametophyte (Ding et al., 2012). Ectopically expression of PIN8 revealed its localization to the ER (Ding et al., 2012). Genetic analysis of the loss-of-function mutants and overexpression lines of PIN5 and PIN8 demonstrated that the two proteins can compensate each other in regulating different developmental processes and auxin homeostasis which suggests their antagonistic function (Ding et al., 2012). To test the hypothesis whether PIN5 and PIN8 transport auxin in opposite directions, auxin transport assay in heterologous yeasts system was performed. Heterologous expression of PIN8 in yeast cells, when compared to the PIN5 and other PIN proteins (Petrásek et al., 2006; Mravec et al., 2009), induced accumulation of radioactively labelled indole-3-acetic acid (IAA) (Ding et al., 2012) which indicate that PIN8 has the property to import auxin. Additional transport assay on ER membrane fractions from PIN5 and PIN8- overexpressing (OE) cells showed increased auxin accumulation of the ER fractions from PIN8OE, and decreased from PIN5OE (Ding et al., 2012). Together this data indicates that PIN8 transports auxin in the opposite direction than other PIN proteins and as such is an auxin influx carrier, like the AUX1 protein. It has been shown that polar localization of PIN proteins depends on tissue-

specific factors (Wiśniewska et al., 2006). Additionally, sequences of PIN proteins encode information about its subcellular localization (Křeček et al., 2009)**.** The PM-localized PIN proteins (PIN1-4 and PIN7) contain transmembrane segments separated by long hydrophilic loop ("long" PINs), whereas PIN5 and PIN8 with reduced and PIN6 with partially reduced hydrophilic loop were shown to localize to the ER (Mravec et al. 2009; Dal Bosco et al. 2012; Ding et al. 2012; Sawchuk et al. 2013). However, recent data also demonstrated PM localization of PIN5 and PIN8 in diverse cell types (Ganguly et al., 2014). A recent study demonstrated that the long hydrophilic loop of "long" PIN proteins encodes molecular cues for intracellular PIN trafficking (Ganguly et al., 2014). Presumably the amino acid sequences of PIN proteins can also encode motifs regulating auxin transport activity. Although the mechanism of PIN proteins in auxin transport is not well understood, it is clear that both, PIN and AUX1/LAX proteins are crucial in this process.

RESULTS

Sequence Analysis of PIN Proteins

Sequence alignments between PIN proteins (CLUSTAL X) identified two domains specific for PIN8 (HPTTG, 94-98 and EEEDEEE, 190-196; Figure 1A) (Ding et al., unpublished).

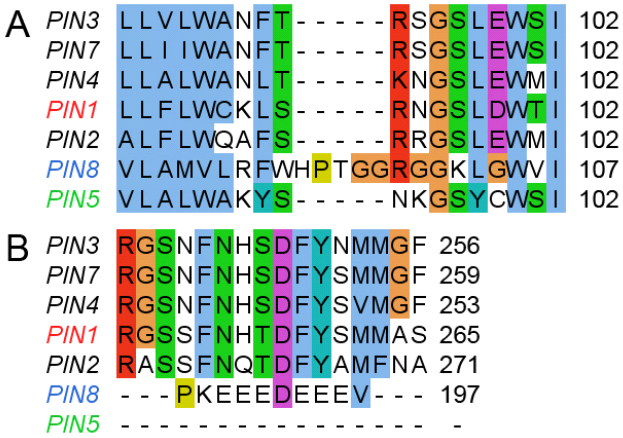

Figure 1. PIN proteins sequence alignment.
(A) and **(B)** Amino acid sequence alignment of PIN proteins using CLUSTAL X indicated that the HPTGG domain was only present in PIN8 **(A)**. The EEEDEEE domain contains conserved aspartic acid (D) among other PIN proteins and is absent in PIN5 **(B)**. Both domains were localized in the heavily charged cytosolic loop in loop connecting two transmembrane domains.

The HPTTG motif existed only in PIN8. The second motif identified in PIN8 (EEEDEEE) contained Asp (D) amino acid conserved between PIN8 and other PIN proteins, preceded and followed by three Glu (E) amino acids characteristic only for PIN8 (Figure 1B) (Ding, unpublished). To assess the role of these domains in PIN8-mediated auxin transport, a site-

directed mutagenesis was performed in *PIN8* by replacing His94 with Ala94 ($PIN8^{H94A}$). Additionally, the HPTTG domain was added after amino acid 93 in PIN5 sequence ($PIN5^{94HPTGG}$) and both constructs were transformed into yeast for auxin transport assays (Ding et al., unpublished). Replacing His94 with Ala94 in the *PIN8* sequence ($PIN8^{H94A}$) inverted the auxin transport direction (Figure 2A and B), as indicated by decreased retention of the radioactively labelled auxins IAA and α-naphthaleneacetic acid (NAA; Fig. 1A and B). However, insertion of this domain into the *PIN5* sequence had only a slight effect on auxin transport (Ding et al., unpublished; Figure 2C).

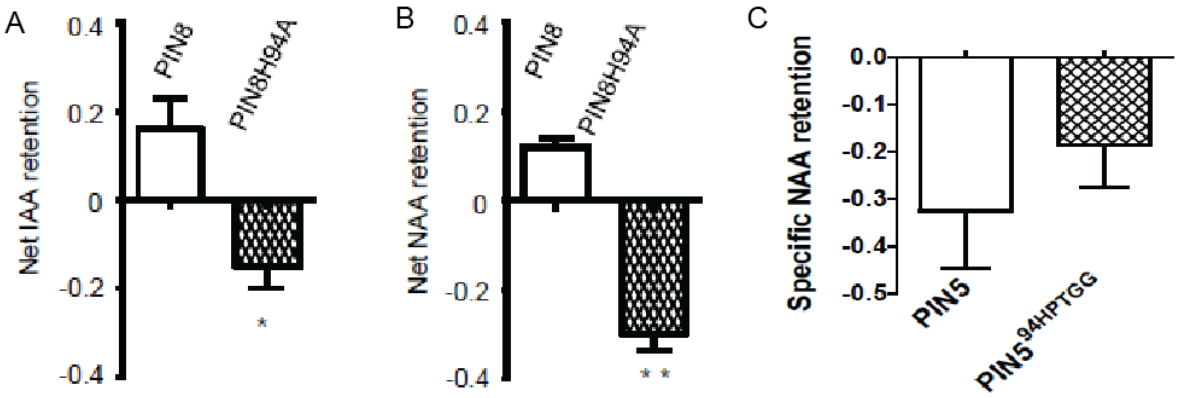

Figure 2. PIN8 and PIN5 have opposite auxin directions.
(A) and **(B)** in the yeast auxin efflux assay, PIN8H94A showed a decreased retention of IAA **(A)** and NAA **(B)** compared to the increased retention of IAA and NAA in the wild-type PIN8 expressing yeast, which implies that PIN8H94A has an opposite auxin transport direction compared to the wild-type PIN8. Data are means ± standard error (SE) of four experiments. Student's *t* test, $*P < 0.05$, $**P < 0.01$.
(C) The introduction of HTPGG domains into PIN5, resulting in PIN5 94HPTGG did not alter PIN5 auxin transport directionalities.

The second motif identified in PIN8 (EEEDEEE) contained Asp (D) amino acid conserved between PIN8 and other PIN proteins, preceded and followed by three Glu (E) amino acids characteristic only for PIN8 (Figure 1b) (Ding, unpublished). The apparent transport rates in the opposite direction can be an indication of the importance of these motifs for different affinities to IAA at the open/closed conformations at the particular side of the membrane. To further study their function, site-directed mutagenesis was performed on *PIN1*, *PIN2*, *PIN5* and *PIN8* (Ding et al., unpublished). For simplicity, mutations related to the first domain ($PIN1^{94HPTGG}$, $PIN2^{94HPTGG}$, $PIN5^{94HPTGG}$, $PIN8^{H94A}$) were named "A", and to the second one ($PIN1^{D258A}$, $PIN2^{D264A}$, $PIN5^{180EEEDEEE}$, $PIN8^{\Delta 190\text{-}196}$) "B" (hereafter). The preliminary results were obtained from the auxin transport assay in yeasts expressing *PIN2*, *PIN2A*, *PIN2B*, *PIN5*, *PIN5A*, *PIN5B*, *PIN8*, *PIN8A* and *PIN8B*. The PIN8 displayed opposite auxin flux compared to PIN2 or PIN5 and PIN2A worked slightly in an import direction (Ding et al., unpublished).

Generation of the Constructs for Yeasts Auxin Transport Assay

Preliminary results on auxin transport mediated by genetically modified PIN proteins prompted us to further analyze the identified domains. A site-directed mutagenesis of the coding sequences (CDS) of PIN1 and PIN2 was performed analogously as described above. As a result the following constructs were obtained: $PIN1^{94HPTGG}$ (PIN1A), $PIN1^{D258A}$ (PIN1B), $PIN1^{94HPTGG,\ D258A}$ (PIN1AB) and $PIN2^{94HPTGG,\ D264A}$ (PIN2AB). The PIN1, PIN1A, PIN1B, PIN1AB, PIN2, PIN2AB were tagged with a haemagglutinin epitope (HA) on their C-terminus and the *NotI* restriction sites were added for the introduction to the yeast expressing pNEV-N vector for auxin transport assay. It has been shown that the expression of PIN proteins in yeasts lead to decreased retention of radioactively labeled auxins suggesting increased auxin efflux (Petrasek et al. 2006; Mravec et al. 2009). Beside the auxin transport in the heterologous yeast system, the ability of the mutated PIN proteins has to be checked *in planta*.

Generation of the Constructs for Auxin Transport Assay in Tobacco Protoplasts

To test the directionality of auxin fluxes, driven by the mutated PIN proteins, we have introduced the *PIN1*, *PIN1A*, *PIN1B*, *PIN1AB*, *PIN2*, *PIN2A*, *PIN2B* and *PIN2AB* genes to the destination vector. The resulting clones were created to perform auxin transport assay in mesophyll protoplasts of transiently transfected tobacco (*Nicotiana benthamiana*).

Generation of the Gateway Constructs for *Arabidopsis* Transformation

To further test whether the two identified domains specific for PIN8 play a role in mediating auxin fluxes, we have introduced the *PIN1*, *PIN1A*, *PIN1B*, *PIN1AB*, *PIN2*, *PIN2A*, *PIN2B* and *PIN2AB* into the destination vectors under the transcriptional regulation of their native promoters, the *AUX1* promoter and cauliflower mosaic virus (CaMV) 35S constitutive promoter for the *Arabidopsis* plant transformation. All of the destination vectors with CaMV 35S promoter contained kanamycin phosphotransferase plant-selectable marker gene. Vectors with the *PIN1*, *PIN2* and *AUX1* promoters contained basta plant selectable marker gene and could be transformed to the SALK T-DNA insertions lines (*pin1-201*, *eir1-4* and *aux1*) which are kanamycin resistant. To examine the subcellular localization of mutated PIN2A, PIN2B, PIN2AB and wild-type PIN2 in plants, GFP sequence was inserted into the constructs, as described in Xu and Scheres, 2005 and expressed under the control of the CaMV 35S promoter.

Plant transformation

To test the functionality of the *PIN1* and *AUX1* promoters, they were introduced into the reporter vectors carrying a double GFP fusion with a nuclear localization signal and

transformed to the Col-0 wild type. Plants transformed with these constructs showed nuclear GFP signal in the root meristematic zone (Figure 3).

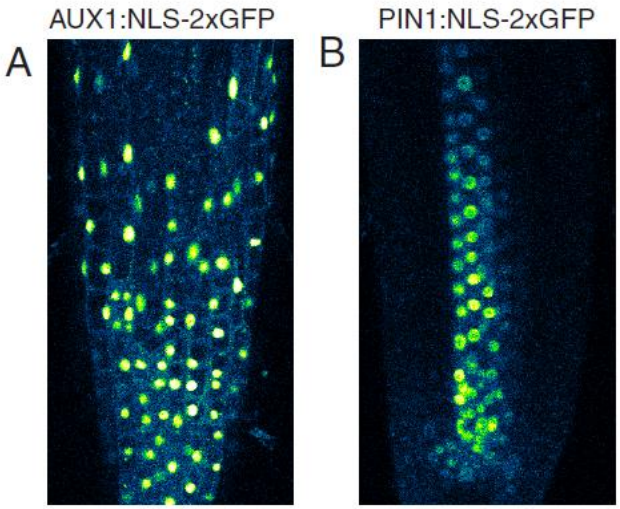

Figure 3. Analysis of the *AUX1* and *PIN1* promoter activity.
(A) and **(B)** *AUX1* and *PIN1* promoter activity visualized by fusion of double GFP with a nuclear localization signal.

Constructs with genes driven by the CaMV 35S promoter were transformed into the Col-0 wild-type plants, whereas those containing *PIN1* and *PIN2* promoters were transformed into the *pin1-201* and *eir1-4* T-DNA insertion lines, respectively. Additionally, constructs with the *AUX1* promoter were introduced into the *aux1* T-DNA mutant background. As *pin1* homozygous mutants are sterile, heterozygous plants were selected on medium supplemented with kanamycin for plant transformation. Generations of plants obtained after transformation with different constructs are summarized in table 3.

DISCUSSION AND PERSPECTIVES

In this study we have generated constructs for the analysis of auxin transport direction in yeasts and protoplasts. Moreover, we obtained plants transformed with variable constructs with mutated PIN proteins. Further analysis of the generated constructs and transformants needs to be conducted in order to dissect the role of two domains specific for PIN8 in mediating auxin transport directionalities. Since no straightforward method is known to show direction of auxin transport mediated by PIN proteins, different approaches have to be combined to address this issue. By comparison of the auxin transport in yeasts and protoplasts or free auxin accumulation in the protoplasts expressing various PIN proteins (Petrasek et al., 2006; Mravec et al., 2009; Ding et al., 2012) we can draw conclusions about the direction of auxin flux. Another option is to use the heterologous *Xenopus laevis* oocyte expression system, which has recently proven useful in studying auxin transport by PIN (Zourelidou et al., 2014). Additionally, genetic analysis of plants carrying modified versions of

PIN proteins, like loss of function and overexpression lines of the PIN5 and PIN8 (Ding et al., 2012), might indicate the possible direction of auxin transport mediated by those proteins. Analysis of the *pin1*, *eir1* and *aux1* mutants transformed with generated constructs can provide us with additional information about directionality of auxin transport. Mutants of the auxin efflux carriers *pin1-201* and *eir1-4* and auxin influx carrier *aux1*, display variable phenotypic defects associated with the transport of auxin and as a result exhibit changed auxin gradients. *pin2* and *aux1* have agravitropic roots whereas *pin1* mutant has fused leaves, *pin*-like inflorescence, defective flowers and three cotyledons (Chen et al., 1998; Luschnig et al., 1998; Marchant et al., 1999; Okada et al., 1991). Mutated *PIN1* and *PIN2,* driven by their native promoters and expressed in the *pin1-201* and *eir1-4* background, respectively, will demonstrate whether these mutants can be complemented by any of the A or B domains. If the two domains mediate directionality of auxin transport, it is expected that mutated versions of PIN1 and PIN2, as opposed to the wild type sequences, will not be able to complement the *pin1-201* and *eir1-4* phenotypes. AUX1, as opposed to the efflux carriers from the PIN protein family, is an influx carrier facilitating auxin entry into the cells from the extracellular matrix. This means it transports auxin in the opposite direction than PM-localized PIN proteins. Restoration of the wild type phenotype of the *aux1* by expression of the mutated *PIN1* and *PIN2* driven by the *AUX1* promoters would indicate that the PIN8 specific domains are involved in mediating auxin transport direction. The transformants will be examined in terms of the free auxin levels, auxin transport and auxin metabolism. Also, various aspects of plant development which require unaffected polar auxin transport can be tested, like root and hypocothyl growth, meristem organization or lateral root growth. Additionally, modelling of PIN8 and comparison to the other known transporters structures can provide additional information about role of the two motifs in different transport directionalities. It is possible that the opposite direction of auxin flux can be caused by different substrate affinities to IAA at the open/closed conformations at the particular side of the membrane.

METHODS

Plasmid Construction

All primers used to generate constructs in this study are summarized in Table 1. Mutated *PIN1A* (insertion of HPTTG, 94-98), *PIN1B* (Asp258 replaced with Ala258), *PIN1AB* and *PIN2AB* (HPTGG after 93 and Asp258 replaced with Ala 258) constructs with the HA-tag (TACCCATACGATGTTCCAGATTACGCT, C-terminal fusion), *NotI* restriction sites and *att*B-flanking sites were obtained through direct gene synthesis (DNA 2.0). Generated constructs were introduced into pDONR221 (Invitrogen) to obtain entry clones PIN1A_pDONR221,

PIN1B_pDONR221, PIN1AB_pDONR221 and PIN2AB_pDONR221 (Table 2, numbers 1-4). The wild type *PIN1* and *PIN2* were amplified from plasmids containing CDS of those genes and inserted into pDONR221 vector with primers containing additional HA-tag, *NotI* and *att*B sites (Table 2, numbers 20-21). All generated entry clones were sub-cloned into the pNEV-N yeast expression vector to generate P1A_pNEV, P1B_pNEV, P1AB_pNEV, P2AB_pNEV and PIN1HA_pNEV and PIN2HA_pNEV control vectors for auxin measurement in yeasts (Table 4). Constructs containing PIN1, PIN2 and AUX1 promoters (PIN1prom_TOPO, PIN2prom_TOPO and AUX1prom_TOPO, respectively) were generated by BP clonase recombination reaction according to the manufacturer's instructions (Invitrogen) (Table 2, numbers 5-7). For the BP reaction PCR-amplified fragments of PIN1, PIN2 and AUX1 promoters (nucleotides -1289 to -5 for PIN1, according to Benkova et al., 2003; -1302 to -1 for PIN2, according to Wiśniewska et al., 2006 and -2479 to -4 for AUX1) and pENTR5'-TOPO vector were taken. Entry clones with numbers 8-19 (Table 2) were generated by BP clonase recombination reaction between PCR-amplified fragments and pDONR221 vector according to the manufacturer's instructions (Invitrogen). Entry clones containing GFP fluorescent marker (Table 2, numbers 16-19) were generated by insertion of GFP into the coding sequence of the wild type and mutated *PIN2* at 1287 position from ATG of wild type *PIN2* (corresponding to the 2312 position in genomic fragment; Xu and Scheres, 2005).
Expression vectors were generated by LR clonase reactions of DNA fragments from entry clones and destination vectors according to the manufacturer's instructions (Invitrogen) (Table 3). For auxin transport assay in protoplasts the pK7WG2D destination vector was used (Table 3, numbers 4-11). This vector contains kanamycin selection marker and free GFP for visualization of transformed cells. The products of LR recombination reactions were used to transform heat shock competent *E*. *coli* strain DH5 alpha.

Plant Material and Plant Transformation.

Obtained constructs (Table 3, numbers 1, 3, 12-38) were transformed to the *Agrobacterium tumefaciens* strain C58C1 and introduced into *A. thaliana* Col-0, *pin1-201* (SALK_047613), *pin2/eir1-4* (SALK_091142) or *aux1-100* plants using the floral dip method (Clough and Bent, 1998). As *pin1* homozygous mutants are sterile, heterozygous plants were selected on medium supplemented with kanamycin for plant transformation. Plants transformed with constructs containing 35S promoter were selected on kanamycin supplemented medium, whereas those with constructs driven by *PIN1*, *PIN2* and *AUX1* promoters were selected on basta containing medium. All the constructs were summarized in a table (including vector name, construct name, and transformed *Arabidopsis* plants recipient pDONR, entry clone and destination vector).

Synthesized Gene Sequences.

PIN2AB: 2059bp (HPTGG after 93; D264 changed to A264)

GGGGACAAGTTTGTACAAAAAAGCAGGCTGCGGCCGCATGATCACCGGCAAAGACATGTACGATGTTTTAGCGGCTATG
GTGCCGCTATACGTTGCTATGATATTAGCCTATGGTTCGGTACGGTGGTGGGGGATATTCACACCGGACCAATGTTCCGGT
ATAAACCGGTTCGTTGCGGTTTTCGCGGTTCCTCTTCTCTCTTTCCATTTCATCTCCTCCAATGATCCTTATGCAATGAATTAC
CACTTCCTCGCTGCTGATTCTCTTCAGAAAGTCGTTATCCTCGCCGCACTCTTTCTTTGGCAGGCGTTTAGCCATCCAACAGG
AGGACGCAGAGGAAGCCTAGAATGGATGATAACGCTCTTTTCACTATCAACACTGCCTAACACGTTGGTAATGGGAATCCC
ATTGCTTAGGGCGATGTACGGAGACTTCTCCGGTAACCTAATGGTGCAGATCGTGGTGCTTCAGAGCATCATATGGTATAC
ATTAATGCTCTTCTTGTTTGAGTTCCGTGGGGCTAAGCTTCTCATCTCCGAGCAGTTCCCGGAGACGGCTGGTTCAATTACT
TCCTTCAGAGTTGACTCTGATGTTATCTCTCTTAATGGCCGTGAACCCCTCCAGACCGATGCGGAGATAGGAGACGACGGA
AAGCTACACGTGGTGGTTCGAAGATCAAGTGCCGCCTCATCAATGATCTCTTCATTCAACAAATCTCACGGCGGAGGACTT
AACTCCTCCATGATAACGCCGCGAGCTTCAAATCTCACCGGCGTAGAGATTTACTCCGTTCAATCGTCACGAGAGCCGACG
CCGAGAGCTTCTAGCTTTAATCAGACAGCATTCTACGCAATGTTTAACGCAAGCAAAGCTCCAAGCCCTCGTCACGGTTAC
ACTAATAGCTACGGCGGCGCTGGAGCTGGTCCAGGTGGAGATGTTTACTCACTTCAGTCTTCTAAAGGCGTGACGCCGAG
AACGTCAAATTTTGATGAGGAAGTTATGAAGACGGCGAAGAAAGCAGGAAGAGGAGGCAGAAGTATGAGTGGGGAATT
ATACAACAATAATAGTGTTCCGTCGTACCCACCGCCGAACCCAATGTTCACGGGGTCAACGAGTGGAGCAAGTGGAGTCA
AGAAAAAGGAAAGTGGTGGCGGAGGAAGCGGTGGCGGAGTAGGAGTAGGAGGACAAAACAAGGAGATGAACATGTTC
GTGTGGAGTTCGAGTGCTTCTCCGGTGTCGGAAGCCAACGCGAAGAATGCTATGACCAGAGGTTCTTCCACCGATGTATC
CACCGACCCTAAAGTTTCTATTCCTCCTCACGACAACCTCGCTACTAAAGCGATGCAGAATCTGATAGAGAACATGTCACCG
GGAAGAAAAGGGCATGTGGAAATGGACCAAGACGGTAATAACGGGGGAAAGTCACCTTACATGGGCAAAAAAGGTAGC
GACGTGGAAGACGGCGGTCCCGGTCCTAGGAAACAGCAGATGCCGCCGGCGAGTGTGATGACGAGACTAATTCTGATAA
TGGTTTGGAGAAAACTCATTCGAAACCCTAACACTTACTCTAGTCTCTTTGGCCTTGCTTGGTCCCTTGTCTCTTTCAAGTGG
AATATAAAGATGCCAACGATAATGAGTGGATCGATTTCGATATTATCTGATGCTGGTCTTGGAATGGCTATGTTTAGTCTT
GGTCTATTTATGGCATTGCAACCAAAGATTATTGCGTGCGGAAAATCAGTAGCAGGGTTTGCGATGGCCGTAAGGTTCTTG
ACTGGACCAGCCGTGATCGCAGCCACCTCAATAGCAATTGGTATTCGAGGTGATCTCCTCCATATCGCCATCGTTCAGGCT
GCTCTTCCTCAAGGAATCGTTCCTTTTGTTTTCGCCAAAGAATATAACGTCCATCCTGATATTCTCAGCACTGCGGTTATATT
CGGAATGCTGGTTGCTTTGCCTGTAACAGTACTCTACTACGTTCTTTTGGGGCTTTACCCATACGATGTTCCAGATTACGCT
GCGGCCGCTTACCCAGCTTTCTTGTACAAAGTGGTCCCC

PIN1A: 1984bp(HPTGG after amino acid 93)

GGGGACAAGTTTGTACAAAAAAGCAGGCTGCGGCCGCATGATTACGGCGGCGGACTTCTACCACGTTATGACGGCTATG
GTTCCGTTATACGTAGCTATGATCCTCGCTTACGGCTCTGTCAAATGGTGGAAAATCTTCACACCAGACCAATGCTCCGGCA
TAAACCGTTTCGTCGCTCTCTTCGCCGTTCCTCTCCTCTCTTTCCACTTCATCGCCGCTAACAACCCTTACGCCATGAACCTCC
GTTTCCTCGCCGCAGATTCTCTCCAGAAAGTCATTGTCCTCTCTCTCCTCTTCCTCTGGTGCAAACTCAGCCATCCAACAGGA
GGACGCAACGGTTCTTTAGATTGGACCATAACTCTCTTCTCTCTCTCGACACTCCCCAACACTCTAGTCATGGGGATACCTCT
TCTCAAAGGCATGTATGGTAATTTCTCCGGCGACCTCATGGTTCAAATCGTTGTTCTTCAGTGTATCATTTGGTACACACTCA
TGCTCTTTCTCTTTGAGTACCGTGGAGCTAAGCTTTTGATCTCCGAGCAGTTTCCAGACACAGCAGGATCTATTGTTTCGAT
TCATGTTGATTCCGACATTATGTCTTTAGATGGAAGACAACCTTTGGAAACTGAAGCTGAGATTAAAGAAGATGGGAAGCT
TCATGTTACTGTTCGTCGTTCTAATGCTTCAAGGTCTGATATTTACTCGAGAAGGTCTCAAGGCTTATCTGCGACACCTAGA
CCTTCGAATCTAACCAACGCTGAGATATATTCGCTTCAGAGTTCAAGAAACCCAACGCCACGTGGCTCTAGTTTTAATCATA
CTGATTTTTACTCGATGATGGCTTCTGGTGGTGGTCGGAACTCTAACTTTGGTCCTGGAGAAGCTGTGTTTGGTTCTAAAG
GTCCTACTCCGAGACCTTCCAACTACGAAGAAGACGGTGGTCCTGCTAAACCGACGGCTGCTGGAACTGCTGCTGGAGCT
GGGAGGTTTCATTATCAATCTGGAGGAAGTGGTGGCGGTGGAGGAGCGCATTATCCGGCGCCGAACCCAGGGATGTTTT
CGCCCAACACTGGCGGTGGTGGAGGCACGGCGGCGAAAGGAAACGCTCCGGTGGTTGGTGGGAAAAGACAAGACGGAA
ACGGAAGAGATCTTCACATGTTTGTGTGGAGCTCAAGTGCTTCGCCGGTCTCAGATGTGTTCGGCGGTGGAGGAGGAAAC
CACCACGCCGATTACTCCACCGCTACGAACGATCATCAAAAGGACGTTAAGATCTCTGTACCTCAGGGGAATAGTAACGAC
AACCAGTACGTGGAGAGGGAAGAGTTTAGTTTCGGTAACAAAGACGATGATAGCAAAGTATTGGCAACGGACGGTGGGA
ACAACATAAGCAACAAAACGACGCAGGCTAAGGTGATGCCACCAACAAGTGTGATGACAAGACTCATTCTCATTATGGTTT
GGAGGAAACTTATTCGTAATCCCAACTCTTACTCCAGTTTATTCGGCATCACCTGGTCCCTCATTTCCTTCAAGTGGAACATT
GAAATGCCAGCTCTTATAGCAAAGTCTATCTCCATACTCTCAGATGCAGGTCTAGGCATGGCTATGTTCAGTCTTGGGTTGT
TCATGGCGTTAAACCCAAGAATAATAGCTTGTGGAAACAGAAGAGCAGCTTTTGCGGCGGCTATGAGATTTGTCGTTGGA
CCTGCCGTCATGCTCGTTGCTTCTTATGCCGTTGGCCTCCGTGGCGTCCTCCTCCATGTTGCCATTATCCAGGCAGCTTTGCC
GCAAGGAATAGTACCGTTTGTGTTTGCCAAAGAGTATAATGTGCATCCTGACATTCTTAGCACTGCGGTGATATTTGGGAT

GTTGATCGCGTTGCCCATAACTCTTCTCTACTACATTCTCTTGGGTCTATACCCATACGATGTTCCAGATTACGCTGCGGCCG
CTTACCCAGCTTTCTTGTACAAAGTGGTCCCC

PIN1B: 1969bp (D258 changed to A258)

GGGGACAAGTTTGTACAAAAAAGCAGGCTGCGGCCGCATGATTACGGCGGCGGACTTCTACCACGTTATGACGGCTATG
GTTCCGTTATACGTAGCTATGATCCTCGCTTACGGCTCTGTCAAATGGTGGAAAATCTTCACACCAGACCAATGCTCCGGCA
TAAACCGTTTCGTCGCTCTCTTCGCCGTTCCTCTCCTCTCTTTCCACTTCATCGCCGCTAACAACCCTTACGCCATGAACCTCC
GTTTCCTCGCCGCAGATTCTCTCCAGAAAGTCATTGTCCTCTCTCTCCTCTTCCTCTGGTGCAAACTCAGCCGCAACGGTTCT
TTAGATTGGACCATAACTCTCTTCTCTCTCTCGACACTCCCCAACACTCTAGTCATGGGGATACCTCTTCTCAAAGGCATGTA
TGGTAATTTCTCCGGCGACCTCATGGTTCAAATCGTTGTTCTTCAGTGTATCATTTGGTACACACTCATGCTCTTTCTCTTTG
AGTACCGTGGAGCTAAGCTTTTGATCTCCGAGCAGTTTCCAGACACAGCAGGATCTATTGTTTCGATTCATGTTGATTCCGA
CATTATGTCTTTAGATGGAAGACAACCTTTGGAAACTGAAGCTGAGATTAAAGAAGATGGGAAGCTTCATGTTACTGTTCG
TCGTTCTAATGCTTCAAGGTCTGATATTTACTCGAGAAGGTCTCAAGGCTTATCTGCGACACCTAGACCTTCGAATCTAACC
AACGCTGAGATATATTCGCTTCAGAGTTCAAGAAACCCAACGCCACGTGGCTCTAGTTTTAATCATACTGCATTTTACTCGA
TGATGGCTTCTGGTGGTGGTCGGAACTCTAACTTTGGTCCTGGAGAAGCTGTGTTTGGTTCTAAAGGTCCTACTCCGAGAC
CTTCCAACTACGAAGAAGACGGTGGTCCTGCTAAACCGACGGCTGCTGGAACTGCTGCTGGAGCTGGGAGGTTTCATTAT
CAATCTGGAGGAAGTGGTGGCGGTGGAGGAGCGCATTATCCGGCGCCGAACCCAGGGATGTTTTCGCCCAACACTGGCG
GTGGTGGAGGCACGGCGGCGAAAGGAAACGCTCCGGTGGTTGGTGGGAAAAGACAAGACGGAAACGGAAGAGATCTTC
ACATGTTTGTGTGGAGCTCAAGTGCTTCGCCGGTCTCAGATGTGTTCGGCGGTGGAGGAGGAAACCACCACGCCGATTAC
TCCACCGCTACGAACGATCATCAAAAGGACGTTAAGATCTCTGTACCTCAGGGGAATAGTAACGACAACCAGTACGTGGA
GAGGGAAGAGTTTAGTTTCGGTAACAAAGACGATGATAGCAAAGTATTGGCAACGGACGGTGGGAACAACATAAGCAAC
AAAACGACGCAGGCTAAGGTGATGCCACCAACAAGTGTGATGACAAGACTCATTCTCATTATGGTTTGGAGGAAACTTATT
CGTAATCCCAACTCTTACTCCAGTTTATTCGGCATCACCTGGTCCCTCATTTCCTTCAAGTGGAACATTGAAATGCCAGCTCT
TATAGCAAAGTCTATCTCCATACTCTCAGATGCAGGTCTAGGCATGGCTATGTTCAGTCTTGGGTTGTTCATGGCGTTAAAC
CCAAGAATAATAGCTTGTGGAAACAGAAGAGCAGCTTTTGCGGCGGCTATGAGATTTGTCGTTGGACCTGCCGTCATGCT
CGTTGCTTCTTATGCCGTTGGCCTCCGTGGCGTCCTCCTCCATGTTGCCATTATCCAGGCAGCTTTGCCGCAAGGAATAGTA
CCGTTTGTGTTTGCCAAAGAGTATAATGTGCATCCTGACATTCTTAGCACTGCGGTGATATTTGGGATGTTGATCGCGTTGC
CCATAACTCTTCTCTACTACATTCTCTTGGGTCTATACCCATACGATGTTCCAGATTACGCTGCGGCCGCTTACCCAGCTTTC
TTGTACAAAGTGGTCCCC

PIN1AB: 1984bp(HPTGG after amino acid 93; D258 changed to A258)

GGGGACAAGTTTGTACAAAAAAGCAGGCTGCGGCCGCATGATTACGGCGGCGGACTTCTACCACGTTATGACGGCTATG
GTTCCGTTATACGTAGCTATGATCCTCGCTTACGGCTCTGTCAAATGGTGGAAAATCTTCACACCAGACCAATGCTCCGGCA
TAAACCGTTTCGTCGCTCTCTTCGCCGTTCCTCTCCTCTCTTTCCACTTCATCGCCGCTAACAACCCTTACGCCATGAACCTCC
GTTTCCTCGCCGCAGATTCTCTCCAGAAAGTCATTGTCCTCTCTCTCCTCTTCCTCTGGTGCAAACTCAGCCATCCAACAGGA
GGACGCAACGGTTCTTTAGATTGGACCATAACTCTCTTCTCTCTCTCGACACTCCCCAACACTCTAGTCATGGGGATACCTCT
TCTCAAAGGCATGTATGGTAATTTCTCCGGCGACCTCATGGTTCAAATCGTTGTTCTTCAGTGTATCATTTGGTACACACTCA
TGCTCTTTCTCTTTGAGTACCGTGGAGCTAAGCTTTTGATCTCCGAGCAGTTTCCAGACACAGCAGGATCTATTGTTTCGAT
TCATGTTGATTCCGACATTATGTCTTTAGATGGAAGACAACCTTTGGAAACTGAAGCTGAGATTAAAGAAGATGGGAAGCT
TCATGTTACTGTTCGTCGTTCTAATGCTTCAAGGTCTGATATTTACTCGAGAAGGTCTCAAGGCTTATCTGCGACACCTAGA
CCTTCGAATCTAACCAACGCTGAGATATATTCGCTTCAGAGTTCAAGAAACCCAACGCCACGTGGCTCTAGTTTTAATCATA
CTGCATTTTACTCGATGATGGCTTCTGGTGGTGGTCGGAACTCTAACTTTGGTCCTGGAGAAGCTGTGTTTGGTTCTAAAG
GTCCTACTCCGAGACCTTCCAACTACGAAGAAGACGGTGGTCCTGCTAAACCGACGGCTGCTGGAACTGCTGCTGGAGCT
GGGAGGTTTCATTATCAATCTGGAGGAAGTGGTGGCGGTGGAGGAGCGCATTATCCGGCGCCGAACCCAGGGATGTTTT
CGCCCAACACTGGCGGTGGTGGAGGCACGGCGGCGAAAGGAAACGCTCCGGTGGTTGGTGGGAAAAGACAAGACGGAA
ACGGAAGAGATCTTCACATGTTTGTGTGGAGCTCAAGTGCTTCGCCGGTCTCAGATGTGTTCGGCGGTGGAGGAGGAAAC
CACCACGCCGATTACTCCACCGCTACGAACGATCATCAAAAGGACGTTAAGATCTCTGTACCTCAGGGGAATAGTAACGAC
AACCAGTACGTGGAGAGGGAAGAGTTTAGTTTCGGTAACAAAGACGATGATAGCAAAGTATTGGCAACGGACGGTGGGA
ACAACATAAGCAACAAAACGACGCAGGCTAAGGTGATGCCACCAACAAGTGTGATGACAAGACTCATTCTCATTATGGTTT
GGAGGAAACTTATTCGTAATCCCAACTCTTACTCCAGTTTATTCGGCATCACCTGGTCCCTCATTTCCTTCAAGTGGAACATT
GAAATGCCAGCTCTTATAGCAAAGTCTATCTCCATACTCTCAGATGCAGGTCTAGGCATGGCTATGTTCAGTCTTGGGTTGT
TCATGGCGTTAAACCCAAGAATAATAGCTTGTGGAAACAGAAGAGCAGCTTTTGCGGCGGCTATGAGATTTGTCGTTGGA
CCTGCCGTCATGCTCGTTGCTTCTTATGCCGTTGGCCTCCGTGGCGTCCTCCTCCATGTTGCCATTATCCAGGCAGCTTTGCC
GCAAGGAATAGTACCGTTTGTGTTTGCCAAAGAGTATAATGTGCATCCTGACATTCTTAGCACTGCGGTGATATTTGGGAT

GTTGATCGCGTTGCCCATAACTCTTCTCTACTACATTCTCTTGGGTCTATACCCATACGATGTTCCAGATTACGCTGCGGCCG
CTTACCCAGCTTTCTTGTACAAAGTGGTCCCC

Legend

GGGGACAAGTTTGTACAAAAAAGCAGGCT - *att*B1
GCGGCCGC - *NotI* restriction site
GCGTTTAGC , AAACTCAGC - sequence preceding HPTGG insertion
CATCCAACAGGAGGA - inserted HPTGG
GCA - D to A substitution
GAT - D amino acid
ACTAAA (GFP) GCGATG - place of GFP insertion
TACCCATACGATGTTCCAGATTACGCT - HA-tag
TTACCCAGCTTTCTTGTACAAAGTGGTCCCC - *att*B2 with two additional TT to maintain the proper reading frame

Table 1. List of Primers Used for Constructs Generation.

No	Name	Sequence
1	*PIN1promF*	5'-CCTCATTATATCATCAACCCATTGC
2	*PIN1promR*	5'-TGTTCGCCGGAGAAGAGAGA
3	*PIN2promF*	5'-TAAAACTGAGATCACTTATTAAAGGC
4	*PIN2promR*	5'-TTTGATTTACTTTTTCCGGCGAGAG
5	*AUX1prom_FP_new*	5'-taaagaagacctgcaacatt
6	*AUX1prom_RP*	5'-tttagcttctagatctgag
7	*PIN2Rgfp*	5'-tcctcgcccttgctcaccatTTTAGTAGCGAGGTTGTCGT
8	*GFPFpin2*	5'-ACGACAACCTCGCTACTAAAatggtgagcaagggcgagga
9	*PIN2F2gfp*	5'-gcatggacgagctgtacaagGCGATGCAGAATCTGATAGAGAACA
10	*GFPRpin2*	5'-cttgtacagctcgtccatgcTGTTCTCTATCAGATTCTGCATCGC
11	*P2F_NotIattb*	5'-GGGGACAAGTTTGTACAAAAAAGCAGGCTGCGGCCGCATGATCACCGGCAAAGA
12	*P2R_HAstopNotIattb*	5'-GGGGACCACTTTGTACAAGAAAGCTGGGTAAGCGGCCGCTTAAGCGTAATCTGGA ACATCGTATGGGTAAAGCCCCAAAAGAACGTAG
13	*P2geneNotI_stop_attb_R*	5'-GCGGCCGCTTAAAGCCCCAAAAGAACGTAGTAGA
14	*P1F_NotIattb*	5'-GGGGACAAGTTTGTACAAAAAAGCAGGCTGCGGCCGCATGATTACGGCGGCGGA
15	*P1R_HAstopNotIattb*	5'-GGGGACCACTTTGTACAAGAAAGCTGGGTAAGCGGCCGCTTAAGCGTAATCTGGA ACATCGTATGGGTATAGACCCAAGAGAATGT
16	*P1geneNotI_stop_attb_R*	5'-GCGGCCGCTCATAGACCCAAGAGAATGTAGTAG

Table 2. Gateway Entry Clones.

No	Construct name	Vector name	Comments	Primers
1	*PIN1A_pDONR221*	pDONR 221	synthesized by company, no stop	
2	*PIN1B_pDONR221*	pDONR 221	synthesized by company, no stop	
3	*PIN1AB_pDONR221*	pDONR 221	synthesized by company, no stop	
4	*PIN2AB_pDONR221*	pDONR 221	synthesized by company, no stop	
5	*PIN1prom_TOPO*	pENTR5'-TOPO	promoter	1, 2
6	*PIN2prom_TOPO*	pENTR5'-TOPO	promoter	3, 4
7	*AUX1prom_TOPO*	pENTR5'-TOPO	promoter	5, 6
8	*PIN2_CDS_stop*	pDONR 221	stop, NotI	11, 13
9	*P1A_stop_221*	pDONR 221	stop, NotI	14, 16

10	*P1B_stop_221*	pDONR 221	stop, NotI	14, 16
11	*P1AB_stop_221*	pDONR 221	stop, NotI	14, 16
12	*P2A_stop_221*	pDONR 221	stop, NotI	11, 13
13	*P2B_stop_221*	pDONR 221	stop, NotI	11, 13
14	*P2AB_stop_221*	pDONR 221	stop, NotI	11, 13
15	*PIN1CDS_stop_221*	pDONR 221	stop, NotI	14, 16
16	*P2A-GFP_221*	pDONR 221	stop, NotI	7, 8, 9, 10, 11, 13
17	*P2B-GFP_221*	pDONR 221	stop, NotI	7, 8, 9, 10, 11, 13
18	*P2AB-GFP_221*	pDONR 221	stop, NotI	7, 8, 9, 10, 11, 13
19	*PIN2-GFP*	pDONR 221	stop, NotI	7, 8, 9, 10, 11, 13
20	*PIN1-HA*	pDONR 221	stop, HA-tag, NotI	14, 15
21	*PIN2-HA*	pDONR 221	stop, HA-tag, NotI	11, 12

Table 3. Gateway Expression Clones.

No	Construct name	Vector name	Entry clones	Destiny	Transformed plants	Obtained T generation
1	*PIN1prom_NLS*	NLS-2xGFP	5	plant transformation	Col-0	T1
2	*PIN2prom_NLS*	NLS-2xGFP	6	plant transformation	Col-0	N/A
3	*AUX1_NLS*	NLS-2xGFP	7	plant transformation	Col-0	T1
4	*PIN1 free GFP*	pK7WG2D	15	a. t. a. in protoplasts		
5	*35SPIN1A,freeGFP*	pK7WG2D	9	a. t. a. in protoplasts		
6	*35SPIN1B,freeGFP*	pK7WG2D	10	a. t. a. in protoplasts		
7	*35SPIN1AB,freeGFP*	pK7WG2D	11	a. t. a. in protoplasts		
8	*PIN2stop,free GFP*	pK7WG2D	8	a. t. a. in protoplasts		
9	*35SPIN2A,freeGFP*	pK7WG2D	12	a. t. a. in protoplasts		
10	*35SPIN2B,freeGFP*	pK7WG2D	13	a. t. a. in protoplasts		
11	*35SPIN2AB,freeGFP*	pK7WG2D	14	a. t. a. in protoplasts		
12	*AUX1:P1A*	pB7m24GW.3	7, 9	plant transformation	aux1-100	T2
13	*AUX1:P1B*	pB7m24GW.3	7, 10	plant transformation	aux1-100	T2
14	*AUX1:P1AB*	pB7m24GW.3	7, 11	plant transformation	aux1-100	T2
15	*AUX1:PIN2*	pB7m24GW.3	7, 8	plant transformation	aux1-100	T2
16	*AUX1:P2A*	pB7m24GW.3	7, 12	plant transformation	aux1-100	T2
17	*AUX1:P2B*	pB7m24GW.3	7, 13	plant transformation	aux1-100	T2
18	*AUX1:P2AB*	pB7m24GW.3	7, 14	plant transformation	aux1-100	T2
19	*P1PIN1*	pB7m24GW.3	7, 15	plant transformation	pin1-201 (SALK_047613)	N/A
20	*P1P1A*	pB7m24GW.3	7, 9	plant transformation	pin1-201 (SALK_047613)	T3
21	*P1P1B*	pB7m24GW.3	7, 10	plant transformation	pin1-201 (SALK_047613)	T3
22	*P1P1AB*	pB7m24GW.3	7, 11	plant transformation	pin1-201 (SALK_047613)	T3
23	*P2PIN2*	pB7m24GW.3	6, 8	plant transformation	eir1-4 (SALK_091142)	T2
24	*P2P2A*	pB7m24GW.3	6, 12	plant transformation	eir1-4 (SALK_091142)	T2
25	*P2P2B*	pB7m24GW.3	6, 13	plant transformation	eir1-4 (SALK_091142)	T2
26	*P2P2AB*	pB7m24GW.3	6, 14	plant transformation	eir1-4 (SALK_091142)	T2
27	*35S:P1_stop*	pK7WG2	15	plant transformation	Col-0	T3
28	*35S:P1A_stop*	pK7WG2	9	plant transformation	Col-0	T3
29	*35S:P1B_stop*	pK7WG2	10	plant transformation	Col-0	T3
30	*35S:P1AB_stop*	pK7WG2	11	plant transformation	Col-0	T3
31	*35S:P2_stop*	pK7WG2	8	plant transformation	Col-0	T3
32	*35S:P2A_stop*	pK7WG2	12	plant transformation	Col-0	T3
33	*35S:P2B_stop*	pK7WG2	13	plant transformation	Col-0	T3
34	*35S:P2AB_stop*	pK7WG2	14	plant transformation	Col-0	T3

35	*35S:P2-GFP*	pK7WG2	19	plant transformation	Col-0	T3
36	*35S:P2A-GFP*	pK7WG2	16	plant transformation	Col-0	T3
37	*35S:P2B-GFP*	pK7WG2	17	plant transformation	Col-0	T3
38	*35S:P2AB-GFP*	pK7WG2	18	plant transformation	Col-0	T3

a. t. a. – auxin transport assay

Table 4. Yeast Expression Clones.

Construct name	Vector name	Entry clone	Resistance in bacteria	Destiny
PIN1HA pNEV	pNEV-N	20	Amp	a. t. a. in yeasts
PIN2HA pNEV	pNEV-N	21	Amp	a. t. a. in yeasts
P1A_pNEV	pNEV-N	1	Amp	a. t. a. in yeasts
P1B_pNEV	pNEV-N	2	Amp	a. t. a. in yeasts
P1AB_pNEV	pNEV-N	3	Amp	a. t. a. in yeasts
P2A_pNEV	pNEV-N	from Z.D.	Amp	a. t. a. in yeasts
P2B_pNEV	pNEV-N	from Z.D.	Amp	a. t. a. in yeasts
P2AB_pNEV	pNEV-N	4	Amp	a. t. a. in yeasts

a. t. a. – auxin transport assay; Z. D. - Zhaojun Ding

REFERENCES

Benková, E., Michniewicz, M., Sauer, M., Teichmann, T., Seifertová, D., Jürgens, G., and Friml, J. (2003). Local, efflux-dependent auxin gradients as a common module for plant organ formation. Cell *115*, 591–602.

Bosco, C.D., Dovzhenko, A., Liu, X., Woerner, N., Rensch, T., Eismann, M., Eimer, S., Hegermann, J., Paponov, I.A., Ruperti, B., et al. (2012). The endoplasmic reticulum localized PIN8 is a pollen-specific auxin carrier involved in intracellular auxin homeostasis. Plant J. *71*, 860–870.

Chen, R., Hilson, P., Sedbrook, J., Rosen, E., Caspar, T., and Masson, P.H. (1998). The *Arabidopsis thaliana* AGRAVITROPIC 1 gene encodes a component of the polar-auxin-transport efflux carrier. Proc. Natl. Acad. Sci. U. S. A. *95*, 15112–15117.

Dharmasiri, N., Dharmasiri, S., and Estelle, M. (2005). The F-box protein TIR1 is an auxin receptor. Nature *435*, 441–445.

Ding, Z., Wang, B., Moreno, I., Dupláková, N., Simon, S., Carraro, N., Reemmer, J., Pěnčík, A., Chen, X., Tejos, R., et al. (2012). ER-localized auxin transporter PIN8 regulates auxin homeostasis and male gametophyte development in *Arabidopsis*. Nat. Commun. *3*, 941.

Friml, J., Wiśniewska, J., Benková, E., Mendgen, K., and Palme, K. (2002). Lateral relocation of auxin efflux regulator PIN3 mediates tropism in *Arabidopsis*. Nature *415*, 806–809.

Friml, J., Vieten, A., Sauer, M., Weijers, D., Schwarz, H., Hamann, T., Offringa, R., and Jürgens, G. (2003). Efflux-dependent auxin gradients establish the apical-basal axis of *Arabidopsis*. Nature *426*, 147–153.

Ganguly, A., Park, M., Kesawat, M.S., and Cho, H.-T. (2014). Functional Analysis of the Hydrophilic Loop in Intracellular Trafficking of *Arabidopsis* PIN-FORMED Proteins. Plant Cell *26*, 1570–1585.

Kepinski, S., and Leyser, O. (2005). The *Arabidopsis* F-box protein TIR1 is an auxin receptor. Nature *435*, 446–451.

Luschnig, C., Gaxiola, R.A., Grisafi, P., and Fink, G.R. (1998). EIR1, a root-specific protein involved in auxin transport, is required for gravitropism in *Arabidopsis thaliana*. Genes Dev. *12*, 2175–2187.

Marchant, A., Kargul, J., May, S.T., Muller, P., Delbarre, A., Perrot-Rechenmann, C., and Bennett, M.J. (1999). AUX1 regulates root gravitropism in *Arabidopsis* by facilitating auxin uptake within root apical tissues. EMBO J. *18*, 2066–2073.

Mravec, J., Skůpa, P., Bailly, A., Hoyerová, K., Křeček, P., Bielach, A., Petrášek, J., Zhang, J., Gaykova, V., Stierhof, Y.-D., et al. (2009). Subcellular homeostasis of phytohormone auxin is mediated by the ER-localized PIN5 transporter. Nature *459*, 1136–1140.

Okada, K., Ueda, J., Komaki, M.K., Bell, C.J., and Shimura, Y. (1991). Requirement of the Auxin Polar Transport System in Early Stages of *Arabidopsis* Floral Bud Formation. Plant Cell *3*, 677–684.

Petrásek, J., Mravec, J., Bouchard, R., Blakeslee, J.J., Abas, M., Seifertová, D., Wisniewska, J., Tadele, Z., Kubes, M., Covanová, M., et al. (2006). PIN proteins perform a rate-limiting function in cellular auxin efflux. Science *312*, 914–918.

Reinhardt, D., Pesce, E.-R., Stieger, P., Mandel, T., Baltensperger, K., Bennett, M., Traas, J., Friml, J., and Kuhlemeier, C. (2003). Regulation of phyllotaxis by polar auxin transport. Nature *426*, 255–260.

Sawchuk, M.G., Edgar, A., and Scarpella, E. (2013). Patterning of Leaf Vein Networks by Convergent Auxin Transport Pathways. PLoS Genet *9*, e1003294.

Swarup, K., Benková, E., Swarup, R., Casimiro, I., Péret, B., Yang, Y., Parry, G., Nielsen, E., De Smet, I., Vanneste, S., et al. (2008). The auxin influx carrier LAX3 promotes lateral root emergence. Nat. Cell Biol. *10*, 946–954.

Swarup, R., Friml, J., Marchant, A., Ljung, K., Sandberg, G., Palme, K., and Bennett, M. (2001). Localization of the auxin permease AUX1 suggests two functionally distinct hormone transport pathways operate in the *Arabidopsis* root apex. Genes Dev. *15*, 2648–2653.

Vieten, A., Sauer, M., Brewer, P.B., and Friml, J. (2007). Molecular and cellular aspects of auxin-transport-mediated development. Trends Plant Sci. *12*, 160–168.

Wisniewska, J., Xu, J., Seifertová, D., Brewer, P.B., Ruzicka, K., Blilou, I., Rouquié, D., Benková, E., Scheres, B., and Friml, J. (2006). Polar PIN localization directs auxin flow in plants. Science *312*, 883.

Xu, J., and Scheres, B. (2005). Dissection of *Arabidopsis* ADP-RIBOSYLATION FACTOR 1 function in epidermal cell polarity. Plant Cell *17*, 525–536.

Yang, Y., Hammes, U.Z., Taylor, C.G., Schachtman, D.P., and Nielsen, E. (2006). High-affinity auxin transport by the AUX1 influx carrier protein. Curr. Biol. CB *16*, 1123–1127.

Zourelidou, M., Absmanner, B., Weller, B., Barbosa, I.C.R., Willige, B.C., Fastner, A., Streit, V., Port, S.A., Colcombet, J., de la Fuente van Bentem, S., et al. (2014). Auxin efflux by PIN-FORMED proteins is activated by two different protein kinases, D6 PROTEIN KINASE and PINOID. eLife *3*.

Chapter 5

Conclusions and Perspectives

In this study, we identified and analyzed two small molecules, ES4 and ES6, which affect ectopic polar localization of PIN1 protein in root epidermis cells; characterized chemicals revealed their effect on ARF/ARF GEF-dependent intracellular trafficking pathway and cell wall biosynthesis, respectively. It has been shown that both, ARF/ARF GEFs and cell wall, are implicated in polar localization of PIN proteins at the plasma membrane (PM) (Doyle et al., 2015; Geldner et al., 2001, 2003; Kleine-Vehn et al., 2008; Richter et al., 2007, 2010, 2012; Steinmann et al., 1999; Feraru et al., 2011). This was concluded based on the PIN localization analysis in ARF GEF- and cell wall biosynthesis-defective mutants and in wild type seedlings treated with chemicals affecting those pathways. Interestingly, although they clearly influenced pathways involved in polar PIN localization, none of the tested ES molecules affected visibly polar localization of natively expressed PIN proteins. Our experimental results showed that ES4 affects endocytosis, exocytosis and vacuolar degradation pathways, all of which are crucial for trafficking of PIN proteins (Figure 1). As shown for ES6, it induced increased expression of auxin response reporter in wild type, which further confirms defects in the PIN auxin transporters localization.

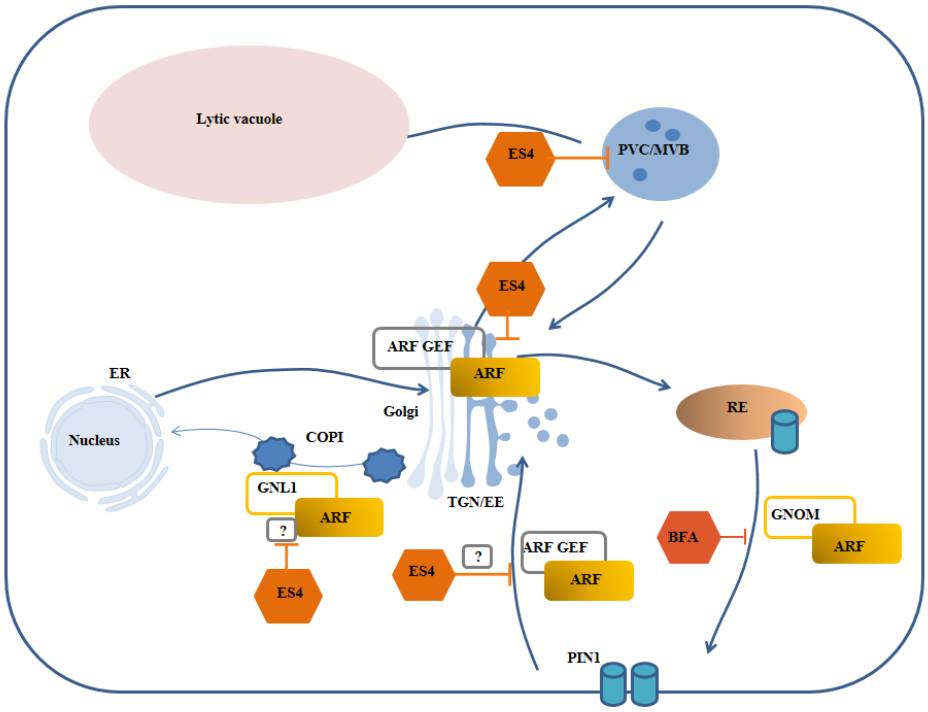

Figure 1. Model illustrating ES4 mode of action.
ES4 presumably affects endocytosis and exocytosis of PIN1. It affects PVC/MVB compartment and degradation pathway. ES4 presumably affects early secretory pathway mediated by COPI through ARF/GNL1.

It remains unclear how ES4 and ES6 induce basal-to apical shift of ectopically localized PIN1. Despite the fact that polarity of native PIN proteins is not affected, ES molecules might influence their mobility and/or abundance at the PM. To visualize the dynamics of PIN

proteins in wild type and PIN2:PIN1-GFP;*pin2* after treatments, Fluorescence Recovery After Photobleaching (FRAP) experiments can be performed in the future. Additionally, western blot assay would provide information about PIN protein abundance after chemical treatments.

The best understood role of ARF GEFs in polar PIN localization is GNOM-mediated basal PIN1 targeting (Geldner et al., 2001; Kleine-Vehn et al., 2008); however, other ARF GEFs were also reported to affect polar PIN localization (Teh and Moore, 2007; Tanaka et al., 2009, 2013; Feraru et al., 2012). Here we demonstrated, that ES4 clearly targets the ARF/ARF GEF dependent pathway but the exact mechanism has to be researched further. It is possible that ES4 acts as a GTP analog. To test this hypothesis and to better understand the connection between ES4 and ARF GEFs, the ES4 competition for GTP binding with ARF1 could be performed to determine whether ES4 compete with GTP to bind to ARF1.

Different factors have been shown to play a role in localization and maintenance of PIN polarity at the PM, including kinases and phosphatases, which are important in apical-basal targeting of PIN proteins (Michniewicz et al., 2007) and cell wall crucial for maintenance of PIN polarity (Feraru et al., 2011). Here we demonstrated that in addition to the effects on PIN polarity and auxin transport, ES6 affects cell wall composition. We also presented, that ES6 might target PP2A phosphatase, since *rcn1* mutant is partially resistant to the ES6 treatments (Figure 2).

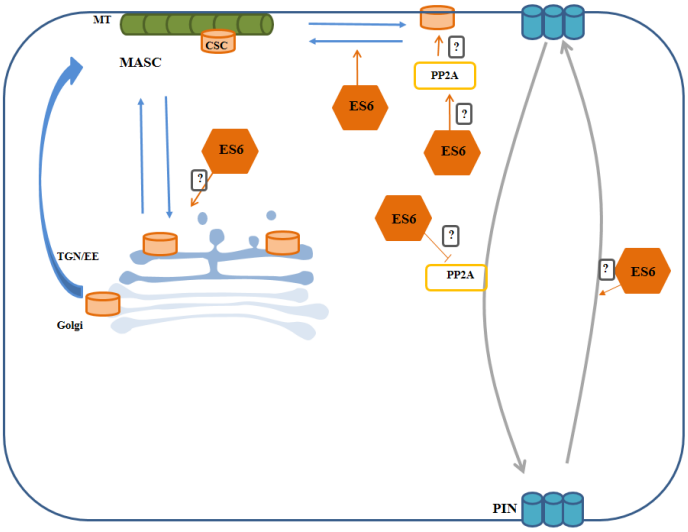

Figure 2. Model illustrating ES6 mode of action.
ES6 induces depletion of CSC from the PM and accumulation in MASCS and presumably in TGN/EE. ES6 presumably affects PP2A dependent pathways and induce basal-to-apical shift of ectopic PIN1 proteins.

It remains unclear, whether ES6 affects cell wall and PP2A pathway independently, or the observable phenotypes interconnect. This hypothesis could be tested by analyzing crosses between *rcn1* and *CESA* marker lines and *DR5::GUS*. Doing so would clarify whether the

rcn1 mutation confers resistance to ES6 treatments in terms of CESA proteins trafficking and auxin response. Additionally, cell wall composition in *rcn1* in the presence of isoxaben and ES6 could be tested, as it was done for wild type. Some chemicals were reported to affect cell wall composition, like isoxaben and CGA 325'615. They could be tested for their effects on auxin reporter accumulation in *DR5::GUS* and on root and hypocotyl growth of *rcn1* to compare their effects with ES6. Results would bring more information about possible link between cell wall biosynthesis and PP2A. The DR5 analyses indicated that ES6 promotes root-to-shoot fluxes; however, localizations of PIN proteins seem not to be affected. Besides the PIN protein family, members of the ATP-binding cassette (ABC) superfamily of transporters, predominantly of its B type (ABCB/multidrug resistance [MDR]/phosphoglycoprotein [PGP]) possess auxin-exporting activity (Geisler et al., 2005; Terasaka et al., 2005). The trafficking of this protein transporters family could be tested for its response to ES6. It is also not excluded, that the effect on the cell wall biosynthesis is not specific, since other chemicals or osmotic stress can induce internalization of Cellulose Synthase Complex (CSC) from plasma membrane and induce accumulation within MASCs (Crowell et al. 2009; Guttierez et al., 2009).

To fully understand the mechanism of action of the characterized chemicals it is necessary to find their target. The method of choice to identify the target include forward genetic screen for mutants resistant to the chemicals. In the screen we found the *es4r1* mutant, carrying mutation in *δ-COPI*, a single copy gene crucial for plant viability. COPI vesicles are mainly involved in retrograde protein transport between Golgi and ER, mediated by GNL1 (Richter et al., 2007; Teh and Moore, 2007). Recently it has been shown, that early secretory trafficking mediated by GNL1 and GNOM is essential for basal polarity establishment (Doyle et al., 2015). This implicates a possible role of δ-COPI in basal-to-apical shift of ectopically localized PIN proteins. This hypothesis can be tested by analyzing genetic interactions between *es4r1* mutant and PIN2:PIN1-HA;*pin2*; ARF-GDP, ARF-GFP and *gnl1* lines in response to ES4 treatment. In any case, the partial resistance only to ES4 indicates that *δ-COPI* is not its direct target and other methods have to be used to identify the target.

To address this issue, biochemical approaches can be applied. However, affinity-based target identification techniques require modification of the chemical. We performed SAR analysis to identify active and non-active sites of the ES molecules for possible modification. Analysis revealed that the whole ES4 structure is possibly essential for its bioactivity since all the tested derivatives of ES4 were biologically inactive. This makes modification of the molecule difficult. To address this problem, Drag Affinity Responsive Target Stability (DARTS) could be performed, a technique that does not require any structural changes of the tested molecule. DARTS relies on the assumption that after the

binding of a small molecule and its protein target stabilizes that target by conformational change or by masking its protease recognition sites and protects it from digestion with applied protease (Lomenick et al., 2009; Lomenick et al., 2011). Comparisons of treated and non-treated samples would reveal the protected target of the small molecule. On the other hand, for the ES6 chemical we identified its active derivate, which indicates that this molecule can be tagged. The new derivative could be tested for other effects described for ES6, such as GUS accumulation or *rcn1* resistance. Obtained results could reveal which molecule is more biologically potent. Additionally, ES6 molecule could be cleaved to better identify its bioactive sties. Moreover, the DARTS technique could also be used to determine the ES6 target.

Utilization of chemical genetics in plant research can help to better understand endomembrane trafficking, hormone transport, and cell wall biosynthesis. Many of the identified and characterized chemicals are commonly used as tools in every day laboratory practice to investigate different processes in plants. Over the course of our research we used several of them: BFA used to investigate PIN trafficking or isoxaben, which specifically affects CESA3 and CESA6 proteins, involved in cell wall biosynthesis (Desprez, 2002; Scheible, 2001). In recent years many other small molecules were used to investigate molecular basis of plant life. Fluorescent brassinosteroide analogue, Alexa Fluor 647–castasterone (AFCS) helped to visualize endocytosis of BRI1-AFCS, the receptor ligand complex (Irani et al., 2012). Characterization of endosidin 8 (ES8) helped to investigate the connection between early secretory pathway and basal polarity establishment (Doyle et al., 2015). Screen for resistance to picolinate-type auxin DAS534 helped to identify homologue of TIR1, which mediates transcriptional repression of auxin responses (Walsh et al., 2006). Here we identified two new small molecules which can help to better understand endomembrane trafficking processes, cell wall biosynthesis and possibly their connection with trafficking and localization of PIN auxin transporters. Additionally, we identified *es4r1* mutant, which together with ES4 can be used to study *δ-COPI* function. So far it was not possible due to the lethality of the full knock-out in the gene.

REFERENCES

Crowell, E.F., Bischoff, V., Desprez, T., Rolland, A., Stierhof, Y.D., Schumacher, K., Gonneau, M., Höfte, H., and Vernhettes, S. (2009). Pausing of Golgi bodies on microtubules regulates secretion of cellulose synthase complexes in *Arabidopsis*. Plant Cell *21*, 1141–1154.

Desprez, T., Vernhettes, S., Fagard, M., Refregier, G., Desnos, T., Aletti, E., Py, N., Pelletier, S., and Hofte, H. (2002). Resistance against Herbicide Isoxaben and Cellulose Deficiency Caused by Distinct Mutations in Same Cellulose Synthase Isoform CESA6. Plant Physiol. *128*, 482–490.

Doyle, S.M., Haeger, A., Vain, T., Rigal, A., Viotti, C., Łangowska, M., Ma, Q., Friml, J., Raikhel, N.V., Hicks, G.R., et al. (2015). An early secretory pathway mediated by GNOM-LIKE 1 and GNOM is essential for basal polarity establishment in *Arabidopsis* thaliana. Proc. Natl. Acad. Sci. U. S. A. *112*, E806–E815.

Feraru, E., Feraru, M.I., Kleine-Vehn, J., Martinière, A., Mouille, G., Vanneste, S., Vernhettes, S., Runions, J., and Friml, J. (2011). PIN polarity maintenance by the cell wall in *Arabidopsis*. Curr. Biol. CB *21*, 338–343.

Feraru, E., Feraru, M.I., Asaoka, R., Paciorek, T., De Rycke, R., Tanaka, H., Nakano, A., and Friml, J. (2012). BEX5/RabA1b regulates trans-Golgi network-to-plasma membrane protein trafficking in *Arabidopsis*. Plant Cell *24*, 3074–3086.

Geisler, M., Blakeslee, J.J., Bouchard, R., Lee, O.R., Vincenzetti, V., Bandyopadhyay, A., Titapiwatanakun, B., Peer, W.A., Bailly, A., Richards, E.L., et al. (2005). Cellular efflux of auxin catalyzed by the *Arabidopsis* MDR/PGP transporter AtPGP1. Plant J. Cell Mol. Biol. *44*, 179–194.

Geldner, N., Friml, J., Stierhof, Y.D., Jürgens, G., and Palme, K. (2001). Auxin transport inhibitors block PIN1 cycling and vesicle trafficking. Nature *413*, 425–428.

Geldner, N., Anders, N., Wolters, H., Keicher, J., Kornberger, W., Muller, P., Delbarre, A., Ueda, T., Nakano, A., and Jürgens, G. (2003). The Arabidopsis GNOM ARF-GEF mediates endosomal recycling, auxin transport, and auxin-dependent plant growth. Cell *112*, 219–230.

Gutierrez, R., Lindeboom, J.J., Paredez, A.R., Emons, A.M.C., and Ehrhardt, D.W. (2009). *Arabidopsis* cortical microtubules position cellulose synthase delivery to the plasma membrane and interact with cellulose synthase trafficking compartments. Nat. Cell Biol. *11*, 797–806.

Irani, N.G., Di Rubbo, S., Mylle, E., Van den Begin, J., Schneider-Pizoń, J., Hniliková, J., Šíša, M., Buyst, D., Vilarrasa-Blasi, J., Szatmári, A.-M., et al. (2012). Fluorescent castasterone reveals BRI1 signaling from the plasma membrane. Nat. Chem. Biol. *8*, 583–589.

Kleine-Vehn, J., Dhonukshe, P., Sauer, M., Brewer, P.B., Wiśniewska, J., Paciorek, T., Benková, E., and Friml, J. (2008). ARF GEF-dependent transcytosis and polar delivery of PIN auxin carriers in *Arabidopsis*. Curr. Biol. CB *18*, 526–531.

Lomenick, B., Hao, R., Jonai, N., Chin, R.M., Aghajan, M., Warburton, S., Wang, J., Wu, R.P., Gomez, F., Loo, J.A., et al. (2009). Target identification using drug affinity responsive target stability (DARTS). Proc. Natl. Acad. Sci. *106*, 21984–21989.

Lomenick, B., Jung, G., Wohlschlegel, J.A., and Huang, J. (2011). Target identification using drug affinity responsive target stability (DARTS). Curr. Protoc. Chem. Biol. *3*, 163–180.

Michniewicz, M., Zago, M.K., Abas, L., Weijers, D., Schweighofer, A., Meskiene, I., Heisler, M.G., Ohno, C., Zhang, J., Huang, F., et al. (2007). Antagonistic regulation of PIN phosphorylation by PP2A and PINOID directs auxin flux. Cell *130*, 1044–1056.

Richter, S., Geldner, N., Schrader, J., Wolters, H., Stierhof, Y.-D., Rios, G., Koncz, C., Robinson, D.G., and Jürgens, G. (2007). Functional diversification of closely related ARF-GEFs in protein secretion and recycling. Nature *448*, 488–492.

Richter, S., Anders, N., Wolters, H., Beckmann, H., Thomann, A., Heinrich, R., Schrader, J., Singh, M.K., Geldner, N., Mayer, U., et al. (2010). Role of the GNOM gene in Arabidopsis apical-basal patterning--From mutant phenotype to cellular mechanism of protein action. Eur. J. Cell Biol. *89*, 138–144.

Richter, S., Müller, L.M., Stierhof, Y.-D., Mayer, U., Takada, N., Kost, B., Vieten, A., Geldner, N., Koncz, C., and Jürgens, G. (2012). Polarized cell growth in *Arabidopsis* requires endosomal recycling mediated by GBF1-related ARF exchange factors. Nat. Cell Biol. *14*, 80–86.

Scheible, W.R., Eshed, R., Richmond, T., Delmer, D., and Somerville, C. (2001). Modifications of cellulose synthase confer resistance to isoxaben and thiazolidinone herbicides in *Arabidopsis ixr1* mutants. Proc. Natl. Acad. Sci. *98*, 10079–10084.

Steinmann, T., Geldner, N., Grebe, M., Mangold, S., Jackson, C.L., Paris, S., Gälweiler, L., Palme, K., and Jürgens, G. (1999). Coordinated polar localization of auxin efflux carrier PIN1 by GNOM ARF GEF. Science *286*, 316–318.

Tanaka, H., Kitakura, S., De Rycke, R., De Groodt, R., and Friml, J. (2009). Fluorescence imaging-based screen identifies ARF GEF component of early endosomal trafficking. Curr. Biol. CB *19*, 391–397.

Tanaka, H., Kitakura, S., Rakusová, H., Uemura, T., Feraru, M.I., De Rycke, R., Robert, S., Kakimoto, T., and Friml, J. (2013). Cell Polarity and Patterning by PIN Trafficking through Early Endosomal Compartments in *Arabidopsis thaliana*. PLoS Genet *9*, e1003540.

Teh, O.K., and Moore, I. (2007). An ARF-GEF acting at the Golgi and in selective endocytosis in polarized plant cells. Nature *448*, 493–496.

Terasaka, K., Blakeslee, J.J., Titapiwatanakun, B., Peer, W.A., Bandyopadhyay, A., Makam, S.N., Lee, O.R., Richards, E.L., Murphy, A.S., Sato, F., et al. (2005). PGP4, an ATP binding cassette P-glycoprotein, catalyzes auxin transport in *Arabidopsis thaliana* roots. Plant Cell *17*, 2922–2939.

Walsh, T.A., Neal, R., Merlo, A.O., Honma, M., Hicks, G.R., Wolff, K., Matsumura, W., and Davies, J.P. (2006). Mutations in an auxin receptor homolog AFB5 and in SGT1b confer resistance to synthetic picolinate auxins and not to 2,4-dichlorophenoxyacetic acid or indole-3-acetic acid in *Arabidopsis*. Plant Physiol. *142*, 542–552.

Additional scientific contributions

Author Contributions:

(Dai et al., 2012)
U.K. performed immunolocalization and quantification of cells with apical, apolar, or basal localization of PIN1 (in stele cells) or PIN2 (in cortical cells) in Col, f1 f3, F1DN, and F3DN roots (Figure 3, Figure 7).

(Baster et al., 2013)
U.K. performed western blot analysis and analysis of vacuolar trafficking in apolarly localized PM proteins- BRI1 and PIP2 (Figure S4).

(Gadeyne et al., 2014)
U.K. constructed vectors and performed tandem affinity purification (TAP-tag) experiments on *Arabidopsis* cell culture cells for CHC2 and CLC1 (Figure 6). U.K. and M.A. performed gravistimulation experiments with *amiR-TML* and *amiR-TPLATE* lines and quantified the results (Figure S5H).

This article is a *Plant Cell* Advance Online Publication. The date of its first appearance online is the official date of publication. The article has been edited and the authors have corrected proofs, but minor changes could be made before the final version is published. Posting this version online reduces the time to publication by several weeks.

A PP6-Type Phosphatase Holoenzyme Directly Regulates PIN Phosphorylation and Auxin Efflux in *Arabidopsis*[C][W]

Mingqiu Dai,[a] Chen Zhang,[b,c,1] Urszula Kania,[d,e,1] Fang Chen,[a] Qin Xue,[a] Tyra Mccray,[a] Gang Li,[a] Genji Qin,[f] Michelle Wakeley,[a,g] William Terzaghi,[a,g] Jianmin Wan,[h] Yunde Zhao,[f] Jian Xu,[b,c] Jiří Friml,[d,e] Xing Wang Deng,[a] and Haiyang Wang[a,h,i,j,2]

[a] Department of Molecular, Cellular, and Developmental Biology, Yale University, New Haven, Connecticut 06520-8104
[b] National University of Singapore, Department of Biological Sciences, Singapore 117543
[c] National Key Laboratory of Crop Genetic Improvement, Huazhong Agricultural University, Wuhan 430070, China
[d] Department of Plant Systems Biology, VIB, Ghent University, 9052 Ghent, Belgium
[e] Department of Plant Biotechnology and Genetics, Ghent University, 9052 Ghent, Belgium
[f] Section of Cell and Developmental Biology, University of California–San Diego, La Jolla, California 92093-0116
[g] Department of Biology, Wilkes University, Wilkes-Barre, Pennsylvania 18766
[h] Institute of Crop Sciences, Chinese Academy of Agriculture Sciences, Beijing 100081, China
[i] Capital Normal University, Beijing 100048, China
[j] National Engineering Research Center for Crop Molecular Design, Beijing 100085, China

The directional transport of the phytohormone auxin depends on the phosphorylation status and polar localization of PIN-FORMED (PIN) auxin efflux proteins. While PINOID (PID) kinase is directly involved in the phosphorylation of PIN proteins, the phosphatase holoenzyme complexes that dephosphorylate PIN proteins remain elusive. Here, we demonstrate that mutations simultaneously disrupting the function of *Arabidopsis thaliana FyPP1* (for Phytochrome-associated serine/threonine protein phosphatase1) and *FyPP3*, two homologous genes encoding the catalytic subunits of protein phosphatase6 (PP6), cause elevated accumulation of phosphorylated PIN proteins, correlating with a basal-to-apical shift in subcellular PIN localization. The changes in PIN polarity result in increased root basipetal auxin transport and severe defects, including shorter roots, fewer lateral roots, defective columella cells, root meristem collapse, abnormal cotyledons (small, cup-shaped, or fused cotyledons), and altered leaf venation. Our molecular, biochemical, and genetic data support the notion that FyPP1/3, SAL (for SAPS DOMAIN-LIKE), and PP2AA proteins (RCN1 [for ROOTS CURL IN NAPHTHYLPHTHALAMIC ACID1] or PP2AA1, PP2AA2, and PP2AA3) physically interact to form a novel PP6-type heterotrimeric holoenzyme complex. We also show that FyPP1/3, SAL, and PP2AA interact with a subset of PIN proteins and that for SAL the strength of the interaction depends on the PIN phosphorylation status. Thus, an *Arabidopsis* PP6-type phosphatase holoenzyme acts antagonistically with PID to direct auxin transport polarity and plant development by directly regulating PIN phosphorylation.

INTRODUCTION

Auxin is a fundamental plant hormone that regulates almost every aspect of plant growth and development, including embryogenesis, organogenesis, apical dominance, tissue regeneration, and tropisms (reviewed in Bennett and Scheres, 2010; Grunewald and Friml, 2010; Peris et al., 2010). Auxin is transported from its sites of biosynthesis to its sites of action by a polarized auxin transport system. Molecular genetic studies in *Arabidopsis thaliana* have lead to the identification and functional characterization of several key players of the polarized auxin transport system, such as the auxin uptake carriers AUXIN RESISTANT1/LIKE AUX1 (AUX1/LAX) (Swarup et al., 2008), the auxin efflux carriers, including PIN-FORMED (PIN) family proteins (Gälweiler et al., 1998; Chen et al., 1998; Müller et al., 1998; Friml et al., 2002; Petrásek et al., 2006), and P-glycoprotein auxin transporters ABCB1 (for ATP BINDING CASSETTE PROTEIN SUBFAMILY B1), ABCB4, and ABCB19 (Terasaka et al., 2005; Bouchard et al., 2006; Blakeslee et al., 2007; Lin and Wang, 2005). PIN proteins are asymmetrically targeted to the plant cell plasma membranes, resulting in distinct polar subcellular localization in a given tissue. For example, PIN1 is localized in the basal (rootward, lower) plasma membrane of stele cells and xylem cells in the vascular system, which is required for long-distance auxin flow from the shoot apex to the root tip (Gälweiler et al., 1998; Friml et al., 2002). PIN2 is expressed in root tissues and is selectively localized to the apical (shootward, upper) side of lateral root cap cells and epidermal cells (Müller et al., 1998; Kleine-Vehn et al., 2008). Polar localization of PIN proteins facilitates auxin flow and determines the direction of local intercellular auxin transport and subsequently regulates plant development (Wiśniewska et al., 2006).

[1] These authors contributed equally to this work.
[2] Address correspondence to haiyang.wang@yale.edu.
The author responsible for distribution of materials integral to the findings presented in this article in accordance with the policy described in the Instructions for Authors (www.plantcell.org) is: Haiyang Wang (haiyang.wang@yale.edu).
[C] Some figures in this article are displayed in color online but in black and white in the print edition.
[W] Online version contains Web-only data.
www.plantcell.org/cgi/doi/10.1105/tpc.112.098905

The EMBO Journal (2013) 32, 260–274
www.embojournal.org

THE EMBO JOURNAL

SCF$^{TIR1/AFB}$-auxin signalling regulates PIN vacuolar trafficking and auxin fluxes during root gravitropism

Paweł Baster[1], Stéphanie Robert[1,2], Jürgen Kleine-Vehn[1,3], Steffen Vanneste[1], Urszula Kania[1], Wim Grunewald[1], Bert De Rybel[1,4], Tom Beeckman[1] and Jiří Friml[1,5,*]

[1]Department of Plant Systems Biology, VIB and Department of Plant Biotechnology and Genetics, Ghent University, Gent, Belgium, [2]Department of Forest Genetics and Plant Physiology, Swedish University of Agricultural Sciences/Umeå Plant Science Center, Umeå, Sweden, [3]Department of Applied Genetics and Cell Biology, University of Applied Life Sciences and Natural Resources (BOKU), Vienna, Austria, [4]Laboratory of Biochemistry, University of Wageningen, Wageningen, The Netherlands and [5]Institute of Science and Technology Austria (IST Austria), Klosterneuburg, Austria

The distribution of the phytohormone auxin regulates many aspects of plant development including growth response to gravity. Gravitropic root curvature involves coordinated and asymmetric cell elongation between the lower and upper side of the root, mediated by differential cellular auxin levels. The asymmetry in the auxin distribution is established and maintained by a spatio-temporal regulation of the PIN-FORMED (PIN) auxin transporter activity. We provide novel insights into the complex regulation of PIN abundance and activity during root gravitropism. We show that PIN2 turnover is differentially regulated on the upper and lower side of gravistimulated roots by distinct but partially overlapping auxin feedback mechanisms. In addition to regulating transcription and clathrin-mediated internalization, auxin also controls PIN abundance at the plasma membrane by promoting their vacuolar targeting and degradation. This effect of elevated auxin levels requires the activity of SKP-Cullin-F-box$^{TIR1/AFB}$ (SCF$^{TIR1/AFB}$)-dependent pathway. Importantly, also suboptimal auxin levels mediate PIN degradation utilizing the same signalling pathway. These feedback mechanisms are functionally important during gravitropic response and ensure fine-tuning of auxin fluxes for maintaining as well as terminating asymmetric growth.
The EMBO Journal (2013) **32**, 260–274. doi:10.1038/emboj.2012.310; Published online 4 December 2012
Subject Categories: signal transduction; plant biology
Keywords: auxin; degradation; gravitropism; PIN

*Corresponding author. Department of Plant Systems Biology, VIB-Ghent University, Technologiepark 927, 9052 Gent, Belgium. Tel.: +32 9 3313913; Fax: +32 9 3313809;
E-mail: jiri.friml@psb.vib-ugent.be
The author responsible for distribution of materials integral to the findings presented in this article in accordance with the policy described in the Instructions for Authors (http://www.embojournal.org) is Jiří Friml (jiri.friml@psb.vib-ugent.be)

Received: 27 September 2012; accepted: 19 October 2012; published online: 4 December 2012

Introduction

The phytohormone auxin is an important regulator of cell morphogenesis shaping and directing growth of organs within different developmental contexts and in response to environmental signals (Vanneste and Friml, 2009). To ensure optimal growth and development, plants have acquired elaborate mechanisms to control the local auxin homeostasis, including control of auxin metabolism (Cheng *et al*, 2006, 2007; Stepanova *et al*, 2008; Tao *et al*, 2008), subcellular compartmentalization (Mravec *et al*, 2009; Barbez *et al*, 2012; Ding *et al*, 2012) and directional auxin transport mediated by plasma membrane-resident transporters, such as ABCB, PIN-FORMED (PIN) and AUXIN-RESISTANT 1 (AUX1) (Bennett *et al*, 1996; Geisler *et al*, 2005; Petrášek *et al*, 2006; Cho *et al*, 2007; Swarup *et al*, 2008; Jones *et al*, 2009). One of the prominent growth responses mediated by auxin transport is root gravitropism. Changes of the orientation relative to the gravity vector are perceived in the root tip, by the sedimentation of statoliths, defined as gravity-sensing organelles (Harrison and Masson, 2008; Leitz *et al*, 2009; Morita, 2010). This process appears to induce the relocation of the auxin efflux carriers (Petrášek *et al*, 2006) PIN3 and PIN7 to the lower side of the gravity-sensing cells, which presumably aligns auxin flux with gravity vector towards the lower side of the root tip (Friml *et al*, 2002; Harrison and Masson, 2008; Kleine-Vehn *et al*, 2010). From there, another auxin efflux carrier, PIN2, which is apically (shootward, upper cell side) localized in the lateral root cap and epidermal cells, mediates the directional auxin flow from the root tip to the elongation zone where control of elongation occurs (Luschnig *et al*, 1998; Müller *et al*, 1998; Abas *et al*, 2006; Wiśniewska *et al*, 2006). Hence, the PIN-mediated establishment of the asymmetric auxin distribution leads to a differential growth between the lower and the upper side of the root. As a consequence, root bends and re-orients in respect to the gravity vector, allowing the efficient exploration of the soil (Firn *et al*, 2000; Swarup *et al*, 2005).

The mechanisms underlying the PIN3 and PIN7 polarization in gravity-sensing columella cells and control of the PIN2 abundance at the plasma membrane for defined gravitropic response remain largely elusive. Nevertheless, some of the molecular processes controlling the subcellular localization of PIN proteins have been characterized (Grunewald and Friml, 2010). PIN proteins internalize continuously via a clathrin-mediated endocytotic pathway (Dhonukshe *et al*, 2007; Kitakura *et al*, 2011) and cycle back to the plasma membrane as shown by pharmacological approaches with a vesicle-budding inhibitor, Brefeldin A (BFA) (Geldner *et al*, 2001). This permanent cycling leads to a dynamic control of their polar localization and abundance at the plasma membrane (Kleine-Vehn *et al*, 2008a), which in turn, determines the rate and direction of the auxin flow (Paciorek *et al*, 2005; Wiśniewska *et al*, 2006). The

Cell

The TPLATE Adaptor Complex Drives Clathrin-Mediated Endocytosis in Plants

Astrid Gadeyne,[1,2,12] Clara Sánchez-Rodríguez,[3,12] Steffen Vanneste,[1,2] Simone Di Rubbo,[1,2] Henrik Zauber,[3] Kevin Vanneste,[1,2] Jelle Van Leene,[1,2] Nancy De Winne,[1,2] Dominique Eeckhout,[1,2] Geert Persiau,[1,2] Eveline Van De Slijke,[1,2] Bernard Cannoot,[1,2] Leen Vercruysse,[1,2] Jonathan R. Mayers,[4] Maciek Adamowski,[1,2,5] Urszula Kania,[1,2,5] Matthias Ehrlich,[3] Alois Schweighofer,[3,6] Tijs Ketelaar,[7] Steven Maere,[1,2] Sebastian Y. Bednarek,[4] Jiří Friml,[1,2,5] Kris Gevaert,[8,9] Erwin Witters,[10,11] Eugenia Russinova,[1,2] Staffan Persson,[3,13,*] Geert De Jaeger,[1,2,13] and Daniël Van Damme[1,2,13,*]

[1]Department of Plant Systems Biology, VIB, Technologiepark 927, 9052 Gent, Belgium
[2]Department of Plant Biotechnology and Bioinformatics, Ghent University, 9052 Gent, Belgium
[3]Max-Planck-Institut für Moleculare Planzenphysiologie, Am Mühlenberg 1, 14476 Potsdam-Golm, Germany
[4]Department of Biochemistry, University of Wisconsin, Madison, WI 53706, USA
[5]Institute of Science and Technology (IST Austria), Am Campus 1, 3400 Klosterneuburg, Austria
[6]Institute of Biotechnology (IBT), University of Vilnius, V. Graiciuno 8, 02242 Vilnius, Lithuania
[7]Laboratory of Cell Biology, Wageningen University, Droevendaalsesteeg 1, 6708PB Wageningen, The Netherlands
[8]Department of Medical Protein Research, VIB, A. Baertsoenkaai 3, 9000 Ghent, Belgium
[9]Department of Biochemistry, Ghent University, 9000 Ghent, Belgium
[10]Department of Biology, Center for Proteome Analysis and Mass Spectrometry, University of Antwerp, 2020 Antwerp, Belgium
[11]Flemish Institute for Technological Research (VITO), 2400 Mol, Belgium
[12]These authors contributed equally to this work
[13]Co-senior authors
*Correspondence: daniel.vandamme@psb.vib-ugent.be (D.V.D.), persson@mpimp-golm.mpg.de (S.P.)
http://dx.doi.org/10.1016/j.cell.2014.01.039

SUMMARY

Clathrin-mediated endocytosis is the major mechanism for eukaryotic plasma membrane-based proteome turn-over. In plants, clathrin-mediated endocytosis is essential for physiology and development, but the identification and organization of the machinery operating this process remains largely obscure. Here, we identified an eight-core-component protein complex, the TPLATE complex, essential for plant growth via its role as major adaptor module for clathrin-mediated endocytosis. This complex consists of evolutionarily unique proteins that associate closely with core endocytic elements. The TPLATE complex is recruited as dynamic foci at the plasma membrane preceding recruitment of adaptor protein complex 2, clathrin, and dynamin-related proteins. Reduced function of different complex components severely impaired internalization of assorted endocytic cargoes, demonstrating its pivotal role in clathrin-mediated endocytosis. Taken together, the TPLATE complex is an early endocytic module representing a unique evolutionary plant adaptation of the canonical eukaryotic pathway for clathrin-mediated endocytosis.

INTRODUCTION

The plasma membrane (PM) forms a fundamental barrier of the cell to communicate with the outside world. Plant cells can remove and add receptors, channels, and other membrane proteins in response to endogenous stimuli such as hormones (Du et al., 2013; Irani et al., 2012; Marhavý et al., 2011; Robert et al., 2010; Sutter et al., 2007), nutrient availability (Barberon et al., 2011; Takano et al., 2010), and pathogen defense (Bar et al., 2009; Robatzek et al., 2006). The process by which membrane materials and extracellular cargoes are internalized is called endocytosis (McMahon and Boucrot, 2011). Clathrin-mediated endocytosis (CME) is the best-characterized endocytic pathway in eukaryotes and is defined by the involvement of the vesicle coat scaffold protein clathrin.

CME requires a series of highly coordinated steps consisting of nucleation, cargo selection, vesicle coat assembly, scission, and vesicle uncoating (McMahon and Boucrot, 2011). The heterotetrameric adaptor protein complex 2 (AP2) represents the core complex for CME in animal cells. Here, clathrin-coated pit nucleation at the PM is hallmarked by the arrival of a clathrin triskelion in association with two AP2 complexes in a phosphatidylinositol 4,5-bisphosphate $PI_{(4,5)}$-P_2-dependent manner. This priming complex subsequently recruits more AP2-clathrin complexes and adaptor proteins required for clathrin coat stabilization (Cocucci et al., 2012; Henne et al., 2010; Kukulski et al., 2012). Among these adaptor elements, the muniscin proteins, complexed with intersectin, epsin, and EGFR pathway

Curriculum Vitae

PERSONAL DETAILS

Name:	Urszula Kania
Date of Birth:	20th November 1985
Place of Birth:	Katowice, Poland
Nationality:	Polish
Current Address:	Witosa 32/9 Katowice 40-832, Poland
Email:	urszula.elzbieta.kania@gmail.com

EDUCATION

2009-2014 PhD study in Plant Biotechnology, VIB Department of Plant Systems Biology and Faculty of Sciences, Department of Plant Biotechnology and Genetics, Ghent University, Belgium Supervisor: Prof. Dr. Jiri Friml

2007 – 2009 University of Silesia, Faculty of Biology and Environmental Protection; Off-Campus Department of Nuclear Medicine and Endocrine Oncology (Cancer Center and Institute of Oncology, Maria- Skłodowska Curie Memorial, Gliwice Branch), Poland
Thesis title: MGMT gene methylation in glioma tumours

2008 - 2009 Lifelong Learning Programme - LLP/ Erasmus, Aarhus University, Faculty of Science, Department of Molecular Biology, Denmark
Project title: MicroRNA as the translational regulation of the multifunctional bHLH transcription factor Twist1

2004 – 2007 Bachelor of Science, University of Silesia, Faculty of Biology and Environmental Protection, Department of Plant Anatomy and Cytology, Poland
Thesis title: Structure of centromeric chromatin

PRESENTATIONS AT SCIENTIFIC MEETINGS

Auxins and Cytokinins in Plant Development International Symposium. June 2014, Prague, Czech Republic (Poster)

16th European Plant Endomembrane Meeting. August, 2013, Ghent, Belgium (Poster)

15th European Plant Endomembrane Meeting. August, 2012, Madrit, Spain (Talk)

VIB Conference. April 2012, Blankenberge, Belgium (Talk)

4th International PhD School on Plant Development. October 2011, Zellingen-Retzbach, Germany (Talk)

The 20th International Conference on Plant Growth Substances. July 2010, Tarragona, Spain (Talk)

PUBLICATIONS

Dai M, Zhang C, **Kania U**, Chen F, Xue Q, McCray T, Li G, Qin G, Wakeley M, Terzaghi W, Wan J, Zhao Y, Xu J, Friml J, Deng XW, Wang H (2012) A PP6-type phosphatase holoenzyme directly regulates PIN phosphorylation and auxin efflux in *Arabidopsis*. *Plant Cell* 24: 2497-514

Baster P, Rober S, Kleine-Vehn J, Vanneste S, **Kania U**, Grunewald W, De Rybel B, Beeckman T, Friml J (2013) SCF(TIR1/AFB)-auxin signalling regulates PIN vacuolar trafficking and auxin fluxes during root gravitropism. *EMBO J* 32: 260-274

Gadeyne A, Sánchez-Rodríguez C, Vanneste S, Di Rubbo S, Zauber H, Vanneste K, Van Leene J, De Winne N, Eeckhout D, Persiau G, Van De Slijke E, Cannoot B, Vercruysse L, Mayers JR, Adamowski M, **Kania U**, Ehrlich M, Schweighofer A, Ketelaar T, Maere S, Bednarek SY, Friml J, Gevaert K, Witters E, Russinova E, Persson S, De Jaeger G, Van Damme D (2014) The TPLATE adaptor complex drives clathrin-mediated endocytosis in plants. *Cell* 156(4):691-704

Kania U, Fendrych M, Friml J (2014) Polar delivery in plants; commonalities and differences to animal epithelial cells. *Open Biol.*4(4):140017

TEACHING EXPERIENCE

Supervision of four bachelor students in their Bachelor Project (3rd Bachelor Biochemistry and Biotechnology, Ghent University).

Project: “Forward genetic screen to identify novel components involved in polar targeting in plants”

TECHNICAL SKILLS

Molecular biology: agarose gel electrophoresis, polyacrylamide gel electrophoresis, DNA and RNA isolation, restriction enzymes analysis, PCR (Quantitative, Real-Time, Nested, Overlap-extension, Touchdown, Methylation-specific), traditional and Gateway cloning

Cell biology: confocal microscopy analysis of immuno-fluorescence and GFP fluorescent probes, after chemical treatment (FM4-64, BrefeldinA, Wortmanin, Concanamycin A, Tyrfostine, Latrunculin A, Oryzalin, Endosidine 4, Endosidine 6)

Biochemistry: TAP (Tandem Affinity Purification)-tag method (preparing constructs, cell culture, protein purification), western blotting

Microscopy: Zeiss and Leica confocal microscops and imaging analysis softwares ImageJ, Zeiss Zen

Robotized systems: Biomek2000 (plasmid isolation), Janus (qRT-PCR), InsituPro Vsi (immuno-chemistry)

Additional: ClustalW, Vector NTI, biolistic transformation of *Nicotiana tabacum* cell culture, cross pollination of *Arabidopsis*, generation of stable transgenic lines in *Arabidopsis* via floral dip, performing genetic screen on the EMS mutagenized plant populations, morphological and subcellular phenotypical characterization of the mutant *Arabidopsis* lines

Acknowledgements

I would like to thank my promotor Jiří for giving me the opportunity to work in his group, encouraging words, patience, support and help, especially during the long process of preparing this dissertation.

I would like to thank all the board committee members, Stéphanie R, Jenny R, Markus G, Danny G, Moritz N, Wout B, Boris P and Kiril M for all the comments and suggestions to improve the manuscript.

All my colleagues in the group, PSB department in Gent and IST Austria, Ana F, Agnieszka B, Agnieszka D, Anas A, Andrej H, Bernard C, Boris P, Camilla B, Candela CM, Cezary W, Christine M, Eduardo CR, Elena F, Elke B, Ellie H, Eva M, Evangelia D, Fabiola OO, Gergely M, Hanka R, Helene R, Hiro T, Hongjiang L, Ignacio M, Jing J, Jose O, Jurgen KV, Kiril M, Kristof V, Krisztina O, Krzysiek W, Łukasz Ł, Maria S, Marta Z, Matyáš F, Mugurel F, Miguel LC, Mike K, Maciek A, Moritz N, Niloufer I, Oana D, Petra N, Petra Z, Peter G, Peter M, Petr V, Ricardo T, Riet DR, Romario M, Saeko K, Satoshi N, Stephen V, Sibu S, Sibylle H, Stéphanie R, Tom V, Tomas P, Tomek N, Wilson AD, Wim G, Xu C, Yuliya S, Yun-Long D, Zhaojun D, for a great atmosphere at work, friendship, smiles, and all the good moments.

A big thank you to the PSB and IST Austria people working in the facilities and administrations, Nancy, Wilson, Nino, Nico, Miguel, Jacky, Kristof, Diane, Sofie, Nathalie, Delphine, Agnieszka, Traude, Katia, Mark, Michael, Vlad for their great job. For proofreading this manuscript, thanks to Martine.

Szczególnie chciałam podziękować mojej rodzinie, Pawłowi, mamie, tacie, Dorocie, Marysi, Łukaszowi, Asi, Maji, Maksowi, Mikeowi za to że są, na dobre i na złe, wierzą we mnie i wspierają w trudnych momentach życia.